EFFECT OF HEAVY METAL SPECIATION ON NITRIFICATION INHIBITION

by

NESLİHAN YAZICI SEMERCİ

BS. in Env. Eng. Marmara University, 1997

M.S. in Env. Eng. Marmara University, 2000

Submitted to the Institute of Environmental Sciences in partial fulfillment of

the requirements for the degree of

Doctor

of

Philosophy

in

Environmental Technology

Boğaziçi University
2007

Dedicated to my daughter ……

ACKNOWLEDGEMENTS

I would like to express my gratitude to my supervisor Prof. Ferhan Çeçen for her guidance, support, encouragement and help, for her valuable comments and generous time in proof readings. It was an opportunity for me to share her extensive knowledge and perspective during this study.

I would also like to express my appreciation to the other members of my thesis jury Prof. Miray Bekbölet, Assoc. Prof. Ayşen Erdinçler, Prof. Orhan Yenigün and Prof. Mehmet Ali Yükselen for spending their valuable time to evaluate this thesis.

The experiments in this study were conducted in Marmara University Environmental Engineering Laboratory. I want to thank all the laboratory staff for their helps. Thanks to Dr. Bülent Mertoğlu and Nuray Güler for molecular analyses. I would also like to thank my undergraduate students for their help in laboratory works in the scope of their graduation project under my supervision. Special thanks to Şerafettin Dede for his technical supports.

The financial support of this study by the Research Fund of Boğaziçi University (Project No: B.A.P. 03S103) and TUBITAK (Project No: ICTAG Ç067, Ç106) is gratefully acknowledged.

Special thanks to Dr. Bilge Kocamemi for her friendship, support and providing me seed sludge of enriched nitrifier culture. Special thanks to my all friends in Marmara University for their support and helps.

Lastly, I would like to thank my family and my husband for their incredible support, understanding, never ending patient and love. To my husband Tolga, I hope you will be around for a long time so I can express my gratitude to you for the rest of my life. As a wife and as a friend.

ABSTRACT

Industrial effluents and high-strength wastewaters such as landfill leachates may contain significant amounts of heavy metals. The presence of heavy metals causes toxicity in biological treatment systems. The toxic and inhibitory characteristics of heavy metals depend on several factors such as exposure time, type of buffer, pH, type and concentration of ligands and acclimation. Therefore, a quite high variation is seen in the reported inhibitory range for metals. Surprisingly, very little information exists on the importance of heavy metal speciation in nitrification inhibition studies. Furthermore, the behaviour of heavy metals under prolonged exposure times, acclimation, adaptation, shifts and changes in bacterial community have not been examined yet. The aim of this study was to investigate the influence of Cd and Zn speciation on nitrification inhibition in batch systems enriched in terms of nitrifiers and to investigate the response of nitrifying biomass to prolonged Cd exposure in a continuous-flow system. These experiments showed that the measurement methodologies applied in assessing heavy metal inhibition should be carefully selected since physical and chemical speciation highly affects inhibition. The activity of nitrifying bacteria in continuous-flow systems could change as a result of shifts in microbial community. It also showed the necessity of incorporation of molecular tools into heavy metal inhibition studies.

ÖZET

Günümüzde, endüstriyel atıksuların ve düzenli depolama sızıntı suyu gibi konsantre atıksuların birçoğu ağır metaller içermektedir. Ağır metallerin varlığı biyolojik arıtma sistemlerini olumsuz yönde etkilemektedir. Ağır metallerin toksik ve inhibitör özellikleri, bakterinin metale maruz kalma süresi, tampon çözeltinin tipi, pH, ligandların tipi ve konsantrasyonu ve aklimasyon gibi birçok parametreye bağlıdır. Literatürde, nitrifikasyon sistemlerinde ağır metal türleşmesinin öneminin çok az incelendiği görülmektedir. Bunun yanısıra, ağır metallerin uzun temas süreleri sonucundaki davranışları, bakterilerin aklimasyonu, adaptasyonu, bakteri türlerindeki değişimler çok fazla incelenmemiştir. Bu çalışmanın amaçlarından biri, kadmiyum ve çinko türleşmesinin nitrifikasyon inhibisyonu üzerindeki tesirlerinin nitrifikasyon bakterileri açısından zenginleştirilmiş kesikli reaktör sistemlerinde incelenmesidir. Zenginleştirilmiş nitrifikasyon bakterilerinin kadmiyum metaline uzun süreli maruz kalması durumundaki tepkisi sürekli reaktör sisteminde incelenmiştir. Kesikli reaktör deneyleri metallerin fiziksel ve kimyasal türleşmesinin inhibisyonu çok etkilediğini, bu nedenle ağır metallerin biyolojik sistemlerdeki inhibisyonunun değerlendirilmesinde uygulanan metodolojilerin çok dikkatli seçilmesi gerektiğini göstermiştir. Nitrifikasyon bakterilerinin sürekli reaktör sistemlerindeki aktiviteleri mikrobiyel türlerdeki değişimler sonucunda değişebilmektedir. Sürekli reaktör deneyleri, moleküler uygulamaların ağır metallerin inhibisyonu çalışmalarına dahil edilmesinin ne kadar gerekli olduğunu göstermiştir.

TABLE OF CONTENTS

ACKNOWLEDGEMENTS iii
ABSTRACT iv
ÖZET v
TABLE OF CONTENTS vii
LIST OF FIGURES xii
LIST OF TABLES xix
LIST OF SYMBOLS/ABBREVIATIONS xxi
1. INTRODUCTION 1
2. FUNDAMENTALS OF NITRIFICATION 3
2.1 Microbiology of Nitrification 4
2.2 Stoichiometry of Nitrification 5
2.3 Growth Kinetics of Nitrification 7
2.4 Effects of Environmental Factors 7
2.5 Enzyme Inhibition 10
3. HEAVY METAL TOXICITY 15
3.1 Properties of Heavy Metals 15
3.2 Heavy Metal Resistance Mechanisms 17
3.2.1 Cadmium Resistance Mechanisms in Microorganisms 18
3.2.2 Zinc Resistance Mechanisms in Microorganisms 19
3.3 Interaction of Metal Species with Biological Interphases 19
3.4 Heavy Metal Removal in Biological Treatment Systems 22
3.4.1 Biosorption 25
3.4.2 Bioaccumulation 27
3.5 Metal Speciation and Bioavailability 29
3.5.1 Metal Complexation by Strong (Anthropogenic) Chelating Agents 30
3.5.2 Chemical Speciation and Toxicity 34
3.5.3 Free Ion Activity Model (FIAM) 35
3.5.4 Biotic Ligand Model (BLM) 36

3.5.4.1 Metal Internalization Fluxes 37
3.5.4.2 Metal Loading Experiments 37
3.5.4.3 Toxicological End Points and Competition Bioassays 38
3.6 Heavy Metal Toxicity in Activated Sludge Systems 39
3.6.1 Mean Cell Residence Time and Acclimation 40
3.6.2 Effective Concentration of Heavy Metals 42
3.7 Review of the Studies on Effects of Heavy Metals in Nitrification Systems 44
3.8 Voltammetric Measurement of Metal Speciation 48
3.8.1 Application of Voltammetry in Environmental Analysis 52
4. STATEMENT OF THE PROBLEM 55
5. MATERIALS AND METHODS 59
5.1 The Maintenance and Growth of the Enriched Nitrifying Sludge 59
5.2 Estimation of Biokinetic Parameters in the Absence of Metals 60
5.3 Batch Experiments with Cadmium (Cd), Zinc (Zn)and Copper (Cu) 61
5.3.1 Preliminary Oxygen Uptake Rate (OUR) Experiments for the Determination of the Inhibition Range 61
5.3.2 Influence of Cd and Zn Speciation on Ntrification Inhibition 63
5.3.2.1 Procedure of Specific Ammonium Utilization Rate Experiments 64
5.3.2.2 Procedure of Long Term Oxygen Uptake Rate Experiments 65
5.3.3 Chemical Speciation Calculations 67
5.4 Biosorption Experiments 69
5.4.1 Sorption Kinetics and Equilibrium Studies 69
5.4.2 Determination of Conditional Stability Constants and Complexation Capacities in Cd and Zn Binding to Bacterial Sites 70
5.5 Experiments in a Continuous-Flow Nitrifying Reactor 72
5.5.1 Experimental Procedure 74
5.5.2 Determination of Nitrifier Activity and Biosorbed Cd 76
5.6 Characterization of Microbial Community in the Continuous-

Flow Nitrifying Reactor 77
5.6.1 DNA Extraction from Sludge Samples 77
5.6.2 PCR (Polymerase Chain Reaction) 78
5.6.3 DGGE (Denaturating Gradient Gel Electrophoresis) 78
5.6.4 Slot-Blot Hybridization 79
5.6.5 FISH (Fluorescence In-Situ Hybridization) 80
5.7 Metal Measurements 81
5.7.1 Sample Digestion 82
5.8. Investigation of Cd and Zn Speciation by Voltammetric Measurements and MINEQL 4.5 + Calculations 86
5.8.1 Measurement of Labile Cd by Voltammetry in the Presence of Complexing Agents 88
5.9 Other Measurements 92
5.10 Reagents 92
6. RESULTS AND DISCUSSIONS 94
6.1 Estimation of Biokinetic Parameters in Ammonium Utilization 94
6.2 The Effect of Cd on Nitrification in Batch Reactor Systems 98
6.2.1 The Effect of Cd, Zn and Cu on the Short Term Specific Oxygen Uptake Rate (SOUR) in the Presence of Phosphate Buffer 98
6.2.2 The effect of Cd, Zn and Cu on the Nitrite Oxidation Determined by SOUR Experiments in the Presence of Phosphate Buffer 100
6.2.3 The effect of Cd on Specific Ammonium Utilization Rate (q_{NH_4-N}) and Specific Oxygen Utilization Rate (SOUR) 102
6.2.4 Effect of Cd Exposure Time on Nitrification Inhibition 107
6.2.5 The effect of Cd-EDTA Complexation on qNH_4-N and SOUR 111
6.2.6 Recovery from Inhibition with EDTA Addition 116
6.2.7 The effect of Cd Speciation on Nitrification 121
6.3 Biosorption of Cd onto Nitrifying Biomass 128
6.3.1 Biosorption of Cd in the Presence of SO_4^{-2} 128

6.3.2 Biosorption of Cd in Ammonium Utilization Experiments 133
6.3.3 Determination of Conditional Stability Constant and Complexation Capacity for Cd binding to Bacterial Sites 134
6.3.4 Kinetic Parameters of Cd biosorption 137
6.4 The Effect of Zn on Nitrification in Batch Reactor Systems 141
6.4.1 The Effect of Zn on Specific Ammonium Utilization Rate (q_{NH_4-N}) and Specific Oxygen Utilization Rate (SOUR) 141
6.4.2 Effect of Zn Exposure Time on Nitrification Inhibition 143
6.4.3 Effect Zn-EDTA Complexation on Nitrification 147
6.4.4 The Effect of Zn Speciation on Nitrification 148
6.5 Biosorption of Zn onto Nitrifying Biomass 152
6.5.1 Biosorption of Zn in the Presence of SO_4^{-2} 152
6.5.2 Biosorption of Zn onto Sludge in Test Mediums Used in Ammonium Utilization Rate Experiments 155
6.5.3 Determination of Conditional Stability Constant and Complexation Capacity for Zn Binding to Bacterial Sites 156
6.5.4 Biosorption Kinetics of Zn 158
6.6 Continuous-Flow Experiments in a Nitrifying Reactor 161
6.6.1 Nitrification Efficiency in the Absence of Cd 161
6.6.2 Estimation of Biokinetic Parameters in the Continuous-flow Reactor 167
6.6.3 Effects of Cd on Ammonium Utilization 170
6.6.4 Relationship Between Inhibition and Cd Biosorption 178
6.6.5 Microbial Community Analyses 183
7. CONCLUSIONS AND RECOMMENDATIONS 190
8. REFERENCES 195
APPENDIX A: NH_4-N, NO_2-N, NO_3-N and MLVSS MEASUREMENT DURUNG THE START-UP PERIOD OF THE NITRIFYING BIOMASS 206
APPENDIX B: NH_4-N CONCENTRATION PROFILES DURING AMMONIUM UTILIZATION RATE EXPERIMENTS FOR BIOKINETIC PARAMETER ESTIMATION 210

APPENDIX C: NH_4-N CONCENTRATION PROFILES IN AMMONIUM UTILIZATION RATE EXPERIMENTS IN THE PRESENCE AND ABSENCE OF Cd 214

APPENDIX D: OUR MEASUREMENT EXPERIMENTS IN THE PRESENCE AND ABSENCE OF Cd 220

APPENDIX E: Cd UPTAKE MEASUREMENT IN AMMONIUM UTILIZATION RATE EXPERIMENTS 226

LIST OF FIGURES

Figure 2.1	Nitrogen Transformations in Biological Treatment Processes	4
Figure 2.2	Mechanism that produces competitive inhibition	12
Figure 2.3	Mechanism that produces uncompetitive inhibition	13
Figure 2.4	Mechanism that produces mixed inhibition	14
Figure 3.1	Schematic representation of the metal transport across the plasma membrane of an organism	20
Figure 3.2	Schematic representations of interactions between various metal species and sensitive sites at a biological membrane	21
Figure 3.3	Heavy Metal Removal Mechanisms by Microbial Action	24
Figure 3.4	Chemical structure of EDTA	30
Figure 3.5	EDTA –Metal Complexes, (a) Mn-EDTA, (b) Co-EDTA	31
Figure 3.6	General scheme showing metal speciation in solution	33
Figure 3.7	Typical current response for differential pulse voltammetry (adapted from Bott, 1995)	50
Figure 5.1	Experimental set-up for short-term oxygen uptake rate (OUR) (1st method) experiments	62
Figure 5.2.	Experimental set-up for the simultaneous measurement of q_{NH_4-N} and SOUR	66
Figure 5.3.	Experimental set-up of the continuous-flow nitrifying reactor	73
Figure 5.4.	The operating conditions in Phases I and II of continuous-flow nitrifying reactor	75
Figure 5.5.	Voltammetry Instrument (VA 797 Computrace)	81
Figure 5.6	Flow Diagram of Cd and Zn Speciation	81
Figure 5.7.	Typical Cd Measurement with Voltammetry	83
Figure 5.8.	Typical Zn Measurement with Voltammetry	84
Figure 5.9.	Change in the labile Cd in the presence of EDTA and NTA	84
Figure 6.1	Typical NH_4-N utilization curves for initial NH_4-N concentration of 22, 50 and 90 mg/L	96
Figure 6.2	Specific ammonium utilization rates at various bulk NH_4-N	

	concentrations	97
Figure 6.3	Inhibition of SOUR in the presence of Cd	98
Figure 6.4	Inhibition of SOUR in the presence of Zn	99
Figure 6.5	Inhibition of SOUR in the presence of Cu	99
Figure 6.6	Inhibition of nitrite oxidation in the presence of Cd based on SOUR measurements	101
Figure 6.7	Inhibition of nitrite oxidation in the presence of Zn based on SOUR measurements	101
Figure 6.8	Inhibition of nitrite oxidation in the presence of Cu based on SOUR measurements	102
Figure 6.9	Inhibition of specific ammonium utilization rate at various a) total and b)initial labile Cd (Cd_{volt}) concentrations	102
Figure 6.10	Inhibition of q_{NH4-N} (a) and decrease of Cd uptake (b) as a function of the initial EDTA concentration	105
Figure 6.11	Inhibition of specific oxygen uptake rate various total initial Cd concentrations	106
Figure 6.12	Inhibition of ammonium utilization rate (q_{NH_4-N}) at various Cd concentrations in the presence of MOPS and phosphate buffer.	107
Figure 6.13	Inhibition of SOUR with respect to time in the presence of 1 and 2 mg/L of influent Cd	109
Figure 6.14	Inhibition of SOUR with respect to time in the presence of 5 and 10 mg/L of influent Cd	110
Figure 6.15	Ammonium utilization curves and SOUR profiles for A1-A2) Control reactor B1-B2) 15 mg/L Cd C1-C2) simultaneous addition of 15 mg/L Cd and $1x10^{-4}$ M EDTA	113
Figure 6.16	Changes in qNH_4-N, SOUR and Cd uptake with time in the presence of 15 mg/L Cd only (2^{nd} reactor)	115
Figure 6.17	Changes in qNH_4-N, SOUR and Cd uptake with time in the presence of 15 mg/L Cd and $1x10^{-4}$ M EDTA (3^{rd} reactor)	115
Figure 6.18	q_{NH_4-N} and NH_4-N measurements after EDTA addition with respect to time	117
Figure 6.19	Recovery of nitrification inhibition with EDTA addition	119

Figure 6.20	Relationship between inhibition and different forms of Cd (a) eq. free Cd calculated by MINEQL, (b) eq. labile Cd measured with voltammetry, (Cd_{volt}) (c) eq. adsorbed Cd calculated with MINEQL (d) initial total and labile Cd	123
Figure 6.21	Change in bulk labile Cd with time for an initial Cd range of 1-10 mg/L	129
Figure 6.22	Change in bulk labile Cd with time for an initial Cd range of 25-100 mg/L	129
Figure 6.23	Adsorption capacity of for an initial Cd concentration of 1-10 mg/L	130
Figure 6.24	Adsorption capacity of for an initial Cd concentration of 25-100 mg/L	130
Figure 6.25	pH profile during sorption process	131
Figure 6.26	Adsorption Isotherms with Freundlich and Langmuir fits	133
Figure 6.27	Comparison of biosorption data in given in Section 6.3.1 and biosorption data of ammonium utilization rate experiments	134
Figure 6.28	Linearization of the Langmuir Isotherm for the determination of the conditional stability constant	135
Figure 6.29	Correlation between Cd^{+2} calculated by MINEQL+ and measured by voltammetry	137
Figure 6.30	Linearization of cadmium biosorption kinetics by Lagergren first-order plots (Initial Cd = 5 mg/L)	138
Figure 6.31	A plot of t/q vs. time according to the pseudo-second order adsorption kinetics for various initial Cd concentrations	139
Figure 6.32	Inhibition of specific ammonium utilization rate at various a) total and b) initial labile Zn (Zn_{volt}) concentrations	141
Figure 6.33	Inhibition of specific oxygen uptake rate various total at various a) total and b) initial labile Zn (Zn_{volt}) concentrations	143
Figure 6.34	SOUR profiles in the absence and presence of 1 and 2 mg/L Zn	144
Figure 6.35	SOUR profiles in the absence and presence of 5 mg/L Zn and 5 mg/L Zn with EDTA	145
Figure 6.36	SOUR profiles in the absence and presence of 9.44 mg/L Zn and 10.7 mg/L Cd	145
Figure 6.37	Variation in the extent of SOUR inhibition with exposure time to 9.44 mg/L Zn and 10.7 mg/L Cd	146
Figure 6.38	Variation in the extent of SOUR inhibition with exposure time to Zn	147

Figure 6.39	Inhibition of specific ammonium utilization rate at various a) free and b) labile Zn (Zn_{volt}) concentrations	148
Figure 6.40	Relationship between inhibition and different forms of Zn (a) eq. free Zn calculated by MINEQL, (b) eq. labile Zn measured with voltammetry, (c) equilibrium adsorbed Zn calculated with MINEQL	149
Figure 6.41	Residuals plots for the Zn inhibition models	151
Figure 6.42	Change in bulk labile Zn with time for an initial Zn range of 1-10 mg/L	152
Figure 6.43	Change in bulk labile Zn with time for an initial Zn range of 25-150 mg/L	153
Figure 6.44	Adsorption capacity of for an initial Zn concentration of 1-10 mg/L	153
Figure 6.45	Adsorption capacity of for an initial Zn concentration of 25-150	154
Figure 6.46	Zn Adsorption according to Freundlich and Langmuir fits	154
Figure 6.47	Comparison of adsorption isotherm in the presence and absence of cations and anions	155
Figure 6.48	Linearization of the Langmuir Isotherm for determination of conditional stability constant for Zn binding Bacterial Sites	157
Figure 6.49	Correlation between labile Zn calculated by MINEQL+ and measured by voltammetry	158
Figure 6.50	Linearization of zinc biosorption kinetics by Lagergren first-order plots (Initial Cd = 5 mg/L)	159
Figure 6.51	A plot of t/q vs. time according to the pseudo-second order adsorption kinetics	159
Figure 6.52	Daily ammonium loadings, effluent NH_4-N, NO_2-N, NO_3-N and bulk MLVSS measurements (Dotted lines show the steady-state concentrations).	164
Figure 6.53	Dependence of nitrite accumulation on free ammonia (NH_4-N= 250 mg/L, NH_4-N loading = 510 mg NH_4-N/g VSS.day)	165
Figure 6.54	Dependence of nitrite accumulation on free ammonia (NH_4-N= 200 mg/L, NH_4-N loading = 370 mg NH_4-N/g VSS.day)	165
Figure 6.55	NO_2-N accumulation profiles during a) Day 50-67 b) Day 81-114	166
Figure 6.56	Relationship between free ammonia concentration and nitrite oxidation inhibition a) Day 81-114 b) Day 50-67	166
Figure 6.57	Ammonium utilization and nitrate production rates in Phase I at	

	different influent NH_4-N loadings	168
Figure 6.58	Steady state q_{NH_4-N} and q_{NO_3-N} values at various bulk NH_4-N concentrations	169
Figure 6.59	Daily ammonium loadings, effluent NH_4-N, NO_2-N, NO_3-N and bulk MLVSS measurements in Phase II with Cd	171
Figure 6.60	Ammonium utilization and nitrate production rates in Phase II with Cd (Dotted lines show the steady-state rates)	175
Figure 6.61	Inhibition in $q_{\max,NH_4-N}$ and $q_{\max,NO_3-N}$ with respect to influent Cd concentrations	177
Figure 6.62	Comparison of the observed and predicted q_{NH_4-N} values at various influent and bulk labile Cd concentrations	178
Figure 6.63	Bulk labile Cd (Cd_{volt}) and biosorbed Cd in Phase II	179
Figure 6.64	Steady-state biosorbed Cd in continuous-flow experiments	180
Figure 6.65	Steady-state soluble bulk labile Cd concentrations in continuous-flow experiments	180
Figure 6.66	Relationship between inhibition and different forms of Cd (a) bulk labile Cd (b) biosorbed Cd	181
Figure 6.67	Photomicrographs of FISH images, (A) All microorganims visualized with DAPI staining (blue) (B) FISH with oligonucleotide probes NSO190 (red) for *Nitrosomonas* species	183
Figure 6.68	Results of slot-blot analyses	186
Figure 6.69	DGGE results of PCR amplified amoA genes (Sample dates are given in Table 6.19)	187
Figure A1.	Influent and effluent NH_4-N concentrations in stock enriched nitrifying culture during start-up and steady state conditions	209
Figure A2.	Effluent NO_2-N concentrations in stock enriched nitrifying culture during start-up and steady state conditions	209
Figure A3.	Effluent NO_3-N concentrations in stock enriched nitrifying culture during start-up and steady state conditions	210
Figure A4.	Biomass Concentration in stock enriched nitrifying culture during start-up and steady state conditions	210
Figure B1.	NH_4-N utilization profile in batch reactors, a) Reactor 1: Initial NH_4-	

	N=5 mg/L b) Reactor 2: Initial NH_4-N=5 mg/L	211
Figure B2.	NH_4-N utilization profile in batch reactors, a) Reactor 1: Initial NH_4-N=25 mg/L b) Reactor 2: Initial NH_4-N=25 mg/L	211
Figure B3.	NH_4-N utilization profile in batch reactors, a) Reactor 1: Initial NH_4-N=50 mg/L, b) Reactor 2: Initial NH_4-N=60 mg/L	212
Figure B4.	NH_4-N utilization profile in batch reactors, a) Reactor 1: Initial NH_4-N=60 mg/L b) Reactor 2: Initial NH_4-N=60 mg/L	212
Figure B5.	NH_4-N utilization profile in batch reactors, a) Reactor 1: Initial NH_4-N=65.5 mg/L b) Reactor 2: Initial NH_4-N=86 mg/L	213
Figure B6.	NH_4-N utilization profile in batch reactors, a) Reactor 1: Initial NH_4-N=95 mg/L b) Reactor 2: Initial NH_4-N=192 mg/L	213
Figure B7.	NH_4-N utilization profile in batch reactors, a) Reactor 1: Initial NH_4-N=25 mg/L b) Reactor 2: Initial NH_4-N=52 mg/L	214
Figure C1.	NH_4-N utilization in batch reactor (a) Exp. No. 1 (b) Exp. No.2	215
Figure C2.	NH_4-N utilization in batch reactor (a) Exp. No. 3 (b) Exp. No.4	215
Figure C3.	NH_4-N utilization in batch reactor (a) Exp. No. 5 (b) Exp. No.6	216
Figure C4.	NH_4-N utilization in batch reactor (a) Exp. No. 7 (b) Exp. No.8	216
Figure C5.	NH_4-N utilization in batch reactor (a) Exp. No. 9 (b) Exp. No.10	217
Figure C6.	NH_4-N utilization in batch reactor (a) Exp. No. 11 (b) Exp. No.12	217
Figure C7.	NH_4-N utilization in batch reactor (a) Exp. No. 13 (b) Exp. No.14	218
Figure C8.	NH_4-N utilization in batch reactor (a) Exp. No. 15 (b) Exp. No.16	218
Figure C9	NH_4-N utilization in batch reactor (a) Exp. No. 17 (b) Exp. No.18	219
Figure C10.	NH_4-N utilization in batch reactor (a) Exp. No. 19 (b) Exp. No.20	219
Figure C11.	NH_4-N utilization in batch reactor (a) Exp. No. 21 (b) Exp. No.22	220
Figure D1.	OUR measurements in qNH_4-N experiments (Exp. No. 3)	221
Figure D2.	OUR measurements in qNH_4-N experiments (Exp. No. 4)	221
Figure D3.	OUR measurements in qNH_4-N experiments (Exp. No. 5)	222
Figure D4.	OUR measurements in qNH_4-N experiments (Exp. No. 12)	222
Figure D5.	OUR measurements in qNH_4-N experiments (Exp. No. 14)	223
Figure D6.	OUR measurements in qNH_4-N experiments (Exp. No. 17)	223
Figure D7.	OUR measurements in qNH_4-N experiments (Exp. No. 18)	224
Figure D8.	OUR measurements in qNH_4-N experiments (Exp. No. 19)	224
Figure D9.	OUR measurements in qNH_4-N experiments (Exp. No. 20)	225

Figure D10.	OUR measurements in qNH_4-N experiments (Exp. No. 21)	225
Figure D11.	OUR measurements in qNH_4-N experiments (Exp. No. 22)	226
Figure E1.	Cd biosorption in ammonium utilization rate experiments a) 1 mg/L b) 2 mg/L	227
Figure E2.	Cd biosorption in ammonium utilization rate experiments a) 2.5 mg/L b) 5 mg/L	227
Figure E3	Cd biosorption in ammonium utilization rate experiments a) 5mg/L b) 5 mg/L	228

LIST OF TABLES

Table 5.1	Composition of the synthetic stock solutions	60
Table 5.2	Conditions in Experiments with Cd	63
Table 5.3	Conditions in Experiments with Zn	64
Table 5.4	Thermodynamic Stability Constants Used in Speciation Calculations	67
Table 5.5	Operational conditions in the continuous-flow nitrifying reactor	74
Table 5.6	Composition of synthetic solution used in continuous flow experiments	74
Table 5.7	PCR primer pairs	78
Table 5.8.	Slot-Blot Hybridization Probes	80
Table 5.9	Probes and target groups	81
Table 5.10	Operational parameters in voltammetric Cd and Zn measurements	85
Table 5.11	Concentration of cations and anions in synthetic feed solution used in batch experiments	86
Table 5.12	Cd species in the feed solution: Comparison of MINEQL +4.5 and voltammetric results at pH=7.5 and pH<2.	87
Table 5.13	Zn species in the feed solution: Comparison of MINEQL +4.5 and voltammetric results at pH=7.5	88
Table 5.14	Cd speciation in the presence of 1.71×10^{-4} M EDTA	90
Table 5.15	Cd speciation in the presence of 1.83×10^{-5} M NTA	91
Table 6.1	Maximum specific ammonium utilization rate ($q_{\max,NH_4-N}$) and half-saturation constant ($K_{S,N}$) at various initial NH_4-N concentrations The comparison of EC_{50} values for Cd in nitrification systems	97
Table 6.2	Results of ammonium utilization rates (q_{NH_4-N}) and specific oxygen uptake rate (SOUR) experiments	103
Table 6.3	Comparison of EC_{50} values for Cd in nitrification systems	104
Table 6.4	Ammonium utilization rates and Cd measurements with respect to time	114
Table 6.5	Equilibrium concentrations of soluble and suspended phase Cd species (Cd_T=12.5 mg/L) before and after 2×10^{-4}M EDTA addition (calculated with MINEQL +4.5 and measured with voltammetry)	120

Table 6.6	Cadmium speciation in ammonium utilization rate experiments	124
Table 6.7	Adsorption Isotherms Constants for Cd	132
Table 6.8	Partition coefficient and conditional stability constant for Cd binding to bacteria	135
Table 6.9	Conditional stability constants for binding of Cd to different organisms	136
Table 6.10	Pseudo-second-order rate constants of Cd biosorption in different test mediums	140
Table 6.11	Summary of ammonium utilization rates and SOUR of Zn experiments	142
Table 6.12	Zinc speciation in ammonium utilization rate experiments at equilibrium	150
Table 6.13	Adsorption Isotherm Constants for Zn	155
Table 6.14	Partition coefficient and conditional stability constant for Zn binding to bacteria	156
Table 6.15	Conditional stability constants for binding of Zn to different organisms	157
Table 6.16	Pseudo-second-order rate constants of Zn biosorption in different test mediums	160
Table 6.17	Steady-state results of continuous-flow experiments at various ammonium loadings	163
Table 6.18.	Maximum specific ammonium utilization rate ($q_{\max,NH_4-N}$) and half saturation constant ($K_{S,N}$) in ammonium utilization in continuous-flow experiments	169
Table 6.19	Results of continuous-flow experiments at various ammonium loadings in the presence of Cd	172
Table 6.20	Sampling information for Slot-Blot hybridization and DGGE analysis	184
Table 6.21	Names and specificity of the probes used in Slot-Blot analysis	184
Table A.1	Performance of the main reactor used in batch experiments	207

LIST OF SYMBOLS / ABBREVIATIONS

Symbol	Explanation	Units used
AMO	Ammonia monooxygenase enzyme	
BR	Biological response	
BR_{max}	Maximum biological response	
C_0	Initial metal ion concentration	mg/L (mol/L)
C_t	Final metal ion concentration	mg/L (mol/L)
Cd_{volt}	Cd concentration measured in voltammetry	
	(Cd^{2+} and Cd in weak complexes)	mg/L (mol/L)
Cd_{bio}	biosorbed Cd concentration calculated with MINEQL +	mg/L (mol/L)
Cd^{2+}	free Cd concentration, mg/L	mg/L (mol/L)
DGGE	Denaturing Gradient Gel Electrophoresis	
DO	Dissolved oxygen	mg O_2/L
DPS	Differential Pulse Polography	
EC_{50}	Effective inhibitor concentration that cause 50% inhibition	
EDTA	Ethylenediaminetetraacetic acid	
EI	Enzyme-inhibitory compound complex	
EIS	Enzyme-substrate-inhibitory compound complex	
$f_{M\text{-}RS}$	Proportion of sensitive sites filled with metal	
$f^{50}_{M\text{-}RS}$	50% occupation of sensitive sites filled with metal	
FA	Free ammonia	mg N/L
FISH	Fluorescence In-Situ Hybridization	
FNA	Free nitrous acid	mg N/L
HAO	Hydroxylamine oxidoreductase enzyme	
i	Inhibition	%
I(A)	Current	A
I	Free inhibitor concentration	mol/L (µg/L)
J_{int}	Metal internalization flux	mol/g.min
		(mol/m^2.min)
J_{max}	Maximum internalization flux	mol/g.min

		(mol/m^2.min)
K	Constant of proportionality	
k_d	Dissociation rate constant	day^{-1}
k_f	Formation rate constant	day^{-1}
k_{int}	Metal internalization rate constant	day^{-1}
K_f	Metal-ligand stability constant	mol/L
K_{ic}	Dissociation constant of EI complex	mol/L (µg/L)
K_{iu}	Dissociation constant of EIS complex	mol/L (µg/L)
K_m	Half-velocity (half-saturation) constant	mol/L (mg/L)
K_m^{app}	Apparent half-velocity constant	mol/L (µg/L)
$K_{S,N}$	Half-saturation constant for ammonia	mg/L
Ko	Half-saturation constant for DO	mg/L
Ks	Half-saturation constant	mg/L
K_S^{app}	Apparent half velocity constant	mg/L
KI	Inhibition constant	µg/L
KL	Langmuir adsorption constant	moles/L
KNS	Conditional stability constant	mol/L
Kp	Partition coefficient	L/g
Kt	Temperature correction factor	
L	Ligand	mol/L (mg/L)
MLVSS	Mixed Liquor Volatile Suspended Solids	mg/L
M	Dry mass of biomass	mg
M^{n+}	Free metal ion	mol/L (mg/L)
$(ML)^{n+}$	Metal complex	mol/L (mg/L)
$M\text{-}A_{cell}$	Metal-nonspecific site complex	g/L
$M\text{-}R_{cell}$	Metal-sensitive site complex	g/L
M-X-cell	activity of the metal-bacterial surface complex	g/L
NH_4^+	Ammonium	mg/L
NH_4-N	Ammonium nitrogen	mg/L
NLSR	Nonlinear Least Square Regression	
NO_2-N	Nitrite nitrogen	mg/L
NO_3-N	Nitrate nitrogen	mg/L

NTA	Nitrilotriacetic acid	
OUR	Oxygen Uptake Rate	mg/L.min
PCR	Polymerase Chain Reaction	
pMMO	Particulate methane monooxygenase enzyme	
R-cell	Concentration of a sensitive site on the surface of the organism	g/L
q	Metal uptake	mg/g (mole/g)
q_{NH4-N}	Specific ammonium utilization rate	mg/g.h
$qNO_3 - N$	Specific nitrate production rate	mg/g.h
$q_{max,N}$	Maximum specific ammonium oxidation rate	mg /g.h
$q_{max,\ NH4-N}$	Maximum specific ammonium utilization rate	mg/g.h
$q^{app}_{mas,NH\,4-N}$	Apparent maximum specific ammonium utilization rate	mg/g.h
q_N	Specific ammonium oxidation rate	g /g.d
S	Substrate concentration	mol/L (mg/L)
S_0	Dissolved oxygen concentration	mol/L (mg/L)
SOUR	Specific Oxygen Uptake Rate	mg/mg.min
T	Temperature	^{0}C
V_{max}	Maximum substrate utilization velocity	mol/L.time
V_m^{app}	Apparent maximum reaction velocity	mol/L.time
V	Volume	mL
VSS	Volatile suspended solids	mg/L
[X-cell]	Concentration of unoccupied binding site	g/L
{-X-cell}	Concentration of free surface site	g/L
y	number of surface sites per unit mass of bacteria	moles/g
Y_N	Yield coefficient for nitrifiers	g/g
Znvolt	Zn concentration measured in voltammetry (Zn2+ and Zn in weak complexes)	mg/L (mol/L)
Zn_{bio}	biosorbed Zn concentration calculated with MINEQL +	mg/L (mol/L)
Zn^{2+}	free Cd concentration, mg/L	mg/L (mol/L
α	Type I error, significance level	
$\mu_{max,A}$	Maximum specific growth rate of autotrophic biomass	1/day
μ_A	Specific growth rate of nitrifying bacteria	1/day

1. INTRODUCTION

The presence of heavy metals can adversely affect the operation of biological treatment processes (Barth et al., 1963, Wang et al., 1999) by accumulating to inhibitory concentrations. Several studies investigated the effects of heavy metals in biological systems alone or in combination with others (Yetiş and Gökçay, 1989, Gökçay and Yetiş, 1991, Mazierski, 1995). A quite high variation is seen in the reported inhibitory range for metals, since different experimental conditions exist in all studies (i.e. exposure time, type of buffer, pH, type and concentration of ligands). In addition to this, interpretation of results is based on different metal forms such as total, labile, free or biosorbed metal. Under these circumstances, it is very difficult to compare the inhibitory concentration ranges.

Although there are a number of studies regarding the effects of heavy metals in biological systems, the main shortcoming of these studies is the inadequacy of incorporating metal bioavailability. Current water quality standards and risk assessment procedures are predominantly based on total or dissolved metal concentrations. However, there is extensive evidence that neither total nor dissolved aqueous metal concentrations are good predictors of metal bioavailability and toxicity (Jansenn et al., 2003). Because the bioavailability of metals depends on chemical form or speciation it is necessary that analytical methods are available to determine or predict the bioavailable fraction of a metal.

Studies demonstrated that short-term batch assays may not adequately reflect the response observed in continuous-flow reactors which are subject to prolonged toxic exposure (Hu et al., 2004). Most importantly, the behaviour of heavy metals under prolonged exposure times, acclimation, adaptation, shifts and changes in bacterial community can best be investigated in continuous-flow experiments. Although toxicity of heavy metals in activated sludge systems and nitrification processes has been studied in numerous works (Dilek and Yetiş, 1991, Zarnovsky et al., 1994, Mazierski, 1995, Madoni et al., 1996, Lee et al., 1997), there is a lack of information on the response of nitrifying bacteria after prolonged exposure to heavy metals.

In this study, in order to investigate the heavy metal inhibition in all aspects, experiments were carried out in batch and continuous-flow reactors with an activated sludge enriched in terms of nitrifiers. The relationship between heavy metal speciation and nitrification inhibition was investigated and modeled according to noncompetitive inhibition model. Direct metal speciation was carried out by voltammetric measurements. Theoretical speciation of metals was calculated by MINEQL + (version 4.5) (Schecher and Mcavoy, 1998) and compared with voltammetric measurements. The response of the nitrifying biomass to Cd was studied by molecular tools.

Chapter 2 provides the theoretical background information on the nitrification process and enzyme inhibition. In Chapter 3, detailed background information about the heavy metal toxicity in biological systems is presented. This chapter also presents the reviews of the studies regarding the effects of heavy metals on nitrification systems. Fundamental information about the voltammetric measurements and applications in environmental analysis are also given in this chapter. In Chapter 4, the main reasons of dealing with this subject are briefly explained. The objectives and methodology of the study are also given in this chapter. Chapter 5 provides all the information about the materials and methods of the study. Some preliminary metal measurements with voltammetry are also given in this chapter. The first part of Chapter 6 presents the results and discussions about the batch experiments carried with Cd. In the second part of Chapter 6, the results and discussions about the batch experiments carried with Zn are given. The third part of Chapter 6 includes the results and discussions about the effect of Cd in a continuous-flow nitrification system. Finally, Chapter 7 provides conclusions and discussions of the significance of research. The chapter ends with recommendations and suggestions for future research.

2. FUNDAMENTALS OF NITRIFICATION

In recent years, the removal or control of nitrogen became an obligation in wastewater treatment as the water sources have been polluted and the demand for reuse of wastewater has increased. Discharges containing nitrogen may accelerate the eutrophication of lakes and reservoirs and may stimulate the growth of algae and rooted aquatic plants in shallow streams. In addition to being aesthetically unpleasant, the presence of algae and aquatic plants may interfere with beneficial uses of the water resources, particularly when they are used for water supplies, fish propagation, and recreation. Significant concentrations of nitrogen in treated effluents may also adverse effects including depletion of dissolved oxygen in receiving waters, exhibiting toxicity toward aquatic life, affecting chlorine disinfection efficiency, presenting a public helath hazard, and affecting the suitability of wastewater for reuse (Metcalf & Eddy, 1993).

Various treatment methods have been used employing chemical, physical and biological systems to limit or control the amount and form of nitrogen discharged by the treatment system. There are several physical and chemical processes used in the past for the removal of nitrogen. The major physical and chemical processes are breakpoint chlorination, selective ion exchange, air stripping and reverse osmosis (EPA, 1993).

Nitrogen entering a biological treatment system in the organic form or ammonia form can be either removed or transformed to another form as shown in Figure 2.1 Removal of nitrogen by biological methods is obtained by assimilation of NH_4-N, NO_2-N, or NO_3-N and their incorporation into cell mass or by conversion of nitrogen gas through nitrification and denitrification. Since the main subject of this study is nitrification process, detailed fundamental information will be only given for this process.

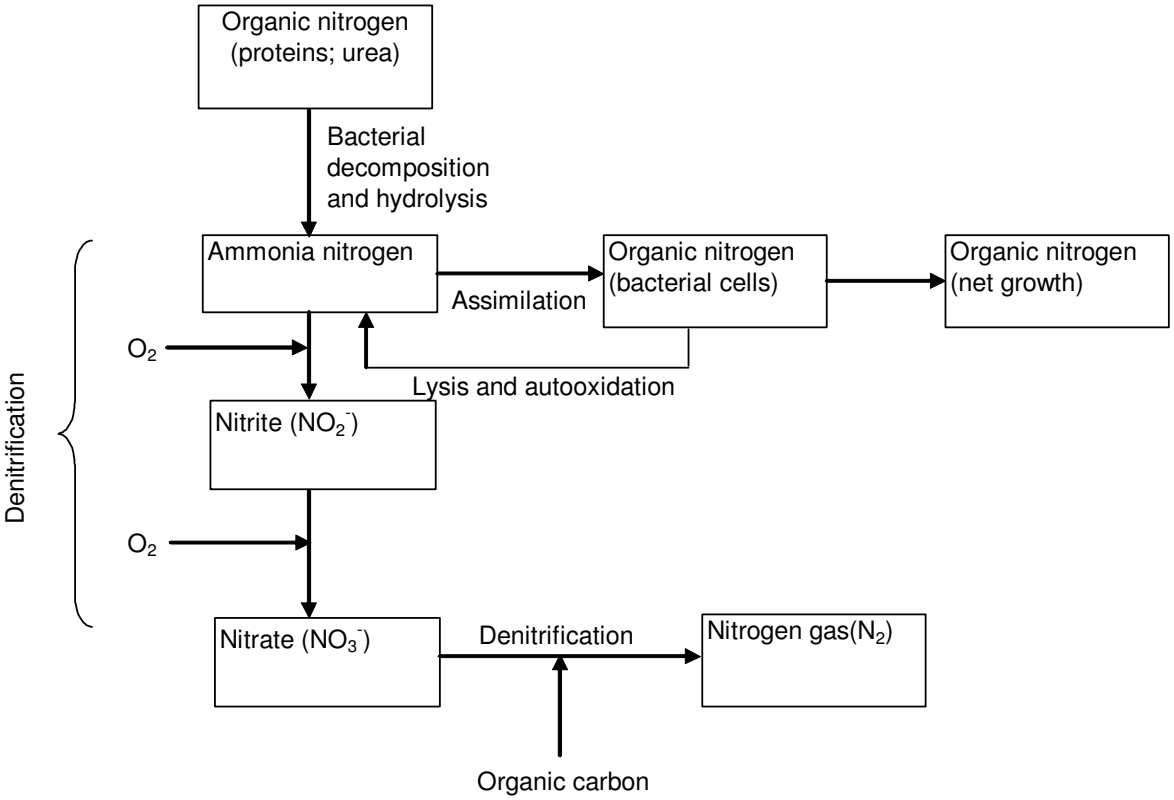

Figure 2.1 Nitrogen transformations in biological treatment processes

2.1. Microbiology of Nitrification

Nitrification is the term used to describe the two-step biological process in which ammonia (NH_4-N) is oxidized to nitrite (NO_2-N) by ammonia oxidizing bacteria (AOB) and nitrite is oxidized to nitrate (NO_3-N) by nitrite oxidizing bacteria (NOB). It should be noted that two groups of autotrophic bacteria are distinctly different. In recent years, the bacteria genera commonly noted for nitrification in wastewater treatment are the autotrophic bacteria *Nitrosomonas* and *Nitrobacter*, which oxidize ammonia to nitrite and then to nitrate, respectively. To date, five genera of NH_4-N oxidizing bacteria (*Nitrosococcus, Nitrosospira, Nitrosolobus, Nitrosorobrio and Nitrosomonas*) are commonly recognized. It should be noted that during 1990s, many more autotrophic bacteria were identified as being capable of oxidizing ammonia (Metcalf & Eddy, 2003). Based on comparative 16S rRNA gene sequence analysis, cultured ammonia-oxidizng bacteria comprise two monophyletic groups within the Proteobacteria. *Nitrosococcus* oceanus belongs to the γ-subclass of Proteobacteria while the members of the genera

Nitrosomonas (including *Nitrococcus mobilis*), *Nitrosospira, Nitrosolobus, Nitrosovibrio* form a close related group within the β-subclass of *Proteobacteria.*

Besides *Nitrobacter*, nitrite can also be oxidized by other NO_2-N oxidizing bacteria (*Nitrococcus*, *Nitrospira*, *Nitrospina* and *Nitroeystis*). Wagner et al. (1995) showed that *Nitrosomonas* was common in activated sludge systems. For nitrite oxidation in activated sludge, Teske et al. (1994) found that *Nitrococsus* was quite prevalent.

2.2. Stoichiometry of Nitrification

The stoichiometric equation for the oxidation of ammonium to nitrite Ammonia Oxidizing Bacteria (AOB) is:

$$2NH_4^+ + 3O_2 \rightarrow 2NO_2^- + 4H^+ + 2H_2O \quad (2.1)$$

Ammonia oxidation is mediated by two different enzymes. Ammonia is first oxidized to hydroxylamine (NH_2OH) by ammonia monooxygenase (AMO) and NH_2OH is further oxidized to NO_2-N by hydroxylamine oxidoreductase (HAO) (Jianlong and Ning, 2004) .

The release of free energy by this reaction has been estimated by various researches to be between 58 and 84 kcal/mole of ammonium (EPA, 1993).

The reaction for the oxidation of nitrite to nitrate by Nitrite Oxidizing Bacteria (NOB) is:

$$NO_2^- + 1/2O_2 \rightarrow NO_3^- \quad (2.2)$$

Nitrite oxidation is mediated by nitrite oxidase, and is believed to proceed without the formation of any chemical intermediates. The reaction has been estimated to release 15.4-20.9 kcal per mole of nitrite (EPA, 1993). The overall oxidation of ammonium is as follows:

$$NH_4^+ + 2O_2 \rightarrow NO_3^- + 2H^+ + H_2O \quad (2.3)$$

Based on the above total oxidation reaction, the oxygen required for complete oxidation of ammonia is 4.57 g O_2/g N oxidized with 3.43 g O_2/g used for nitrite production and 1.14 g O_2/g NO_2 oxidized. When synthesis is considered the amount of oxygen required is less than 4.57 g O_2/g N (Metcalf & Eddy, 2003).

Neglecting cell tissue, the amount of alkalinity required to carry out the reaction given in Eq. (2.3) can be estimated by rewriting Eq (2.3) as follows:

$$NH_4^+ + 2HCO_3^- + 2O_2 \rightarrow NO_3^- + 2CO_2 + 3H_2O \quad (2.4)$$

In the above equation, for each g of ammonia nitrogen (as N) converted, 7.14 g of alkalinity as $CaCO_3$ will be required. Along with obtaining energy, a portion of the ammonium ion is assimilated into cell tissue. The biomass synthesis reaction can be represented as follows:

$$4CO_2 + HCO_3^- + NH_4^+ + H_2O \rightarrow C_5H_7O_2N + 5O_2 \quad (2.5)$$

In this reaction, the chemical formula $C_5H_7O_2N$ is used to represent the synthesized bacterial cells. The growth of AOB and NOB can be given as following:

$$13NH_4^+ + 15CO_2 \xrightarrow{AOB} 10NO_2^- + 3C_5H_7NO_2 + 23H^+ + 4H_2O \quad (2.6)$$

$$10NO_2^- + 5CO_2 + NH_4^+ + 2H_2O \xrightarrow{NOB} C_5H_7NO_2 + 10NO_3^- + H^+ \quad (2.7)$$

From theoretical energy release relationships, yield values of 0.29 g VSS/g NH_4^+ and 0.084 g VSS/g NO_2^--N can be calculated.

2.3. Growth Kinetics of Nitrification

The kinetics of growth and substrate removal for autotrophic bacteria can be expressed with the same equations used earlier for heterotrophic bacteria. The specific growth rates of *Nitrosomonas* and *Nitrobacter* with NH_4-N and NO_2^-N as the respective growth-limiting substrates, can be expressed by the Monod equation (Grady and Lim, 1980)

$$\mu_A = \mu_{\max,A}\left(\frac{S}{K_S + S}\right) \tag{2.8}$$

where;

μ_A = maximum specific growth rate of autotrophic bacteria, day^{-1}

S = concentration of NH_4-N or NO_2^-, mg/L

K_S = half-saturation constant for NH_4-N or NO_2^-, mg/L

Comparison of values for $\mu_{max,A}$, maximum specific growth rate for autotrophs with the typical values for heterotrophs shows the former one to be at least an order of magnitude smaller than the latter (Grady and Lim, 1980). This implies that much longer solids retention time for biological systems designed to achieve nitrification versus only carbon oxidation (Shammas, 1986).

2.4. Effects of Environmental Factors

When designing treatment systems, parameters such as temperature, pH, dissolved oxygen concentration, aeration characteristics and many others are significant in the removal efficiency of the nitrification process. The effect of each parameter should be taken into consideration before designing a nitrification system. In this section most significant parameters affecting nitrification rate are briefly summarized.

Temperature:

The nitrification process occurs over a range of approximately 4 - 45^{o}C, with about 35^{o}C optimum for *Nitrosomonas* and 35 - 42^{o}C optimum for *Nitrobacter* (EPA, 1993). Temperature has a strong effect upon the growth rate of nitrifying bacteria just as it has

upon heterotrophs. Several workers have shown that the effect of temperature on μ_A fits an Arrhenius-type equation over the physiological range (Grady and Lim, 1980). Wong-Chong and Loehr found that deactivation of the *Nitrobacter* occurred at lower temperatures than did deactivation of *Nitrosomonas* and that the temperature dependency of both genera was a function of pH. An acceptable Arrhenius-type expression of the effect of temperature on the maximum growth rate of *Nitrosomonas* over range of 5-30^{o}C is:

$$\mu_{\max,A,T} = \mu_{\max,A\ 15} e^{[K_t (T-15)]} \tag{2.9}$$

where:

$\mu_{max,\ A,T}$ = maximum specific growth rate at any temperature T (^{o}C), day^{-1}

$\mu_{max,A,15}$ = maximum specific growth rate 15 ^{o}C, day^{-1}

K_t = temperature correction factor

For *Nitrosomonas* the reported value for temperature correction factor (K) lies between 0.095 and 0.12 whereas for *Nitrobacter* it is between 0.056 and 0.069. Half saturation constant (K_S) also varied with temperature for *Nitrosomonas*;

$$K_{sT} = K_{s15} e^{[0.118(T-15)]} \tag{2.10}$$

and for *Nitrobacter;*

$$K_{sT} = K_{s15} e^{[0.146(T-15)]} \tag{2.11}$$

The reported values of K_{s15} were 0.405 and 0.625 mg/L for *Nitrosomonas* and *Nitrobacter*, respectively.

pH :

Reactor pH conditions have been found to have significant effect on the rate of nitrification. Nitrification causes a destruction of alkalinity and a potential exists for a drastic drop in pH. Also nitrifying bacteria are very sensitive to pH (Grady and Lim, 1980).

Generally, the optimum pH for nitrification ranges between 8 and 9. There is a wide range in reported pH optima; however the general trend is that as the pH decreases, the rate of nitrification decreases. The optimum pH for *Nitrosomonas* is 8.5 to 8.8 and that for *Nitrobacter* is 8.3 to 9.3 (Shammas, 1986).

An equation was proposed to depict the effect of pH on μ_A for N*itrosomonas* when the pH is below 7.2:

$$\mu_A = \mu_{\max,A}\left[1 - 0.8333(7.2 - pH)\right] \tag{2.12}$$

where, $\mu_{,\max,A}$ is the maximum μ_A, which is assumed to be constant between pH 7.2 and 8.0.

Dissolved Oxygen Concentration:

The concentration of dissolved oxygen (DO), has a significant effect on the rates of nitrifier growth and nitrification in biological waste treatment systems. By modeling the growth of *Nitrosomonas* according to the Monod equation, with DO as the growth limiting substrate concentration, values for the half-saturation coefficient, $K_{O,}$ has been reported as 0.15-2.0 mg/L O_2 (EPA, 1993)

The intrinsic growth rate of *Nitrosomonas* is not limited at DO concentrations above 1.0 mg/L, but that DO concentrations greater than 2.0 mg/L may be required in practice. When designing the aeration or oxygen addition component of a suspended growth nitrification system, it is recommended that a minimum DO level of 2.0 mg/L be specified at all times throughout the biological reactor to prevent peak load ammonia bleed-through (EPA, 1993). The combined effect of all of these factors can be expressed by putting them into equation:

$$\mu_A = \mu_{\max,A}\left(\frac{S}{K_S + S}\right)\left(\frac{S_o}{S_o + K_o}\right) \tag{2.13}$$

where:

S = concentration of NH_4-N or NO_2^-, mg/L

S_0 = Dissolved oxygen concentration, mg/L

K_o = Half-saturation constant for dissolved oxygen, mg/L

Inhibitors:

Besides temperature, pH and dissolved oxygen, nitrifying organisms are susceptible to a wide range of organic and inorganic inhibitors. Certain inorganics, including specific metals, are inhibitory to nitrifiers. Inhibitory inorganic compounds reported are zinc, free cyanide, perchlorate, copper, mercury, chromium, nickel, silver, cobalt, thiocyanate, sodium cyanide, sodium azide, hydrazine, sodium cyanate, potassium chromate, cadmium, arsenic (trivalent), fluoride, lead (EPA, 1993).

Nitrifying organisms are also sensitive to certain forms of nitrogen. Both *Nitrosomonas* and *Nitrobacter* are sensitive to their own substrate, ammonium and nitrite nitrogen respectively and more so to the substrate of another. Un-ionized ammonia (NH_3), or free ammonia (FA), and un-ionized nitrous acid (HNO_2), or free nitrous acid (FNA), are believed to be inhibitory to nitrifiers above certain concentrations. FA begins to inhibit *Nitrosomonas* at a concentration of 10-150 mg/L and *Nitrobacter* in the range of 0.1-1.0 mg/L. FNA begins to inhibit *Nitrosomonas* and *Nitrobacter* at concentrations of 0.22-2.8 mg/L (EPA, 1993). The FA and FNA concentrations are directly correlated to pH and temperature, and the concentration of ammonia plus ammonium and nitrite plus nitrous acid respectively.

2.5. Enzyme Inhibition

Substances that cause a reduction in the rate of an enzyme-catalyzed reaction when present in the reaction mixture are called *inhibitors* (Cornish-Bowden, 1995). Some of these (e.g. urea) are non-specific protein denaturants. Inhibition can arise in a wide variety of ways, however, and there are many different types of inhibitors. One class is that of *irreversible inhibitors* or *catalytic poisons* where the loss of activity is time dependent and cannot be recovered during the timescale of interest. These are substances that combine with the enzyme in such a way as to decrease its activity to zero. If the inhibited enzyme is totally inactive, irreversible inhibition behaves as a time-dependent loss of enzyme concentration (i.e.. lower V_{max}), in other cases, involving incomplete inactivation, there may be time-dependent changes in both K_S and V_{max}. Heavy metal ions (e.g. mercury and lead) should generally be prevented from coming into contact with enzymes as they

usually cause such irreversible inhibition by binding strongly to the amino acid backbone (Cornish-Bowden, 1995).

The second class is that of *reversible inhibitors* where activity may be restored by the removal of the inhibitor. These are substances that form dynamic complexes with the enzyme that have different catalytic properties from those of the uncombined enzyme. If the enzyme has no catalytic activity at all when saturated with inhibitor the inhibition may be described as *complete inhibition* or *linear inhibition*. If the enzyme-inhibitor complex has some residual catalytic activity, this is called *partial inhibition,* from the fact that some activity remains when the enzyme is saturated with inhibitor, or hyperbolic inhibition from the shapes of the curves obtained by plotting apparent Michelis-Menten parameters against inhibitor concentration (Cornish-Bowden, 1995)

Both linear and hyperbolic inhibition may be in principle be sub-classified according to the particular apparent Michaelis-Menten parameters that are affected. These are;

- Competitive Inhibition (specific inhibition)
- Uncompetitive Inhibition (catalytic inhibition)
- Mixed inhibition

In competitive inhibition, the degree of inhibition usually decreases as the substrate increases since the inhibitor and substrate competes with each other for the same active site of the enzyme (Beg and Atiqullah, 1983). The mechanism may be represented in general as shown in Figure 2.2. The defining equation for competitive inhibition is shown in Eqn. 2.14.

$$V = \frac{V_{\max} S}{K_S (1 + I / K_i) + S} \tag{2.14}$$

in which I is the free inhibitor concentration and V_{max} is substrate utilization and K_S is the half-saturation constant. The equation is the form of the Michelis-Menten equation and can be written as (Eqn. 2.15):

$$V = \frac{V_{\max}^{app} S}{K_m^{app} + S} \tag{2.15}$$

where $V_{\max}^{app}$ and K_S^{app} are the apparent values of V_{max} and K_S and are given by $V^{app}=V_{max}$, $K_S^{app}=K_S(1+I/K_i)$. Hence, the effect of a competitive inhibitor is to decrease the apparent value of V_{max}/K_S by a factor of $(1+I/K_i)$ while leaving that of V_{max} unchanged. Competitive inhibition is most noticeable at low substrate concentrations but can be overcome at sufficiently high substrate concentrations as the V_{max} remains unaffected.

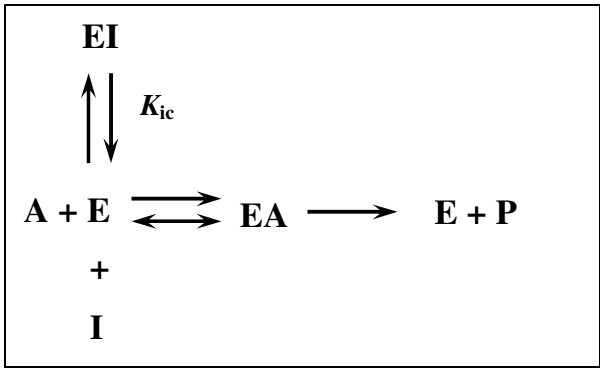

Figure 2.2. Mechanism that produces competitive inhibition (adapted from Cornish-Bowden, 1995)

Uncompetitive inhibition is at the other extreme of competitive inhibition. It is the case where the inhibitor decreases the apparent value of V_{max} with no effect on V/K_S. This type of inhibition occurs when the inhibitor binds to a site which only becomes available after the substrate (S) has bound to the active site of the enzyme. This inhibition is most commonly encountered in multi-substrate reactions where the inhibitor is competitive with respect to one substrate (e.g. S_2) but uncompetitive with respect to another (e.g. S_1). The mechanism may be represented in general terms as shown in Figure 2.3.

The inhibition is most noticeable at high substrate concentrations and cannot be overcome as both the V_{max} and K_S are equally reduced. The rate equation for uncompetitive inhibition is:

$$V = \frac{V_{\max}^{app} S}{K_S^{app} + S} \tag{2.16}$$

where $V_{max}{}^{app}$ and $K_S{}^{app}$ are the apparent V_{max} and K_S given by $V_{\max}^{app} = V_{\max} /(1 + I / K_{iu})$ and $K_S^{app} = K_S /(1 + I / K_{iu})$. Hence the effect of an uncompetitive inhibitor is to decrease the both the K_S and V_{max}.

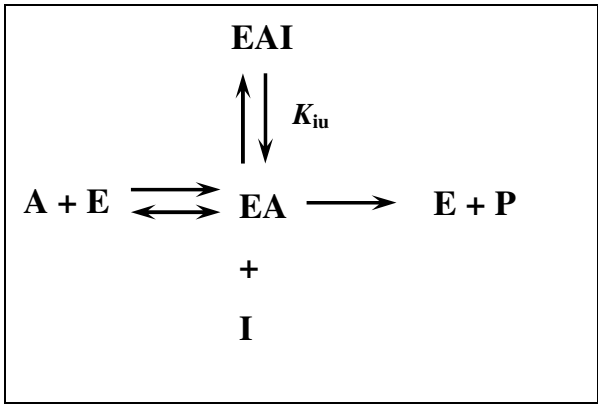

Figure 2.3. Mechanism that produces uncompetitive inhibition (adapted from Cornish-Bowden, 1995)

The simplest formal mechanism for the mixed inhibition is one in which the inhibitor can bind both to the free enzyme to give a complex EI with dissociation constant, K_{ic}, and also to the enzyme-substrate complex to give a complex EAI with dissociation constant, K_{iu}, as shown in Figure 2.4. In this type of inhibition both $V_{\max}^{app} / K_S^{app}$ and V^{app} vary with the inhibitor concentration according to the following equations:

$$V^{app} = \frac{V_{\max}}{1 + \dfrac{I}{K_{iu}}} \tag{2.17}$$

$$K_S^{app} = \frac{K_S (1 + I / K_{ic})}{1 + I / K_{iu}} \tag{2.18}$$

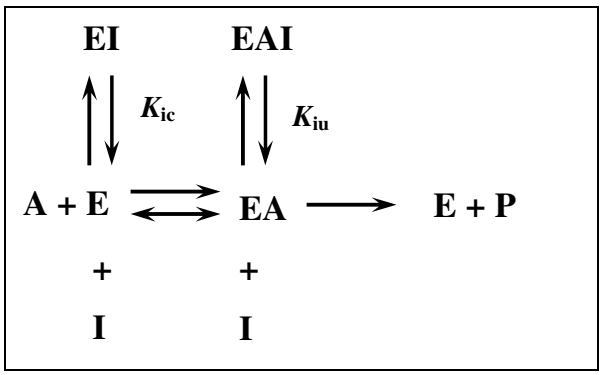

Figure 2.4. Mechanism that produces mixed inhibition (adapted from Cornish-Bowden, 1995)

Most elementary books on inhibition discuss the two types, competitive inhibition and non-competitive inhibition. In this type of inhibition, the substrate concentration does not affect the degree of inhibition. The inhibitor blocks a portion of the initially present enzyme. Thus the available enzyme for substrate will decrease. The rate equation for noncompetitive inhibition is:

$$V = \frac{V_{\max}^{app} S}{K_S + S} \tag{2.19}$$

where V_{max}^{app} is the apparent V_{max} and given by $V_{\max}^{app} = V_{\max} /(1 + I / K_i)$. Hence the effect of a noncompetitive inhibitor is to decrease the V_{max} and leaving K_S unchanged.

3. HEAVY METAL TOXICITY

3.1. Properties of Heavy Metals

The metals are abounded on earth for long time and about 75% of the elements are classified as metals in periodic table. Scientists are familiar with the term "Heavy Metal" but a very few of us have the insight of this terminology. It is alleged that metals that are toxic in nature are heavy metals, but the fact is that there is no authentic evidence behind this statement. Sometimes heavy metals are considered as groups of metals and semimetals (metalloids) that have been associated with contaminants and potential toxicity. The term heavy metal has been used inconsistently. There is no exact definition of heavy metals in literature.

The definitions for "heavy metal" are as follows:

- Metals with element densities above 7 g/cm^3.
- Metals with a specific gravity greater than 4.
- Metals with atomic weight greater than that of sodium, i.e. greater than 23, thus starting with magnesium.
- Metals with atomic weights greater than 40, thus starting with scandium.

However, any authoritative body such as IUPAC (International Union of Pure and Applied Chemists), which makes recommendations regarding the names of newly discovered elements and forms other chemistry related standards, has never defined the term "heavy metals" (http://www.cpp.org.pk/articles/heavy_metals.html).

Most heavy metals are transition elements with incompletely filled “d” orbitals. These d orbitals provide heavy metal cations with the ability to form complex compounds which may or may not be redox active. Thus, heavy metal cations play an important role as “trace elements” in sophisticated biochemical reactions. They play an integral role in the life processes of microorganisms. Some metals such as calcium (Ca), cobalt (Co), chromium (Cr(III)), copper (Cu), iron (Fe) and zinc (Zn) are required nutrients and are

essentials. On the other hand, other metals (silver (Ag), aluminum (Al), cadmium (Cd), gold (Au), lead (Pb) and mercury (Hg)) have no biological roles and are not essential.

Essential metals function as catalysts for biochemical reactions, are stabilizers of protein structures and bacterial cell walls, and serve maintaining osmotic balance. Essential transition metals like iron, copper and nickel are involved in redox processes. Still other essential metals like magnesium and zinc stabilize various enzymes and DNA through electrostatic forces. Iron, magnesium, nickel and cobalt are part of complex molecules with a wide array of functions; and potassium and sodium are required for regulation of intracellular osmotic pressure (Bruins et al., 2000) However, metals at high concentration are toxic to microorganisms. Toxicity occurs through the displacement of essential metals from their native binding sites or through ligand interactions. Nonessential metals bind with greater affinity to thiol-containing groups and oxygen sites than do essential metals (Bruins et al., 2000). Heavy metal ions form unspecific complex compounds in the cell, which leads to toxic effects. Some heavy metal cations, e.g. Hg^{2+}, Cd^{2+} and Ag^{2+}, form strong toxic complexes, which make them too dangerous for any physiological function. Even highly reputable trace elements like Zn^{2+} or Ni^{2+} and especially Cu^{2+} are toxic at higher concentrations (Nies, 1999).

To have any physiological or toxic effect, most heavy metal ions have to enter the cell (Nies, 1999). Because some essential metals are necessary for enzymatic functions and bacterial growth, uptake mechanism exist that allow for the entrance of metal ions into cell. There are two general uptake systems for heavy metal ions: one is fast and unspecific. It is driven only by chemiosmotic gradient across the cytoplasmic membrane of bacteria and ATP is not required. The second type of uptake system has high substrate specificity, is slower and often uses ATP hydrolysis as the energy source (Nies, 1999). While the first mechanism is more energy efficient, it results in an influx of a wider variety of heavy metals, and when these metals are present at high concentrations, they are more likely to have toxic effects once inside the cell (Spain, 2003).

The relative response of microorganisms to the presence of heavy metals can be classified in relation with the heavy metal concentration into three zones as demonstrated by McCarty (1964);

- the zone of increasing stimulation
- the zone of decreasing stimulation and
- the toxicity zone.

The addition of small amounts of heavy metals to the cell environment is usually beneficial to the cell growth, up to the point at which the optimum concentration is surpassed and a relative decrease of the stimulation effect was observed. Further increase of the heavy metal concentration will have an adverse effect on the cell growth, until a complete reduction of the microbial activity and the failure of the system (McCarty, 1964). Gökcay and Yetiş (1991) and Yetiş et al. (1999) showed that acclimatized sludge was stimulated in the presence of Cr(VI) and observed an approximately two times increase in maximum specific growth rate, μ_m value and stimulatory effects on the biomass yield in the presence of 25 mg/L of Cr(VI). Gikas and Romanos (2006) have recently found similar results about the effects of Cr(VI) on the growth of activated sludge. Cr(VI) was found to stimulate microbial growth for concentrations up to about 25 mg/L, exhibiting maximum growth stimulation at 10 mg/L, whilst the lethal dose was found to be between 80 and 160 mg/L.

3.2. Heavy Metal Resistance Mechanisms

To survive under metal stressed conditions, bacteria have developed heavy metal resistance systems. These systems are mostly plasmid-mediated and very specific and have been found virtually in all eubacterial groups studied. Metal resistance systems may have developed shortly after prokaryotic life started and are present in nearly all bacterial types. They arose because the bacteria exist in an environment that has always contained metals (Bruins et al., 2000).

There are differences between chromosomal and plasmid based metal resistance systems. Essential metal resistance systems are usually chromosome-based and more complex than plasmid systems. Plasmid-encoded systems, on the other hand, are usually toxic-ion efflux mechanisms. A cell may develop metal resistance systems in an attempt to protect sensitive cellular components. Limiting metal access or altering cellular components decreases their sensitivity to metals. Several factors determine the extent of

resistance in a microorganism: the type and number of mechanisms for metal uptake, the role of each metal plays in normal metabolism, and the presence of genes located on plasmids or chromosomes that control metal resistance. Six mechanisms were postulated to be involved in resistance to metals which will be described briefly (Bruins et al., 2000):

- Metal exclusion by permeability barrier
- Active transport of the metal away from the cell/organism
- Intracellular sequestration of the metal by protein binding
- Extracellular sequestration
- Enzymatic detoxification of the metal to a less toxic form
- Reduction in metal sensitivity of cellular targets

3.2.1. Cadmium Resistance Mechanisms in Microorganisms

Cadmium is a nonessential metal that is toxic at low concentration. The solubility product of CdS is $1.4x10^{-29}$ M^2 but $2.91x10^{-25}$ M^2 for ZnS. Thus, cadmium is more toxic than zinc. The effects of cadmium may be summed up under the general headings “thiol binding and protein denaturation”, “interaction with calcium metabolism and membrane damage” and interaction with zinc metabolism”, or loss of a protective function (Nies, 1999).

Cadmium enters bacteria and other cells through divalent ion transport systems. Divalent ion transport systems are normally required to transport essential metals such as magnesium, phosphate and sulfate. Nutrient transport systems are often up-regulated in times of need or starvation. An adverse consequence of this is the co-transport of other cations that may be toxic to the organism (Bruins et al., 2000).

Cadmium resistance occurs through all biochemical resistance mechanisms with the exception of enzymatic detoxification. Unlike Hg(II) or Ar(V), Cd(II) does not undergo enzymatic detoxification. Enzymatic resistance through NAD(P)H-dependent reaction is not energetically favored for metals like Cd(II), Zn(II), Ni(II) and Co(II). Covalent modification of the divalent form of these metals is also not biologically favorable because this form is more unstable and toxic (Bruins et al., 2000). The most prominent metal resistance system for Cd(II) is by efflux pumps (Nies, 1999, Bruins et al., 2000).

3.2.2. Zinc Resistance Mechanisms in Microorganisms

Zinc occurs exclusively as the divalent cation Zn^{2+}. With its completely filled d orbitals, the zinc cation is not able to undergo redox changes under biological conditions. It is important in forming complexes (such as zinc fingers in DNA) and as a component in cellular enzymes (Nies, 1999). Bacterial cell accumulates zinc by a fast, unspecific uptake mechanism and it is normally found in higher concentrations (Spain, 2003), but is less toxic than other heavy metals.

Two general efflux mechanisms are responsible for bacterial resistance to zinc. One is a P-type ATPase (is defined as an ATPase that forms a phosphorylated intermediate while catalyzing a reaction) efflux system that transport zinc ions across the cytoplasmic membrane by energy from ATP hydrolysis. The other mechanism involved in Zn efflux is an RND-driven (RND refers to a family of proteins that are involved in the transport of heavy metals) transporter system that transports zinc across the cell wall (not just the membrane) of gram-negative bacteria and is powered by a proton gradient and not ATP (Spain, 2003, Nies, 1999).

3.3. Interaction of Metal Species with Biological Interphases

Trace metal interactions with aquatic organisms generally involve the following steps (Campbell, 1995):

- advection or diffusion of the metal in the bulk solution to the cell membrane surface
- sorption/surface complexation of the metal at binding sites on the cell membrane surface
- uptake (transport) of the metal through the cell membrane into the organism.

In the bulk solution (Fig. 3.1, right-hand side), the metal may be present as the free-metal ion, or as one or more dissolved metal-ligand complexes. On approaching the surface of the cell, these metal forms will normally encounter the cell wall. The macromolecules making up this highly porous external layer contain a variety of simple functional groups, dominated by O-containing donor groups (-COH;-COOH;-$P(O)(OH)_2$) (Campbell et al., 2002). At neutral pH values many of these functional groups will be

ionized, affording a hydrophilic matrix of negatively charged sites through which the metal and its complexes must migrate, eventually reaching the plasma membrane (Fig. 3.1, left-hand side). The important features of this membrane barrier are its overall hydrophobic, phospholidic character, the presence of proteins-some of which may traverse the lipid bilayer-and the existence of transport proteins and/or ion channels that facilitate the movement of ions across the membrane (Simkiss and Taylor, 1995).

Potential binding sites for the incoming metal encountered can be divided into two classes: *physiologically inert* sites, where the metal binds without obviously perturbing the normal cell function, and *physiologically active* sites, where the metal affects cell metabolism. In the latter case, metal binding may affect cell metabolism directly, e.g. if the binding site corresponds to a membrane-bound enzyme, or indirectly, if the bound metal subsequently transported across the plasma membrane into the cell. Once within the cell, the metal may interact with a variety of intracellular sites, resulting in positive or negative consequences (Campbell et al., 2002).

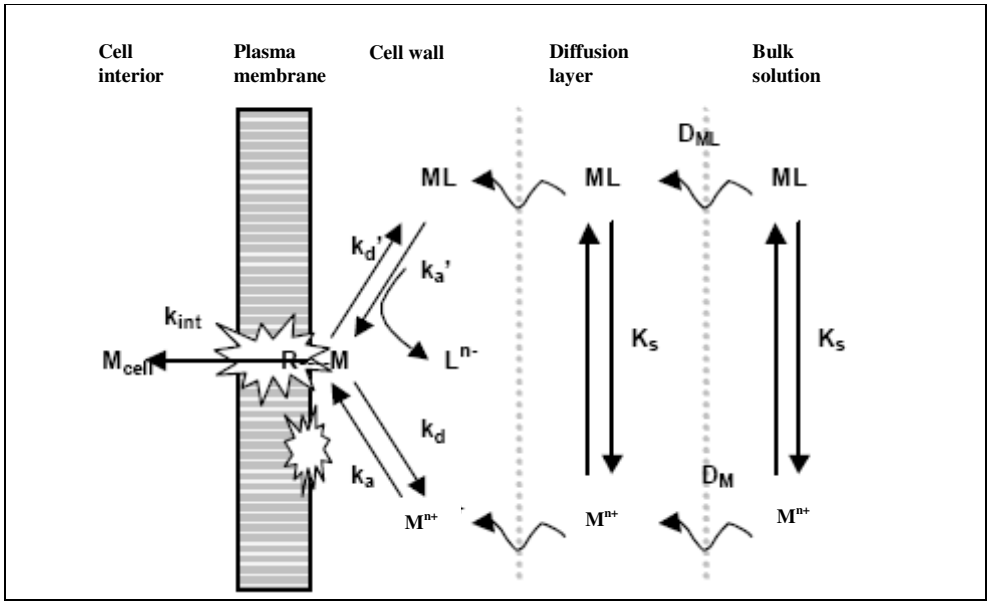

Figure 3.1. Schematic representation of the metal transport across the plasma membrane of an organism (adapted from Campbell et al., 2002).

The major transport route of metal ions over a biological membrane is generally assumed to occur through specific (M-R_{cell}) (e.g. specific carrier ligands, transporters, ion channels) or nonspecific (M-A_{cell}) adsorption of the metal to the surface of the cell (Figure 3.2, adapted from Escher and Sigg, 2004). To invoke a biological effect, the metal must first react with sensitive sites (M-R_{cell}) on the biological membrane (Eqn. 3.1)

$$M^{n+} + R-cell \underset{k_d}{\overset{k_f}{\leftrightarrow}} M-R_{cell} \xrightarrow{k\,\mathrm{int}} ML_{\mathrm{int}} + R-cell \qquad (3.1)$$

where R-cell refers to the free concentration of a sensitive site on the surface of the organism; k_f, k_d and k_{int} are the formation, dissociation and internalization rate constants.

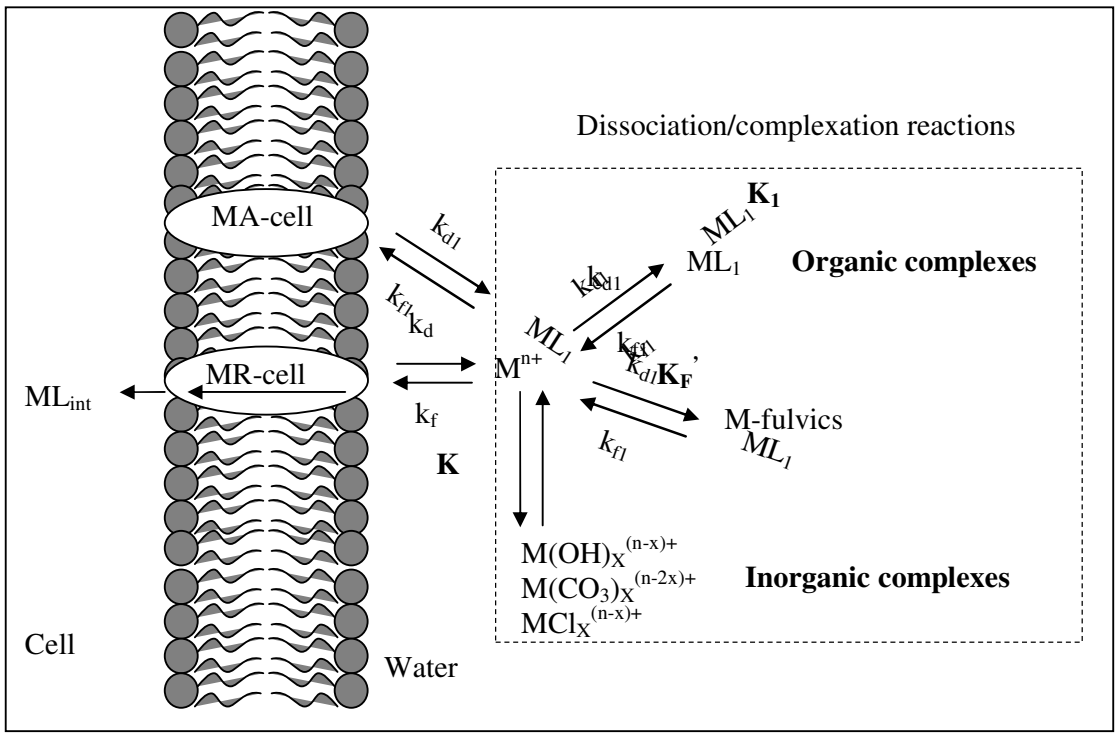

Figure 3.2. Schematic representations of interactions between various metal species and sensitive sites at a biological membrane (adapted from Escher and Sigg, 2004)

The metal-sensitive site complexes (M-R_{cell}) can be transported over the membrane. It is often assumed that the rate-limiting step for the metal uptake is the active transport of the M-R_{cell} over the membrane leading to internalization of the metal (Escher and Sigg, 2004). Equilibrium among the metal species in solution and those bound to the surface will

be attained if transport across the biological membrane is rate-limiting. In that case, for metal concentrations below saturation of the uptake sites, biological uptake fluxes will be directly proportional to any of the metal species in equilibrium (M-R_{cell} or M^{n+} in Eqn 3.1) and can be expressed with simple steady state-models, the free ion activity model (FIAM) or the biotic ligand model (BLM).

In the opposite case, for which biological internalization is rapid compared to either physical transport or chemical reactivity of the metal, biological uptake fluxes will be better related to some other fraction of the metal species in solution (e.g. mobile or labile) (Escher and Sigg, 2004). Labile complexes refer to metal species that dissociate and hence contribute to the free metal ion flux over the time scale that metal species are resident in the diffusive boundary layer surrounding the organism (Bowles et al., 2006). If the metal transport from the bulk solution to the membrane surface is slow compared to the actual uptake by the organism, the free metal ion will become depleted near the membrane surface, and as a result, (labile) metal complexes –if present- will dissociate, resulting in enhanced diffusional flux and enhanced metal uptake (Degryse et al., 2006). Recently, Degryse et al. (2006) measured the uptake of cadmium (Cd) by spinach (*Spinacia oleracea*) from solution in the absence or presence of synthetic ligands. At the same free ion concentration, the uptake of Cd ranged over almost 3 orders of magnitude and largest in treatments with fast dissociating (i.e. labile) complexes. Similar results were found for the diffusional fluxes in these solutions. Degryse et al. (2006) concluded that Cd uptake is rate-limited by diffusion of the free ion to the root surface, even in stirred solution, resulting in apparent exceptions from the free ion activity model. This result showed us the free ion concept should be reconsidered when transport limitations of the metal ion to the uptake site prevail.

3.4. Heavy Metal Removal in Biological Treatment Systems

A variety of suitable methods exist for the removal of heavy metals from industrial wastes when they are at high concentrations. These are chemical precipitation, electrode deposition, ion exchange, reverse osmosis, evaporative recovery and membrane technology applications (Yetiş et al., 1998). There are numerous reports in the literature about the removal of soluble heavy metals in biological treatment systems. Generally, about 5 to

20% removal occurs in primary sedimentation basin and an additional 10 to 80% removal occurs in the activated sludge process with biosorption, binding of heavy metal to biomass, and with other processes. Activated sludge treatment can reduce influent levels of iron, copper, lead, nickel, and zinc by 30 to 90 percent (Cheng et al., 1975).

Heavy metal uptake (removal) by secondary sludge follows a two-phase process-a rapid initial phase of great magnitude followed by a slow secondary phase of less magnitude. The first step, which is called biosorption or extracellular uptake is related to the surface characteristics of microorganisms to where metals bind. The second, and relatively unimportant one that is called bioaccumulation or intracellular uptake, might be the entrance of metal inside the cell (bioaccumulation or intracellular uptake). The removal achieved in bioaccumulation is relatively insignificant in comparison with that of the biosorption. The biosorption phase only takes from minute to an hour (Cheng et al., 1975, Nelson et al., 1981, Çeçen et al., 2001). Influencing factors include pH, the concentration of metal present in the wastewater (Yetiş et al., 1998) and the composition and characteristics of wastewater and sludge (Battistoni et al., 1993).

Metal binding to microorganism is mediated primarily by physical-chemical factors. Although living and dead cells are capable of metal accumulation, there are differences in the mechanisms involved, depending on the extent of metabolic dependence (Sala et al., 2002)**.** Sludge viability does not significantly affect metal biosorption (Cheng et al., 1975). As a result, active metabolic processes can be considered to be relatively unimportant. Studies show that mercury (II), lead (II) and cadmium (II) are among the group of the most removable metals and nickel (II) is the least removable metal (Barth et al., 1963, Cheng et al., 1975).

The ability of several organisms, ranging from bacteria to fungi, yeasts and algae, to remove and/or concentrate metals is well documented by extensive literature and numerous review papers published mostly over the last decade (Nelson, 1981, Volesky et al., 1993 Volesky, 1999, Figueria et al., 1997, Arıcan and Yetiş, 2006). At least four mechanisms have been identified up to now for the removal of metal ions from aqueous solutions by microbial action and schematically summarized in Figure 3.3.

Bioadsorption (biosorption): consisting of exocellular or pericellular binding of metals, which may involve either:

- cation adsorption which may be similar to the behavior of the commercially carboxylic cation exchange resin; or
- metal deposition : precipitation at microbial surface that may occur as surface complexation or chelation or as entrapment by extracellular organelles.

Bioaccumulation: consisting of intracellular uptake of metals which may occur by

- intracellular uptake of metals
- uptake via undefined processes
- uptake via anion transport pathways

Formation of insoluble compounds with formation and precipitation of :

- -metal sulfides
- -metal oxides

Miscellaneous microbe-metal reactions: e.g. volatilization

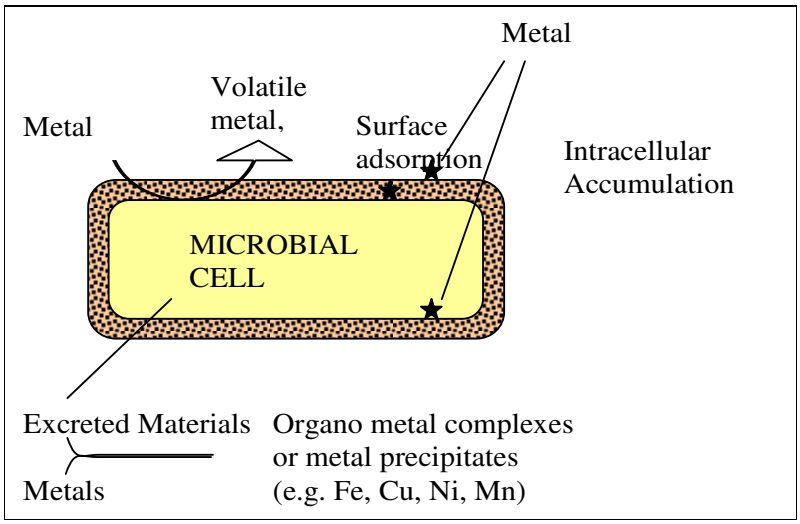

Figure 3.3. Heavy Metal Removal Mechanisms by Microbial Action (Kelly et al., 1979)

Biosorption and bioaccumulation are two different processes. The first may be referred to as a passive process, in the sense that it is not related to any physiological function and may occur even if the microorganism is dead. Surface binding of metals is typically rapid, reversible and independent of energy metabolism. Weakly acidic functional groups, present in the cell wall, are involved in the mechanism of heavy metal binding. It

was suggested in some studies that an ion exchange mechanism exists involving a competition between hydrogen and heavy metal ions for the cell surface binding sites (Artola et al., 1997). Anionic ligands responsible for cation surface binding include phosphoryl, carboxyl, sulphydryl and hydroxyl groups of membrane proteins and lipids and of cell wall structural components. Bioaccumulation, by contrast, is dependent on metabolic energy, ATPase and transmembrane proton gradient.

3.4.1. Biosorption

Biosorption may be defined as the removal of metal or metalloid species, compounds and particulates from solution by biological material. This technology has been recognized a potential alternative to existing technologies for removing heavy metals from industrial wastewater (Artola et al., 1997). Using microorganisms as biosorbents for heavy metals is an attractive alternative to existing methods for toxicity reduction and recovery of valuable metals from industrial effluents, because of good performance and low cost of biosorbent material. Living, dead or resting cells of different species of bacteria, fungi and algae have served as biomass sources with varying metal binding capacities (Yetiş et al., 1998).

Biosorption is primarily an adsorption-type phenomenon, which takes place through the electrostatic attraction of metal cations to the negatively charged surface of the microbial cell. It exhibits this property, acting just as a chemical substance, as an ion exchanger of biological origin. It seems that the bulk of the metal binding capacity is related, for each microbial species, to the chemical format of the cell wall. Hence, although the metal binding mechanism is basically the same, the metal binding agent changes depending on the microbial species.

Biosorption uses raw materials which are either abundant (seaweeds) or wastes from other industrial operations (fermentation wastes). The metal sorbing performance of certain types of biomass can be more or less selective for heavy metals. That depends on:

- the type of biomass
- the mixture in the solution
- the type of biomass preparation
- the chemical-physical environment

It is important to note that concentration of a specific metal could be achieved either during the sorption uptake by manipulating the properties of a biosorbent, or upon desorption during the regeneration cycle of the biosorbent (Volesky, 1999).

The physiological state of the organisms, the age of the cells, the availability of micronutrients during their growth and the environmental conditions during the biosorption process (such as pH, temperature, and presence of certain co-ions) are important parameters that affect the performance of a living biosorbent. The effects of metal concentration on the efficiency of the biosorbent are also influenced by metal solution chemical features (Sala et al., 2002).

pH: Many researches have reported that hydrogen ion concentration, or pH, is the most important factor affecting heavy metal uptake by sludge particulates (Wang et al., 1999). The adsorption of metal on both organic and inorganic surfaces is influenced by pH (Nelson et al., 1981). It has been reported that pH can affect both the metal speciation through protonation of both the solid surface sites and the dissolved organic ligand as well as dissolution of organic matter from sludge particulates. Nelson et al. (1981) found that cadmium (II) and zinc (II) adsorption increased steadily from 15 to 20% at pH 4 to greater than 90% at pH 10. In contrast, copper (II) seemed to reach the maximum adsorption density in the pH range from 7 to 8, then decreased markedly at pH values greater than and less than 7 to 8.

The pH of the solution in which interactions between metal ions and organic material take place is an important factor in determining the association of metal ions with organic functional groups. Hydrogen ion will compete with other cations, including the metals, for binding sites on the sludge functional groups. As the pH of the solution is increased, resulting in an increase of free binding sites, the formation of metal-organic complexes may also increases. Changes in environmental pH can influence the uptake of metals in at least two ways: (i) by affecting the metal speciation and (ii) by its effect on the biological surface uptake sites (Campbell and Stokes, 1985).

Sludge age: It was shown that higher sludge age causes increase in biosorption. This behavior is consistent with the hypothesis that exocellular polymers are largely responsible

for uptake of metal ions by bacteria. The generation of exocellular polymers has been shown to depend on the growth phase of the bacteria, with slower growing or endogenous cultures exhibiting greatest production.

The effect of sludge age on biosorption is different for various metals. The sludge age parameter had no effect on mercury partition while a different behavior was observed for cadmium and nickel (Battistoni et al., 1993). The cadmium affinity decreased in older sludges. The similar observation was reported by Nelson et al. (1981) on 5-day-old activated sludges taken from a treatment plant. The nickel uptake, on the contrary, was increased with sludge age and showed a remarkable difference between 10 and 15 days. These experimental results show that different sludge sorption sites should be considered for the metal.

The amount of metal bound to the cell wall is found to be larger than that accounted for in terms of stoichiometric interaction between metal ion and active sites on the wall. To explain this situation a two-stage mechanism, substantiated by electron microscopic observations, was proposed: during the first stage the only metal ions taken up are those which become stoichiometrically bound to the active sites in the wall; afterwards (second stage) the metal ions bound to the cell wall act as nucleation sites for the deposition of others from solution, with the formation of aggregates, called crystalloids.

Biomass Concentration: Earlier experiments clearly indicated that the total amount of metal taken up by the sludge floc increased as the concentration of VSS increased (Cheng et al., 1975). Similarly, the uptake of metal increases with initial metal concentration at a constant biomass or biosorbent concentration (Cheng et al., 1975, Yetiş et al., 1998, Bux et al., 1999).

3.4.2. Bioaccumulation

Bioaccumulation is the second phase of the process of metal uptake by living microorganisms. It is dependent on metabolic energy, ATPase activity and the transmembrane proton gradient and is referred to as active absorption, as opposed to the passive physicochemical adsorption-retention assigned to biosorption. Passive adsorption

is rapid and independent of the presence of specific nutrients, whereas active absorption is slow and nutrient dependent.

Bioaccumulation of metals into a cell generally requires specific transport systems and depends on the tolerance of the organism to relatively high concentrations of "toxic" elements in the intracellular cytoplasm and other subcellular components, but may be dependent or independent of the cell's metabolism. In the latter case, those chemical or physical factors affecting biological reactions do not affect bioaccumulation. It was shown that metal cations can reach cytoplasm by utilizing the highly specific "micronutrient" transport systems evolved by microorganisms. In this respect, a distinction should be made between metabolically essential and non-metabolic metals. The former, including K, Fe, Mg and traces of Cu, Ni, utilize their specific transport systems. The non-metabolic metals (Co, Ni, Cu, Cd and Ag) primarily utilize the pathways existing for the uptake of metabolically essential metals. The extent of metal accumulation is generally much lower than that achieved by biosorption, ranging from 0.5 to 2.0 % of the organism's dry weight. In order to maintain the ionic balance in its cytoplasm, on uptake of a metal cation, the microorganisms must release cations of an equivalent charge: depending on the organism, these cations may be protons, magnesium or potassium.

Accumulation of trace metals onto organisms is most often described by the sum of several metal body burdens including the metal bound to the cell wall, the cell membrane, specific carrier proteins, and intracellular ligands. On the contrary, acute effects due to trace metals are generally best related to either the concentration of free metal ion in solution (basis of the free ion activity model, FIAM, as described in Section 3.5.1), or to the metal bound to sensitive (biologically active) sites at biological surface (basis of the Biotic Ligand Model, BLM, as described in Section 3.5.2). Both FIAM and BLM are based on the underlying hypotheses that metal internalization fluxes are a good indicator of metal toxicity and that the metal must cross or react with sensitive sites on the biological membrane to invoke a toxic effect. The differentiation between metals that has been internalized by the cell and that adsorbed indiscriminately to cell components is thus extremely relevant and necessary when relating biological effects to measurements of chemical speciation (Hassler et al., 2004a).

There are plenty of techniques available for distinguishing surface bound metal from intracellular metals such as cation exchange (Bowles et al., 2006), acid washes (Chu et al., 1997) and the use of complexing agents such as EDTA [$C_{10}H_{16}N_2O_6$] (Hu et al., 2003, Hassler et al., 2004b, Wilkinson et al, 2004) and citrate (Hu et al., 2003). Of the above techniques, EDTA extraction method appears to be the most widespread one (Hassler et al., 2004b).

3.5. Metal Speciation and Bioavailability

Metal ions exist in numerous forms in water. A bare metal ion cannot exist as a separate entity in water. In order to secure the highest stability of their outer electron shells, metal ions in water are bond to other species. These species may be water molecules or other species present in water. However, some other species in water bind much more strongly than water to metal ions. Complexation is a reaction whereby heavy metal ions replace one or more coordinated water molecules in the co-ordination sphere with other nucleophilic groups or *ligands*. The species that bind with the metal ion is called ligand, and the negatively, neutral or positively charged product in which the ligand is bound with the metal ion is called a complex or coordination compound (Morel, 1993).

Ligands that bond in one place to a metal ion and bonds in two or more places to a metal ion are called as unidendate ligands as multidentate ligands (or chelating agents), respectively. Some of the common examples of these ligands are CO_3^{-2}, NH_3, F^-, CN^-, $S_2O_3^{-2}$, ethylenediaminetetraacetic acid (EDTA) and sodium nitrilotriacetate (NTA) (Manahan, 1994, Saari et al., 1998)

Complexation reaction of dissolved metal ions with various ligands can be written as follows (Saari et al., 1998):

$$M^{n+} + L \Leftrightarrow (ML)^{n+} \tag{3.2}$$

where; M^{n+} = metal ion, L=ligand; and $(ML)^{n+}$ = metal complex

The equilibrium constant for this reaction is termed a stability or formation constant, K_f and expressed as follows (Saari et al., 1998):

$$K_f = \frac{[ML^{n+}]}{[M^{n+}][L]} \tag{3.3}$$

The greater the metal-ligand stability constant (K_f), the more stable the complex. In general, since a chelating agent may bond to a metal ion in more than one place simultaneously, chelates are more stable than complexes involving unidentate ligands. Thus, complexes of unidentate ligands are of relatively importance. Of considerably more importance are complexes with chelating agents (Manahan, 1994, Saari et al., 1998).

3.5.1. Metal Complexation by Strong (Anthropogenic) Chelating Agents

Natural water and wastewaters contain a variety of substances capable of forming complexes with the dissolved metal ions. These complexing agents can be either inorganic (e.g., Cl^-, CO_3^{-2}, S^{-2}, PO_4^{-3}, NH_3) or organic (e.g. amino acids, proteins, humic acids). Natural water sources contain the bulk of ligands that are mainly multidentate organic molecules. These are natural organic matter, including humic, tannic and fulvic acids (HA, TA, & FA). Moreover, NTA [$N(CH_2COO^-)_3$] and EDTA [$C_{10}H_{16}N_2O_6$] are the most observed and the most important synthetic ligands in domestic and industrial wastewaters (Alder et al., 1990). Metal complexation by strong artificial chelating agents such as EDTA (Figure 3.4) or NTA is probably the best studied topic in aquatic coordination chemistry, and the effects of these chelating agents in complex mixtures have been thoroughly analyzed.

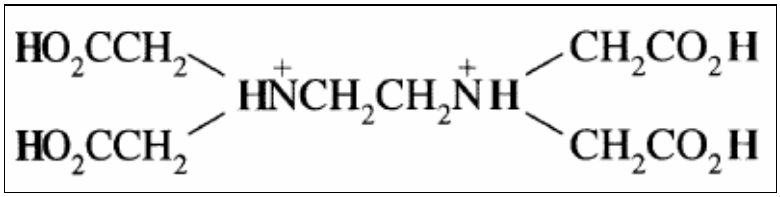

Figure 3.4. Chemical structure of EDTA

NTA is an alternative detergent builder to replace phosphates in combination with zeolite A and polycarboxylates. Sodium tripolyphosphate (STTP) was for a long time practically the only builder in laundry detergents. Because of its contribution to the eutrophication of the lakes and rivers, the use of phosphates in laundry detergents is banned in a lot of countries (Alder et al., 1990).

The synthetic complexing agent ethylenediaminetetraacetic acid (EDTA) is widely used in industrial, pharmaceutical, and agricultural applications. These include boiler-scale cleaning, leather tanning, textile dyeing, metal cleaning, separation of metals, and as an ingredient to stabilize soaps, germicides, herbicides, vegetable oils, beer, wine, carbonated beverages, milk, dressing and sauces and canned fish products (Gardiner, 1976). Due to its non-biodegradability (Alder et al., 1990) it is present in sewage effluents (Karia and Giger, 1996), fresh water and groundwaters (Gardiner, 1976). It has been detected in wastewater effluents at concentrations as high as 19 µM (Alder et al., 1990, Kari and Giger 1996, Nowack et al., 1996), while the concentrations of other chelating agents are typically at least an order of magnitude lower (Alder et al., 1990, Nowack et al., 1998) because they are used in smaller quantities and or partially or completely removed during wastewater (Alder et al., 1990). EDTA forms very stable complexes with heavy metals (Figure 3.5) and have therefore often been suspected to remobilize adsorbed or precipitated heavy metals from river sediments or aquifers (Gardiner, 1976, Alder et al., 1990, Morel, 1993).

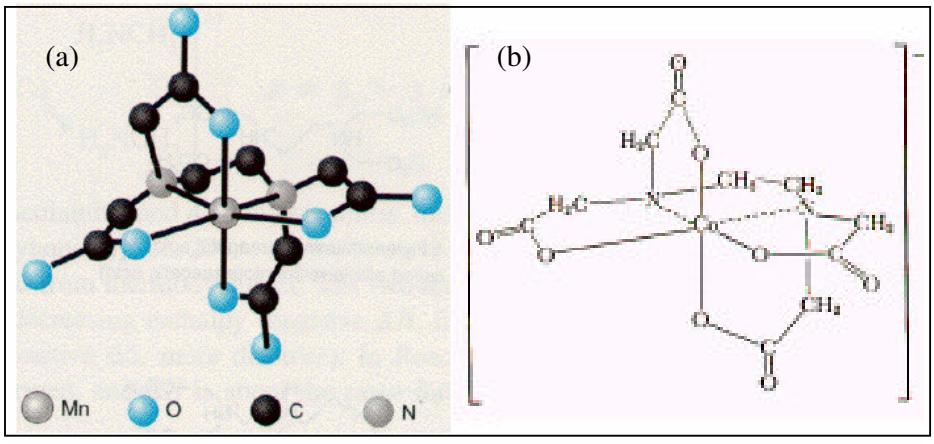

Figure 3.5. EDTA –Metal Complexes, (a) Mn-EDTA, (b) Co-EDTA

The resulting complexes with the organic and inorganic ligands can markedly alter the chemical form (speciation) of the metal in solution (Neubecker et al., 1983). When environmental chemists use the term "speciation" with reference to metals, they generally mean the distribution of the metal in question among various possible forms or "species". It is often useful to distinguish between the *physical* speciation of a metal, i.e. its distribution among dissolved, colloidal or particulate forms, and the *chemical* speciation of the metal. This latter term is generally taken to mean the distribution of the metal among various distinct chemical species in solution, and it includes both the distinction between "complexed" and "uncomplexed" metals (Figure 3.6) and the distinction between different oxidation states (Twiss et al., 2000).

Complexation of heavy metals by organic and inorganic ligands is important for two reasons. The first is that the biological availability and toxicity of heavy metals are dependent on the chemical form of the metal. It was observed that after addition of a strong complexing agent to an algal medium, growth was inhibited due to iron deficiency, and other studies have shown that solutions containing toxic metals are detoxified by the addition of natural and synthetic ligands (van Sprang et al., 2001, Hu et al., 2002).

The speciation of a metal is a critical factor to consider when assessing the metal's environmental impact. Physical, chemical and biological behaviors are all dependent on the chemical state of the metal in solution. For example, adsorption to sediments can be either reduced or enhanced depending on the existing complex. It has been reported that $PbCO_3$ is much more strongly bound to silica than Pb^{+2}. On the other hand, the formation of soluble chloro complexes may cause the release of mercury from sediments. Biological effects also strongly depend on speciation. The toxicity of several transition elements to microorganisms decreases as a result of complexation, indicating that the free metal ion is the toxic form. In other instances, growth of microorganisms was shown to decrease as a result of the complexation of essential nutrients (Neubecker et al.,1983).

Soluble metal complex formation competes with precipitation (Wang et al., 1999). Metals normally removed by hydroxide, carbonate or sulfite precipitation remain soluble if a strong complexing agent is present (Tünay et al., 1994). A metal that cannot be removed in primary treatment passes to the secondary treatment and adversely affects the biological

treatment systems. It was observed that when physicochemical methods were applied for heavy metal removal to leachates that contain high concentrations of ammonia, organic material, the removal was difficult due to metal complexes (Çeçen et al., 2000).

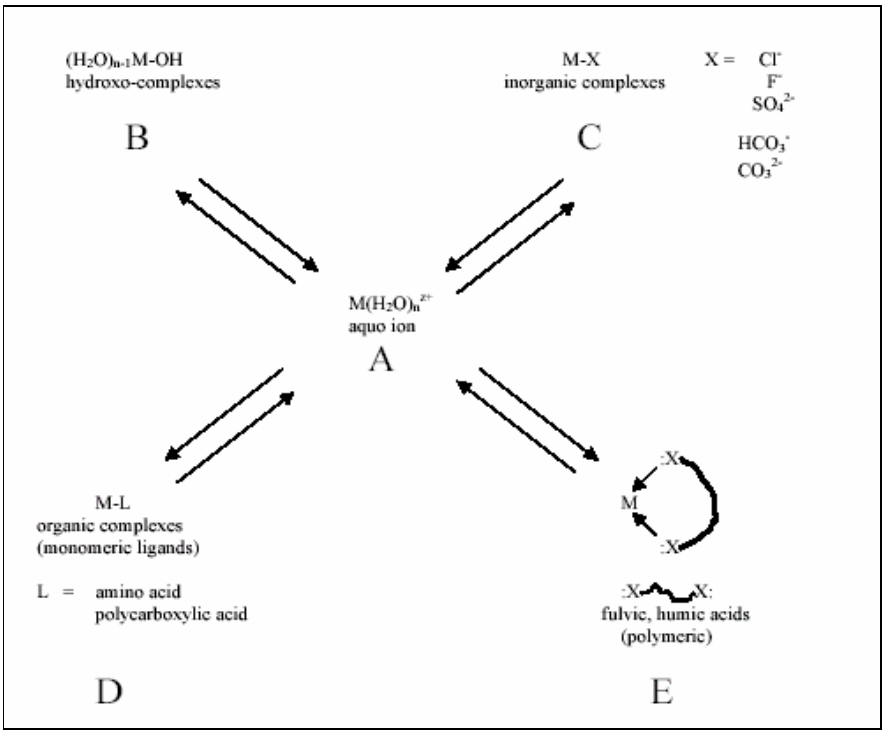

Figure 3.6. General scheme showing metal speciation in solution (adapted from Twiss et al., 2000)

Unlike organic chemicals, heavy metals are not biodegradable and can bioaccumulate to potentially inhibitory concentrations (Hu et al., 2002). The effects of heavy metals on biological treatment systems singly or in combination with others were investigated in several studies (Yetiş et al., 1989, Gökçay et al., 1991, Mazierski, 1995, Dilek et al., 1998). Toxicity of metals decreases when the organic loading is high due to the complexation of heavy metals with organic material. Also, addition of chelates to wastewater is a method to prevent metal inhibition in a biological system. (Tyagi, 1991, van Sprang et al., 2001, Hu et al., 2002).

Any complexing agent, which reduces the proportion of uncomplexed metal ion in a system, increases the solubility of the metal. Many authors have studied the effect of chelating agents, in particular NTA, on the extent of adsorption of trace metal ions onto naturally occurring solids.

The potential impact of synthetic chelating agents on sewage treatment plant and receiving waters has been given considerable attention recently in the context of the replacement of tripolyphosphate (TPP) by nitrilotriacetate (NTA) in household detergents (Gardiner, J., 1975, Woodiwiss et al., 1979, Stoveland et al., 1979).

The strong affinity of synthetic chelating agents for metal ions could lead to a reduction in the extent of removal of trace metals during sewage treatment, increased mobility of metals in water courses, modification of the toxicity of trace metals to fish and other aquatic organisms and interference in some analytical methods (Gardiner, 1976, van Sprang et al., 2001). The biological degradation of NTA was investigated in several studies (Stoveland et al., 1979, Alder et al., 1990). Unlike NTA, the degradation of EDTA was not observed in the biological step of a sewage treatment plant. Also, EDTA cannot be removed by bank filtration (Gardiner et al., 1990). The degradation of EDTA was not even expected in a nitrifying plant (Alder et al., 1990).

All of these studies regarding the heavy metal complexes were accomplished with heterotrophic bacteria. There are very few studies about the impact of metal-organic material complexation on nitrification systems (Hu et al., 2002). In recent studies, it was indicated that elevated dosages of EDTA itself impair nitrification (Hu et al., 2002).

3.5.2 Chemical Speciation and Toxicity

It is currently well accepted that in order to predict trace metal effects on aquatic organisms, it is necessary to take chemical speciation into account rather than to simply measure the total metal concentration. To quantitatively relate chemical speciation to biological effects, the metal bioavailability has been explained by simplified models such as the free ion activity model (FIAM) or more recently the biotic ligand model (BLM). Although the FIAM and BLM are based on the measurement of different fundamental

parameters, that is the activity of the free ion in solution for FIAM or the metal adsorbed to sensitive sites at the biological surface for BLM, they both are steady state models (Hassler et al., 2004a) with similar assumptions and similar conceptual framework. Indeed, in any attempt to relate bulk solution measurements to bioavailability, it is necessary to take into account;

- mass transport of the metal and metal complexes in the bulk solution
- complexation and dissociation reactions in the immediate vicinity of the organism and
- surface complexation to a cellular ligand (or carrier ligand), which can either lead to the internalization of the metal or trigger a biological reponse.

3.5.3. Free Ion Activity Model (FIAM)

The key assumptions of the FIAM have been given by Campbell (1995):

1. The cell membrane is the primary site for metal interactions with aquatic organisms
2. The interactions of a free surface site on the cell membrane, {R-cell}, with a metal, M^{n+}, can be described as a surface complexation reaction given by Eqn. 3.1.

The activity of the surface complex, {MR-cell}, can be calculated by using Eqn. 3.4:

$$\{M - R_{cell}\} = K\{R_{cell}\}[M] \tag{3.4}$$

where K is the adsorption constant or conditional stability constant (L/mol), {M-R_{cell}} is the activity of the surface complex (g/L) and [M] is the activity of the free metal ion (mg/L).

3. Rapid equilibrium is established between metal species in the aqueous medium and those at the cell membrane surface
4. Biological response whether it be expressed as uptake/accumulation and/or lethal (i.e. survival) or sub-lethal (e.g. behavior, growth or reproduction) toxicity, is directly proportional to the activity of the surface complex, M-R_{cell}. Therefore, BR can be derived from the following relationship:

$$BR=kK\{R_{cell}\}[M] \quad (3.5)$$

where k is constant of proportionality.

5. In the range of metal activities eliciting a BR, the activity of the free surface sites, $\{R_{cell}\}$, remains virtually constant and the activity of the surface complex, $M\text{-}R_{cell}$ is directly proportional to $[M^{n+}]$ in solution and
6. During the exposure to a metal, the nature of the cell membrane remains unchanged.

3.5.4. Biotic Ligand Model (BLM)

The key assumptions underlying the BLM have been outlined by Brown and Markich, 2000):

1. A surface binding site binds reversibly with a metal to form a surface complex (this is consistent with assumption (2) of the FIAM)
2. Biological response results from the equilibrium or steady-state occupation of surface binding sites, $\{R_{cell}\}$ (this is consistent with assumption (3) of the FIAM)
3. Biological response is directly proportional to the fraction of the total number of binding sites on the cell membrane, $\{R_{cell}\}_{T,}$ bound by the metal (i.e. $\{M\text{-}R_{cell}\}$) (this is similar to the assumptions (5) of the FIAM)
4. The maximum BR (BR_{max}) occurs when the total number of binding sites on the cell membrane, $\{R_{cell}\}_T$, are bound by the metal.
5. The activity of the metal bound to binding sites, $M\text{-}R_{cell}$, is small compared to the activity of the metal in the aqueous solution, [M].

Constants for the interaction of the metal with biological surface in BLM have been estimated by measuring metal internalization fluxes (bio-uptake), metal loading, and metal toxicity. Each determination provides a different measurement of the stability constants and each technique has its own advantages and disadvantages (Sloveykova and Wilkinson, 2005).

3.5.4.1. Metal Internalization Fluxes: Organisms are placed in contact with metal from the exposure medium and the quantity of accumulated metal is monitored as a function of time. Metal uptake rates (normalized for cell number or biomass) or fluxes (normalized for cell surface area) are determined from the slope of the plot of accumulated metal as a function of contact time. Internalized or cellular metal that has crossed a biological membrane may be distinguished from total metal burdens, often using chemical extraction techniques (given in detail Section 2.3.3). Metal internalization fluxes are determined and plotted against concentrations in the bulk solution against concentrations in the bulk solution over several orders of magnitude (Sloveykova and Wilkinson, 2005). The Michelis-Menten equation (Eqn. 2.4) is used to quantify the saturation flux and the half saturation constant of the metal, K_M.

$$J_{\text{int}} = J_{\max} \frac{[M]}{K_M + [M]} \tag{3.6}$$

where J_{int} is the metal internalization flux, mole/gMLSS.min (or mole /m^2.min), J_{max} is the maximum (or saturation) internalization flux mole /gMLSS.min (or mole /m^2.min) and K_m half-saturation constant of the metal (mole/L).

The major disadvantage of this approach is that it assumes that the biological effects are directly related to the rate of metal crossing the biological membrane (internalization flux), as opposed to the concentration of cellular metal (flux integrated over time) or some other internalized metal fraction. While this assumption is reasonable when predicting acute toxicity, it is less likely to be valid when evaluating chronic effects. Furthermore, the method is technically difficult in that it requires determinations of metal uptake fluxes over several orders of magnitude of dissolved metal, including saturating concentrations that would not normally be environmentally relevant (Sloveykova and Wilkinson, 2005).

3.5.4.2. Metal Loading Experiments: Total metal contents (both intracellular and extracellular, {M-R_{TOT}}) of unicellular organisms including algae and bacteria are often determined by bioaccumulation experiments or by whole cell titrations in which increasing concentrations of metal are added to cell suspensions. Data can be interpreted using

relatively simple treatment such as Langmuir adsorption isotherm (one site, eqn. 3.7), a Scatchard plot (multiple sites, eqn. 3.8) or by more complex treatments such as the Non-Ideal Competitive Adsorption (NICA)-Donnan approach that take into account both the polyelectrolytic and polyfunctional nature of the cell surface (Sloveykova and Wilkinson, 2005).

$$\{M-R_{TOT}\}=\{M-R_{TOT}\}_{\max}\frac{K_M[M]}{1+K_M[M]} \tag{3.7}$$

$$\frac{\{M-R_{TOT}\}}{[M]}=K_M\{M-R_{TOT}\}_{\max}-K_M\{M-R_{TOT}\} \tag{3.8}$$

Both graphical and numerical methods can be used to determine the concentration of total binding sites and the equilibrium constant, K_{NS}, corresponding to the formation of a cellular surface complex. In the Langmuir treatment, the reciprocal of adsorption density, $1/\{M\text{-}R_{TOT}\}$ is generally plotted as a function of the reciprocal (equilibrium) concentration of trace metal in solution to obtain the affinity constant and the total adsorption capacity. Similarly, (a Scatchard) plot of $\{M\text{-}R_{TOT}\}/[M]$ versus $\{M\text{-}R_{TOT}\}$ should yield a straight line with a slope equal to the conditional stability constant and intercept equal to the maximum binding capacity (Sloveykova and Wilkinson, 2005). Conditional stability constants and the number of binding sites for fish gills and metal were determined by Langmuir isotherm (Playle, 1998) or Scatchard analysis. Conditional adsorption constant (K_{NS}) and total site concentration (R_{TOT}) determined in this manner take into account both physiologically sensitive sites and the non-specific sites that are unlikely to participate in the internalization process (Sloveykova and Wilkinson, 2005).

3.5.4.3. Toxicological End Points and Competition Bioassays: The conceptual framework of the BLM assumes that there is a direct relationship between the degree of toxic effect and the proportion of sensitive sites that are filled with metal, f_{M-Rs}, such that the observed severity of the biological response will increase progressively as the sensitive sites on the organisms are filled. In such a case, a 50% effect could be expected for a metal concentration in solution corresponding to a 50% occupation of sensitive sites (f_{M-RS}^{50})(Sloveykova and Wilkinson, 2005).

3.6. Heavy Metal Toxicity in Activated Sludge Systems

Many municipal activated sludge plants receive combined wastewaters containing heavy metals. These metals typically include copper, zinc, nickel, cadmium and others that originate predominantly from industrial discharges. Historically, there has been little concern for the presence of these metals in the wastewater, as long as they were at sub-toxic levels. Increasingly stringent effluent regulations, together with recent indications of the detrimental effects of trace metal discharges on the receiving environment and biota, have resulted in a need to assess the interaction and removal efficiency of heavy metals within the activated sludge (Cheng, 1975, Savvides et al., 1995).

The discharge of toxic materials into wastewater treatment plants is of concern for a number of reasons. First, biological activity may be inhibited, resulting in lower treatment efficiencies. Second, toxicants may pass through treatment facilities into receiving waters, where they threaten aquatic life. Third, toxic materials removed from wastewater may concentrate in the sludge to the extent that benefits of land disposal are impaired (Codina, 1994). Finally, the presence of heavy metals in wastewater can adversely affect the operation of biological treatment processes, management, development and selection of alternatives for municipal wastewater treatment and ultimate solids disposal; and reuse and discharge of the effluent (Wang et al., 1999).

Both heterotrophic bacteria responsible for the oxidation of organic matter and nitrifying bacteria that use inorganic matter as a carbon source are adversely affected by heavy metals. As indicated in several studies, nitrifying bacteria, *Nitrosomonas* and *Nitrobacter,* are more susceptible to heavy metal toxicity than the bacteria primarily responsible for the oxidation of carbonaceous biological oxygen demand (Stoveland et al., 1979). Barth et al. (1963) conducted a study to find the effects of a mixture of heavy metals on sewage treatment processes and concluded that although a total concentration of 8.9 mg/L of four metals had no great effect on overall efficiency of a pilot scale activated sludge plant, the nitrification in such a plant was almost completely inhibited and nitrifying organisms did not acclimatize to the metals during the entire test period.

The toxicity of heavy metals in activated sludge systems has been studied in numerous works (Dilek and Yetiş, 1991, Zarnovsky et al., Mazierski, 1995, Madoni et al., 1996, Lee, 1997). Toxicity of heavy metals in biological systems was related to the factors such as type, concentration and the form of soluble metal (cation or complex), history of the activated sludge (acclimated or nonacclimated), operational parameters (pH), microorganism concentration, mean cell residence time and the presence of other compounds in wastewater (Tyagi et al., 1991, Zarnovsky et al., 1994). Since there are too many factors, differences may exist in published results. Due to the complexity of the process, more measurement is necessary in order to compare the results obtained by using different methods and generalize the heavy metal toxicity assessment procedure. Among the factors affecting heavy metal toxicity in activated sludge systems the most important ones are summarized in the following sections.

3.6.1. Mean Cell Residence Time (Sludge Age) and Acclimation

Research works at various mean cell residence times indicate that heavy metal toxicity decreases at longer mean cell residence times. Neufeld and Hermann (1975) demonstrated that it was possible to achieve satisfactory level of effluent quality by varying the mean cell residence time in activated sludge that has been previously acclimated to heavy metals. Zarnovsky et al. (1994) evaluated the effect of cadmium in non-acclimated and acclimated activated sludge samples in short and long term tests, respectively. Toxicity of 3 mg/L of Cd inhibited non-acclimated samples in an instantaneously increasing way with respect to the time of cadmium to biomass contact. For 3 mg/L of Cd, the percentage of maximum inhibition decreased as the sludge age increased. In their study, a continuous-flow completely mixed lab-scale reactor was also operated at sludge retention times (SRT) of 6.6, 10.0 and 16 days to examine the effect of sludge age on Cd toxicity to the acclimated sludge and to compare the behavior of Cd in non-acclimated and acclimated activated sludge systems. For the acclimation of the activated sludge to Cd, the synthetic wastewater containing 6 mg/L of Cd was introduced to the system for 60 days. The maximum time of inhibition ranged between 5 and 9 hours for non-acclimated sludge and between 2 and 5 hours in the case of acclimated sludge after the starts of the tests. Since acclimated sludge should biosorb a certain amount of Cd during acclimation, it took much less time to reach the threshold biosorbed Cd

concentration (saturation of sensitive sites with Cd) compared to the non-acclimated ones. This result also showed the importance of biosorbed metal concentration in explaining heavy metal toxicity.

In another study, Staisnakis et al. (2002) studied the effect of mean cell residence time and biomass acclimation to Cr(VI) on heterotrophic bacterial kinetics. Their results showed that the heterotrophic yield coefficient, Y_H, values obtained at various Cr(VI) concentrations appeared to be highly dependent on sludge age. A stimulating effect was observed by an increase in Y_H value at Cr(VI) concentration of 1 mg/L and a sludge age of 20 days only. At sludge age values of 5 and 10 days and Cr(VI) concentrations of 1 mg/L, calculated Y_H values were approximately equal to the values obtained in the control reactor (without Cr(VI)) addition. At a sludge age of 2.5 days, even 1 mg/L of Cr(VI) resulted in a significant Y_H decrease. In the same study, similar results were obtained for acclimatized biomass. The only difference was that the stimulating effect at a sludge age of 20 days was observed for both 1 and 10 mg/L. Further increase of Cr(VI) to 25 mg/L decreased the Y_H value below that of the control reactor.

On the basis of the works of Yetiş and Gökçay (1989) and Gökçay and Yetiş (1991), toxicity in an activated sludge, in terms of process performance, was strictly dependent on the mean cell residence time. The effect of sludge age can be attributed to the higher amount of extracellular polymers excreted by activated sludge at long sludge ages that tend to adsorb metals and consequently rendering them unavailable to bacteria.

A constant input level of heavy metal may not affect biological treatment performance. Acclimatized sludges maintain high removal efficiencies even if exposed to a high concentration of heavy metals such zinc, cadmium and mercury (Neufeld and Hermann, 1975). In contrast, shock loads manifest remarkable effects on activated sludge with major evidence for the non-acclimatized ones (Battistoni et al., 1993). Most of the studies conducted about heavy metal toxicity concentrate on non-acclimatized microorganisms and the fact that the microorganisms may be acclimatized to such metals has often been overlooked (Gökçay and Yetiş, 1991). Dilek and Yetiş (1991) reported that copper levels up to 10 mg/L had no inhibitory effects on the kinetic parameters of the continuous flow-nitrification process.

Resistance of biological treatment systems to metal toxicity may be greatly enhanced by proper acclimation. Acclimation usually involves the use of alternative pathways, which are not distrupted (or least distrupted to a lesser degree) by the presence of heavy metals. This process is, nevertheless, limited and the cell may not be able to further acclimation at relatively higher concentrations, resulting in complete containment of biological activity (Gikas and Romanos, 2006). During acclimation, either resistant organisms are selected and/or microbes are metabolically adapted to metal. In the case of metabolic adaptation, microorganisms are thought to synthesize new enzymes to substitute the metal-inactivated ones or create alternative shunt pathways (Yetiş and Gökçay, 1989).

3.6.2. Effective Concentration of Heavy Metals

There is a high variability in the effective concentration that cause 50% inhibition, EC_{50} or threshold heavy metal concentrations reported in literature. For example, Gerneay et al. (1997) and Hu et al. (2002), investigated the inhibitory effects of Cd on an enriched nitrifying sludge by specific oxygen uptake rate (SOUR) measurements. Although similar procedures were used for the determination of nitrification activity in both studies, the reported EC_{50} concentration was 8.30 mg/L in terms of total Cd in the study of the Gerneay et al., (1997) and 31.47 mg/L in terms of free Cd in the study of Hu et al. (2002).

In general, heavy metals are considered as toxic compounds that inhibit the growth of microorganisms, although their growth is often stimulated by the presence of trace amounts of selected metals (Gikas and Romanos, 2006). Gikas and Romanos (2006) found that Cr (VI) and Cr(III) stimulate activated sludge growth rates for concentrations up to about 25 and 15 mg/L, respectively. Gökçay and Yetiş (1991) also observed similar results for Cr(VI) in activated sludge system. They reported that Cr(VI) did not adversely affect the activated sludge kinetics and up to 25 mg/L Cr (VI) the bacterial activity was improved.

The concentration of metals necessary to inhibit biological systems varies with the stage of a culture and characteristics of microorganisms. Jönsson et al. (2001) conducted inhibition tests with activated sludge originating from different treatment plants and obtained different results for the same metal concentration. Sludges originated from

treatment plants that mainly received domestic wastewater, were more sensitive to inhibitors than sludges from treatment plants with a considerable industrial load from a variety of industrial branches. The difference in results was attributed to the adaptation of the sludge exposed to small amounts of a variety of toxic substances. It is very well known that activated sludge often exposed to small amounts of a variety of toxic substances may build up a general resistance (Nies, 1999, Spain, 2003).

Growth of *Nitrosomonas* inoculum was found to be completely inhibited at concentrations of nickel, chromium and copper as low as 0.25, 0.25 and 0.5 mg/L, respectively. Loveless and Painter (1968) reported that growth of inoculum in "crude" distilled water with copper concentrations of 0.05-0.08 mg/L and zinc concentrations of 0.05-0.1mg/L was completely inhibited.

Concentrations of the metals that can be tolerated by nitrifiers in activated sludge are much higher than those in pure cultures. Barth et al. (1963) reported that the aeration phase of a biological treatment could tolerate concentrations of up to 10 mg/L of chromium (Cr^{+3}), copper (Cu^{+2}), nickel (Ni^{+2}) or zinc (Zn^{+2}), either singly or in combination, with less than 5% loss in treatment efficiency. Moreover, they reported that the continuous dosage range of nickel that will not give significant reduction in treatment efficiency is 1.0-2.5 mg/L. Conversely, Yetiş and Gökçay (1989) indicated that a nickel concentration up to 10 mg/L and a chromium concentration up to 25.0 mg/L did not adversely affect the growth rate of microorganisms. Similarly, Lee (1997) studied the effects of copper and nickel on a pure nitrification culture and concluded that there was no visible inhibition on nitrification until the nickel and copper concentrations in the reactors were approximately 100 mg/L and 25 mg/L, respectively.

3.7. Review of the Studies on Effects of Heavy Metals in Nitrification Systems

There are several studies regarding the effects of heavy metals on activated sludge in biological systems. There are only a few studies on this area carried out with nitrifying bacteria. Brief information about the results of these studies is given below.

Lee (1997) studied the toxic responses of copper and nickel on an autotrophic culture of strict nitrifiers, *Nitrosomonas sp*. and *Nitrobacter sp.* They computed the concentrations of inorganic ligand ammonia and copper species using the MINTEQA2/PRODEFA2 (Allison et al., 1991) equilibrium model and found the relationships between chemical species and nitrification inhibition. They observed that *Nitrosomonas sp.* carrying out the first step of the nitrification process is more sensitive to copper and nickel than *Nitrobacter sp. c*arrying out the second step. In this study, it was concluded that of all the chemical species determined by MINTEQA2/PRODEFA2, $Cu(NH_3)_4^{+2}$ were probably those responsible for the inhibitory effects on ammonia oxidation. Similarly, the tetramine of nickel, $Ni(NH_3)_4^{+2}$, highly correlated with the percent inhibition of ammonia oxidation.

Bramm and Klapwijk (1981) studied the effects of free copper on nitrification in an activated sludge and showed that the effect of copper on nitrification depends on the concentration of mixed liquor suspended solids and pH. The concentration of total Cu has to be increased as the mixed liquor suspended solids increased to reach the same free copper concentration due to the complexation capacity of the sludge itself. Related to this result, as the mixed liquor suspended solids concentration increased, the required total copper concentration to attain the same degree of inhibition increased too. They found a linear relationship between the reduction in nitrification capacity and the adsorbed copper.

In the same study, it was also shown that the presence of strong complexing agents such as NTA and EDTA eliminated the toxic effect of copper. It was also shown that addition of NTA provided the recovery from inhibition. This result certainly showed that copper adsorbed to extracellular sites on the surface of the bacteria cell caused the reduction in nitrification capacity since only extracellular metal can be extracted with the addition of complexing agents (Hassler, 2004b). The time required to recover the nitrification capacity was found to be related to time elapsed between the addition of NTA

and addition of copper. This is evidence that kinetic rather than thermodynamic parameters might be responsible for the slow extraction of Cu from the cell wall of the bacteria.

In another study, Hu et al. (2002) investigated the effect of Cd and Ni on nitrification kinetics in an enriched nitrifying system in the presence and absence of complexing agents and SO_4^{2-}. Dissolved Cd and Ni concentration were measured with flame atomic absorption spectrophotometry. Free Cd and Ni concentrations were manipulated by varying the concentration of complexing agents while keeping total metal concentration constant or by varying the concentration of metal while keeping complexing agents concentration constant. Free Cd concentration was measured with ion selective electrode whereas the concentration of free Ni was calculated with MINEQL + (version 4.5). Exposure (or contact) time of metal to nitrifying bacteria was set at 15 minutes. Cd and Ni speciation were determined with the MINEQL + (Version 4.5) chemical equilibrium speciation algorithm. pH was adjusted to 7 with the MOPS buffer which is a special organic buffer that does not form complexes with metals (Hu et al., 2002, Twiss et al., 2001, Degryse et al., 2006) and also does not interfere with voltammetric measurements (Degryse et al., 2006). Conditional stability constants of Cd-biomass and Ni-biomass were estimated from metal partition experiments as $10^{1.1}$ (or 12.6 moles of Cd /moles of biomass) and $10^{1.4}$ (or 12.6 moles of Ni /moles of biomass).

In the same study (Hu et al., 2002), in the presence of complexing agents very poor correlations were obtained between the total Ni or Cd concentration and the inhibitory effect on ammonium oxidation. Total metal concentration was correlated to ammonium oxidation in the presence of the sulfate ion. Similar to the findings of Bramm and Klapwijk (1981), there was a strong correlation between free Cd and Ni concentrations and nitrification inhibition. Ni inhibition results were fitted to an empirical noncompetitive inhibition model and Cd inhibition results were fitted to a simple linear model. This study was the most recent one on the evaluation of the FIAM model in relation to bacterial activity. From another point of view, the reported EC_{50} values in this study are very far from the previously reported ones. The concentration of free metal cation causing 50% inhibition was estimated at 58.7 mg/L and 30.28 mg/L for Ni and Cd, respectively.

Studies demonstrated that short-term assays may not adequately reflect the response observed in continuous-flow reactors subject to prolonged toxic exposure (Hu et al., 2004). For the same metal concentration, a much higher inhibition could be observed in continuous-flow reactors for shock loadings.

Hu et al. (2004) demonstrated that the observed inhibition as a function of the free metal cation concentration was two (for Zn) to more than 10 times (for Cu) higher in the continuous-flow reactor than in a batch reactor. Even with the same activated sludge and inhibition measurement procedure, the results were very different. The discrepancy between the results was attributed to the slow internalization kinetics of metals. In this study, the contact time of metal with bacteria in short-term experiments was 40 minutes, whereas it was 35 days in continuous-flow experiments. In batch experiments, the reported degree of inhibition was less than 50% for free Cu and Ni concentrations of 1.91 and 29.35 mg/L, respectively. On the contrary, in continuous-flow experiments, they observed almost 90% inhibition for free Cu and Ni concentrations of 0.064 and 11.74 mg/L, respectively.

The results obtained from continuous-flow systems can be implemented in real systems such as in the determination of threshold concentrations and the design of biological reactors. Most importantly, the behavior of heavy metals under prolonged exposure times, acclimation, adaptation and shifts and changes in bacterial community changes can only be obtained with continuous-flow experiments.

Lee (1997) investigated the effect of Cu and Ni on enriched nitrifying bacteria in a continuous-flow reactor. They observed that 5 mg/L Cu suppressed nitrification partially and no further increase in toxicity was exhibited until copper concentration was increased to 25 mg/L which is dissimilar to the results of Hu et al. (2004). Their observations were similar in the case of nickel. There was no visible inhibition until the influent Ni concentration reached 150 mg/L. The observed inhibition at 150 mg/L was only 40% which is very low compared with literature data. 94% inhibition was observed at 250 mg/L which could be observed only in industrial wastewaters and leachates.

Under prolonged exposure periods, the nitrifying bacteria can acclimate to heavy metal by building up heavy metal resistance systems. As described in Section 2.3, heavy

metal resistance can be mediated by a series of systems like the permeability barrier, intra- and extra-cellular sequestration, active transport efflux pump, enzymatic detoxification and reduced sensitivity of cellular targest to metal ions. In certain situations, microbial community changes were observed and resulted in resistant bacteria dominates the systems (Principi et al., 2006, Moussa et al., 2006).

3.8. Voltammetric Measurement of Metal Speciation

Trace heavy metals are very important in the environment due to their toxicity although they are presenting at very low concentrations. They may accumulate at very low concentrations in food chain. The development of new methods is required and challenged for quantifying trace metals is required and challenged. Most of the sensitive and selective methods recently available such as ICP-MS, ICP-AES and GF-AAS are too expensive and are not practically applied in developing countries.

Voltammetry is a promising technique for the determination of trace metals. It is relatively low-cost but provides high sensitivity and can be used for the simultaneous determination of multi-elements (Jakumnee et al., 2001). It has been used in a lot of studies for metal speciation (Bott, 1995, Scoullos and Pavlidou, 2001, Rossiter et al., 2001).

Analytical chemists routinely use voltammetric techniques for the quantitative determination of a variety of dissolved inorganic and organic substances. Inorganic, physical, and biological chemists widely use voltammetric techniques for a variety of purposes, including fundamental studies of oxidation and reduction processes in various media, adsorption processes on surfaces, electron transfer and reaction mechanisms, kinetics of electron transfer processes, and transport, speciation, and thermodynamic properties of solvated species. Voltammetric methods are also applied to the determination of compounds of pharmaceutical interest and, when coupled with HPLC, they are effective tools for the analysis of complex mixtures (Settle, 1997).

Historically, the branch of electrochemistry, now called voltammetry, was developed from the discovery of polarography in 1922 by the Czech chemist Jaroslav Heyrovsky, for which he received the 1959 Nobel Prize in chemistry. The early voltammetric methods experienced a number of difficulties, making them less than ideal for routine analytical use. However, in the 1960s and 1970s significant advances were made in all areas of voltammetry (theory, methodology, and instrumentation), which enhanced the sensitivity and expanded the repertoire of analytical methods. The coincidence of these advances with the advent of low-cost operational amplifiers also facilitated the rapid commercial development of relatively inexpensive instrumentation.

General uses of voltammetric techniques are as follows (Settle, 1997):

- Quantitative determination of organic and inorganic compounds in aqueous and nonaqueous solutions
- Measurement of kinetic rates and constants
- Determination of adsorption processes on surfaces
- Determination of electron transfer and reaction mechanisms
- Determination of thermodynamic properties of solvated species
- Fundamental studies of oxidation and reduction processes in various media
- Determination of complexation and coordination values

and common applications are:

- Quantitative determination of pharmaceutical compounds
- Determination of metal ion concentrations in water to sub–parts-per-billion levels
- Determination of redox potentials
- Detection of eluted analytes in high-performance liquid chromatography (HPLC) and flow injection analysis
- Determination of number of electrons in redox reactions
- Kinetic studies of reactions

The common characteristic of all voltammetric techniques is that they involve the application of a potential (E) to an electrode and the monitoring of the resulting current (i) flowing through the electrochemical cell. In many cases the applied potential is varied or the current is monitored over a period of time (t). Thus, all voltammetric techniques can be described as some function of E, $I(A)$, and t. They are based on the current response of an analyte to an applied potential waveform (Figure 3.7). The magnitude of the peak current is proportional to the concentration of the analyte in solution (Bott, 1995, Thomas and Henze, 2001).

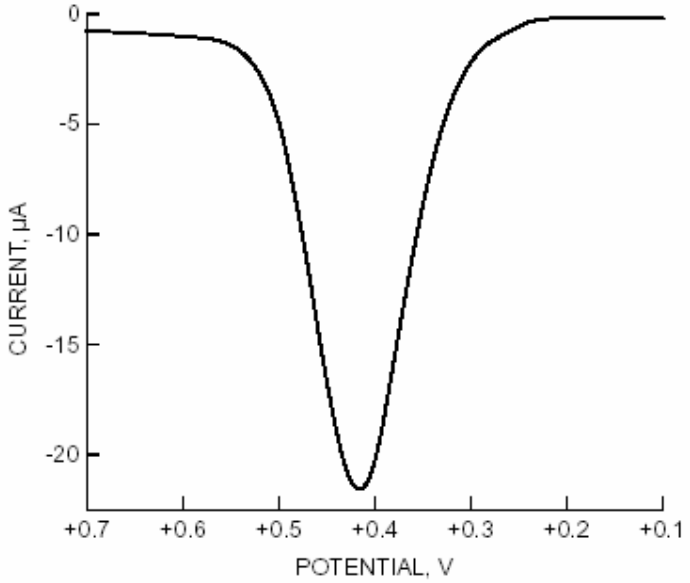

Figure 3.7. Typical current response for differential pulse voltammetry (adapted from Bott, 1995)

Voltammetry exhibits a wide dynamic range, from sub-ppb to ppm or higher. For the higher concentrations (ppm or high ppb), direct measurement by differential pulse voltammetry (DPS) or square-wave voltammetry is possible; for lower concentrations these voltammetric techniques are combined with a preconcentration step. These latter techniques are referred as stripping techniques. For many metal/metalloids ions (e.g., lead, cadmium, copper, zinc, antimony and bismuth), Anodic Stripping Voltammetry at a mercury electrode is used (Bott, 1995, Thomas and Henze, 2001).

Voltammetric measurement are considered active techniques (as opposed to passive techniques such as potentiometry) because the applied potential forces a change in the concentration of an electroactive species at the electrode surface by electrochemically reducing or oxidizing it. The analytical advantages of the various voltammetric techniques include excellent sensitivity with a very large useful linear concentration range for both inorganic and organic species (10^{-12} to 10^{-1} M), a large number of useful solvents and electrolytes, a wide range of temperatures, rapid analysis times (seconds), simultaneous determination of several analytes, the ability to determine kinetic and mechanistic parameters, a well-developed theory and thus the ability to reasonably estimate the values

of unknown parameters, and the ease with which different potential waveforms can be generated and small currents measured.

The electrochemical cell, where the voltammetric experiment is carried out, consists of a working (indicator) electrode, a reference electrode, and usually a counter (auxiliary) electrode. In general, an electrode provides the interface across which a charge can be transferred or its effects felt. Because the working electrode is where the reaction or transfer of interest is taking place, whenever we refer to the electrode, we always mean the working electrode. The reduction or oxidation of a substance at the surface of a working electrode, at the appropriate applied potential, results in the mass transport of new material to the electrode surface and the generation of a current. Even though the various types of voltammetric techniques may appear to be very different at first glance, their fundamental principles and applications derive from the same electrochemical theory (Thomas and Henze, 2001).

A variety of voltammetric techniques are available which are capable of measuring very small quantities of **uncomplexed metal ions** in solution:

- Pulse Polarogrophy (PP)
- Differential pulse polagrogphy (DPP)
- Anodic stripping voltammetry (ASV)
- Differential pulse anodic stripping voltammetry (DPASV)

For concentrations in the 10^{-7} to 10^{-4} mol/L range the test solution is usually analysed directly using differential pulse polagrophy (DPP) and a dropping mercury electrode (DME) or fast linear scan voltammetry with mercury or solid electrodes. For the lower concentrations, stripping techniques following electrolytic (i.e. ASV) or adsorptive accumulation at the electrode (usually mercury) are used.

These methods are attractive because of great sensitivity and specificity towards the free form of metal. The concentration of the metal detected by voltammetry is not necessarily equal to the total metal concentration of the sample but rather to the concentration of the labile (free) metal. Electrochemically labile metal is that fraction of

the total metal which is reducible at the electrode surface. This can include free (uncomplexed) metal as well as metal arising from weak complexes or complexes which can dissociate rapidly. By addition of acid or sample digestion, non-labile forms are rendered labile and total metal analyses can be obtained.

DP or Differential Pulse Voltammetry is the most universal and frequently used voltammetric measurement mode. It is equally well suited for irreversible and reversible systems and offers a high sensitivity. For DP voltammetry, rectangular pulses with a constant amplitude are superimposed on a stepwise rising direct voltage ramp. The current I (A) is measured as a function of the voltage U immediately before the pulse and at the end of the pulse. From the differences between the two current measurements, peak-shaped curves are obtained which are evaluated using linear, polynomial, horizontal or exponential baselines.

3.8.1. Application of Voltammetry in Environmental Analysis

One of the major applications of voltammetry in environmental analysis has been speciation studies (Florence, 1986, Scoullos and Pavlidou, 2001, Jakumnee et al., 2001). Speciation analysis is defined as the determination of the concentrations of different physicochemical forms of the element which make up its total concentration in the sample. Metals can exist in a range of physicochemical forms in environmental samples, including hydrated metal ions, inorganic and organic complexes, and adsorbed on organic and inorganic colloidal particles. The toxicity of a metal ion varies with its physicochemical form, and the predominant reason for speciation studies is to measure the “toxic” fraction of the metal. Typically, the most toxic forms are the hydrated metal ions and labile complexes (i.e., dissociation can readily occur), and the least toxic forms are strongly bound metal complexes and metal adsorbed on colloidal particles (indeed, in unpolluted natural waters, metals are usually present in one of these latter two forms). Metal complexes with very lipophilic organic ligands can also be highly toxic due to the ability of these complexes to cross cell membranes (Bott, 1995). The toxicity of some metal ions also varies with oxidation state. For example, As(V), Cr(III), Tl(III), and Sb(V) are nontoxic, whereas As(III), Cr(VI), Tl(I), and Sb(III) are toxic. However, these pairs of oxidation states can be distinguished electrochemically, since only one of each pair is

electrochemically active (Bott, 1995). The concentration of the electroinactive oxidation state can be calculated by measuring the total metal ion concentration following conversion of the electroinactive oxidation state to the electroactive oxidation state. For example, the concentration of Sb(III) can be determined in 0.2–0.5 M hydrochloric acid, and the total Sb concentration can be determined following reduction of Sb(V) to Sb(III). However, it is important to realize that it is generally impossible to measure the concentrations of individual species; for example, Cd^{2+}, $CdSO_4$, $CdCl^-$, and $CdCO_3$ cannot be distinguished by ASV. It is only possible to divide the species into groups based on gross behavioral differences (Bott, 1995). Furthermore, the distribution between the groups that is measured experimentally cannot be the same as that present in the original environment, since the measurement process (e.g., filtration, pH changes, the application of an electric field) alters the equilibria between the different forms of the species. The limitations apply not only to voltammetric techniques, but also to all techniques that are used for speciation studies. However, Florence (1986) has observed that the aim of speciation studies is not to provide a detailed species distribution, but rather to provide an estimation of the fraction of the metal present in a toxic form.

The simplest voltammetric speciation studies involve separation of the metal species into two groups—labile and inert. Labile species are species that can be detected by ASV, such as hydrated metal ions, and metal ions dissociated from weakly bound complexes or weakly adsorbed on colloidal particles. However, the composition of the labile fraction can vary with experimental conditions (e.g., pH, temperature, buffer composition, and the rate of stirring), and hence the exact conditions used must be specified (Bott, 1995). The inert fraction consists of the species that do not dissociate the metal under the conditions used. The total metal fraction can be measured following prolonged UV irradiation in an acidic medium (Thomas and Henze, 2001) (which promotes dissociation of the metal from all types of ligands and colloids), and hence the inert fraction can be calculated from the two experiments. It is assumed in this approach that metal complexes are not directly reduced during the deposition step; however, this assumption is not necessarily valid, particularly at very negative deposition potentials (Figura and McDuffie, 1979). The validity can be tested by using a range of deposition potentials, and plotting the anodic stripping current versus deposition potential (Bott, 1995). If only ionic metal is reduced, then the peak current increases from zero to a limiting value over a small potential range; however, if

metal complexes are directly reduced, the peak current increases continuously as the deposition potential is made more negative. In order to avoid the possibility of directly reducing metal complexes, it is recommended that the minimum deposition potential be measured for each metal (i.e., just sufficiently negative to give the maximum anodic stripping current) and that the metals be determined in separate experiments using the appropriate minimum deposition potential (Bott, 1995).

4. STATEMENT OF THE PROBLEM

Recent studies show that the bioavailability and toxicity of dissolved metals are strongly related to the free metal concentration rather than to the total (Hu et al., 2002, Bram and Klapwijk, 1981, Campell, 1995, Twiss et al., 2001, Lee, 1997, Hassler et al., 2004). Free Ion Activity Model (FIAM) was applied to correlate toxicity and free metal ion (Hu et al., 2002, Bram and Klapwijk, 1981, Ma et al., 2003). In certain situations, exceptions to Free Ion Activity Model (FIAM) can arise which were discussed in detail by Campbell (1995). Degryse et al. (2006) and Campbell et al. (2002) showed that metals in the form of hydrated ions, labile organic and weak inorganic ligands such as chloride, sulfate, carbonate etc. may also contribute to toxicity by dissociating into the free form. Hence, besides free metal ion, the influence of the labile metal concentration should also be considered when searching the relationship between metal speciation and biological response (uptake or toxicity). Similar to the FIAM, the Biotic Ligand Model (BLM) was developed to understand the relationship between metal adsorbed to sensitive sites at the biological surfaces and biological response (Hassler et al., 2004, Ma et al., 2003, Brown and Marrkich, 2000, Jansen et al., 2002). Much of the pioneering work on metal-organism interactions has been carried out with unicellular algae through the application of FIAM and BLM models alone or in combination.

In biotreatment systems, soluble or total metal concentrations are usually measured by atomic absorption spectroscopy (AAS) and chemical equilibrium models such as MINEQL 4.5 or WHAM are used for the determination of free metal ion concentration or metal speciation. On the other hand, in the application of the BLM model in metal-surface complexation, the conditional stability constant has to be determined for the calculation of biosorbed metal concentration. The use of labile metal concentration for the interpretation of inhibitory concentration could eliminate the necessities mentioned above.

In the first part of the study, the relationship between Cd and Zn speciation and nitrification inhibition was investigated by testing the applicability of FIAM and BLM models in batch systems. Based on these considerations, the objectives of the first part were as follows:

- to investigate the relationship between heavy metal speciation and nitrification inhibition. The labile metal concentration is suspected to be the inhibitory form and consists of free metal (M^{+2}) and metal in weak complexes. Therefore, voltammetry was employed to differentiate between the total and the labile metal. Cd and Zn was selected as the model heavy metals since these metals are susceptible to complexation and mostly found in municipal and industrial wastewater treatment plants. Cd and Zn speciation was adjusted with the use of the organic compound ethylenediamine tetraacetic acid (EDTA).
- to study the recovery from inhibition using EDTA as a washing agent
- to model inhibition in terms of free, labile and biosorbed forms of Cd.

Besides the above mentioned objectives, biosorption of Cd and Zn was investigated in nitrification systems. Conditional stability constants (Log K) and binding site concentrations were determined in the presence and absence of inorganic ligands such as HCO_3^-, CO_3^{2-} and the organic ligand EDTA. Determination of conditional stability constants is necessary for the theoretical determination of physical and chemical Cd and Zn speciation in biological systems.

Shock loads cause much higher inhibition in continuous-flow systems than in batch ones (Battistoni et al., 1993, Hu et al., 2004). On the other hand, a constant input of heavy metal may not affect biological treatment (Yetiş and Gökçay, 1989). Acclimatized sludges maintain their high removal capacities even if they are exposed to high concentrations of heavy metals such zinc, cadmium and mercury (Neufeld and Hermann, 1975). Resistance of biological treatment systems to metal toxicity may be greatly enhanced by proper acclimation. Acclimation usually involves the use of alternative pathways, which are not disrupted (or least disrupted to a lesser degree) by the presence of heavy metals. This process is, nevertheless, limited and the cell may not be able to further acclimation at relatively higher concentrations, resulting in complete containment of biological activity (Gikas and Romanos, 2006). During acclimation, either resistant organisms are selected and/or microbes are metabolically adapted to metal. In the case of metabolic adaptation, microorganisms are thought to synthesize new enzymes to substitute the metal-inactivated ones or create alternative shunt pathways (Yetiş and Gökçay, 1989). The inhibitory effects of metals in continuous flow systems were mostly investigated in activated sludge systems

containing both heterotrophic and autotrophic bacteria. There are only a few studies investigating the response of nitrifying bacteria to long-term heavy metal input. Futhermore, in these studies, it has not been clarified fully yet that the main reason of observing lower inhibitory levels in continuous-flow systems regarding to batch systems was due to selection of resistant organisms or metabolic adaptation of microorganisms to a specific metal. Therefore, in the second part of the study the influence of continuous Cd feeding on nitrification was investigated in a continuous flow nitrifying reactor and the followings are the objectives of the continuous-flow experiments;

- to evaluate the inhibitory effect of Cd on nitrification in continuous-flow experiments,
- to compare the inhibition pattern in batch and continuous flow regimes
- to observe recovery of cells that have been contacted with Cd for a long period of time and
- to investigate the microbial diversity in the biomass experiencing long term Cd introduction

The methodology to comply with the above mentioned objectives is summarized in Table 4.1.

Table 4.1. Methodology of the Study

PHASE I	PHASE II: BATCH EXPERIMENTS	PHASE III: CONTINUOUS-FLOW EXPERIMENTS	PHASE IV : MICROBIAL COMMUNITY ANALYSES
1. Sludge Maintenance & Growth	1. Suspended-growth batch experiments with Cd and Zn	Continuous-flow experiments in a nitrification system	• Monitoring and analysis of microbial diversity in the continuous-flow nitrification system in the absence and presence of Cd by ○ FISH ○ DGGE ○ SLOT-BLOT
• Start up of the main batch reactor for maintenance of enriched nitrifier culture • Batch experiments for biokinetic parameter estimation	• Short-term OUR experiments • Long-term OUR experiments • Batch experiments • Biosorption experiments • Speciation calculations • FIAM and BLM applications • Data evaluation	• Set-up and start-up for continuous flow nitrification system • Biokinetic parameter estimation in the absence of metals • Evaluation of effects of Cd in the continuous flow nitrification system • Data evaluation	
2. Metal Measurements with Voltammetry			• Data evaluation
• Method development for Cd, Zn and Cu			
3. Metal Speciation Calculations			
• Application of the chemical equilibrium programs MINEQL and Visual MINTEQA2			

5. MATERIALS AND METHODS

5.1. The Maintenance and Growth of the Enriched Nitrifying Sludge

The seed sludge enriched in terms nitrifiers was taken from another study (Alpaslan and Çeçen, 2005) and was cultured in a 16 L batch reactor operated on a fill-and-draw principle. This sludge has been used throughout the study. 1 L of the mixed liquor was removed directly from the tank to operate the system at a sludge age of 16 days. It was fed daily with an inorganic substrate mixture consisting ammonium sulfate $(NH_4)_2SO_4$ as an energy source, sodium bicarbonate ($NaHCO_3$) as an inorganic carbon source and macro- and micro nutrients necessary for nitrifying biomass. The composition of the stock feed solution is given in Table 5.1. Every day just before feeding, 8 L of the reactor volume was decanted after an approximate settling period of 30 minutes. The reactor feeding was performed daily by adding 200 mL mineral solution and 450 ml ammonia and alkalinity solution into the 16 L reactor from the their stock solutions.

The temperature of the reactor was kept around 25 ^oC with an aquarium heater. The pH of the bulk medium was around 8.3±0.5. The aeration of the reactor was performed by using three aquarium air stones connected to an air/vacuum pump (Millipore Corp.). The complete mixing conditions were also provided by these air stones which acted as diffusers of the reactor.

At the start-up period of the reactor, ammonium (NH_4^+-N), nitrite (NO_2^--N) and nitrate (NO_3^-- N) nitrogen ions were measured daily to monitor the performance of the main reactor (Table A.1, Figure A1-A4 Appendix A). Average values of MLSS and MLVSS measured after attainment of steady state were 818±42 and 764±23 mg/L, respectively. After attainment of steady-state, the temperature, pH, DO and MLVSS in the reactor was controlled regularly, to keep the sludge characteristics almost constant throughout the study.

Table 5.1. Composition of the synthetic stock solutions

Name of Chemicals	Stock Concentration g/L	Final Concentration in main batch reactor mg/L	mg/L	
$(NH_4)_2SO_4$	37.75	1416	300	as NH_4-N
$NaHCO_3$	95	3563	2121	as $CaCO_3$
Mg SO_4. $7H_20$	2	50.0	4.93	as Mg
$CaCO_3$	0.103	2.58	1.03	as Ca
$FeSO_4.7H_2O$	0.4	10.00	2.01	as Fe
$MnSO_4.H_2O$	0.2	5.00	1.62	as Mn
K_2HPO_4	0.325	8.13	3.65	as K
			1.44	as P

5.2. Estimation of Biokinetic Parameters in the Absence of Metals

The biokinetic parameters, maximum specific ammonium utilization rate ($q_{max,NH4-N}$) and half-saturation constant ($K_{s,NH4-N}$) of nitrifying culture were determined only for the ammonium oxidation step of the nitrification process. Several batch experiments were conducted at an initial NH_4-N concentration of 5, 10, 25, 50, 60, 70, 85, 100, 200 mg/L. At least three measurements were done for the same initial NH_4-N concentration to check the validity of results and repeatability of the measurements.

Before starting the experiments, 500 mL the mixed liquor from stock nitrifying culture was rinsed twice to remove remaining ammonia and nitrite ions and diluted to 1000 mL that resulted MLVSS concentration of 350±50 mg/L. In a following step, sludge was fed with a predetermined volume of synthetic feed solution and mineral solution from their stock solutions (Table 5.1) to obtain desired initial NH_4-N concentration in the range of 5-200 mg/L. All experiments were conducted at a constant temperature of 25^0C by using a water bath. Samples were aerated by means of porous aquarium diffusers located at the bottom of the vessels to provide a dissolved oxygen concentration approximately 9 mg/L and also to maintain complete mixing conditions. The pH was kept at 7.5±0.2 by using phosphate buffer consisting of 8.67 mM of $H_2PO_4^-$ and 34.67 mM of HPO_4^{-2} ions.

NH_4-N concentration was measured in the supernatant at the beginning and at certain time intervals. Experiments with high initial NH_4-N concentrations lasted at least 2 hours whereas measurements with initial NH_4-N concentrations of less than 25 mg/L continued until a bulk NH_4-N of less than 1 mg/L. MLVSS concentrations were measured in duplicate at the beginning and end of the experiments. Ammonium utilization rates were determined from the slope of the NH_4-N concentration versus time plots (Appendix B-Figure B1-B4) by linear regression analysis. Specific ammonium utilization rates were calculated by dividing ammonium utilization rate to MLVSS concentration.

5.3. Batch Experiments with Cadmium (Cd), Zinc (Zn), Copper (Cu)

5.3.1. Preliminary Oxygen Uptake Rate (OUR) Experiments for the Determination of the Inhibition Range

The objective of Oxygen Uptake Rate (OUR) experiments was to assess the inhibitory effects of cadmium (Cd), zinc (Zn) and copper (Cu) on the nitrifying biomass by measuring the oxygen consumption during nitrification.

The effects of Cd, Zn and Cu on nitrifying biomass were investigated for each step of the nitrification by adding the ammonium or nitrite as an initial substrate in OUR experiments. Initial ammonium and nitrite ion concentrations in OUR experiments were chosen as 50 mg/L to provide unlimited substrate conditions. Before starting with OUR experiments, biomass was washed twice to remove the remaining ammonia and nitrite ions.

The DO concentrations were recorded at 15 s intervals and lasted approximately 10 minutes. The level of DO affects OUR when its concentration was less than 4 mg/L (EPA, 1983). Therefore, the recording phase was stopped when the bulk DO concentration of the closed bottle was less than 4 mg/L to provide oxygen unlimited conditions. The VSS concentrations were measured at twice at the end of each test. The SOUR value of the biomass was calculated for each set of experiment using the following formula;

$$SOUR = \frac{OUR}{MLVSS} \tag{5.1}$$

The biomass suspensions were aerated with pure oxygen gas before the predetermined volume of the substrate (NH_4^+-N or NO_2^-- N) was added from their stock solutions. The pH of the assay was maintained at a final pH of 7.5±0.2 during the test using the phosphate buffer (Section 5.2). The experimental work was carried out in a capped glass bottle with 300 mL working volume, which was filled with the sludge and the synthetic feed solution. The temperature of the bottle was kept constant at 25^0C. Complete mixing of the reactor content was provided by a magnetic stirrer. The dissolved oxygen probe was inserted into the bottle and the DO concentrations were recorded at 15 s intervals for 10 minutes at each Cd concentration. The recording was started as soon as the metal solution was added into the reactor. The oxygen uptake rate was measured from the slope of the oxygen versus time curve. The MLVSS concentrations were determined at the same time to calculate the specific OUR. Then, the inhibition at each metal concentration was calculated. The experimental set- up for the oxygen uptake rate experiments according to the first method is given in Figure 5.1. In these experiments, the initial Cd, Zn and Cu concentrations varied between 5-150 mg/L, 2.5-150 mg/L and 5-150 mg/L, respectively.

Figure 5.1. Experimental set-up for short-term oxygen uptake rate (OUR) (1^{st} method) experiments

5.3.2. Influence of Cd and Zn speciation on nitrification inhibition

The influence of Cd and Zn speciation on nitrification was evaluated with simultaneous NH_4-N, OUR and Cd or Zn measurements. The effects of chemical Cd and Zn speciation on nitrification were investigated in the presence and absence of the organic complexing agent, EDTA. In some experiments, the concentration of free Cd or Zn was manipulated at constant analytical Cd or Zn concentrations by varying the concentration of EDTA or at a constant concentration of EDTA by varying the total Cd or Zn concentrations. The metal measurements during the experimental period allowed the differentiation of the effects of chemical and physical metal speciation. The operational conditions in experiments with Cd and Zn are given in Table 5.2 and 5.3, respectively.

Table 5.2. Conditions in Experiments with Cd

Experiment No	MLVSS mg/L	Initial Cd mg/L	EDTA M	pH
1	260	-	-	7.3
2	390	-	-	7.4
3	420	-	-	7.5
4	588	-	-	7.5
5	207	-	-	7.6
6	210	-	-	7.7
7	382	-	$1x10^{-5}$	7.7
8	340	-	$2x10^{-5}$	7.7
7	303	1	-	7.2
8	300	1	-	7.4
9	266	2	-	7.4
10	293	2.5	-	7.7
11	278	5	-	7.4
12	473	5	-	7.5
13	387	5	-	7.4
14	350	5	-	7.7
15	496	5	$1x10^{-4}$	7.3
16	560	10	-	7.3
17	465	10	$1x10^{-4}$	7.3
18	498	15	-	7.5
19	250	15	-	7.7
20	220	15	$1x10^{-4}$	7.6
21	350	15	$8x10^{-5}$	7.7
22	370	15	$1.2x10^{-4}$	7.5
23	360	20	-	7.3
24	407	25	-	7.4

Table 5.3. Conditions in Experiments with Zn

Experiment No	MLVSS mg/L	Initial Zn mg/L	EDTA M	pH
1	390	-	-	7.4
2	240	1	$2x10^{-5}$	7.7
3	240	2	$2x10^{-5}$	7.5
4	232	2.5		7.5
5	410	2.5	-	7.5
6	316	2.5	$2x10^{-5}$	7.7
7	256	5	-	7.6
8	373	5	-	7.6
9	316	5	$2x10^{-5}$	7.6
10	240	6	$2x10^{-5}$	7.7
11	267	10	-	7.5
12	423	12	$2x10^{-5}$	7.5
13	257	25	-	7.5

5.3.2.1 Procedure in Specific Ammonium Utilization Rate Experiments. A sample of mixed liquor was put into l000 mL glass bottles from the stock nitrifying biomass and was contacted with metal. A supplementary sample of mixed liquor without metal was set up as control. The temperatures of samples were kept at 25^0C. Samples were aerated and thus completely mixed by means of porous aquarium diffusers located at the bottom of the reactors. The pH of the activated sludge samples was set to 7.5±0.2 by adding of 100 mL MOPS [(3-(N-morpholino)propanesulfonic acid] buffer which does not form metal complexes and also does not interfere in voltammetry (Campbell, 1995). Also 15 mL $NaHCO_3$ from their stock solution was added to 1000 mL batch reactors. This yielded a final concentration of 0.02 M MOPS and 0.015 M $NaHCO_3$. Before addition of metal and ammonium nitrogen, reactor contents were aerated approximately for 5 minutes to allow pH to rise to 7.5. As a final step ammonium and the relevant metal were simultaneously added to the reactor.

NH_4-N and metal concentrations were measured in samples filtered through 0.45 μm syringe filters (Milipore Corp.) at the beginning and specified time intervals over a period of 2-4 hours. Ammonium utilization rates were determined from the slope of the concentration versus time plots for each metal concentration. VSS concentrations were measured in duplicate at the end of the tests for the calculation of specific ammonium utilization (q_{NH4-N}) and specific oxygen uptake rates (SOUR).

5.3.2.2. Procedure of Long-Term Oxygen Uptake Rate Experiments. A portion of the mixed liquor taken from the parent bottle was put into 100 mL capped glass vessel at certain time intervals. The temperature of the vessel was kept constant at 25^0C. Complete mixing of the reactor was provided by a magnetic stirrer. A decrease in DO in the vessel due to the substrate oxidation and temperature of the solution was measured by a DO probe and continuously recorded for 5 s intervals by a personal computer interfaced to the DO meter (WTW Oxi 730).

Inhibition was quantified in terms of the reduction in $q_{NH4\text{-}N}$ and SOUR of biomass with respect to the control reactor using the following formula;

$$i(\%) = \frac{rate_{control} - rate_{metal}}{rate_{control}} \text{ x } 100 = (1 - \frac{rate_{metal}}{rate_{control}}) \text{ x} 100 \qquad (5.2)$$

Schematic view of the experimental set up is given in Figure 5.2. The results of these experiments are shown in Figures D1-D10 in Appendix D.

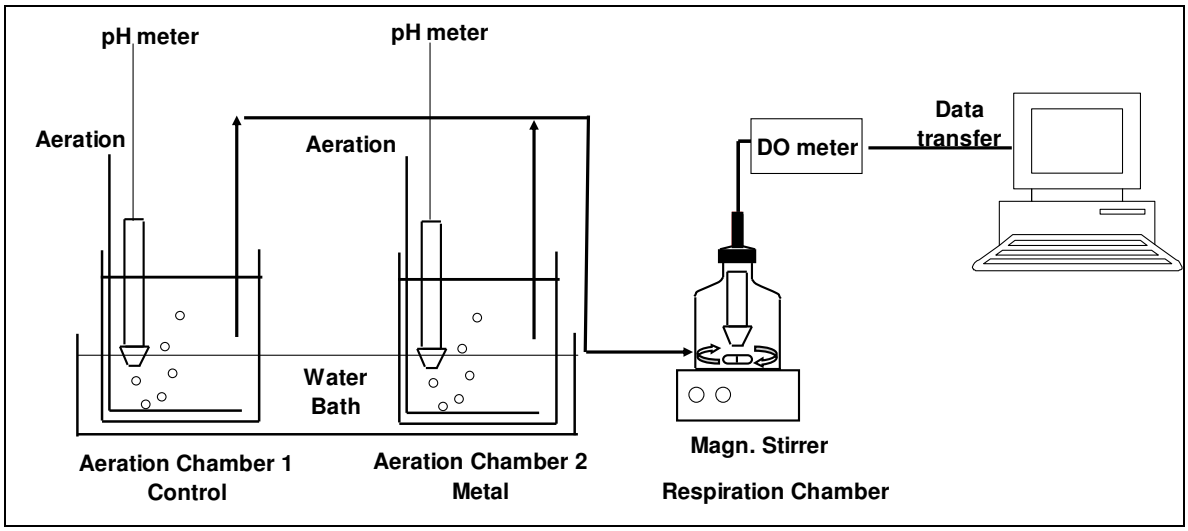

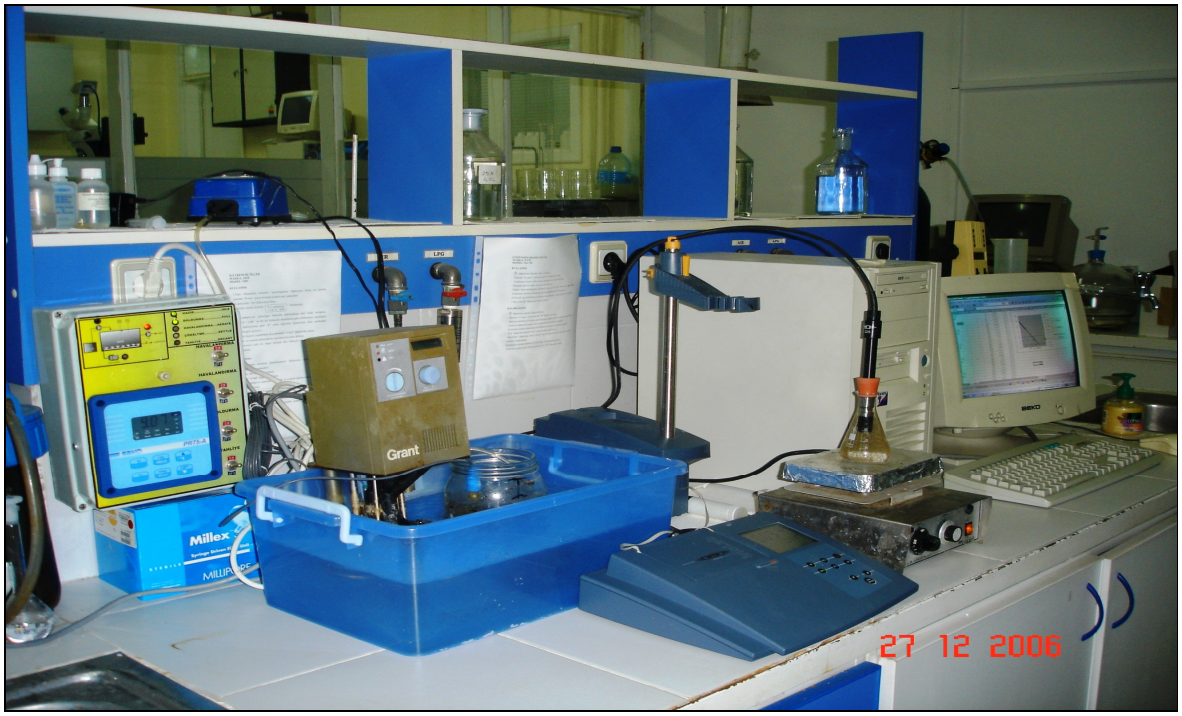

Figure 5.2. Experimental set-up for the simultaneous measurement of q_{NH_4-N} and SOUR

5.3.3. Chemical Speciation Calculations

Cd and Zn speciation calculations were performed by using the MINEQL + (Version 4.5) chemical equilibrium program, from Environmental Research Software. The program was developed to solve mass balance expressions using equilibrium constants (Schecher and McAvoy, 1994). The ionic strength correction was based on Davies Equation. Stability constants were updated using the stability constant database given in MINTEQA2/PRODEFA2 User Manual Supplement for Version 4.0 (Hydrogeologic, Inc. and Allison Geoscience Consultants, Inc.). All speciation calculations were performed for 25^0C. The list of stability constants used in Cd and Zn speciation calculations is given in Table 5.4. Distribution of Cd and Zn in the soluble and suspended phases was calculated with the incorporation of conditional stability constants for metal-biomass species and binding site concentration (complexation capacity) of biomass. The details for determination of conditional stability constants and complexation capacities are given in Section 5.3.5.

Table 5.4. Thermodynamic Stability Constants Used in Speciation Calculations

Species Name	Log K	Species Name	Log K
Cd Species		**Zn Species**	
$Cd(OH)_3^-$	-32.505	$Zn(OH)_3^-$	-28.091
$Cd(OH)_4^{2-}$	-47.288	$Zn(OH)_4^{2-}$	-40.488
$CdOH^+$	-10.097	$ZnOH^+$	-8.997
$Cd(OH)_{2aq}$	-20.294	$Zn(OH)_{2(aq)}$	-17.7940
Cd_2OH^{3+}	-9.397	$ZnHCO_3^+$	11.8290
$CdHCO_3^+$	10.686	$Zn(SO_4)_2^{2-}$	3.28
$CdCO_3(aq)$	4.3578	$ZnSO_{4(aq)}$	2.34
$CdSO_4^{2-}$	3.50	ZnEDTA	18.00
$CdSO_4(aq)$	2.37	ZnHEDTA	21.40
CdEDTA	18.20	ZnNTA	11.95
CdHEDTA	21.50	ZnNTA2	14.88
CdNTA	11.07	$Zn(CO_3)aq$	4.76
CdNTA2	15.03		

Table 5.4 (Continued)

Other species			
Species Name	Log K	Species Name	Log K
$CaNTA^{3-}$	7.608	$CaHPO_{4(aq)}$	15.035
$CaOH^{+}$	-12.697	$CaHEDTA^{4-}$	15.90
$FeOH_3$	-28.991	$CaHCO_3^{+}$	11.599
$FeOH_{2(aq)}$	-20.494	$KHPO_4^{-}$	13.255
$FeOH^{+}$	-9.397	$MgHPO_{4(aq)}$	15.1750
$FeOHNTA^{3-}$	13.23	MgHEDTA	14.97
$MgOH^{+}$	-11.397	$MnHEDTA^{4-}$	19.10
$MnOH^{+}$	-10.597	$NH_3(aq)$	-9.244
$Mn(OH)_3^{-}$	-34.80	$H_2PO_4^{2-}$	19.573
$H_2CO_{3(aq)}$	16.681	HPO_4^{2-}	12.375
HCO_3^{-}	10.3290	H_3PO_4	21.7210
$MgHCO_3^{-}$	11.339	HSO_4^{-}	1.99
$MnHCO_3^{+}$	11.6290	EDTAH	10.948
$NaHCO_{3(aq)}$	10.079	EDTAH2	17.221
$FeH_2PO_4^{2-}$	22.273	EDTAH4	22.50
$FeHEDTA^{4-}$	19.06	EDTAH5	24.00
$NH_4SO_4^{-}$	1.03	NTAH	10.278
$MgCO_3(aq)$	2.92	NTAH2	13.22
$NaCO_3^{-}$	1.270	NTAH3	15.22
$FeSO_{4(aq)}$	2.39	NTAH4	16.22
FeNTA	10.19	$CaCO_{3(aq)}$	3.20
KSO_4^{-}	0.85	$CaEDTA^{4-}$	12.42
$MgSO_{4(aq)}$	2.26	MgNTA	6.5
MgEDTA	10.57	$MnSO_{4(aq)}$	2.25
MnEDTA	15.60	MnNTA	8.573

5.4. Biosorption Experiments

In this study, Cd and Zn solutions were prepared by using $3CdSO_4.8H_2O$ and $ZnSO_4.7H_2O$, respectively in all experiments.

Uptake of Cd or Zn onto biomass was studied under the following conditions:

1. Biosorption of Cd or Zn onto sludge in test mediums consisting of Cd or Zn and SO_4^{-2} for an initial metal range of 1-100 mg/L.
2. As it is known that the presence of the inorganic complexing ions such as as HCO_3^-, CO_3^{-2}, SO_4^{-2} could change the Cd or Zn speciation. Furthermore, the BLM model takes competing ions such as Mg^{2+}, Na^+, Ca^{2+} into account implicitly. Therefore, biosorption of Cd or Zn onto sludge was also followed in ammonium utilization rate (q_{NH4-N}) experiments to investigate the influence of anions and cations on Cd and Zn biosorption.

5.4.1. Sorption Kinetics and Equilibrium Studies

In order to determine the contact time required for equilibrium, dynamic biosorption experiments were conducted first. Uptake of Cd and Zn onto biomass was studied in 1000 mL glass vessels placed into a water bath (Grant type) to maintain a constant temperature of 25^0C. Since most of the thermodynamic constants are available for 25^0C, all experiments were conducted at this temperature. In accordance with batch runs in ammonium utilization rate experiments, 300 mg/L mixed liquor suspended solids was contacted with $8.92x10^{-3}$ -1.34 mM Cd (1-150 mg/L) and 0.015 -2.29 mM Zn (1-150 mg/L). Again mixing was done by air and metal measurements were carried out for 24 hours. The pH varied in the range of 7-7.2. Sampling was more frequent at the beginning of each experiment. After settlement of sludge, the metal in the supernatant was measured by voltammetry. The metal uptake onto and/or into sludge was calculated as follows:

$$q = \frac{(C_o - C_t)xV}{M} \tag{5.3}$$

where, q is the metal uptake (mg metal/g biomass), C_o and C_t are initial and final metal ion concentrations (mg/L), respectively, M is the dry mass of biomass and V is the volume of the solution. In terms of metal, equilibrium in the bulk medium was reached in 30 min. At each equilibrium metal concentration, q was determined and an isotherm was generated.

5.4.2. Determination of Conditional Stability Constants and Complexation Capacities in Cd and Zn Binding to Bacterial Sites

Different methodologies exist to determine the conditional stability constant and concentrations of binding site ([X-cell]), such as measurement of metal internalization fluxes, metal loading and metal toxicity (Slaveykova et al., 2005, MINEQL Manual (1998), Nelson et al., 1981). In this study, the metal loading approach was followed using the Langmuir adsorption isotherm.

The interaction of a free surface site on the cell membrane, {-X-cell}, with a metal M^{Z+}, can be described as a surface complexation reaction (Brown et. al., 2000, Nelson et al., 1981)

$$[M]+\{X-cell\}\xleftrightarrow{K}\{\ M-X-cell\ \} \tag{5.4}$$

$$K=\frac{M-X-cell}{\{X-cell\ \}[M]} \tag{5.5}$$

where, K is the equilibrium constant or the conditional stability constant for binding of the metal to sensitive sites at the cell surface, M is the free metal species (mg/L), X-cell is the unoccupied bacterial surface site (sensitive site) (g/L), M-X-cell is the activity of the metal-bacterial surface complex (g/L).

A mass balance can be written for a given bacterial surface in which the total mass, X-cell, is equal to the sum of unoccupied and occupied (complexed) sites by metal ion:

$$\{\text{X-cell}\}_T=\{M-X-cell\ \}+\{\ X-cell\ \}/\ y \tag{5.6}$$

where, X-cell$_T$ is the total bacterial (surface) mass (g/L) and y is the number of surface sites per unit mass of bacteria (moles/g). The Langmuir isotherm can be derived by substitution of Eqn. 5.6 into Eqn. 5.4. With some rearrangement, an explicit equation for {M-X-cell} can be obtained:

$$\frac{\{M-X-cell\ \}}{\{X-cell\}_T} = \frac{y[M]}{y/K_p + [M]} \tag{5.7}$$

The standard form of the Langmuir isotherm is as follows:

$$q = \frac{q_{\max}[M]}{K_L + [M]} \tag{5.8}$$

where, q is the adsorption density of free metal species (moles/g), q_{max} is the maximum adsorption density of free metal species, (moles/g), [M] is the equilibrium solution concentration of free metal species (moles/L), and K_L is the Langmuir adsorption constant (moles/L).

Equations 5.7 and 5.8 are analog to each other and the following relations can be found:

$$q = \{M\text{-}X\text{-}cell\}/\{X\text{-}cell\}_T \tag{5.9}$$

$$y = q_{max} \tag{5.10}$$

$$y/K_p = K_L \tag{5.11}$$

The Langmuir adsorption constant, K_L is related to the conditional stability constant K in Eq.5.8 and is used in the MINEQL model. This K_L is proportional to the reciprocal of the partition coefficient, K_p. Both K_p and y can be calculated using Equations 5.10 and 5.11 if a Langmuir type isotherm can be derived from adsorption experiments. Alternatively, if adsorption is linear with respect to the metal concentration, then the slope is equal to K_p.

5.5. Experiments in a Continuous-Flow Nitrifying Reactor

The continuous-flow experiments in the absence and presence of Cd were performed in a completely mixed suspended growth reactor shown schematically in Figure 5.3. Cd was the metal of choice in continuous-flow experiments since inhibition was observed at much lower concentrations compared to Zn (Section 6.2.7 and 6.4.4). The detailed technical information about the continuous flow system is given in Table 5.5. The reactor was operated for 480 days.

A completely mixed 20 L aeration tank was connected by a plastic tube to a 10 L settling tank. The reactor was operated at a sludge retention time (SRT) of 20 days and hydraulic retention time (HRT) of 1.0 day. 1 L of the mixed liquor was daily removed from the aeration tank. A temporized peristaltic pump was utilized to recycle the settled sludge at a flowrate of 10 L/day. Biomass adhered to the walls of the clarifier was manually scraped. Treated water was daily collected into a 20 L effluent tank. The reactor was aerated and completely mixed by 2 circular aquarium air stone diffusers which are connected to an air pump (Millipore Inc.). Since the activity of nitrifying bacteria is considerably influenced by environmental conditions, the temperature, pH, and DO parameters were constantly controlled. The pH of the reactor was controlled by a pH control unit. 1 M sodium bicarbonate ($NaHCO_3$) and 0.5 M hydrochloride acid (HCl) solutions were automatically added to the aeration tank to maintain the reactor pH at 7.5 ±0.2 and to supply the required inorganic carbon. The temperature within the activated sludge unit was maintained constant at 25º C by the aquarium heater. DO levels was kept around 6-7 mg/L and complete mixing inside the reactor was provided by aeration. Treated water from secondary clarifier was collected in a 20 L bottle to have composite samples.

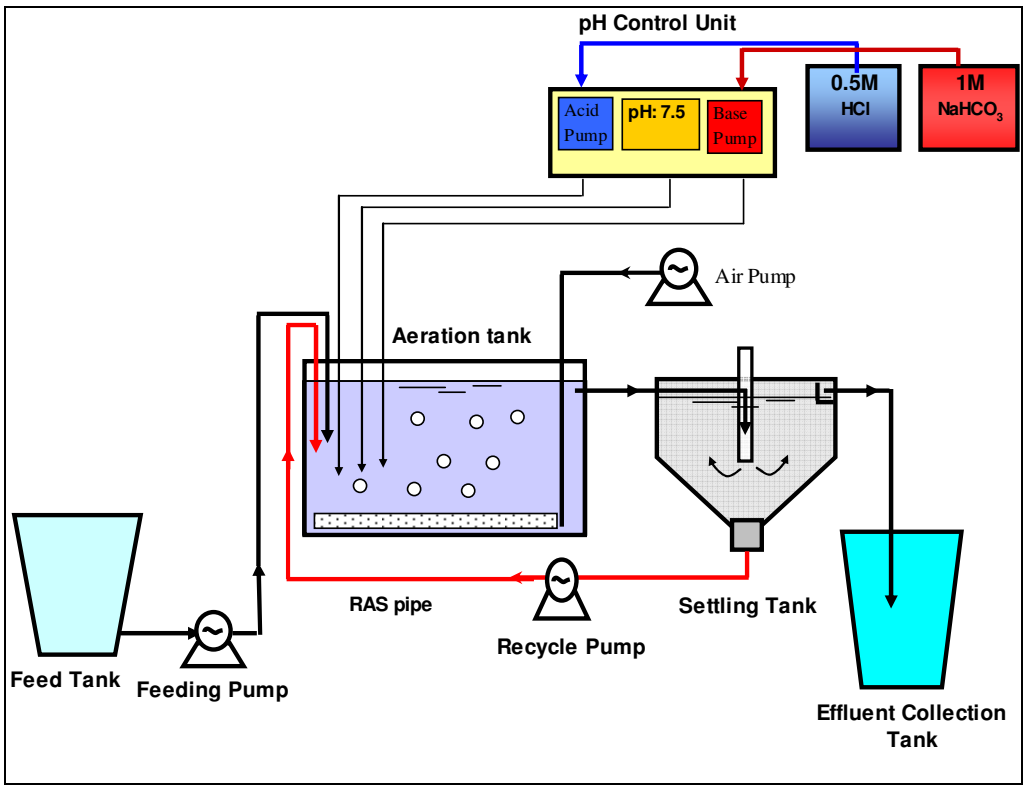

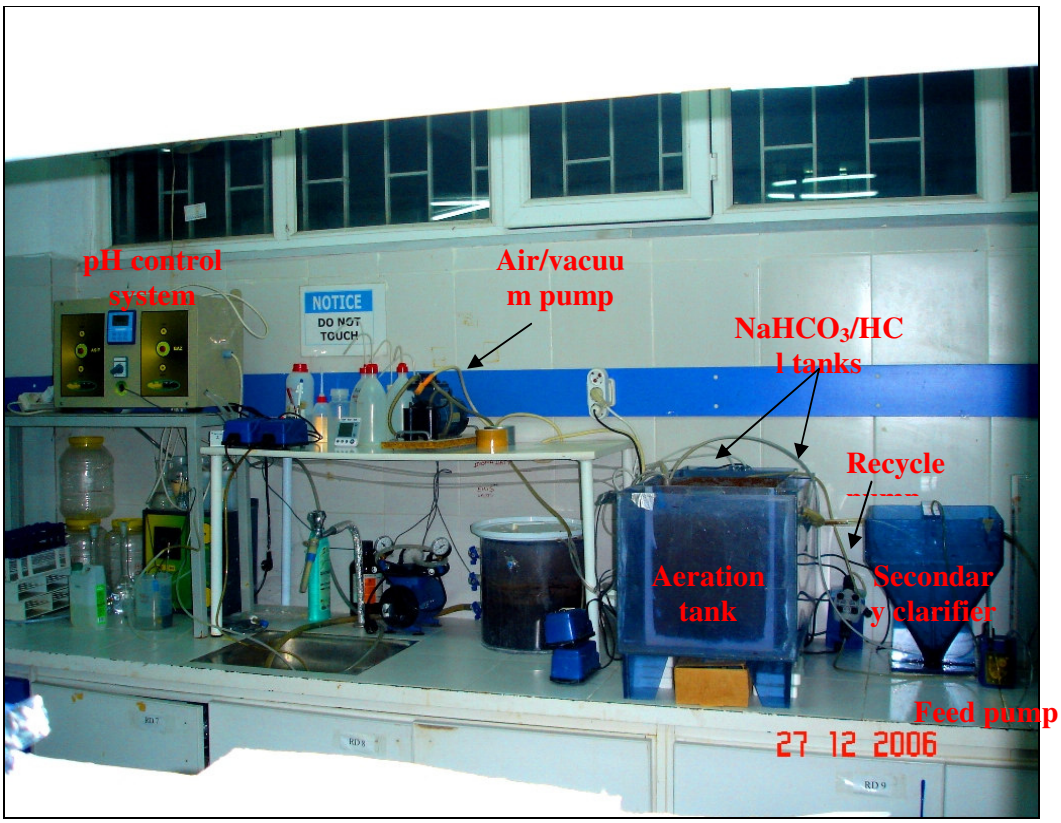

Figure 5.3. Experimental set-up of the Continuous-Flow Nitrifying Reactor

Table 5.5. Operational conditions in the continuous-flow nitrifying reactor

Influent Feed Flowrate, L/day	10
Reactor Volume, L	20
Sludge Retention Time (SRT), day	20
Hydraulic Retention Time (HRT), day	1
Recycle Flowrate, L/day	10
Waste Activated Sludge, L/day	1

The composition of the synthetic feeding solutions used in this study is given in Table 5.6. This synthetic feed was devoid of organic carbon to discourage heterotrophic growth in the reactor and to encourage the predominance of nitrifiers.

Table 5.6. Composition of the synthetic solution used in continuous-flow experiments

Chemical	Stock Concentration, g/L	Final Concentration, mg/L	
$MgSO_4.7H_2O$	2	50	4.93 as Mg
$CaCO_3$	0.103	2.575	1.03 as Ca
$FeSO_4.7H_2O$	0.4	10	2.01 as Fe
$MnSO_4.H_2O$	0.2	5	1.62 as Mn
K_2HPO_4	0.325	8.13	3.65 as K
$(NH_4)_2SO_4$	37.75	50-250 mg/L	

5.5.1. Experimental Procedure

Phase I: In the absence of Cd, the biokinetic parameters were determined by operating the reactor at various influent ammonium loadings (0.19 to 0.60 mg NH_4-N/mg VSS.day). The influent ammonium was changed to a new value upon attainment of steady-state at each initial ammonia concentration.

Phase II: Cd was continuously fed and its level was gradually increased in each run throughout the experimental period. These experiments were performed to comply the following objectives;

- to evaluate the inhibitory effect of Cd on nitrification in continuous-flow experiments,
- to compare the inhibition pattern in batch and continuous-flow regimes
- to observe recovery of cells that have been contacted with Cd for a long period of time and to investigate the microbial diversity in the biomass experiencing long-term Cd introduction

The influent ammonium concentration was chosen as 200 mg/L NH_4-N during this phase to provide substrate independent removal. Increments in Cd feeding were adjusted such that less than 50% decrease took place in ammonium utilization or nitrate production rates. The influent Cd loading to the system was increased in increments of 2 mg/L Cd. When the decreases in $qNH_4 - N$ and $qNO_3 - N$ were higher than or close to 50%, Cd feeding was stopped and the system was fed with NH_4-N only. Throughout this period, extensive Cd measurements were performed to investigate the desorption of Cd from cells. The aim was to assess a relationship between biosorbed Cd and inhibition. At each influent Cd concentration, the reactor was operated for at least 14 days. This period was necessary to reach steady-state conditions and to acclimate nitrifying bacteria to Cd. The operating conditions in Phases I and II are shown in Figure 5.4.

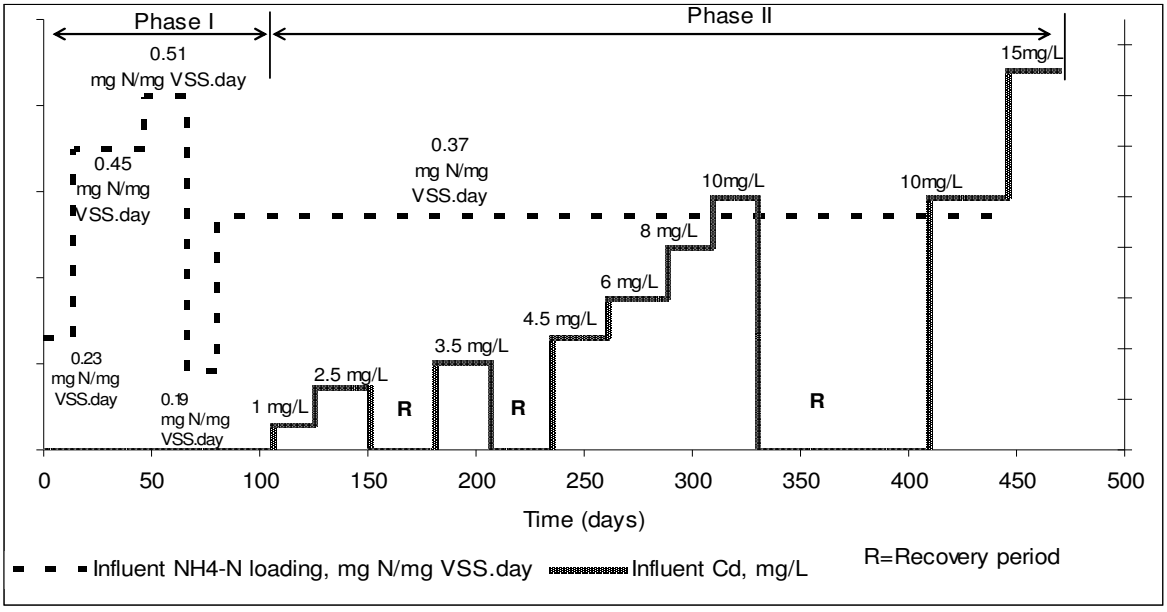

Figure 5.4. The operating conditions in Phases I and II of Continuous-Flow Nitrifying reactor

5.5.2. Determination of Nitrifier Activity and Biosorbed Cd

Throughout the experimental period, samples were daily taken from the feed tank, effluent collection tank (composite samples) and from the aeration tank (grab sample). NH_4-N, NO_2-N and NO_3-N concentrations were then measured. Ammonium utilization and nitrate production rates were used for controlling the efficiency and performance of the system and calculated by Eq.5.12 and Eq.5.13.

$$q_{NH_4-N} = \frac{Q(NH_4-N_{\text{inf}} - NH_4-N_{eff})}{V.X} \tag{5.12}$$

$$q_{NO_3-N} = \frac{Q(NO_3-N_{eff} - NO_3-N_{\text{inf}})}{V.X} \tag{5.13}$$

where NH_4-N_{inf}, NH_4-N_{eff} are the influent and effluent ammonium concentrations, respectively, mg/L, NO_3-N_{inf} and NO_3-N_{eff} are the influent and effluent NO_3-N concentration in grab and composite samples, mg/L, Q is the influent flowrate, L/day, X is the biomass concentration, mg/L, V is the volume of the aeration tank, L.

Free ammonia (NH_3-N) concentration was calculated by using Eq. 5.14.

$$\text{NH}_3\text{-N} = \frac{NH_4-N}{1+10^{(9.25-pH)}} \tag{5.14}$$

Cd concentration was measured in samples taken from the feed tank, inside the reactor and from the secondary clarifier. Labile Cd in the bulk solution was measured by voltammetry in samples filtered through 0.45 μm syringe filters (Millipore Corp., USA). Biosorbed Cd was calculated by measuring the total Cd and subtracting the soluble Cd from the total as shown in Eq. 5.15.

$$Cd_{bio}(\frac{mg\ \ Cd}{g\ \ MLSS}) = Total\ \ Cd\ \ - Soluble\ \ Cd \tag{5.15}$$

5.6. Characterization of Microbial Community in the Continuous-Flow Nitrifying Reactor

The microbial ecology, community shifts and quantity changes in the microbial community of the continuous-flow reactor were investigated with Denaturation Gradient Gel Electrophoresis (DGGE) and Fluorescence In-Situ Hybridization (FISH) techniques. Sampling and analyses for molecular characterization were done by Bülent Mertoğlu and Nuray Güler, at the Marmara University Environmental Engineering Department, as also reported in a project (Saatçi et al., 2006).

Sludge samples were taken at certain times during continuous-flow experiments with ammonium only and at the end of each Cd loading period, especially inhibition periods. Samples were taken from the wasted sludge and then concentrated by centrifuging for 0.5 h at 7000 rpm. Concentrated sludge samples were extracted and fixed for DNA extractions and FISH samples. The fixed cells were stored at -20^0C.

5.6.1. DNA Extraction from Sludge Samples

1.2 mL of concentrated sludge sample was taken into a 1.5 mL microcentrifuge tube centrifuge at 14000 rpm for 5 min. TE buffer (at pH = 8.0) was added till 0.75mL and 0.3 mL of phenol and 3 spoon full of 0.1 mm sized zirconia beads were also added to the sample tube. The tube was beat-beaten for 5 s at 2500 rpm using Mini Bead-beater-8 (Biospec Products). After beat-beating, the sample containing tube was centrifuged at 14,000 rpm for 10 min. 0.6 mL of supernatant was taken into a clean 1.5 mL microcentrifuge tube and gently mixed with 0.6 mL of Binding matrix of Fast DNA SPIN kit, and then allowed to settle for 5 min at room temperature. The mixture was centrifuged for 1 min and the supernatant was discarded. 0.5 mL of SEWS-M Solution (Salt Ethanol Wash Solution – Fast DNA SPIN kit) was added and mixed gently. After 1 min centifugation at 14,000 rpm, the supernatant was removed. For further removal from ethanol the tube was centrifuged for additional 10 s and the supernatant was discarded with the help of a pipet. As the final step, 100 µL of DES (DNA Elution Solution – Fast DNA SPIN kit) was added to the tube, gently mixed and incubated for 2 min at room temperature. After centrifugation at 14,000 rpm for 1 min, the supernatant containing

dissolved DNA was transferred to a new tube. DNA extraction results were controlled using agarose gel electrophoresis.

5.6.2. PCR (Polymerase Chain Reaction)

The variable regions of the ribosomal DNA and *amoA* genes of nitrifying bacteria were amplified by PCR to use for slot blot hybridization, denaturing gradient gel electrophoresis (DGGE) and cloning. PCR primer pairs used in this study for amplification of DNA isolates are shown in Table 5.7.

Table 5.7. PCR primer pairs

Primer	Target	Sequence (5' – 3')
27 for	Bacterial forward	AGA GTT TGA TCC TGG CTC AG
1510 rev	Bacterial reverse	GGT TAC CTT GTT ACG ACT T
amoA – 1F	*amoA* forward	GGG GTT TCT ACT GGT GGT
amoA – 2R	*amoA* reverse	CCC CTC KGS AAA GCC TTC TTC
amoA – 1F – C	*amoA* forward with clamp	GGG GTT TCT ACT GGT GGT
GC 968 for	Bacterial forward with clamp	CGC CCG GGG CGC GCC CCG GGC GGG GCG GGG GCA CGG GGG GAA CGC GAA GAA CCT TAC
1401 rev	Bacterial reverse	CGG TGT GTA CAA GAC CC

5.6.3. DGGE (Denaturating Gradient Gel Electrophoresis)

Denaturing gradient gel electrophoresis (DGGE) of PCR-amplified genes can be used to evaluate the diversity of complex microbial systems. In DGGE, the separation of equal length DNA fragments is based on sequence-dependent melting behavior in a polyacrylamide gel containing a concentration gradient of increasing denaturant. DGGE is a powerful technique whereby the diversity of PCR-amplified genes from a large number

of samples can be compared in one gel to reveal changes in community structure over time or space.

DGGE of PCR products generated by the 16S rDNA and amoA primers were performed with the BioRad D-Code Universal Mutation Detection System (BioRad). Polyacrylamide gels with a gradient of 30–70% denaturant and 20–50% denaturant for 16S rDNA and amoA DGGEs respectively were made with a gradient maker (BioRad) according to the manufacturer's guidelines. A top gel without denaturant was cast above the denaturing gel before the polymerization started. Gels were run for 16 h at 80 Vand 15 h at 100 V in 0.5X TAE buffer at a constant temperature of 60 °C for 16S rDNA and amoA DGGEs respectively.

The gels were stained with silver nitrate. The photochemically derived silver stain was originally described for protein staining and later applied to nucleic acids. Silver nitrate reacts with biopolymers under acidic conditions and subsequently silver ions are selectively reduced to metallic silver by formaldehyde under alkaline conditions. The silver stain detects nucleic acids in polyacrylamide gels very sensitively and therefore small amounts of PCR products are needed for DGGE analysis.

Following the staining, gels were fixed for 5 min and washed in deionized water to provide a permanent record of the experiment. After second fixation, preservation solution (50 ml 96% ethanol, 20 ml glycerol, and 130 ml deionized water) was added and rocked for at least 7 min and gels were covered with porous hydrophilic cellophane. Finally, gels were dried overnight at 40°C.

5.6.4. Slot-Blot Hybridization

Slot-blot hybridization was performed with DIG-labelled oligonucleotide to investigate the variations and activity of microbial populations. Extracted DNA was used for domain-specific probes for Bacteria. All microorganisms were detected by using Universal Specific Oligonucleotide probe. The analyses were performed with oligonucleotide probes given in Table 5.8.

Table 5.8. Slot-Blot Hybridization Probes

Probe name	Sequence	Target group
EUB 338	GCT GCC TCC CGT AGG AGT	Bacteria domain
NSO190	CGA TCC CCT GCT TTT CTC C	Ammonia Oxidizing Bacteria
NSM 156	TAT TAG CAC ATC TTT CGA T	Ammonia Oxidizing Bacteria
NIT3	CCT GTG CTC CAT GCT CCG	*Nitrobacter*
NTSPA 662	GGA ATT CCG CGC TCC TCT	*Nitrospira*

5.6.5. FISH (Fluorescence In-Situ Hybridization)

Fluorescence In-Situ Hybridization (FISH) is a microbial method that allows the detection of whole-bacterial cells and the analysis of chromosomes via the labeling of specific nucleic acids with fluorescently labeled oligonucleotide probes. Basically, the FISH method uses fluorescent molecules to vividly paint genes or chromosomes so that they can be detected and identified. First, short sequences of single-stranded DNA, called probes, are prepared. These probes hybridize, or bind, to complementary nucleic acids and, because they are labeled with fluorescent tags, allow researchers to see the location of those sequences of DNA. When the results are viewed, usually with a scanning laser microscope, they can be visually stunning. Unlike most other techniques used to study microorganisms, which require that the cells be actively dividing, FISH can also be performed on nondividing cells, making it a highly versatile procedure. The FISH method involves four steps: fixation, hybridization, washing, and detection.

Hybridization must be carried out in a properly sealed moisture chamber to prevent evaporative concentration of the hybridization solution, which might result in nonspecific binding of the fluorescent probe to the cell.

Hybridizations were performed at 46°C for 2 h with 10 µL hybridization buffer (0.9 M NaCl, 20 mM Tris/HCl, pH 8.0, 0.01% SDS) containing each labeled probe (30 ng/well for Cy3 and 50 ng/well for FLUOS) (MWG Biotech, Ebersberg). A list of the oligonucleotide probes used in FISH is given in Table 5.9.

Table 5.9. Probes and target groups

Prob Name	Labeled	Target group	Formamide (%)
EUB 338	FLUOS	Bacteria	20
ALF 1b	Cy3	α- proteobacteria	35
BET 42a	Cy3	β- proteobacteria	35
GAM 42a	Cy3	γ- proteobacteria	35
NSO 190	Cy3	Ammonia Oxidizing β- proteobacteria	35
NIT 3	Cy3	*Nitrobacter*	35
NTSPA 662	Cy3	*Nitrospira*	35

5.7. Metal Measurements

Metal concentrations were measured by voltammetry (VA 797 Computrace, Metrohm Inc.,). The picture of the voltammetry is shown in Figure 5.5.

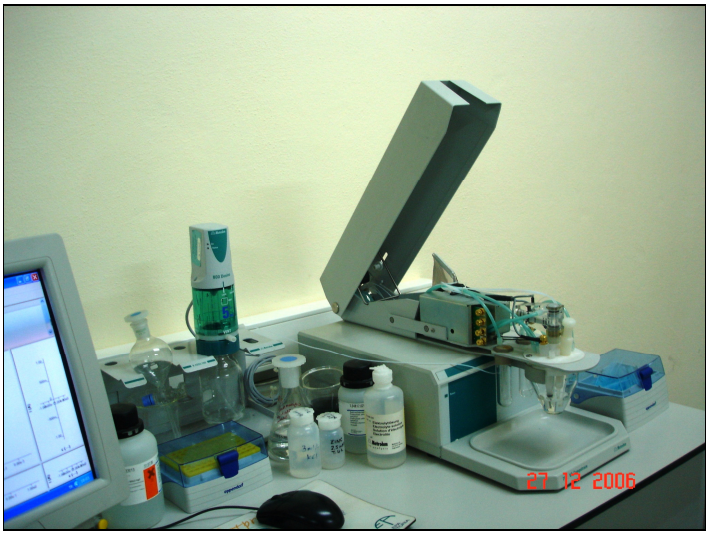

Figure 5.5. Voltammetry Instrument (VA 797 Computrace)

The soluble metal in this study was measured by two different ways: First, the metal in the untreated sample was measured at is natural pH (around 7.5 for the batch experiments). Then the metal was also measured after adjusting pH to < 2 after digestion.

The metal concentration measured in the first determination is the fraction of metal that is present as hydrated ions, labile organic and weak inorganic complexes with ligands such as chloride, sulfate and carbonate etc. The concentration measured in the second determination includes the amount of metal present as inert organic complexes in addition to that present as hydrated ions and labile complexes. The total metal concentration in the soluble phase and solids associated phase was measured after digesting a predetermined volume of wet sludge. The flow diagram for the theoretical and voltammetric Cd speciation is presented in Figure 5.6. Operational parameters of voltammetry for Zn and Cd measurements are given in Table 5.10. 3 mol/L of KCL solution (Metrohm Ltd., Switzerland or Merck KGaA, Germany) solution was used as a supporting electrolyte. Pure nitrogen (N_2) gas (99.996% pure) was used as the inert gas to de-aerate the analyte solution and for the operation of Multi Mode Electrode (MME). Samples for Cd and Zn measurements are shown in Figure 5.7 and 5.8, respectively.

5.7.1. Sample Digestion

Samples were digested by UV photolysis using a UV digester (UV Digester Metrohm Inc.). 0.5 mL concentrated H_2O_2 (30%), 0.5 mL hydrochloric acid (HCl, 98%) and 10 mL samples were put into the quartz vessels. Concentrated HCl acid was used instead of HNO_3^- since high NO_3^- concentrations interfered with voltammetric measurements. Sample loss during digestion was controlled by adjusting the sample temperature to less than 100^0C by cooling systems of UV digester. Samples were digested at a temperature of 90^0C for 4 hours.

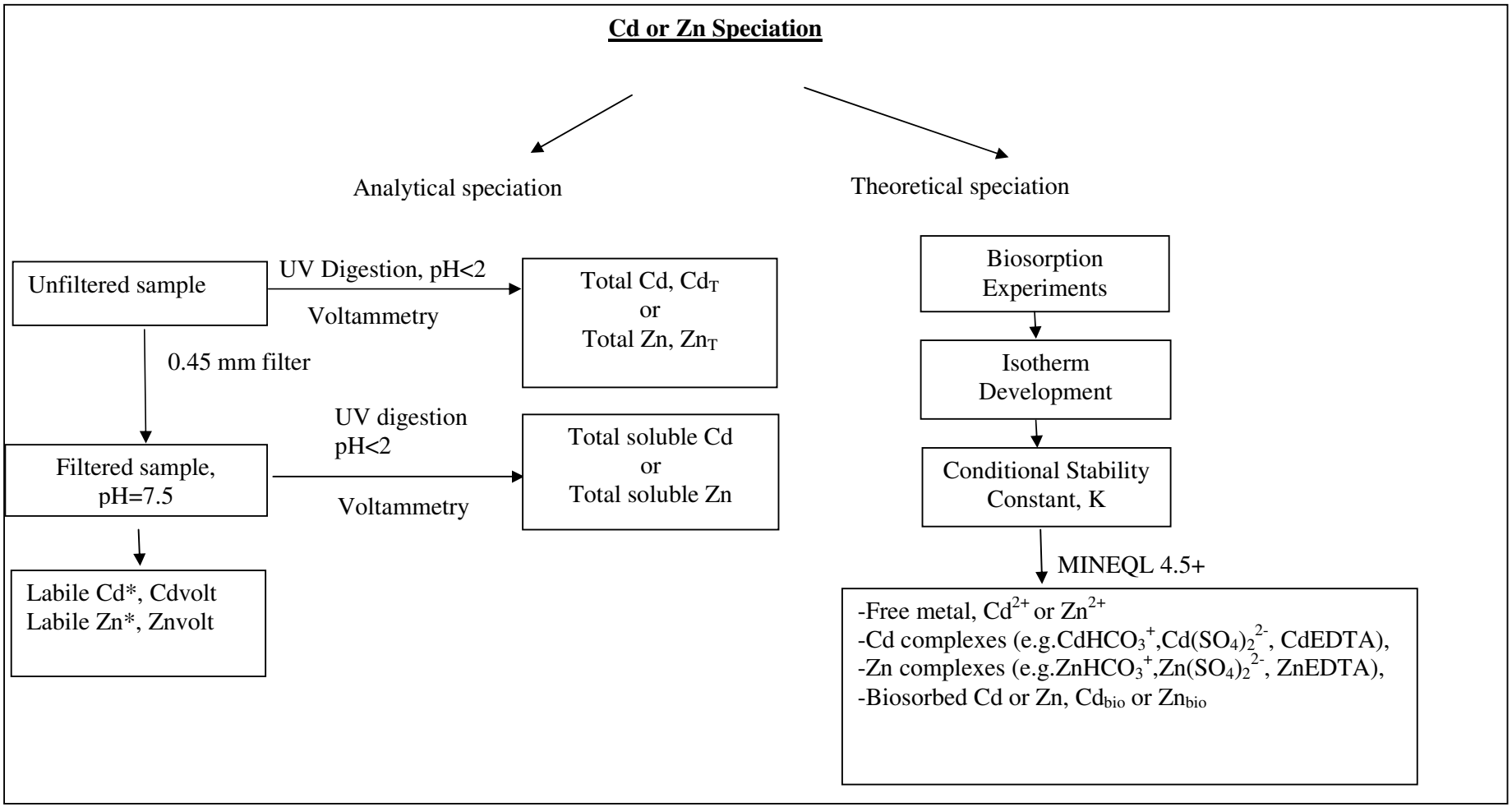

* Labile Cd = Cd_{volt}= free Cd (Cd^{2+}) + Cd in weak complexes , * Labile Zn = Zn_{volt}= free Zn (Zn^{2+}) + Zn in weak complexes

Figure 5.6. Flow Diagram of the Cd and Zn Speciation

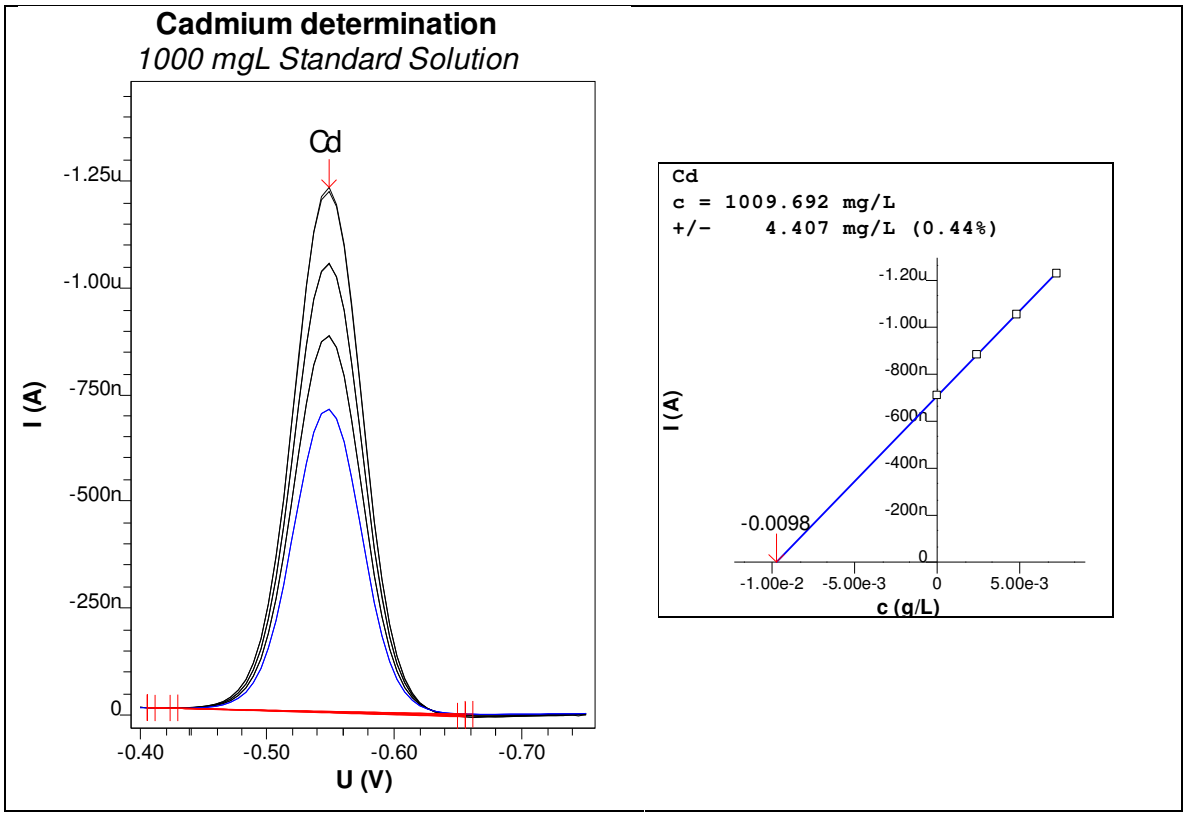

Figure 5.7. Typical Cd Measurement with Voltammetry

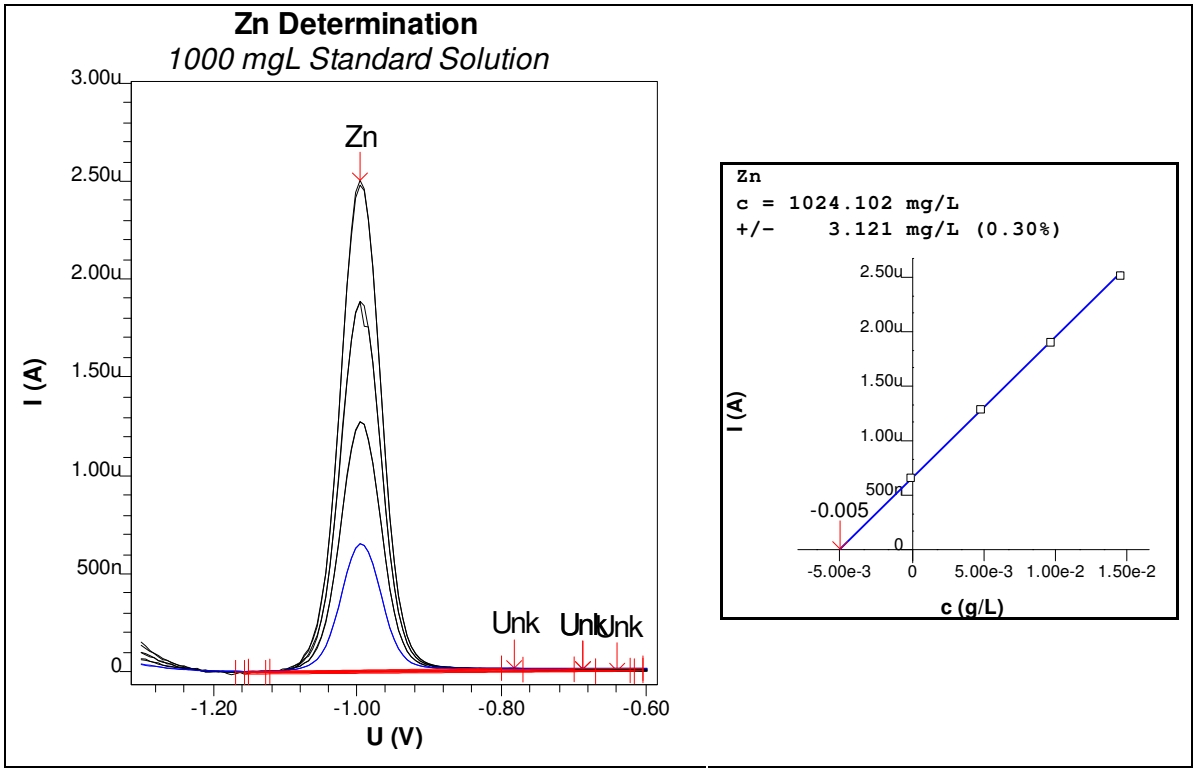

Figure 5.8. Typical Zn Measurement with Voltammetry

Table 5.10. Operational parameters in voltammetric Cd and Zn measurements

Parameters	Cd	Zn
Mode	Differential pulse	Differential pulse
Calibration method	Standard addition	Standard addition
Electrode	DME (Dropping mercury electrode)	DME (Dropping mercury electrode)
Initial purge time	400 s	400 s
Equilibration time	5 s	5 s
Start potential	-0.2 V	-0.9V
End potential	-0.7 V	-1.2 V
Pulse amplitude	0.0505 V	0.0505 V
Pulse time	0.4 s	0.4 s
Voltage step	0.00595 V	0.00595 V
Sweep rate	0.0419 V/s	0.0419 V/s
Peak potential	-0.585 ± 0.08 V	-0.980 ± 0.08 V

5.8. Investigation of Cd and Zn Speciation by Voltammetric Measurements and MINEQL 4.5 + Calculations

The influence of cations and anions in the feed solution in Table 5.11 on the free and labile metal concentration was investigated by voltammetric measurements and compared with MINEQL + 4.5 calculations. Total and labile metal (M_{volt}) measurements were carried out with voltammetry as described in Section 5.7. Concentration of metal species in bulk solution was calculated with MINEQL +4.5. The pH of the solution was set to 7.5 by MOPS buffer ([(3-(N-morpholino)propanesulfonic acid, pKa=7.2) at a concentration of 20 mM.

Table 5.11. Concentration of cations and anions in the synthetic feed solution used in batch experiments

	Final concentration in batch reactor	
Cations	mg/L	mole/L
Ca^{2+}	1.03	$2.57x10^{-5}$
Fe^{2+}	2.01	$3.59x10^{-5}$
K^{+}	3.64	$9.33x10^{-5}$
Mg^{2+}	4.93	$2.03x10^{-4}$
Mn^{2+}	1.63	$2.96x10^{-5}$
Na^{+}	345	$1.50x10^{-2}$
NH_4^{+}	66.82	$3.71x10^{-3}$
Anions		
SO_4^{2-}	208-225	$2.17x10^{-3}$-$2.22x10^{-4}$
CO_3^{2-}	1.55	$2.57x10^{-5}$
HCO_3^{-}	915	$1.50x10^{-2}$
HPO_4^{2-}	4.5	$4.67x10^{-5}$

Speciation of the metals in the presence of 5, 10 and 20 mg/L Cd and 5, 10 and 25 mg/L Zn is illustrated in Table 5.12 and 5.13, respectively.

Table 5.12. Cd species in the feed solution: Comparison of MINEQL +4.5 and voltammetric results at pH=7.5 and pH<2.

Species	Stability Constant, Log K (Table 5.5)	Total Cd, mg/L 5	10	20
		MINEQL results		
Cd^{2+}	-	3.32	6.63	13.23
$CdOH^{+}$	-10.08	0.01	0.01	0.02
$CdHCO_3^{+}$	12.40	0.06	0.11	0.23
$Cd(CO_3)(aq)$	5.39	0.72	1.44	2.86
$Cd(CO_3)_2^{2-}$	7.22	0.02	0.04	0.07
$Cd(SO_4)_2^{2-}$	3.50	0.04	0.08	0.17
$Cd(SO_4)(aq)$	2.46	0.82	1.66	3.35
Total Cd according to MINEQL calculations, mg/L		4.99	9.97	19.93
Cd measured by voltammetry at pH =7.5 (Cd_{volt}), mg/L		4.06	8.39	16.65
Cd measured by voltammetry at pH<2 (total Cd), mg/L		4.53	8.58	17.33

The most important Cd species is the free Cd^{+2} as predicted by MINEQL. On the other hand, Cd_{volt} was slightly higher than this value due to the presence of labile complexes with low stability constants, which may dissociate into free form. A possible ligand in the medium is the HCO_3^- ion, which is an inorganic carbon source for nitrifiers. As seen in Table 5.13, the presence of bicarbonate leads to a number of Cd-carbonate species of significant concentration with variable stability constants. It seems that the $CdCO_3(aq)$ did not dissociate or slowly dissociated into the electroreducible free Cd in the time scale of voltammetric measurement in the dropping mercury (DME) mode. Therefore, the new labile Cd could be calculated by substracting the concentration of $Cd(CO_3)_{(aq)}$ from the total Cd. The new labile Cd concentrations would be then 4.26, 8.5 and 7.10 mg/L for 5, 10 and 20 mg/L, respectively. As seen in Table 5.12 the voltammetrically determined Cd concentrations at pH 7.5 are very close to these concentrations.

Similar to the results of Cd measurement, Zn is highly present as free form. The labile Zn measured by voltammetry, Zn_{volt}, was approximately 20% lower than the theoretical calculations for all Zn concentrations. If the same hypothesis was applied for Zn, then the labile Zn would be 3.54, 7.09 and 17.82 mg/L for 5, 10 and 25 mg/L of total

Zn, respectively. The labile Zn concentrations calculated by this way are very close to Zn_{volt} concentrations (Table 5.13).

Table 5.13 Zn species in the feed solution: Comparison of MINEQL +4.5 and voltammetric results at pH=7.5

		Total Zn, mg/L		
Species	Stability Constant, Log K (Table 5.5)	5	10	25
		MINEQL results		
Zn^{2+}	-	2.50	5.0	12.50
$ZnOH^{+}$	-8.997	0.05	0.10	0.26
$ZnHCO_3^{+}$	11.829	0.63	1.25	3.08
$Zn(CO_3)_{(aq)}$	4.76	1.46	2.91	7.17
$Zn(SO_4)_2^{2-}$	3.28	0.01	0.81	0.04
$Zn(SO_4)_{(aq)}$	2.34	0.36	0.73	1.97
Total labile Zn according to MINEQL calculations, mg/L		5.0	10.0	25.0
Zn measured by voltammetry at pH =7.5 (Zn_{volt}), mg/L		3.11	7.5	16.99

During speciation measurements, some preliminary controls were also carried out to examine the probable formation of dissolved solids, especially, otavite $(CdCO_3)_s$ to ensure that the metal concentrations that were at sub-solubility limits to avoid precipitation. In these experiments, the concentration of HCO_3^- was gradually increased from $1.11x10^{-4}$ to $7x10^{-3}$ M at a constant Cd concentration of $4.46x10^{-4}$ M. The solution pH was set to 7.0±0.05 with 20 mM MOPS addition. In any case, dissolved solids were absent in the system.

5.8.1. Measurement of Labile Cd by Voltammetry in the Presence of Complexing Agents

Some preliminary Cd measurements were carried out in the presence of complexing agents in order to test the operational parameters in Table 5.11. For this purpose, various Cd test solutions were prepared. In these solutions, the concentration of labile Cd was manipulated by changing the total Cd concentration while keeping EDTA or NTA constant at $1.71x10^{-4}$ M and $1.83x10^{-5}$ M, respectively. The concentrations of free Cd, CdEDTA or CdNTA were also calculated with the MINEQL +4.5 program and shown in Table 5.15

and 5.16, respectively. The total Cd concentration was also measured after UV digestion as described in Section 5.7.1. As seen in Tables 5.14 and 5.15, it is easy to differentiate strong Cd complexes from labile Cd by voltammetric measurement, since only the electroreducible form of Cd (free Cd) gave a signal in voltammetric measurement. The t-test was applied and the labile Cd calculated with MINEQL and measured by voltammetry as illustrated in Figure 5.9, were found to be not significantly different from each other ($p > 0.05$).

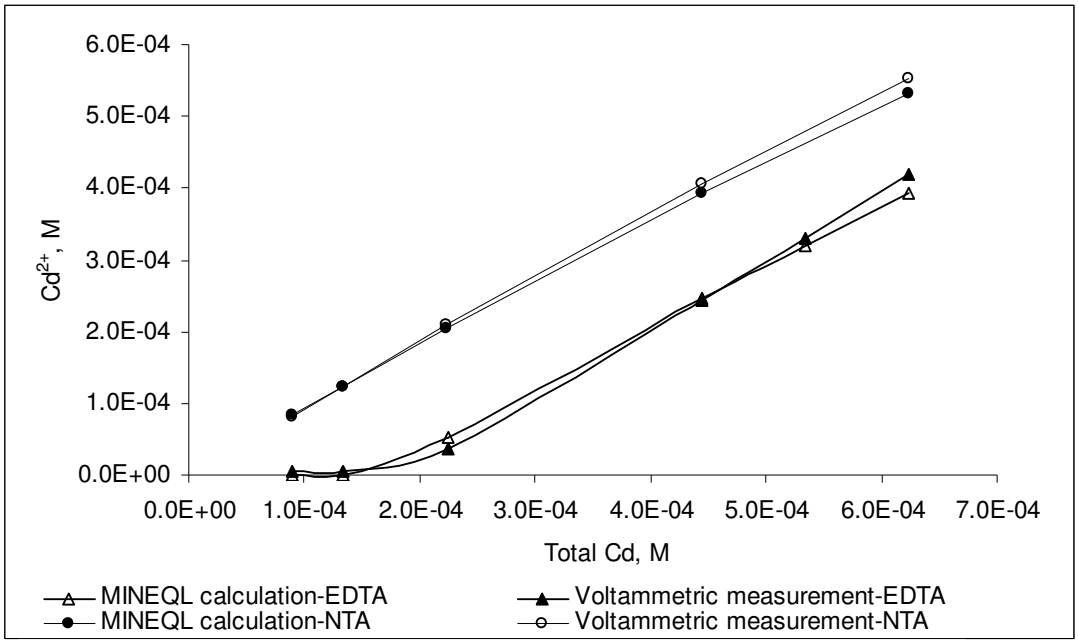

Figure 5.9. Change in the labile Cd in the presence of EDTA and NTA

Table 5.14. Cd speciation in the presence of $1.71x10^{-4}$ EDTA

Initial Cd Concentration		MINEQL calculations				Voltammetric measurement		Voltammetric measurement	
Cd		CdEDTA,		Cd^{+2}		Labile Cd, Cd_{volt}		Total Cd, Cd_T	
mole/L	mg/L	mole/L	mg/L	mole/L	mg/L	mole/L	mg/L	mole/L	mg/L
$8.899x10^{-5}$	10	$8.87x10^{-5}$	9.95	$2.86x10^{-7}$	0.032	$4.89x10^{-6}$	0.548±0.014	$7.24x10^{-5}$	8.123±0.032
$1.335x10^{-4}$	15	$1.32x10^{-4}$	14.80	$1.31x10^{-6}$	0.147	$4.55x10^{-6}$	0.510±0.031	$1.18x10^{-4}$	13.464±0.031
$2.25x10^{-4}$	25	$1.69x10^{-4}$	18.95	$5.25x10^{-5}$	5.901	$3.60x10^{-5}$	4.03±0.017	$2.02x10^{-4}$	22.542±0.144
$4.449x10^{-4}$	50	$1.71x10^{-4}$	19.17	$2.46x10^{-4}$	27.65	$2.44x10^{-4}$	27.38±0.206	$4.39x10^{-4}$	49.2±0.505
$5.339x10^{-4}$	60	$1.71x10^{-4}$	19.17	$3.20x10^{-4}$	35.97	$3.31x10^{-4}$	37.09±0.292	$5.64x10^{-4}$	63.2±0.995
$6.229x10^{-4}$	70	$1.71x10^{-4}$	19.17	$3.92x10^{-4}$	44.07	$4.19x10^{-4}$	46.96±0.406	$6.33x10^{-4}$	71.0±0.805

Table 5.15. Cd speciation in the presence of $1.83x10^{-5}$ NTA

Initial Cd Concentration		MINEQL calculations				Voltammetric measurement	
Cd		CdNTA,		Cd^{+2}		Labile Cd, Cd_{volt}	
mole/L	mg/L	mole/L	mg/L	mole/L	mg/L	mole/L	mg/L
$8.899x10^{-5}$	10	$1.83x10^{-5}$	2.05	$7.066x10^{-5}$	7.92	$8.16x10^{-5}$	9.152±0.132
$1.335x10^{-4}$	15	$1.83x10^{-5}$	2.05	$1.146x10^{-4}$	13.86	$1.22x10^{-4}$	13.671±0.221
$2.25x10^{-4}$	25	$1.83x10^{-5}$	2.05	$2.06x10^{-4}$	23.10	$2.09x10^{-4}$	23.469±0.335
$4.449x10^{-4}$	50	$1.83x10^{-5}$	2.05	$4.27x10^{-4}$	47.83	$4.06x10^{-4}$	48.408±0.480
$6.229x10^{-4}$	70	$1.83x10^{-5}$	2.05	$6.05x10^{-4}$	67.79	$6.40x10^{-4}$	71.763±0.789

5.9. Other Measurements

- NH_4-N Analysis: NH_4^+-N concentrations were analyzed by method 4500-NH_3 C (Nesslerization Method) in Standard Methods (APHA, AWWA, WEF, 1998) with HACH DR/2000 spectrophotometer.

- NO_2-N Analysis: NO_2-N concentrations ranging from 0 to 150 mg/L were analyzed by Ferrous Sulfate Method (Method 8153) with Hach DR/2000 spectrophotometer by using Nitriver 2 powder pillows. NO_2-N concentrations ranging from 0 to 0.3 mg/L NO_2-N were analyzed by Diazotization Method (Method 8057) with Hach DR/2000 spectrophotometer by using Nitriver 3 powder pillows.

- NO_3-N Analysis: NO_3-N concentrations were analyzed by Cadmium Reduction Method (Method 8039) with HACH DR/2000 spectrophotometer by using Nitra Ver5 powder pillows. The sample was pretreated with 30 g/L bromine water and 30 g/L phenol solution to prevent interference of NO_2^-.

- SS and VSS Analyses: SS and VSS analyses were performed using Method 2540D and Method 2540E in Standard Methods (APHA, AWWA, WEF, 1998) respectively.

- DO and pH measurements: The DO concentrations and pH were measured by using WTW OxiLevel-2 DO meter and WTW Inolab-1 pH meter, respectively.

5.10. Reagents

Ultrapure water from Arium 611, Sartorious, Germany was used for the preparation of all stock solutions. All glassware and plasticware was cleaned by soaking in 10% (v/v) nitric acid (Merck Tracepur, Germany) for a minimum of 24 h followed by rinsing with ultrapure water.

- Stock Cd Solution: Merck cadmium sulfate hydrate ($3CdSO_4.8H_2O$) was used for the preparation of Cd solutions. Cadmium stock solution (1000 mg/L) was prepared by dissolving this compound.

- Stock Zn Solution: Merck zinc sulfate hydrate ($ZnSO_4.7H_2O$) was used for the preparation Zn solutions. Zinc stock solution (1000 mg/L) was prepared by dissolving this compound.

- MOPS buffer solution: Merck 3-Morpholinopropane sulfonic acid ($C_7H_{15}NO_4S$) was used for the preparation 200 mM MOPS buffer solutions by dissolving this compound.

- Stock EDTA solution: Merck EDTA salt was used for the preparation 0.1 M stock EDTA.solution

- **Cadmium standard solution**: Merck Cadmium standard solution (traceable to SRM) from NIST in HNO_3 acid (0.5 mol/L 1000 mg/L Cd) was used in voltammetric measurement as Cd calibration solution.

- **Zinc standard solution**: Merck Zinc standard solution (traceable to SRM) from NIST in HNO_3 acid (0.5 mol/L 1000 mg/L Zn) was used in voltammetric measurement as Zn calibration solution.

6. RESULTS AND DISCUSSIONS

6.1. Estimation of Biokinetic Parameters in Ammonium Utilization

The maximum specific ammonium utilization rate $q_{\max,NH_4-N}$ and half-saturation constant ($K_{S,N}$) for ammonium were determined. Specific ammonium utilization rates of the nitrifying bacteria are independent of the NH_4-N concentration if the NH_4-N concentration is significantly higher than the half-saturation constant according to the Monod equation:

$$q_{NH_4-N} = q_{\max,NH_4-N} \frac{NH_4 - N}{K_{S,N} + NH_4 - N} \tag{6.1}$$

where

$q_{\max,NH_4-N}$ = maximum specific ammonium utilization rate, mg NH_4-N/g VSS.day

NH_4-N = growth limiting substrate concentration (NH_4-N), mg/L and

$K_{S,N}$ = half-saturation constant, mg/L

As well known, heavy metals are noncompetitive inhibitors (Beg et al., 1982, Hu et al., 2002, Ren and Frymier, 2003, Mazierski, 1994, Lewandowski, 1987). In this type of inhibition, inhibitors decrease the maximum ammonium utilization rate without changing half-saturation constant as shown in Eq. 6.2 and explained in Section 2.5. In order to follow the decrease in maximum specific ammonium utilization rate in the presence of heavy metals, it is necessary to work in a NH_4-N concentration range where bacteria reach their maximum activity.

$$q_{NH_4-N\,inhibited} = \frac{q_{\max,NH_4-N,app}\, S}{K_{S,N} + S} = \frac{q_{\max,NH_4-N} S}{(1 + \frac{I}{K_i})(K_{S,N} + S)} \tag{6.2}$$

where

$q_{NH_4-N_{inhibited}}$ = specific ammonium utilization rate under inhibition conditions, mg NH_4-N/g VSS.day

$q_{\max,NH_4-N,app}$ = apparent maximum specific ammonium utilization rate, mg NH_4-N/g VSS.day

S = growth limiting substrate concentration (NH_4-N), mg/L

K_i = inhibition coefficient, mg/L

I = inhibitor concentration, mg/L

For this purpose, the specific ammonium utilization rates (q_{NH_4-N}) determined at various initial NH_4-N were evaluated with respect to bulk NH_4-N. By definition, the specific substrate utilization rate equals to the one-half of the maximum substrate utilization rate when the bulk substrate concentration equals the half saturation constant. It can be determined from the substrate versus time plot if microorganism concentration is essentially constant with time (Williamson and McCarty, 1975). Due to low growth kinetics, the change in nitrifying biomass concentration is negligible (EPA, 1993). Hence, the specific ammonium utilization rate should be almost constant during batch experiments as long as substrate-independent conditions are provided (Eq. 6.1).

Decrease of NH_4-N with respect to time was linear until the bulk NH_4-N concentration was in the range of 1.5-2 mg/L. When bulk NH_4-N concentration was less than 2 mg/L, a smooth transition from zero-order to first-order rate was observed. The transition NH_4-N concentration changed depending on the initial NH_4-N / MLVSS ratio. When microorganisms were in excess compared to the NH_4-N concentration, NH_4-N utilization took place very fast and the transition NH_4-N concentration could not determined easily. On the other hand, when both biomass and substrate concentrations were low, the time scale of the experiment expanded so that the substrate concentration remained near K_S for a reasonable length of time (Williamson and McCarty, 1975). Although this method has some advantages, poor estimates of K_s, are still obtained if the half-saturation coefficient is small.

Typical ammonium utilization curves for an initial NH_4-N concentration of 22, 50 and 90 mg/L are shown in Figure 6.1. Transition NH_4-N concentrations were shown with arrows on the curves. Least square nonlinear regression technique was applied to determine the half-saturation constant, $K_{S, N}$ and the maximum specific ammonium utilization rate, $q_{, max, NH4-N}$ at each initial NH_4-N concentration. The results were summarized in Table 6.1.

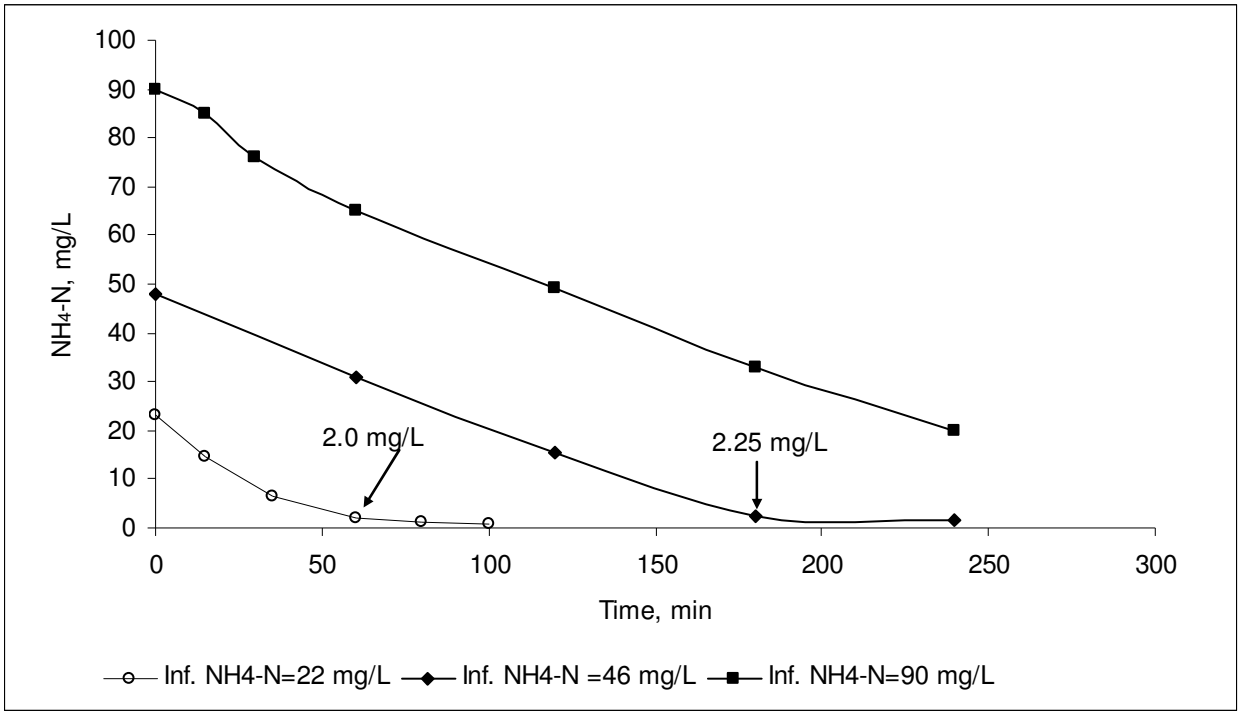

Figure 6.1. Typical NH_4-N utilization curves for initial NH_4-N concentration of 22, 50 and 90 mg/L

Table 6.1. Maximum specific ammonium utilization rate ($q_{\max,NH_4-N}$) and half-saturation constant ($K_{S,N}$) at various initial NH_4-N concentrations

Initial NH_4-N mg/L	Maximum Specific Ammonium Utilization Rate ($q_{\max,NH_4-N}$) mg NH_4-N/g VSS.h	Half-Saturation Constant ($K_{S,N}$) mg/L	R^2
50	81.2±1.67	0.67±0.088	0.95
50	86.3±1.64	0.77±0.096	0.95
22	68.9±2.71	1.60±0.199	0.98
22	75.8±5.01	1.18±0.223	0.97
55	62.6±3.09	0.51±0.105	0.95
55	67.1±3.22	0.34±0.205	0.94

As seen from Table 6.1, evaluation of the data with respect to the bulk NH_4-N concentrations resulted in $q_{\max,NH_4-N}$ and $K_{S,N}$ values in the ranges of 62-86 mg NH_4-N/g VSS.h and 0.34-1.6 mg NH_4-N/L, respectively. Average value for $q_{\max,NH_4-N}$ and $K_{S,N}$ were calculated as 73.5 ±9.1 mg NH_4-N/g VSS.h and 0.84±0.4 mg/L, respectively. Model and experimental results are shown in Figure 6.2.

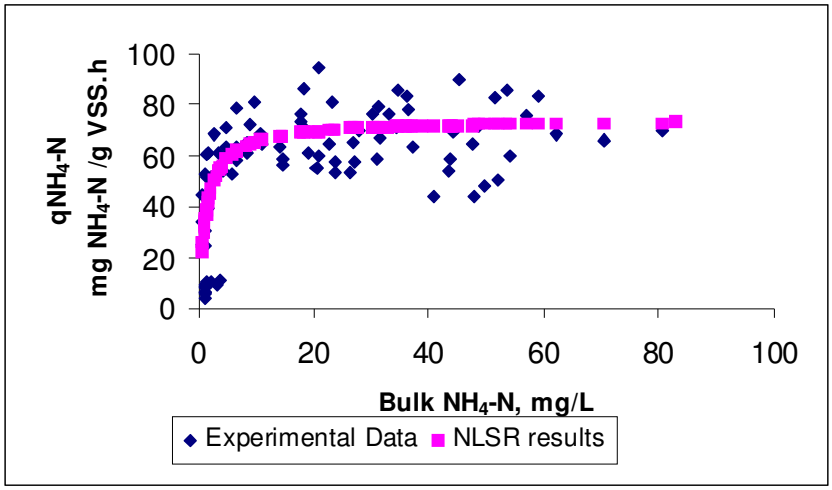

Figure 6.2. Specific ammonium utilization rates at various bulk NH_4-N concentrations

6.2. The effect of Cd on Nitrification in Batch Reactor Systems

6.2.1. The effect of Cd, Zn and Cu on the Short-Term Specific Oxygen Uptake Rate (SOUR) in the Presence of Phosphate Buffer

Short-term OUR experiments were conducted to determine the instant effects of Cd, Zn and Cu on nitrification. The initial metal range in ammonium utilization experiments was also adjusted according to the results of these experiments. The metal concentration for Cd, Zn and Cu was 5-150 mg/L, 2.5-150 mg/L and 5-150 mg/L, respectively. The percent decrease in SOUR for Cd, Zn and Cu is illustrated in Figure 6.3, 6.4 and 6.5, respectively. Since dissolved oxygen was both used in ammonium and nitrite oxidation steps, the percent reductions in SOUR experiments reflected the inhibition of both steps.

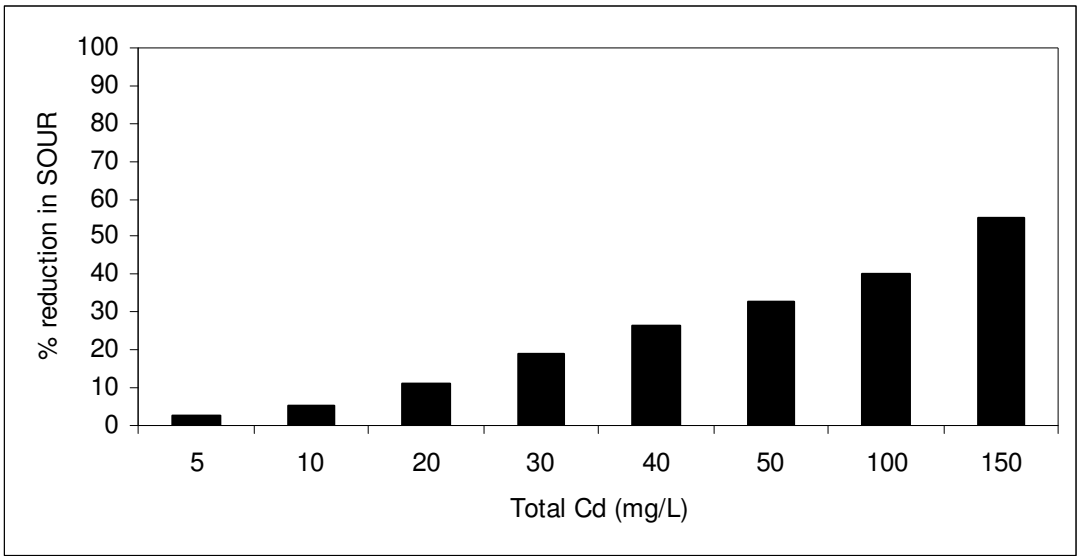

Figure 6.3. Inhibition of SOUR in the presence of Cd

SOUR associated with ammonium and nitrite oxidation decreased as the initial metal concentrations increased. According to these measurements, the initial metal concentration that caused 50% inhibition was 50 and 150 mg/L for Zn and Cd, respectively. The recorded inhibition in the presence of Cu was less than 50% in the initial range of 20-150 mg/L.

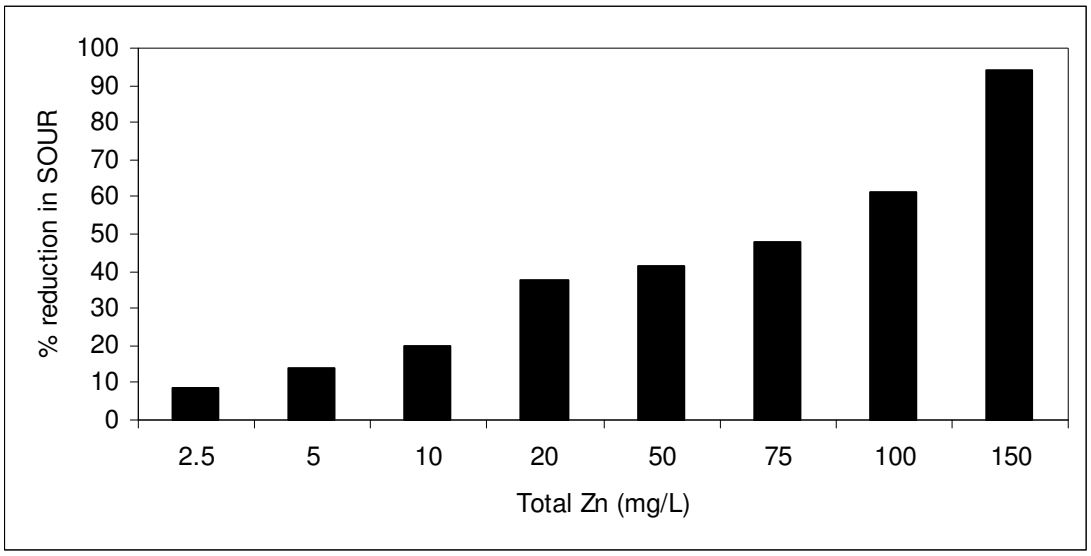

Figure 6.4. Inhibition of SOUR in the presence of Zn

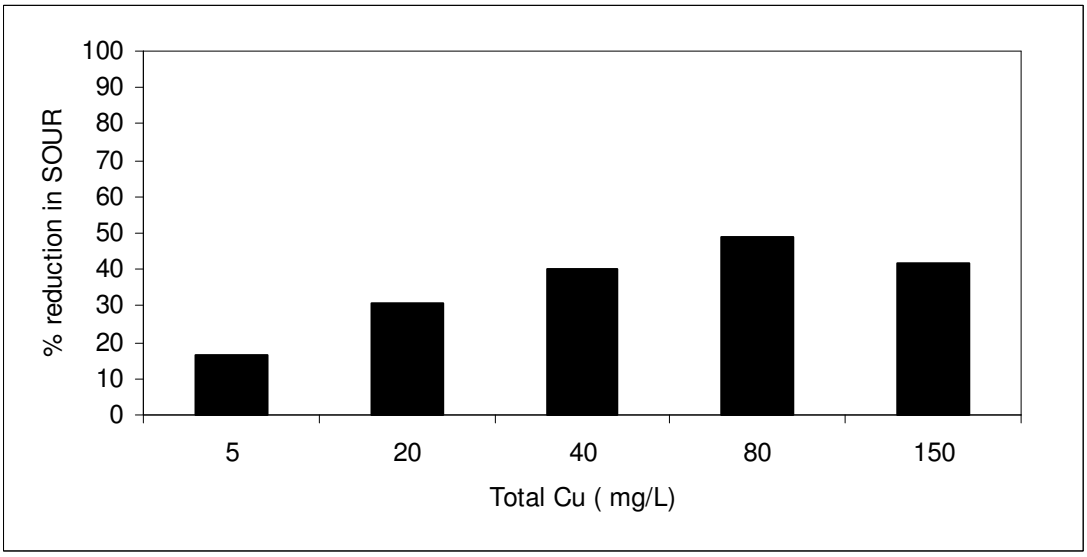

Figure 6.5. Inhibition of SOUR in the presence of Cu

It is well documented that the metal must first react with sensitive sites on the biological membrane to invoke a biological effect. Cd uptake progressed very slowly, as mentioned in literature (Hu et al., 2004). This was also observed in this study. Biosorption experiments showed that, at least 30 minutes were necessary for the completion of Cd sorption (Section 6.2.6). In short-term SOUR experiments, the DO recording was started as soon as the metal

was added into the measurement vessel and the total duration of the experiment was only 10 min (Section 5.3.1). In such a short period of time, equilibrium could not be established between Cd and its complexes in solution and Cd on the surface of the cell. This could be the main reason of observing very low inhibition levels in the case of Cd. Long-term OUR measurements with a total duration of at least 1 h showed that as the contact time of Cd with bacteria increased, the recorded inhibition increased tremendously. On the other hand, Zn is an essential metal and higher internalization fluxes would be expected for such essential metals (Hassler et al., 2004a). This could be the reason of observing higher inhibition levels in the case of Zn. Due to high internalization fluxes, Zn showed its inhibitory effect immediately and the extent of inhibition did not change with time in long-term OUR measurements as shown in Section 6.3.2.

Nevertheless, the observed EC_{50} values are not comparable with previously published values. For example Gerneay et al. (1997) applied similar OUR measurements and EC_{50} values for Cd and Cu were as 8.3 and 173 mg/L, respectively. As explained in Section 5.3.1, the pH of the solution was set to 7.5 by using phosphate buffer. The reason of contradictory results could be attributed to the formation of dissolved solids in the presence of phosphate buffer. Since no metal measurements were carried out in these experiments, the soluble metal concentrations could not be established. Comparison of the observed inhibition levels in the presence of different type of buffers will be given in Section 6.2.3.

6.2.2 The Effect of Cd, Zn and Cu on the Nitrite Oxidation Determined by SOUR Experiments in the Presence of Phosphate Buffer

In these experiments, nitrite (NO_2^-) was added to the respirometry vessel along with metals as a substrate to assess either the effect of Cd, Zn or Cu on nitrite oxidation. The results are illustrated in Figures 6.6 to 6.8. The extent of inhibition in the presence of Cd and Cu was similar and varied between 25% and 45%, whereas it was less than 50% in the presence of Zn.

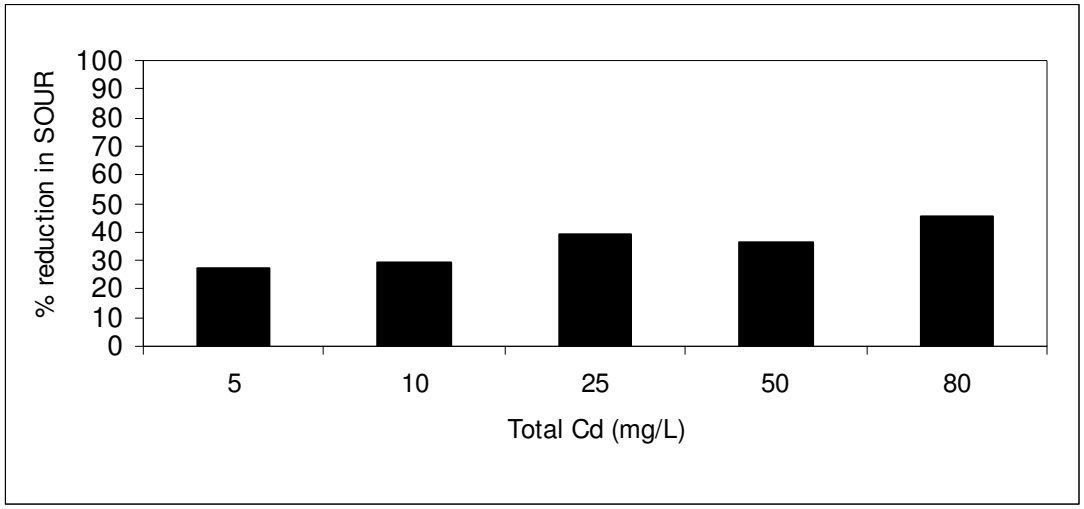

Figure 6.6. Inhibition of nitrite oxidation in the presence of Cd based on SOUR measurements

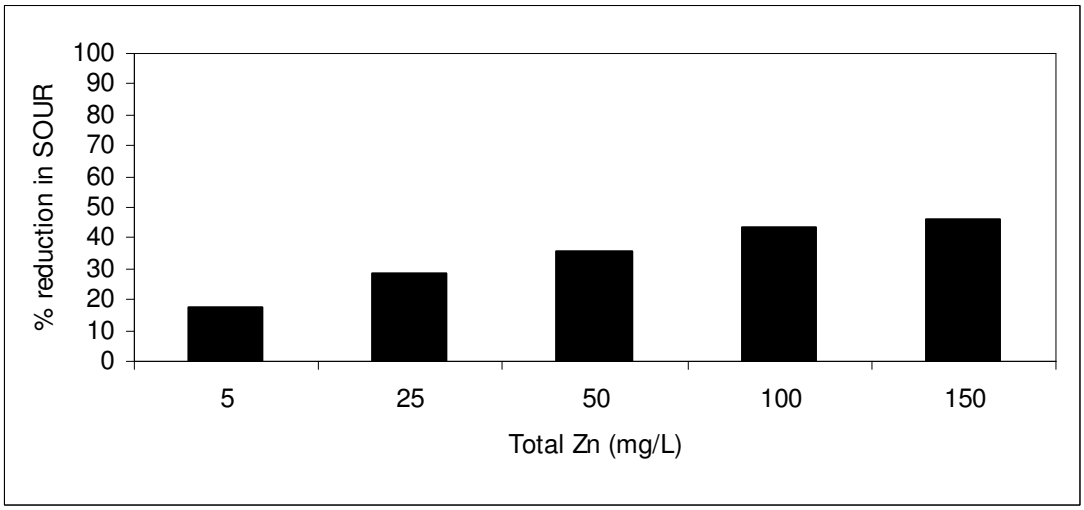

Figure 6.7. Inhibition of nitrite oxidation in the presence of Zn based on SOUR measurements

It was decided to carry out further specific ammonium utilization rate and long term oxygen uptake rate experiments with Cd and Zn since Cd is the best known toxic heavy metal and Zn is an essential metal which becomes toxic at high concentrations.

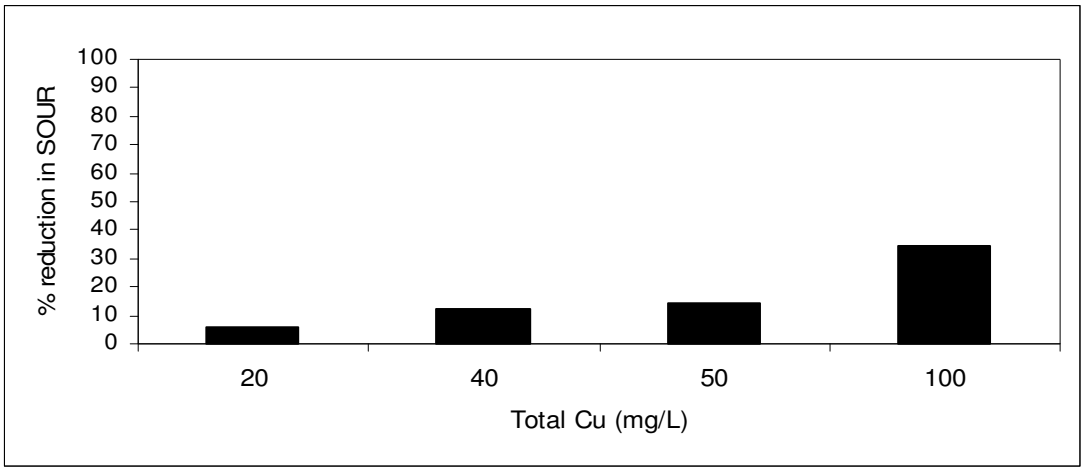

Figure 6.8. Inhibition of nitrite oxidation in the presence of Cu based on SOUR measurements

6.2.3. The effect of Cd on specific ammonium utilization rate (q_{NH_4-N}) and specific oxygen utilization rate (SOUR)

Specific ammonium utilization rates (q_{NH_4-N}) were evaluated with respect to initial and labile Cd concentrations in the range of 1-25 mg/L as shown in Figure 6.9 and summarized in Table 6.2.

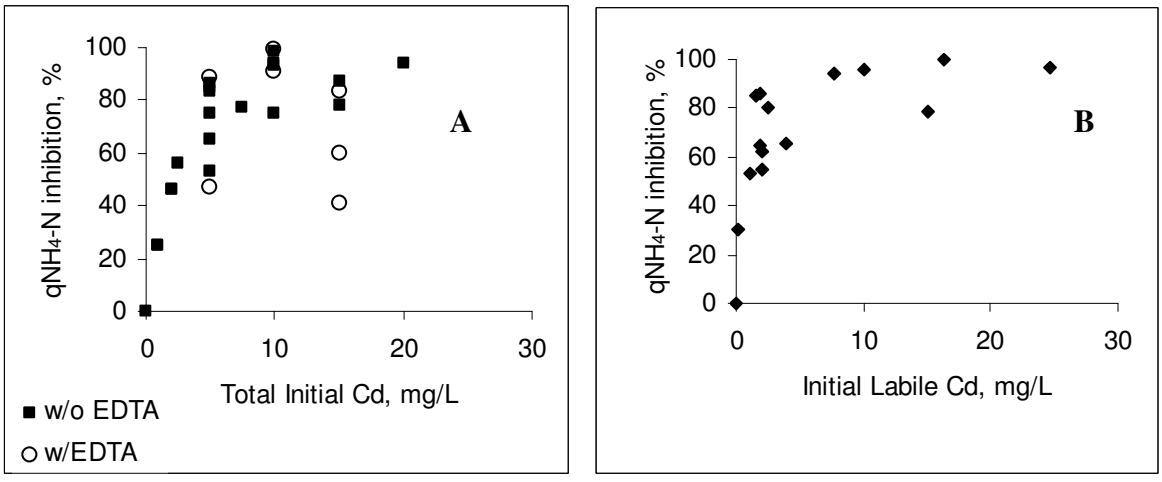

Figure 6.9. Inhibition of specific ammonium utilization rate at various a) total and b) initial labile Cd (Cd_{volt}) concentrations

Table 6.2. Results of ammonium utilization rates (q_{NH_4-N}) and specific oxygen uptake rate (SOUR) experiments

Experiment No	VSS	pH	Total Cd	Cd_{volt}		EDTA	Specific Ammonium Utilization Rate (qNH_4-N)		Specific Oxygen Uptake Rate (SOUR)		% reduction in qNH_4-N		% reduction in SOUR	
	mg/L	-	mg/L	mg/L		mol/L	mg NH_4-N /g VSS.h		mg O_2/g VSS.min		%		%	
				Initial	Final		Initial	Final	Initial	Final	Initial	Final	Initial	Final
1	260	7.3	-	-	-	-	32.0	32.0	-	-	-	-	-	-
2	390	7.4	-	-	-	-	37.0	37.0	-	-	-	-	-	-
3	420	7.5	-	-	-	-	44.0	44.0	2.10	2.30	-	-	-	-
4	588	7.5	-	-	-	-	42.5	42.5	2.20	2.40	-	-	-	-
5	207	7.6	-	-	-	-	49.0	49.0	1.99	2.32	-	-	-	-
6	210	7.7	-	-	-	-	53.3	53.3	-	-	-	-	-	-
7	303	7.2	1	1.06	0.49	-	23.8	15.8	-	-	30	53	-	-
8	266	7.4	2	2.02	0.86	-	27.1	18.1	-	-	20	47	-	-
9	293	7.7	2.5	1.87	0.95	-	28.8	14.9	-	-	15	56	-	-
10	278	7.4	5	1.82	0.95	-	9.60	6.00	-	-	72	83	-	-
11	473	7.5	5	2.46	1.06	-	12.7	4.80	-	-	63	86	-	-
12	387	7.4	5	4.24	2.24	-	42.0	17.8	2.05	0.7	4	65	12	70
13	350	7.7	5			-								
14	496	7.3	5	4.85	1.64	$1x10^{-4}$	10.9	7.20	0.85	0.14				
15	560	7.3	10	7.71	3.39	-	1.80	2.20	-	-	95	94	-	-
16	465	7.3	10	8.70	5.13	$1x10^{-4}$	12.9							
17	498	7.5	15	15.0	8.98	-	30.1	9.50	2.09	0.86	6	78	5	61
18	250	7.7	15	10.7	5.90	-	20.0	6.40	1.13	0.10	59	87	51	96
19	220	7.6	15	4.04	1.65	$1x10^{-4}$	31.8	28.8	1.91	1.61	35	41	17	30
20	350	7.7	15	1.62	1.03	$8x10^{-5}$	40.0	18.0	0.53	0.21	26	83	77	92
21	370	7.5	15	0.19	0.10	$1.2x10^{-4}$	54.1	27.6	2.14	2.04	13	60	7	11
22	360	7.3	20	16.3	10.9	-	2.80	2.10	-	-	92	94	-	-
23	407	7.4	25	24.6	7.73	-	1.63	1.23	-	-	96	97	-	-

The data in Figure 6.9 were obtained from the same set of experiments. In these experiments, MOPS buffer was used to eliminate the possibility of dissolved solid formation in the presence of phosphate buffer. For most of the cases, the extent of inhibition increased as the total or initial labile Cd increased. The degree of inhibition reached 50% for a total Cd of 2-2.5 mg/L (0.0178 to 0.022 mM) and for initial labile Cd of 1.0-2.0 mg/L. Although several studies investigated the effects of heavy metals alone or in combination with others, there is still no quantitative agreement for the inhibitory range of Cd in nitrification systems. A quite high variation in the inhibitory range can be result of the inhibition measurement methodologies and/or Cd speciation in test mediums. Furthermore, comparison of results is difficult since interpretation is based on different Cd forms. For example, Gerneay et al. (1997) and Hu et al. (2002) investigated the inhibitory effects of Cd on an enriched nitrifying sludge by specific oxygen uptake rate (SOUR) measurements and found the EC_{50} concentration as 8.30 mg/L in terms of total Cd and 31.47 mg/L in terms of free Cd, respectively.

The EC_{50} of Cd in this study with respect to total Cd is far from the values given in the literature as seen in Table 6.3.

Table 6.3. Comparison of EC_{50} values for Cd in nitrification systems

Test Culture	EC_{50} concentration, mg/L	Extent of inhibition %	Methodology	Contact time, min	References
enriched nitrifier	8.30[a]	50	Batch	10	Gerneay et al, 1997
enriched nitrifier	31.47[b]	50	Batch	15	Hu et al., 2002
enriched nitrifier	1.5[c]	50	Batch	60	this study

[a] Total Cd concentration, [b]free Cd concentration [c] initial labile Cd concentration

Recent studies have shown that the total aqueous concentration of a metal is not a good predictor of its bioavailability and toxicity. Bioavailability and toxicity are strongly related to speciation of the metal. Chemical speciation of metal changes as a result of

inorganic and organic complexation reactions (Twiss et al., 2001). The influences of Cd speciation on nitrification inhibition and application of FIAM and BLM models will be discussed in Section 6.2.5.

A poor correlation was found between total Cd and inhibition, especially for EDTA added cases, as illustrated in Figure 6.9a. For a total Cd of 15 mg/L (0.14 mM), inhibition ranged from 30% to 95.70%. On the contrary, the inhibition expressed in terms of $q_{NH4\text{-}N}$ correlated better with the initial labile Cd (6.9b). As a result of EDTA additions, the q_{NH_4-N} inhibitions relatively decreased as shown in Figure 6.10a. It is well known that EDTA addition reduces nitrification inhibition due to the formation of strong complexes with a high stability constant (Log K=18.20 M^{-}). Formation of such complexes reduced the free Cd concentration and further prevented Cd biosorption as shown in Figure 6.10 b. There is a linear correlation between the percent decrease in q_{NH_4-N} and adsorption (R^2= 0.99) (data not shown). This showed that there is a strong relationship between metal biosorption and inhibition which will be evaluated in detail in further sections.

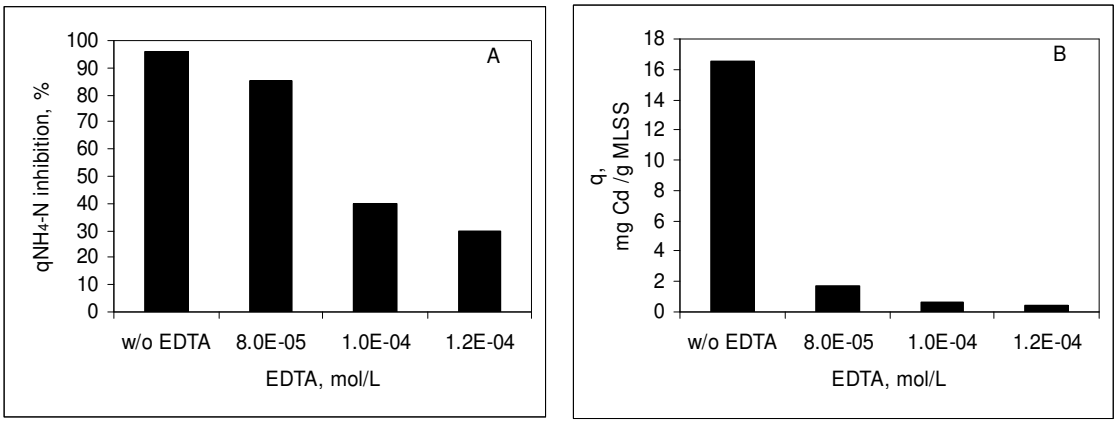

Figure 6.10. Inhibition of $q_{NH4\text{-}N}$ (a) and decrease of Cd uptake (b) as a function of the initial EDTA concentration

Specific oxygen uptake rates (SOUR) were evaluated with respect to initial Cd concentrations in the range of 1-25 mg/L as shown in Figure 6.11 and summarized in Table 6.2. Similar to the inhibition levels determined by q_{NH_4-N} measurements in Section (6.2.3), the percent decrease in SOUR increased as the initial Cd concentration increased.

Inhibition levels for the same Cd concentration were variable, especially for EDTA added cases. The EC_{50} value was around 2 mg/L in terms of total initial Cd. In general, the inhibition levels determined with SOUR measurements were 5-10% higher than those determined with q_{NH_4-N}. This showed that the nitrite oxidation step was inhibited to a lesser extent than the ammonium oxidation step which is consistent with the previous studies (Lee et al., 1997).

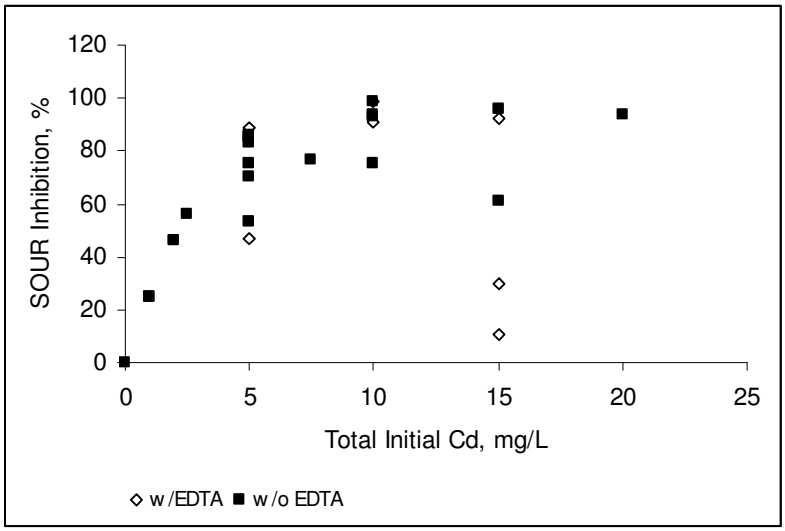

Figure 6.11. Inhibition of specific oxygen uptake rate various total initial Cd concentrations

The inhibition levels determined with long-term SOUR experiments were extremely different from the short-term SOUR experiments reported in Section 6.2.1. For example, for 5 mg/L of initial Cd, the recorded inhibition in short-term SOUR was approximately 5% whereas it ranged between 70 to 90 % in long-term SOUR. As explained in Section 6.2.1, the potential reasons of discrepancy could be the difference in the exposure time, which was 10 minutes in short-term and at least 60 minutes in long-term SOUR experiments. Another reason may be the reduction in the labile metal concentration in the presence of phosphate buffer. The effect of Cd exposure time on the extent of inhibition was given in Section 6.2.4.

The effect of phosphate buffer was investigated by conducting q_{NH_4-N} measurements for an initial Cd concentration of 0, 20, 50 and 100 mg/L. These

concentrations were selected intentionally since they covered the Cd concentration range applied in short-term OUR experiments. The pH of the reactors in the first set was controlled by phosphate buffer whereas the MOPS buffer was used in the second reactor set. The exposure time (contact time of Cd with biomass) in both reactor sets was 24 hours. The results of these experiments are shown in Figure 6.12. The initial labile Cd was measured at the beginning of experiments (shown at the top of the bars for each Cd concentration). As clearly seen, the initial labile Cd concentrations were higher in the case of MOPS addition due to noncomplexing properties. On the other hand, phosphate buffer decreased the concentration of labile Cd by forming complexes. Hence, the use of phosphate buffer was certainly one of the main reasons of observing low inhibition levels in short-term experiments and should be used very carefully for the determination of inhibition levels of metals.

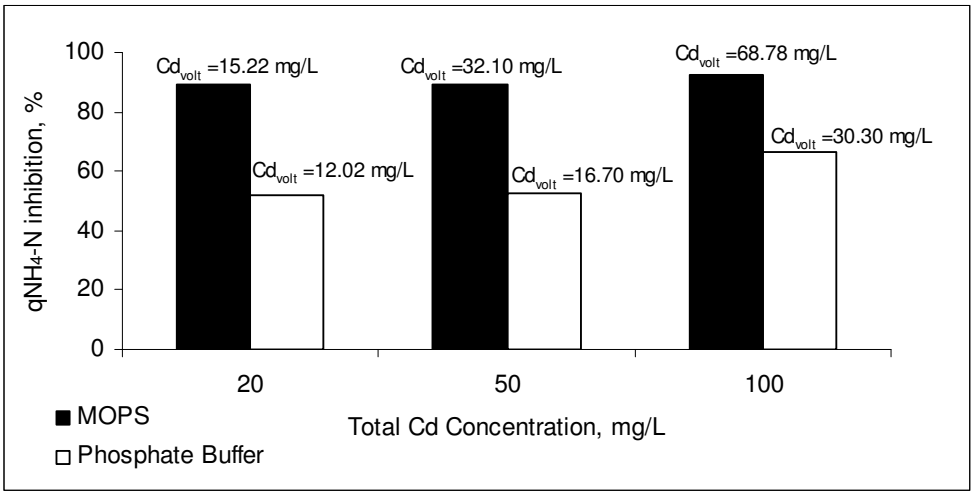

Figure 6.12. Inhibition of ammonium utilization rate (q_{NH_4-N}) at various Cd concentrations in the presence of MOPS and phosphate buffer.

6.2.4 Effect of Cd exposure time on nitrification inhibition

The effect Cd exposure on nitrification inhibition was investigated in long-term SOUR experiments. Some typical profiles in long-term SOUR measurements are shown in Figure 6.13 and 6.14. In these experiments Cd was added to the respirometric vessel after SOUR reached its maximum value. Preliminary experiments in the absence of Cd showed that SOUR generally reached its maximum value in 20-30 minutes (data not shown).

SOUR started to decrease instantaneously with Cd addition. During the course of a batch operation, the inhibitory effect of Cd on nitrification increased accordingly. Increase of the inhibition with respect to time was certainly related with the uptake of Cd into/onto sludge. As seen in Figure 6.13 and 6.14, there was an initial rapid inhibition stage followed by a second slow inhibition which is very similar to the uptake or biosorption of metals.

The duration of the initial rapid phase was almost constant for all metal concentrations and determined as 60 minutes. In this time course, metals certainly achieve equilibrium between the sludge and bulk phases, but metal internalization may still not take place (Hu et al,. 2003). The second stage of inhibition lasted to the end of the experiment. In some experiments, the second stage was not observed due to the duration of the experiment. The initial inhibition could be a result of Cd binding onto sensitive sites on the surface of the membrane, whereas the final inhibition could be associated with the sensitive sites inside the membrane.

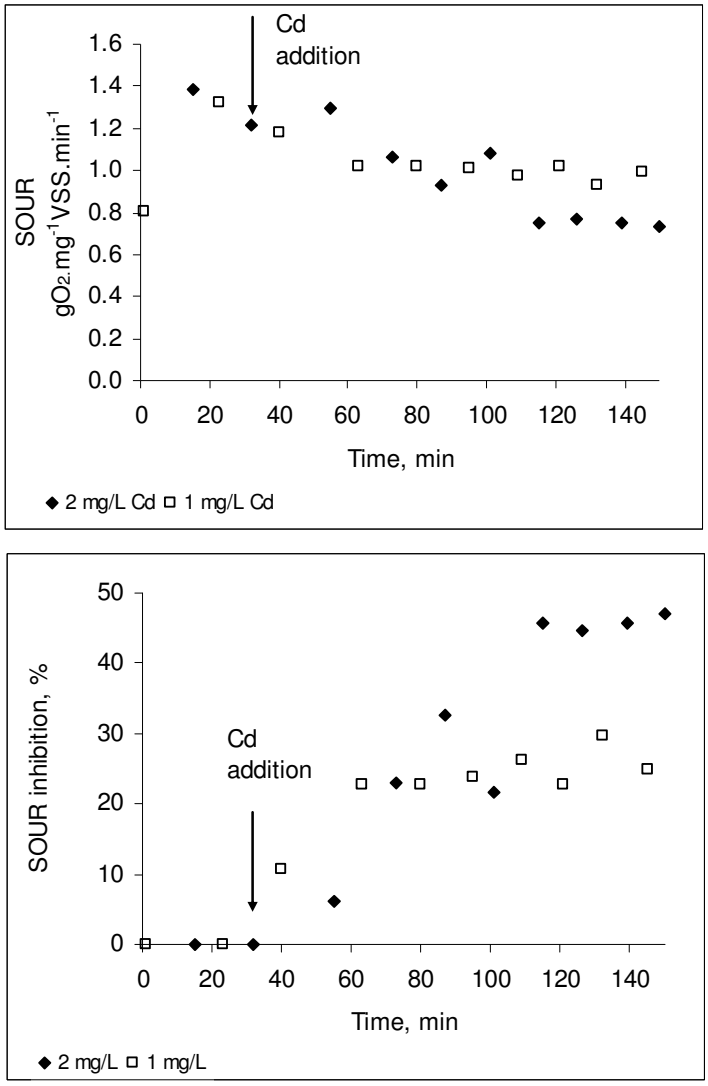

Figure 6.13. Inhibition of SOUR with respect to time in the presence of 1 and 2 mg/L of influent Cd

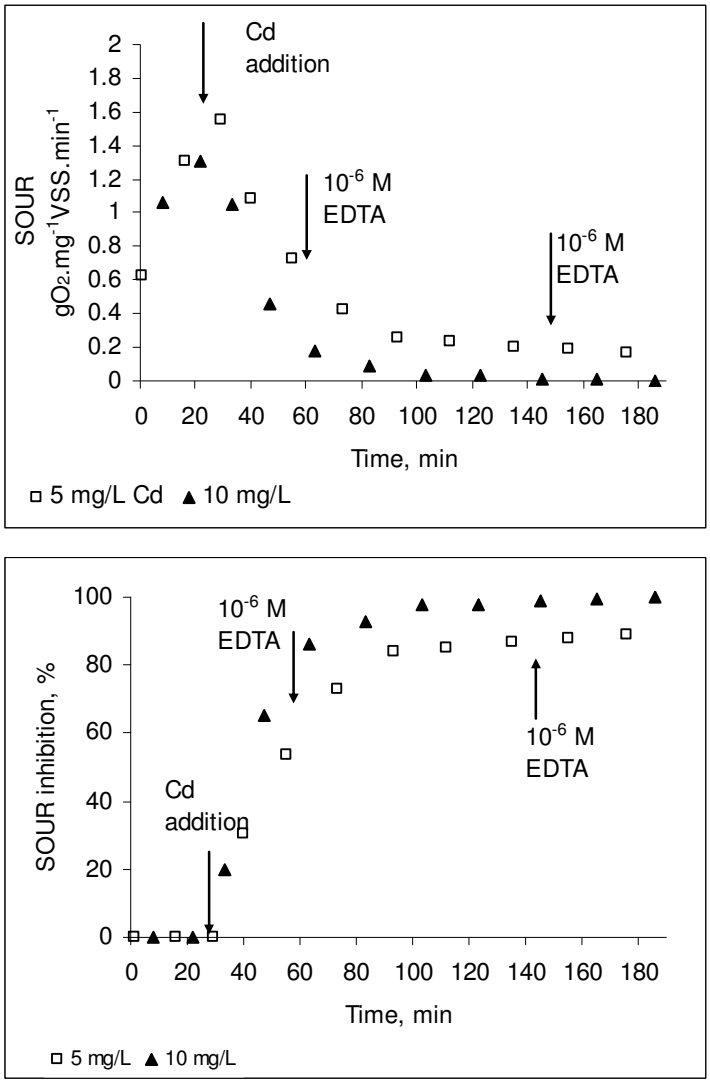

Figure 6.14. Inhibition of SOUR with respect to time in the presence of 5 and 10 mg/L of influent Cd

Overall, the results revealed that short-term SOUR responses to Cd may lead to inaccurate results. Hence, it is essential that inhibition is monitored in a long period of time to allow the uptake of metals. In a following section, the importance of Cd uptake in the determination of inhibition levels will be discussed.

6.2.5 The effect of Cd-EDTA complexation on qNH_4-N and SOUR

Complexation reaction of Cd with EDTA proceeds according to the following equation:

$$Cd + EDTA \rightarrow CdEDTA \tag{6.2}$$

Due to the high stability of the Cd-EDTA complex (log K=18.20), dissociation into free Cd is not possible. In order to understand the mechanisms in the presence of EDTA, the effect of Cd-EDTA complexation on nitrification was further investigated.

Three batch reactors were operated in parallel and qNH_4-N, SOUR and metal uptake measurements were simultaneously carried out. The first nitrification reactor was used as a control and contained only biomass and ammonium. The second reactor contained also a total Cd of 15 mg/L ($1.34x10^{-4}$ M), whereas the third one was fed with 15 mg/L Cd and $1x10^{-4}$ M EDTA. The reactors were operated under identical conditions (pH=7.5, MLSS=300 mg/L, MLVSS=240 mg/L, T=25^0C). Specific ammonium utilization rates (q_{NH_4-N}) and specific oxygen uptake rates were shown in Figure 6.15 and summarized in Table 6.4.

In the control reactor, NH_4-N utilization was linear (R^2=0.98) throughout the experimental period (Figure 6.15a) which indicated zero-order removal. The average specific ammonium utilization rate was found as 49 mg NH_4-N /g VSS.h. SOUR was initially 1.99 mg O_2/gVSS.min and reached a maximum value of 3.0 mg O_2/gVSS.min at 62 min. The corresponding NH_4-N utilization rate was 47 mg NH_4-N/g VSS.h. The decrease in SOUR to 2.32 mg O_2/gVSS.min at time 200 min could be due to nitrite

accumulation which led to a lower oxygen consumption (Figure 6.15a). This situation was also observed in previous batch experiments (data not shown).

As seen in Figure 6.15b, in the presence of 15 mg/L of Cd alone, ammonium utilization was not linear and leveled of at some value. The q_{NH4-N} value decreased gradually within the experimental time and was calculated as 20, 20**,** 12, 10 and 8.7 mg NH_4-N/g VSS.h at 0, 30, 120, 150 and 180 minutes. Reductions in q_{NH4-N} were 59, 59, 76, 79 and 82 %, respectively. Preliminary experiments had shown that ammonium utilization followed a zero-order reaction at NH_4-N concentrations exceeding 5 mg/L (Section 6.1). Therefore, the decrease in q_{NH4-N} was the result of nitrification inhibition by Cd addition and could not be attributed to substrate limitations since the lowest NH_4-N concentration was 45 mg/L in the reactor. Similarly, the SOURs were reduced by inhibition and were found as 1.13, 0.72, 0.22 and 0.10 mg O_2/gVSS.min at time 0, 38, 66 and 208 minutes (Figure 6.15b). The corresponding percent reductions in SOUR were found as 51, 68, 91 and 96%. The reductions in SOUR were approximately 14% higher than those in q_{NH4-N}. This could be attributed to the fact that SOUR represents the consumption of O_2 in both ammonium and nitrite oxidation steps (EPA, 2003).

When Cd and EDTA were simultaneously added to the third reactor, there was a small reduction in q_{NH4-N} and SOUR compared with the control reactor. The q_{NH4-N} and SOUR did not change much with time as in the case of the second reactor (Figure 6.15c). They decreased slightly to 28.8 mg NH4-N/g VSS.h and 1.61 mg O_2/g VSS.min. In the presence of Cd alone, the inhibition progressed with time due to uptake of Cd into/onto biomass. However, in EDTA added cases, ammonium utilization was linear and SOUR levels did not change much with respect to time (Figure 6.15c).

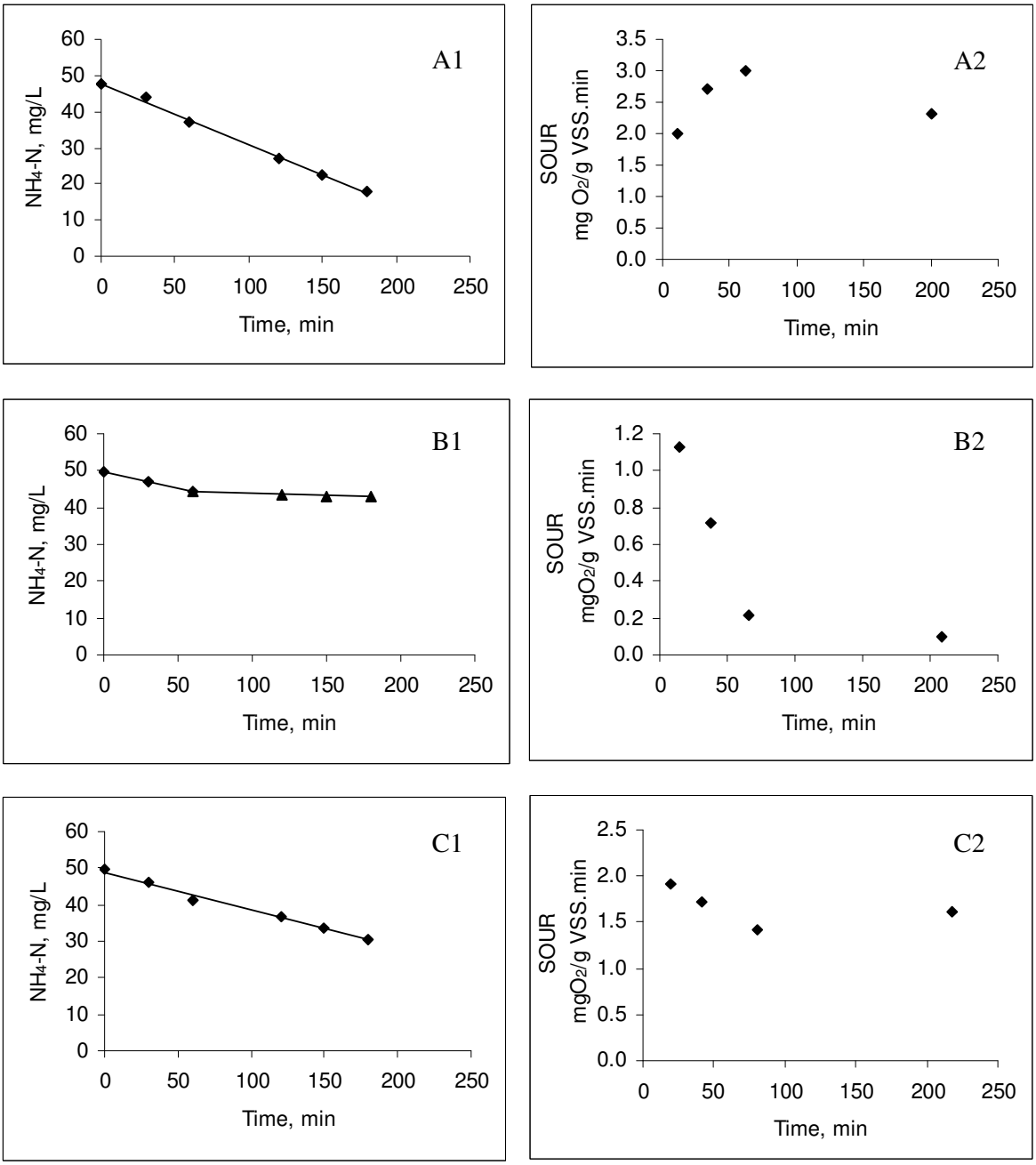

Figure 6.15. Ammonium utilization curves and SOUR profiles (A1-A2) Control reactor, (B1-B2) 15 mg/L Cd, (C1-C2) simultaneous addition of 15 mg/L Cd and $1x10^{-4}$ M EDTA

Table 6.4. Ammonium utilization rates and Cd measurements with respect to time

Time, Min	Labile Cd (Cd_{volt}) mg/L	NH_4-N utilization rate (mg NH_4-N/L.h)	q_{NH4-N} (mg NH_4-N/g VSS.h)
Reactor I –Control Reactor - 50 mg/L NH_4-N			
0	-	0.12	34.0
30	-	0.18	50.8
60	-	0.17	49.6
120	-	0.17	48.4
150	-	0.16	47.6
180	-	0.03	9.6
Reactor II –50 mg/L NH_4-N +15 mg/L Cd			
0	14.75	0.083	20
30	7.75	0.083	20
60	6.95	0.050	12
120	6.17	0.042	10.1
150	5.88	0.036	8.7
180	5.90	0.027	6.4
Reactor III – 50 mg/L NH_4-N +15 mg/L Cd + $1x10^{-4}$M EDTA			
0	4.04	0.12	32
30	2.23	0.14	38.6
60	1.89	0.11	29.5
120	1.76	0.11	29.1
150	1.88	0.11	28.8
180	1.65	0.03	9.4

The relationship between Cd uptake and inhibition rate was evaluated by comparing the Cd uptake and q_{NH_4-N} or SOUR inhibition with respect to time. In the case of Cd alone (Figure 6.16) and simultaneous Cd and EDTA addition (Figure 6.17), Cd uptake was completed in 150 and 30 min, respectively, as reported in previous studies (Nelson et al., 1981). This coincides with the change in reductions in q_{NH4-N} and SOUR with time. The inhibition stayed constant after approximately 150 minutes in the first case, whereas it reached a constant value after 30 min in the latter one. These results support that there was a relationship between Cd uptake onto sludge and inhibition. Biologically active metal species are reported to be transported to the cell surface of any organism before they exert an effect (Campbell et al., 2002). Diffusion is the first transport step from the bulk solution towards the bacterial cell and is driven by the metal concentration gradient between the bulk solution and the cell wall. In EDTA added cases, only a slight change was observed in the percent reduction in SOUR and q_{NH4-N} with time. This could be attributed to the decrease of the concentration gradient as a result of EDTA complexation with Cd species

in bulk solution. Increases in inhibition percents with respect to time sustain the suggestion that extracellular and/or intracellular metal uptake causes toxicity in biological systems. This subject will be discussed in detail in Section 6.2.5.

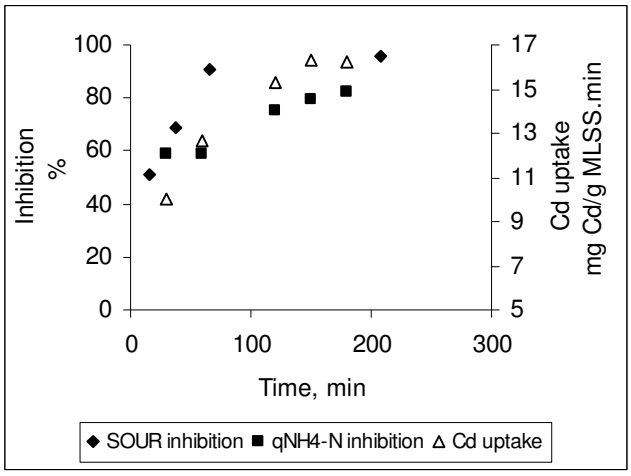

Figure 6.16. Changes in qNH_4-N, SOUR and Cd uptake with time in the presence of 15 mg/L Cd only (2^{nd} reactor)

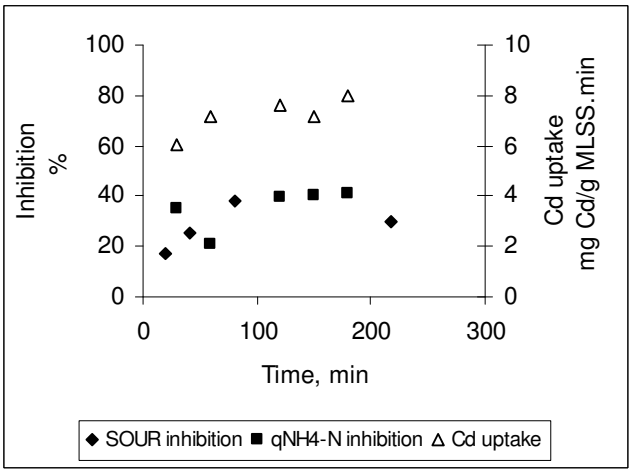

Figure 6.17. Changes in qNH_4-N, SOUR and Cd uptake with time in the presence of 15 mg/L Cd and $1x10^{-4}$ M EDTA (3^{rd} reactor)

6.2.6. Recovery from inhibition with EDTA addition

EDTA is used as a washing agent to remove metals from bacterial surfaces (Hassler et al., 2004b). Strong washing agents such as EDTA rapidly extract the metal bound to the cell wall in the first few minutes. To investigate the recovery of q_{NH_4-N} and SOUR inhibition and to find out the Cd species responsible for the percent reductions in qNH_4-N and SOUR, $1x10^{-4}$ M EDTA was added to the batch reactor (2^{nd} reactor described in Section 6.2.5) where biomass had been contacted with 15 mg/L Cd for 6.5 h. After EDTA addition, q_{NH_4-N} and SOUR measurements were carried out in the next 22 and 41 hours, respectively.

With EDTA addition, a recovery in NH_4-N removal was observed, which was almost absent with 15 mg/L Cd addition as seen in Figure 6.18. After 22 hours, the specific ammonium utilization rate increased from 8.7 to 12.2 mg NH_4-N /g VSS.h (Figure 6.18). From these figures the percent increase in q_{NH_4-N} with respect to that before EDTA addition was calculated as 28%. SOUR increased from 0.10 to 0.55 mg O_2/g VSS.min. SOUR further increased from 0.55 to 0.74 mg O_2/g VSS.min after 41 hours from EDTA addition corresponding increase. The corresponding recovery from SOUR inhibition with respect to the value before EDTA addition after 20 and 41 hours were 19.8% and 28%, respectively. The results suggest that inhibition of nitrification by Cd is a reversible process. Braam and Klapwijk (1981) observed similar results for nitrification inhibition with copper.

However, EDTA addition did not cause complete recovery from inhibition. The reason may be explained based as follows: EDTA complexes with Cd in 1:1 ratio. In this experiment, $1.34\ x10^{-4}$ M (15 mg/L) Cd was added to the biomass. Due to the high stability constant of the CdEDTA ($K_{Cd\text{-}EDTA} = 10^{18.10}$), theoretically, $1x10^{-4}$ M EDTA should extract $1x10^{-4}$ M (11.2 mg/L) extracellular Cd from the biomass. Hence, the remaining $3.376x10^{-5}$ M (3.786 mg/L) Cd could have caused the nitrification inhibition. The observed inhibition in qNH4-N and SOUR at the end of the 22 and 41 hours was 75% and 67%. The expected inhibition at 3 mg/L of total Cd was approximately 60% according to the data given in Figure 6.9 and 6.11, which definitely coincides with the inhibition observed after EDTA

addition. The results of this run indicated that sensitive sites affected by Cd could be located on the surface of the cell. In other words, the extracellular Cd fraction caused nitrification inhibition. Since no Cd measurements were carried out after EDTA addition, the results could not be supported metal measurements.

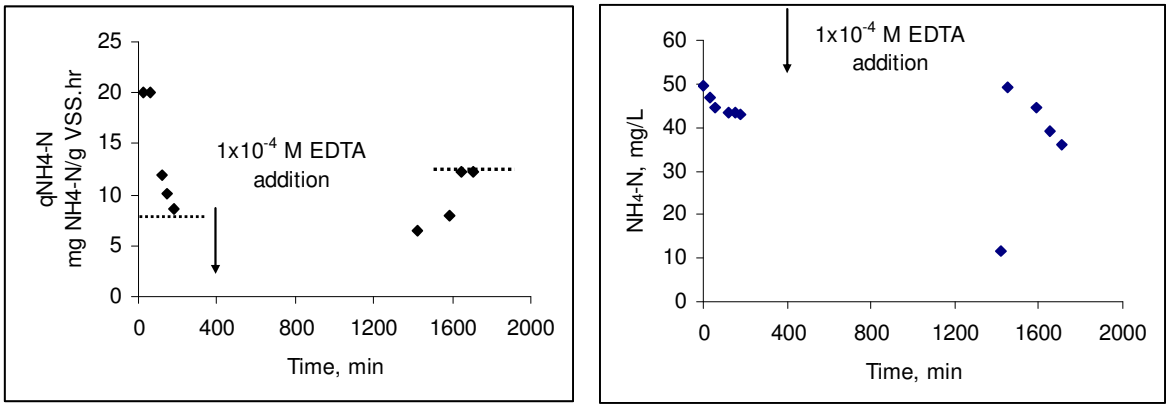

Figure 6.18. q_{NH_4-N} and NH_4-N measurements after EDTA addition with respect to time

To support our interpretation about the location of sensitive sites and to investigate the importance of the EDTA/Cd ratio on nitrification inhibition recovery, another set of experiments was conducted. For this purpose, EDTA was added to two parallel batch reactors, which had been contacted with Cd for 30 min (Figure 6.19) to investigate the recovery from SOUR inhibition and the Cd species leading to inhibition. SOUR measurements were carried out at certain time intervals. In the present study, the use of EDTA removed the biosorbed Cd and thus led to a relief from inhibition as seen in Figure 6.19a and 6.19b. Adsorbed Cd was quantitatively extracted at approximately 98% for a molar EDTA/Cd ratio of 1.82. Actually, the ratio was slightly lower than the effective EDTA concentration since Ca, Mn, Mg, Fe and Na also form complexes with EDTA. Thermodynamically, the distribution of $2x10^{-4}$ M EDTA among dissolved species was as follows: 55.7 % CdEDTA, 17.3% FeEDTA, 14.8% MnEDTA, 2.9% MgEDTA, 8.6% CaEDTA. Concentration of Cd species in the test medium under experimental conditions is given in Table 6.5. As seen from Table 6.5, calculated labile Cd concentration was 4.06 mg/L which was very close to the labile Cd measured with voltammetry after 30 minutes (Cd_{volt}= 4.61 mg/L). This showed that the distribution of Cd in soluble and suspended

phase was predicted successfully with the conditional stability constant (log K=4.47 M^{-}) (Section 6.2.7).

Cd extraction from cell surface led to a noticeable recovery and the same SOUR level was reached as before Cd addition (Figure 6.19). Recovery from inhibition was abrupt with EDTA addition and the recovery rate was almost the same at different Cd concentrations as seen from Figure 6.19 (slope of the SOUR curve during recovery). Extraction of adsorbed Cd was completed in an EDTA contact time of 2 min. As shown in Figure 6.19b, almost no Cd remained on the biomass. It is a known fact that efflux of internalized metal does not occur when the contact time with EDTA is less than 5 min for different Cd loadings (Hassler et al., 2004b). Our findings indicate that Cd sorbed to sensitive sites on the membrane surface (extracellular fraction) could be responsible for inhibition since only surface-bound Cd could be removed with EDTA extraction (Hassler et al., 2004b). The recovery efficiency is highly related with the extraction efficiency, which in turn is dependent on the effective $EDTA_{eff}$ /Cd ratio. This ratio should be at least 1:1 to achieve considerable extraction (Hassler et al., 2004b) since Cd forms 1:1 complexes with EDTA. Therefore, for practical purposes, it is likely that a nitrifying sludge exposed to Cd for a long time and retaining Cd may recover from inhibition by EDTA addition. But, in real cases the Cd and EDTA are simultaneously present in a municipal wastewater treatment plant in a concentration range of 0.2-1.2 µg/L and 30 to 50 µg/L, respectively (Alder et al., 1990, Petrasek et al.,1983). Therefore, Cd is already complexed at the beginning and inhibition is not as severe as when Cd is alone.

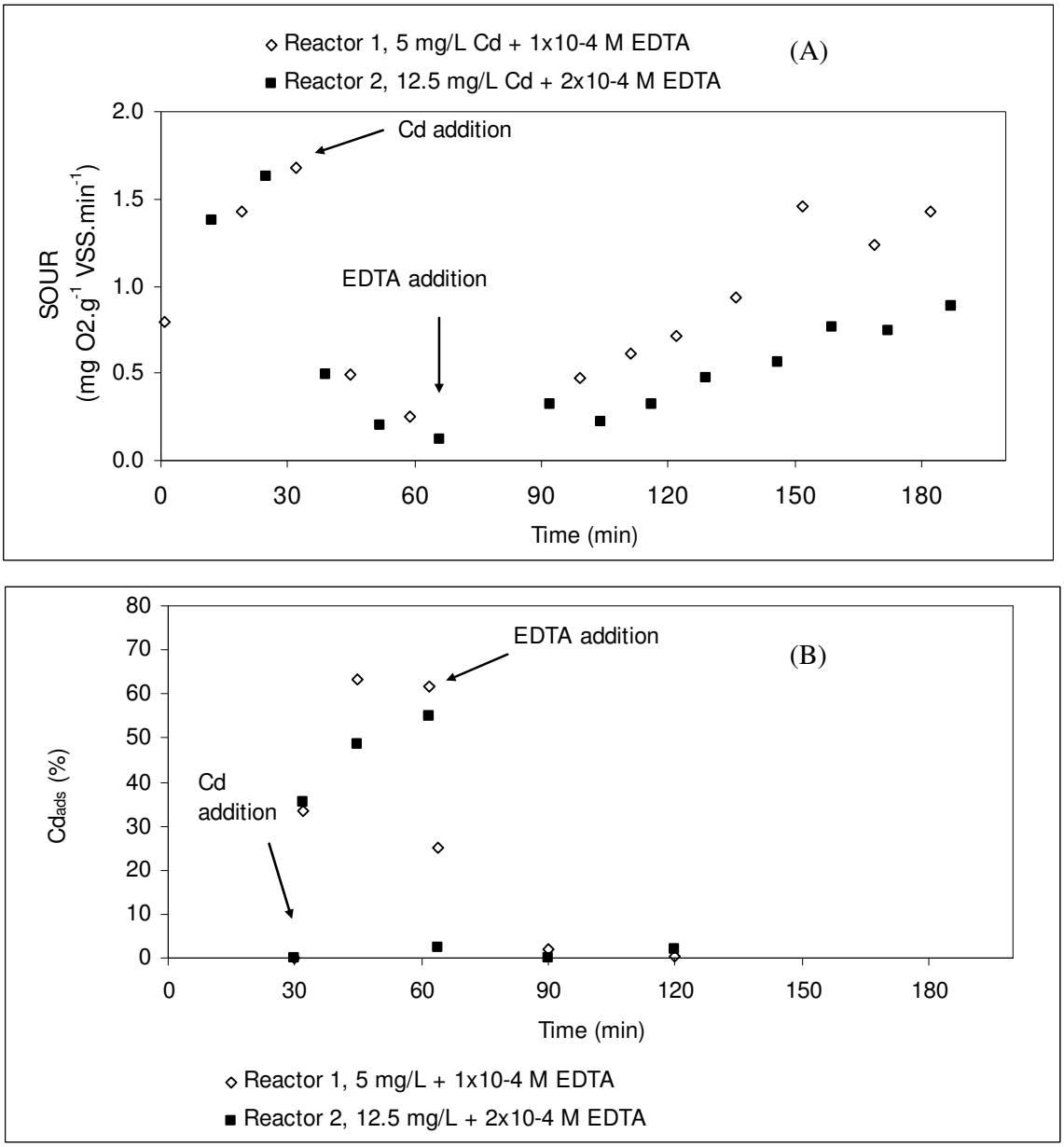

Figure 6.19. Recovery of nitrification inhibition with EDTA addition

Table 6.5. Equilibrium concentrations of soluble and suspended phase Cd species (Cd_T=12.5 mg/L) before and after $2x10^{-4}$M EDTA addition (calculated with MINEQL +4.5 and measured with voltammetry)

	Before EDTA addition		After EDTA addition	
	mol/L	mg/L	mol/L	mg/L
Cd^{2+}	$2.231x10^{-5}$	2.50	$7.23x10^{-11}$	<0
CdBiomass	$7.488x10^{-5}$	8.397	$3.32x10^{-10}$	<0
$Cd(OH)_3^-$	$9.268x10^{-15}$	<0.0	$2.999x10^{-20}$	<0
$Cd(OH)_4^{2-}$	$1.378x10^{-21}$	<0.0	$4.47x10^{-27}$	<0
$CdOH^+$	$6.847x10^{-8}$	0.008	$2.216x10^{-13}$	<0
$Cd(OH)_{2aq}$	$2.209x10^{-10}$	<0	$7.144x10^{-16}$	<0
Cd_2OH^{3+}	1.354x10-^{11}	<0	$1.42x10^{-22}$	<0
$CdHCO_3^+$	$4.118x10^{-7}$	0.0462	$1.334x10^{-11}$	<0
$CdCO_3$(aq)	$9.821x10^{-6}$	1.10	$3.178x10^{-11}$	<0
$CdSO_4^{2-}$	$9.806x10^{-8}$	0.011	$3.202x10^{-13}$	<0
$CdSO_4$(aq)	$3.47x10^{-6}$	0.3891	$1.126x10^{-11}$	<0
CdEDTA	-	-	$1.115x10^{-4}$	12.5
CdHEDTA	-	-	$2.459x10^{-9}$	<0
Fe[EDTA]	-	-	$3.464x10^{-5}$	-
FeH[EDTA]	-	-	$4.396x10^{-10}$	-
FeOH[EDTA]	-	-	$1.319x10^{-6}$	-
$Fe(OH)_2$[EDTA]	-	-	$6.687x10^{-9}$	-
Mn[EDTA]	-	-	$2.958x10^{-5}$	-
MnH[EDTA]	-	-	$1.034x10^{-9}$	-
Mg[EDTA]	-	-	$5.74x10^{-6}$	-
MgH[EDTA]	-	-	$1.59x10^{-9}$	-
Ca[EDTA]	-	-	$1.72x10^{-5}$	--
CaH[EDTA]	-	-	$5.743x10^{-10}$	-
Na[EDTA]	-	-	$2.268x10^{-11}$	-
Labile Cd, MINEQL	$4.5x10^{-5}$	4.06	-	12.50
Adsorbed Cd, Cd_{bio}	$8.741x10^{-5}$	9.80	-	0
Labile Cd, Cd_{volt}*	$4.916x10^{-5}$	4.61	-	12.19

*Labile Cd measured with voltammetry before and after EDTA addition

6.2.7. The effect of Cd speciation on nitrification

In order to evaluate the effects of Cd speciation on nitrification inhibition, percent reductions in specific ammonium utilization rates (i) shown in Table 6.2, on page 95 were correlated to different forms of Cd in the test medium (Table 5.1). Steady-state models such as Free Ion Activity Model (FIAM) or the Biotic Ligand Model (BLM) suppose that the metal and its complexes are in equilibrium. Therefore, equilibrium concentrations of Cd were used through the modelling of inhibition according to Cd speciation.

Equilibrium concentrations of Cd in the soluble phase and bound to bacterial surface were calculated thermodynamically by MINEQL+ (version 4.5) as explained in Section 5.3.3.

The test medium used in all batch experiments throughout the study contains inorganic complexing ions such as HCO_3^-, CO_3^{-2}, SO_4^{-2} and PO_4^{-3}. These ions form weak inorganic Cd complexes and could be dissociated into free Cd during voltammetric measurements. Degryse et al. (2006) have recently observed that weak dissolved Cd complexes can increase Cd uptake when transport limitations of the Cd to the uptake site prevail. Therefore, in addition to the free Cd and surface bound Cd during specific ammonium utilization rate experiments, labile Cd measured by voltammetry (shown as Cd_{volt}) was also used.

In the absence of EDTA, equilibrium concentrations of the free, labile and surface-bound Cd represented approximately 33%, 46% and 54% of the total Cd, respectively. Equilibrium concentrations of Cd species in the presence of inorganic and/or organic complexing agents during batch experiments are shown in Table 6.6.

In this study, bulk NH_4-N concentration is always greater than the $K_{S,N}$. In such cases ($K_{S,N} \ll S$) expression of specific ammonium utilization rate in the presence of noncompetitive inhibitors (Eq. 6.2) will be simplified as

$$q_{NH_4-N\,inhibited} = \frac{q_{\max,NH_4-N}}{(1+\frac{I}{K_i})} = q_{\max,NH_4-N}(\frac{K_i}{K_i+1}) \qquad (6.3)$$

and by substituting Equation 6.1 and and 6.3 into Equation 5.2 , the degree of inhibition (i) can be expressed as a function of the inhibitor concentration and the inhibition constant as given in Equation 6.4.

$$i = (\frac{I}{K_i + I})\,\text{x}100 \qquad (6.4)$$

where

i = degree of inhibition, %

I = metal concentration, mg/L

K_i = inhibitor coefficient, mg/L

Correlations of ammonium utilization rate inhibition (i) with different forms of Cd are given in Figure 6.20. A saturation-type relationship as in Equation 6.5 was obtained between inhibition and the respective metal concentration as also done in other studies (Hu et. al., 2002). Inhibition constant, K_i, in Equation 6.4 and K_M given in Equation 6.5 are analogous to each other. Thus, Cd was found to be a noncompetitive inhibitor.

$$i = i_{\max}\,\frac{I}{K_M + I}\,\text{x}100 \qquad (6.5)$$

where, $i_{\max}$ and i represents the q_{NH_4-N} inhibition percentages, %

I= either biosorbed Cd (Cd_{bio}), Cd in voltammetry (Cd_{volt}), free Cd in MINEQL (Cd^{2+}), mg/L

K_M=Cd concentration that caused 50% reduction in q_{NH_4-N} rate, analog to EC_{50}, mg/L

Least square nonlinear regression was applied to find the model parameters in Eq.6.3 using the data given in Table 6.2 and 6.6. Then, the maximum inhibition percentage, $i_{\max}$ and EC_{50} (or K_M) values were obtained for each form of Cd as shown on related Figures 6.20a-c. With these values the model curves in Figure 6.20a-c were drawn to compare

experimental and model results. Inhibition could be expressed with all three forms of Cd. That suggested that both Free Ion Activity Model (FIAM) and Biotic Ligand Model (BLM) were applicable under the conditions of this study. In each case, the nonlinear regression had a high correlation coefficient and the residuals were randomly distributed. The 95% confidence intervals shown in Figure 6.20a-c further demonstrate the validity of the models. Here the superiority of using voltammetry was highlighted for Cd speciation in nitrification. Voltammetric results show that the true values of free and labile Cd, correlate better with inhibition values in the absence and presence of complexing agents and eliminate the need of assumptions in chemical equilibrium models.

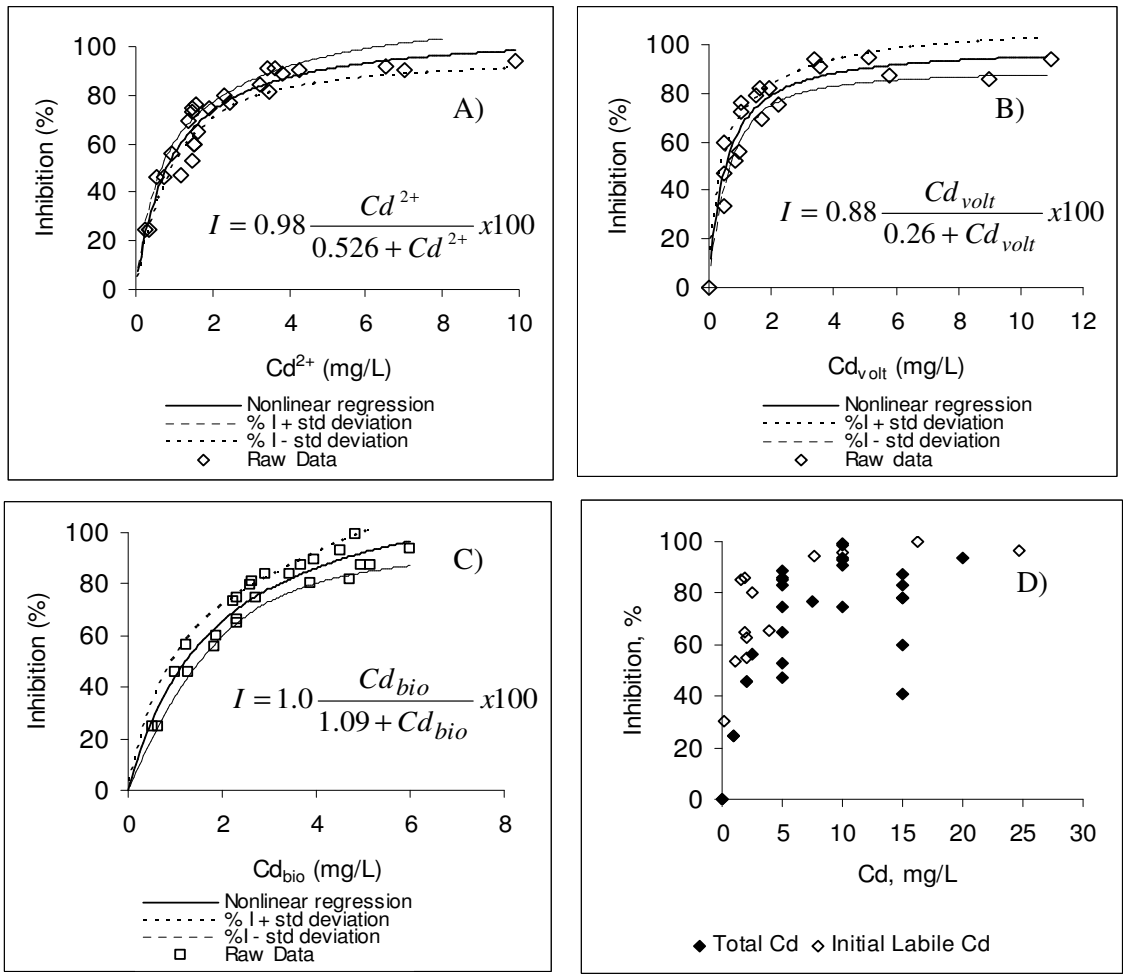

Figure 6.20. Relationship between inhibition and different forms of Cd (a) eq. free Cd calculated by MINEQL, (b) eq. labile Cd measured with voltammetry, (Cd_{volt}) (c) eq. adsorbed Cd calculated with MINEQL (d) initial total and labile Cd

Table 6.6. Cadmium speciation in ammonium utilization experiments

Sample No	Total Cd	EDTA	Calculated Labile Cd (free Cd+Cd in weak inorganic complexes)			Cd in strong complexes	Surface bound Cd (Cd_{bio})	Cd measured by volt.
	mol/L [mg/L]	mol/L	mol/L [mg/L]			mol/L [mg/L]	mol/L [mg/L]	mol/L [mg/L]
			Cd^{2+}	Inorganic Cd complexes	Total labile	CdEDTA	Cd-bacteria	Cd_{volt}
1	$4.45x10^{-5}$ [4.99]	-	$1.33x10^{-5}$ [1.491]	$6.18x10^{-6}$ [0.690]	$1.95x10^{-5}$ [2.185]	-	$2.49x10^{-5}$ [2.792]	$8.48x10^{-6}$ [0.951]
2	$2.23x10^{-5}$ [2.5]	-	$5.92x10^{-6}$ [0.664]	$3.22x10^{-6}$ [0.360]	$9.14x10^{-6}$ [1.025]	-	$1.31x10^{-5}$ [1.469]	$8.44x10^{-6}$ [0.947]
3	$8.92x10^{-6}$ [1.0]	-	$2.40x10^{-6}$ [0.269]	$6.64x10^{-7}$ [0.070]	$3.06x10^{-6}$ [0.310]	-	$5.84x10^{-6}$ [0.655]	$4.44x10^{-6}$ [0.498]
4	$1.78x10^{-5}$ [1.99]	-	$4.94x10^{-6}$ [0.554]	$1.61x10^{-6}$ [0.180]	$6.55x10^{-6}$ [0.735]	-	$1.12x10^{-5}$ [1.256]	$7.6x10^{-6}$ [0.855]
5	$4.45x10^{-5}$ [4.99]	-	$1.34x10^{-5}$ [1.503]	$5.82x10^{-6}$ [0.650]	$1.92x10^{-6}$ [2.155]	-	$2.51x10^{-5}$ [2.815]	$9.49x10^{-6}$ [1.064]
6	$8.89x10^{-5}$ [9.96]	-	$3.19x10^{-5}$ [3.577]	$1.38x10^{-5}$ [1.550]	$4.57x10^{-5}$ [5.130]	-	$4.28x10^{-5}$ [4.80]	$3.028x10^{-5}$ [3.396]
7	$1.78x10^{-4}$ [19.9]	-	$8.0x10^{-5}$ [8.971]	$3.49x10^{-5}$ [3.920]	$1.15x10^{-4}$ [12.89]	-	$6.20x10^{-5}$ [6.953]	$9.767x10^{-5}$ [10.95]

Table 6.6. (Contiuned)

Sample No	Total Cd	EDTA	Calculated Labile Cd (free Cd+Cd in weak inorganic complexes),			Cd in strong complexes	Surface bound Cd (Cdbio)	Cd measured by volt.
	mol/L [mg/L]	mol/L	mol/L [mg/L]			mol/L [mg/L]	mol/L [mg/L]	mol/L [mg/L]
			Cd^{2+}	Inorganic Cd complexes	Total labile	CdEDTA	Cd-bacteria	Cd_{volt}
8	$4.45x10^{-5}$ [4.99]	-	$1.39x10^{-5}$ [1.559]	$4.85x10^{-6}$ [0.540]	$1.87x10^{-5}$ [2.102]	-	$2.57x10^{-5}$ [2.882]	$2.0x10^{-5}$ [2.240]
9	$1.34x10^{-4}$ [15.02]	-	$5.77x10^{-5}$ [6.470]	$2.03x10^{-5}$ [2.280]	$7.80x10^{-5}$ [8.750]	-	$5.56x10^{-5}$ [6.235]	$8.0x10^{-5}$ [8.975]
10	$1.34x10^{-4}$ [15.02]	$1.0x10^{-4}$	$1.05x10^{-5}$ [1.177]	$4.82x10^{-6}$ [0.540]	$1.53x10^{-5}$ [1.718]	$8.51x10^{-5}$ [9.543]	$2.09x10^{-5}$ [2.344]	$1.48x10^{-5}$ [1.661]
11	$1.34x10^{-4}$ [15.02]	-	$3.35x10^{-5}$ [3.757]	$1.17x10^{-5}$ [1.310]	$4.52x10^{-5}$ [5.063]	-	$1.39x10^{-5}$ [1.559]	$5.19x10^{-5}$ [5.815]
12	$1.34x10^{-4}$ [15.02]	$8.0x10^{-5}$	$1.53x10^{-5}$ [1.716]	$8.33x10^{-6}$ [0.930]	$2.36x10^{-5}$ [2.650]	$7.88x10^{-5}$ [8.840]	$2.75x10^{-5}$ [3.084]	$8.9x10^{-6}$ [1.00]
13	$1.34x10^{-4}$ [15.02]	$1.2x10^{-4}$	$5.19x10^{-6}$ [0.582]	$2.08x10^{-6}$ [0.23]	$7.27x10^{-6}$ [0.816]	$1.14x10^{-4}$ [12.784]	$1.17x10^{-5}$ [1.312]	$1.7x10^{-6}$ [0.193]

If Atomic Absorption Spectroscopy (AAS) is used, the total soluble metal and not the free Cd concentration can be measured. Therefore, in order to apply the inhibition model basing on free and biosorbed Cd, using the equations in Figure 6.20a and 6.20c, one should know the exact composition and pH of water or wastewater. Most of the time, the determination of composition is difficult and time consuming**.** The stability constant of the organic matter-metal complex and adsorption constant of Cd binding to sensitive sites should be known to calculate the free Cd ion or biosorbed Cd. On the other hand, the inhibition model based on Cd_{volt} (labile Cd concentration) is easy to use in practical applications. It only requires the measurement of the labile metal concentration with voltammetry.

The measurement methodologies applied in assessing heavy metal inhibition in biological systems should be carefully selected since physical and chemical speciation highly affects inhibition. A quite high Cd level may surprisingly lead to low inhibition in nitrification due to the complexing potential of Cd with inorganic and organic ligands. The diffusion of the metal to the sensitive sites could be retarded as a result of the decrease in the concentration gradient between the Cd in the bulk solution and on the surface of biomass. The complexation of metal may inhibit biosorption. In such cases, short-term activity measurement methods having a total duration of 5 or 10 min may lead to misleading information about the inhibitory values, especially for metals with slow uptake kinetics like Cd.

Inhibition was completely reversible when EDTA concentration was in excess compared to the metal concentration. This recovery from inhibition with EDTA addition supports the idea that rather Cd sorbed to sensitive sites on the membrane surface (extracellular fraction) could be responsible for nitrification inhibition. Both the FIAM and BLM models basing on the free metal ion activity and the biosorbed metal concentration were successfully applied in this study. A novelty in this study was to determine labile Cd analytically by voltammetry for nitrification inhibition. The good correlation between labile Cd and nitrification inhibition indicated that also weak Cd complexes could contribute to inhibition besides free Cd. This leads to the result that the labile metal concentration should also be considered in reporting inhibition levels. Therefore, the use of voltammetry is recommended in the assessment of the

relationship between inhibition and metal speciation. The major findings in this section were reported in the form of a paper (Semerci and Çeçen, 2007).

6.3. Biosorption of Cd onto Nitrifying Biomass

As explained in Section 5.4, uptake of Cd onto biomass was studied under the following test mediums conditions;

3. Biosorption of Cd onto biomass in test mediums consisting of Cd and SO_4^{-2} for an initial Cd range of 1-100 mg/L.
4. Biosorption of Cd onto biomass in ammonium utilization rate (q_{NH_4-N}) experiments. In these experiments the test mediums contained inorganic complexing ions such as HCO_3^-, CO_3^{-2}, SO_4^{-2}.

6.3.1. Biosorption of Cd in the presence of SO_4^{-2}

Changes in labile Cd (Cd_{volt}) concentration for an initial Cd range of 1-10 and 25-100 mg/L during the course of the adsorption experiments are shown in Figure 6.21 and 6.22. Completion of sorption is achieved when the Cd concentration remains constant in the bulk liquid. For all initial Cd concentrations, there was an initial rapid uptake stage followed by a second slow uptake as illustrated in Figure 6.23 and 6.24. The results showed that the metal sorption was more efficient in the initial rapid uptake stage. At 1 mg/L Cd, 88% of biosorption was complete within the 60 minutes of contact and microorganisms slowly took up the remaining 8.10% during the 120 minutes of contact. These results agree with the two-stage adsorption mechanisms proposed in the literature (Nelson et al., 1981, Arican et al., 2002). The first rapid uptake completed within the first hour corresponds to the passive uptake, while the second slow stage seems to be metabolism-dependent intracellular uptake. There was a slight increase in pH during biosorption and equilibrium pH varied with the initial Cd (Figure 6.25). In the pH range of 6-8, activated sludge bacteria are negatively charged and hydrolyzed metal enhances the adsorption of metal on to negatively charged surface. Hence, the pH increase observed during biosorption may be an indication of passive Cd uptake which is also consistent with previous studies (Arican and Yetiş, 2002, Benguella and Benaissa, 2002).

Adsorption occurred rapidly and nearly reached to equilibrium within approximately 40 minutes for initial Cd concentrations of 1, 2.5, 5 and 10 mg/L which is consistent with previous studies (Nelson et al., 1981). On the other hand, the time necessary to reach equilibrium for 25, 50 and 100 mg/L Cd, increased to 60 minutes.

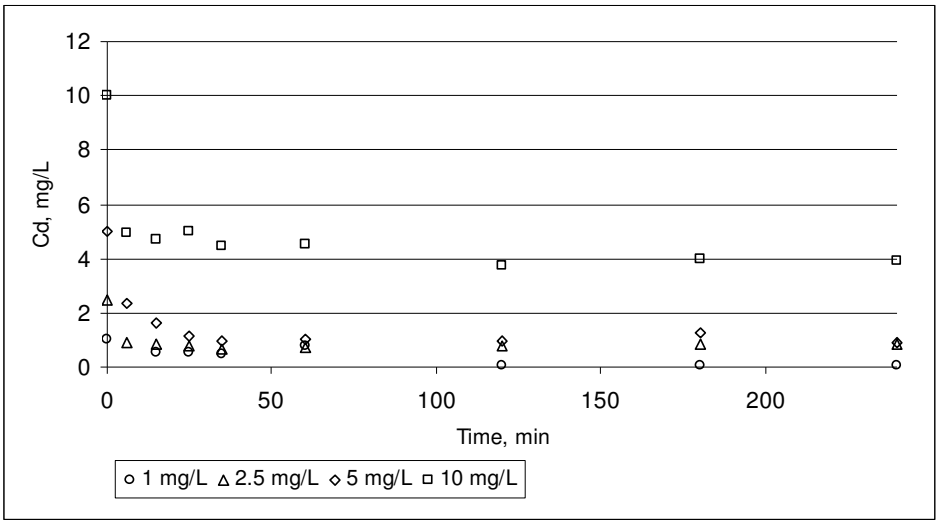

Figure 6.21. Change in bulk labile Cd with time for an initial Cd range of 1-10 mg/L

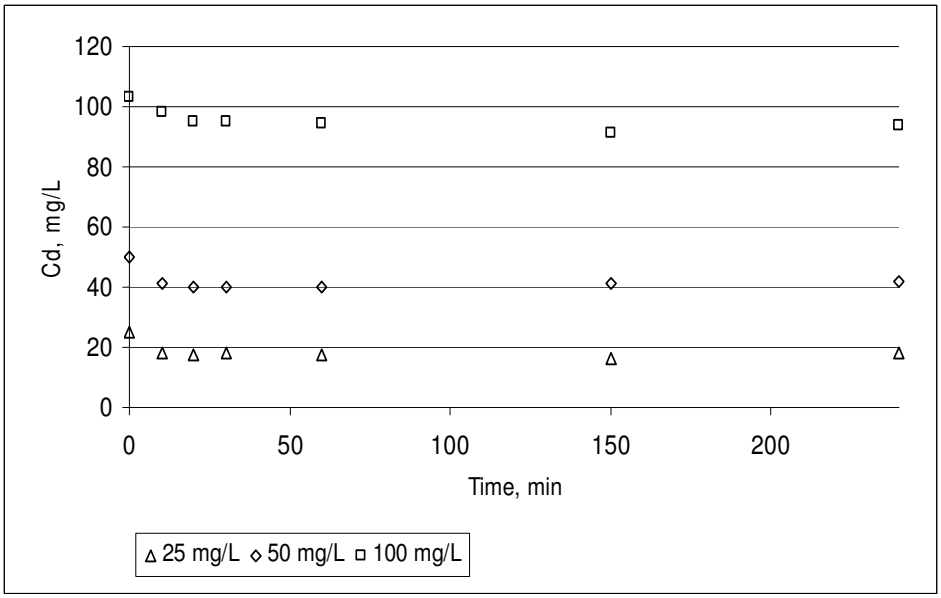

Figure 6.22. Change in bulk labile Cd with time for an initial Cd range of 25-100 mg/L

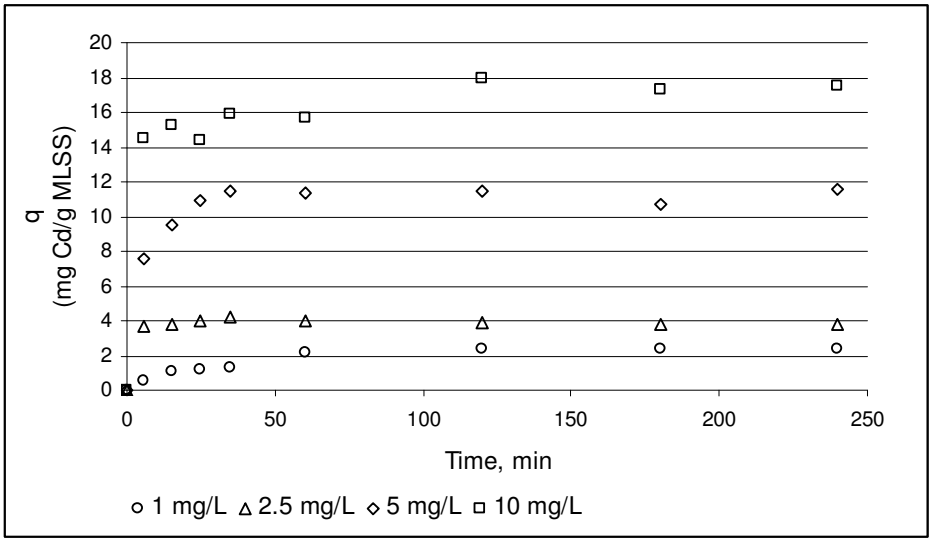

Figure 6.23. Adsorption capacity of for an initial Cd concentration of 1-10 mg/L

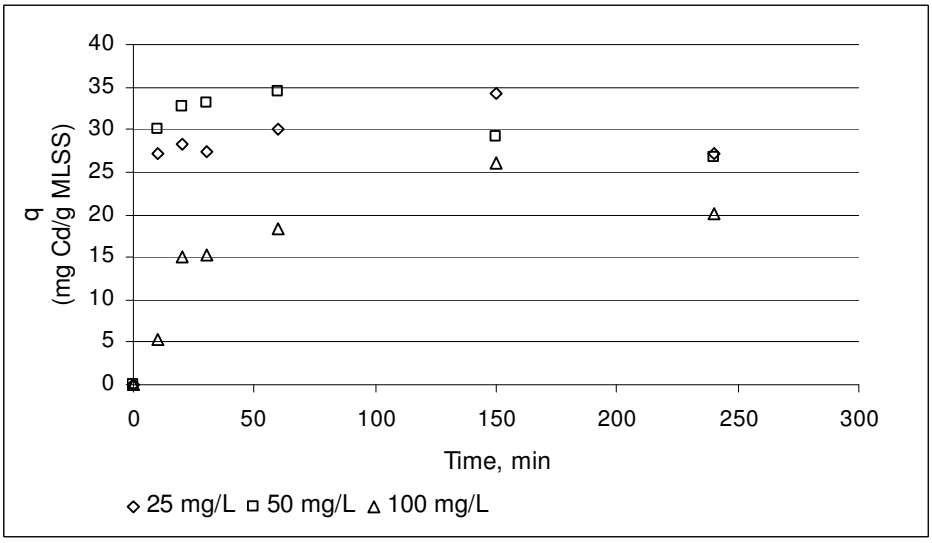

Figure 6.24. Adsorption capacity of for an initial Cd concentration of 25-100 mg/L

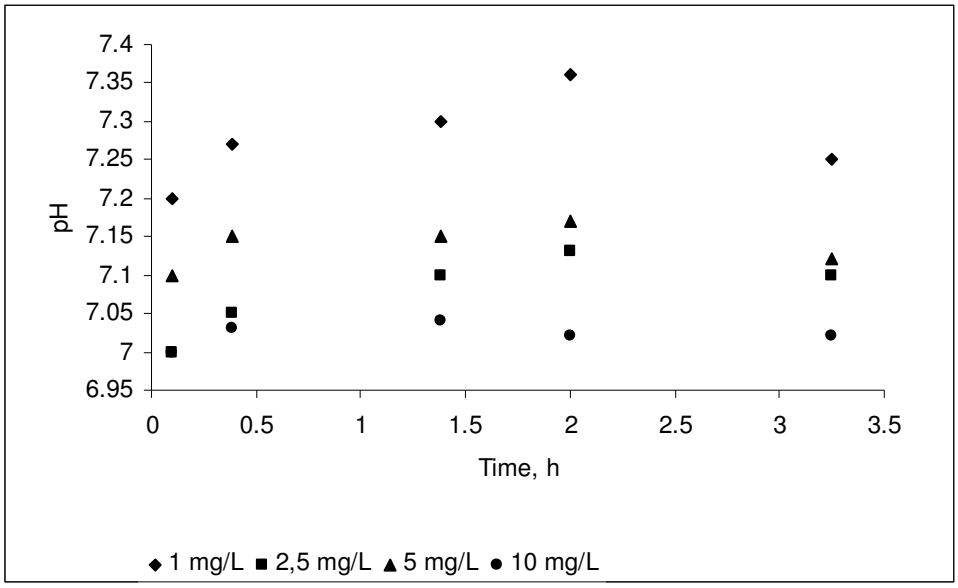

Figure 6.25. pH profile during sorption process of 1-10 mg/L Cd

Equilibrium concentrations of Cd were used to construct adsorption isotherms. In order to investigate the sorption isotherm two equilibrium models were analyzed: the Langmuir and the Freundlich isotherm equations.

The Langmuir adsorption isotherm assumes that the adsorbed layer is one molecule in thickness and that all sites are equal, resulting in equal energies and enthalpies of adsorption. The Langmuir adsorption isotherm is often used to describe sorption of a solute from a liquid solution as:

$$q_e = \frac{q_{\max} K_L C_e}{1 + K_L C_e} \tag{6.6}$$

The constants q_{max} (Langmuir monolayer saturation capacity) and K_L (Langmuir isotherm constant) can be determined from a linearized form of Equation 6.6, represented by Equation 6.7.

$$\frac{C_e}{q_e} = \frac{1}{q_{\max} K_L} + \frac{C_e}{q_{\max}} \tag{6.7}$$

A plot of C_e/q_e versus C_e gives a straight line of slope $1/K_L q_{max}$ and an intercept of $1/q_{max}$.

The Freundlich equation predicts that the metal concentrations on the adsorbent will increase as long as there is an increase in the metal concentration in the liquid and expressed by the following equation:

$$q = K_f C_e^{1/n} \tag{6.8}$$

and the equation may be linearized by taking logarithms:

$$\log(q_e) = \frac{1}{n}\log(C_e) + \log(K_f) \tag{6.9}$$

where K_f (Freundlich isotherm constant) and 1/n (Freundlich exponent) are empirical constants dependent on several factors.

Langmuir and Freundlich constants obtained by linear regression analysis are given in Table 6.7. Langmuir isotherm best fits the experimental results over the experimental range and conditions with high correlation coefficients. Although Freundlich isotherm represents the equilibrium data reasonably well, the fit is not as good as the Langmuir isotherm. The adsorption isotherm data were plotted in Figure 6.26.

Table 6.7. Adsorption Isotherm Constants for Cd

Freundlich Isotherm Constant		
K_f	1/n	R^2
6.495±0.083	0.4187±0.073	0.867
Langmuir Isotherm Constant		
q_{max}	K_L	R^2
30.95±0.00068	3.12±0.027	0.997

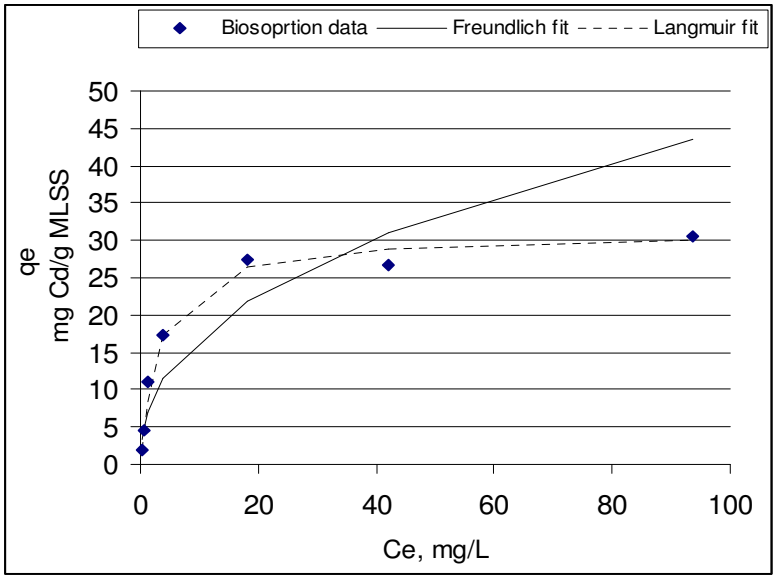

Figure 6.26. Adsorption Isotherms with Freundlich and Langmuir fits

6.3.2. Biosorption of Cd in ammonium utilization experiments

Uptake of Cd onto biomass was also followed in ammonium utilization rate experiments for an initial Cd range of 1-25 mg/L. Adsorption occurred rapidly and nearly reached equilibrium within 30 minutes for all Cd concentrations. Equilibrium concentrations of Cd were used to construct an adsorption isotherm. The adsorption isotherm data were plotted in Figure 6.27 together with the adsorption data given in Figure 6.26 and found to have almost similar characteristics. Since the initial Cd concentrations were in the range of 1-25 mg/L, the adsorption capacities fall into the linear portion of the isotherm curve. Cd biosorption followed during ammonium utilization rate experiments was in good agreement with the Langmuir adsorption model given Section 6.3.1 as illustrated in Figure 6.27.

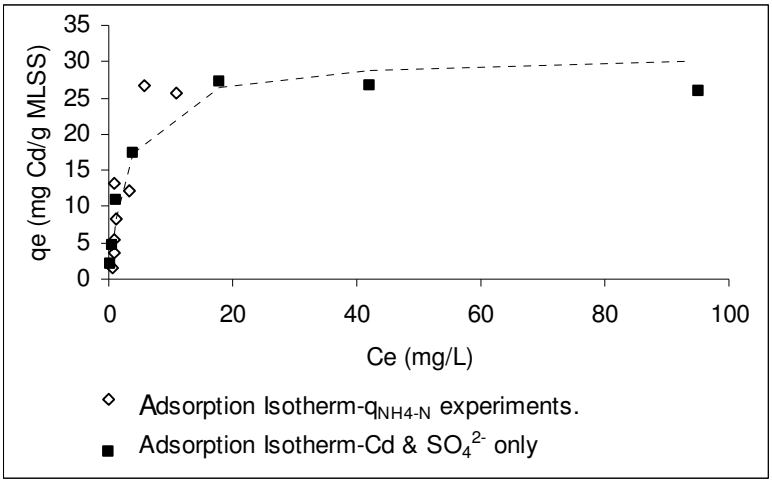

Figure 6.27. Comparison of biosorption data in given in Section 6.3.1 and biosorption data of ammonium utilization rate experiments

The biosorption characteristics of Cd in the presence and absence of cations and anions were found to be almost the same for an initial Cd concentration of range of 1-25 mg/L. The similarity was also tested by comparing the conditional stability constants for two cases in Section 6.3.3.

6.3.3. Determination of the Conditional Stability Constant and Complexation Capacity for Cd Binding to Bacterial Sites

The partition coefficient was determined from the linear portion of the Figure 6.26 and 6.27 and summarized in Table 6.8. By linearization of the Langmuir isotherm, the conditional stability constant (K) and site concentration for the Cd-bacteria ({Cd-X-cell}) binding were also determined as shown in Figure 6.28 and summarized in Table 6.8.

As seen in Table 6.8., the conditional stability constants and site concentration (complexation capacity) were not much different from each other in the presence and absence of cations and inorganic ligands. This indicates that the affinity of Cd to binding sites is higher than other cations and complexation of cations with cell surface could be eliminated through the application of BLM model.

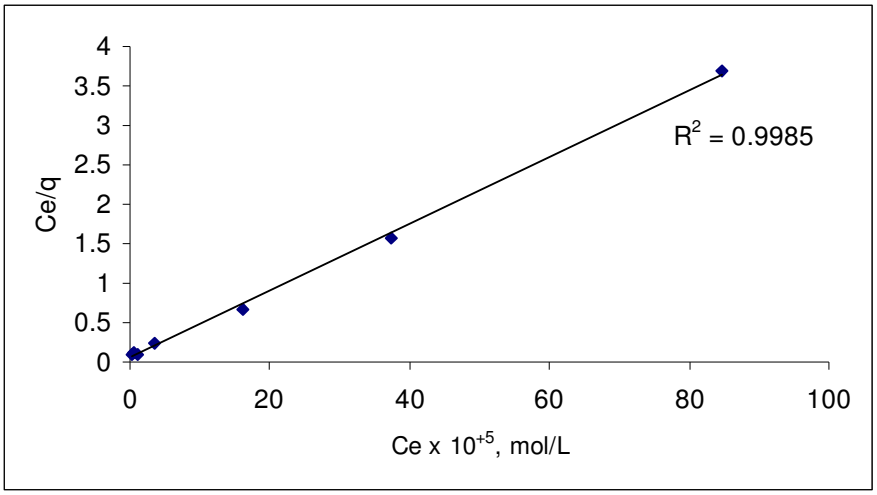

Figure 6.28. Linearization of the Langmuir Isotherm for the determination of the conditional stability constant

Table 6.8. Partition coefficient and conditional stability constant for Cd binding to bacteria

	Partition coefficient, K_p, L/g	Conditional stability constant, LogK	Site concentration for the Cd-bacteria mol Cd/g MLSS
Uptake of Cd in the presence of SO_4^{-2} only	3.77	4.47	$2.76x10^{-4}$
Uptake of Cd in the presence of inorganic and organic ligands	1.96	4.24	$2.14x10^{-4}$

Comparison of the conditional stability constants of Cd for different types of organisms are presented in Table 6.9. As seen in Table 6.9, conditional stability constant values determined in this study are very close to the values given in previous studies especially for bacteria cases. The pH of the test solution in our experiments was around 7.5 whereas it was 7.0 in the study of Hu et al., 2004. The difference between the conditional stability constants for enriched nitrifying bacteria (Hu et al., 2003) could be due pH.

Table 6.9. Conditional stability constants for binding of Cd to different organisms

Organism		Log K	Reference
Bacteria	*Bacillus subtilis*	2.7, 4.2	Daughney and Fein, 1998
	Bacillus licheniformis	3.9, 5.1	Daughney and Fein, 1998
	nitrifying bacteria (mixed culture)	1.1	Hu et al., 2002
	nitrifying bacteria (mixed culture)	4.24	This study
	nitrifying bacteria (mixed culture)	4.47	This study
Phytoplankton	*Chlorella pyrenoidosa*	5.5	Hart et al., 1979
	Chlorella vulgaris	4.4	Ting et al., 1989
Fish	*Caprinus caprio*	6.5	Jansen et al.,2002

Conditional stability constant (or in other words Langmuir adsorption constant, K_L) or partition coefficient, K_p were then incorporated into the MINEQL +(Version 4.5). As done in this study, comparative evaluation of K_p or K_L with two different methods, such as voltammetry and MINEQL, is often not made in literature. At low Cd concentrations, consistent results were obtained with these methods (Figure 6.29). The t-test was applied and the results were not significantly different from each other ($p > 0.05$) in the Cd range of 1-25 mg/L. As the initial Cd concentration increased (e.g. 50 mg/L), the difference between these two methods became statistically significant at equilibrium metal levels (Cd^{+2}=22.32 mg/L in MINEQL, Cd_{volt}=42 mg/L). Therefore, for calculation of biosorption at high Cd levels, the use of voltammetry is advised since it gives more reliable results than theoretical sorption predicted from chemical equilibrium.

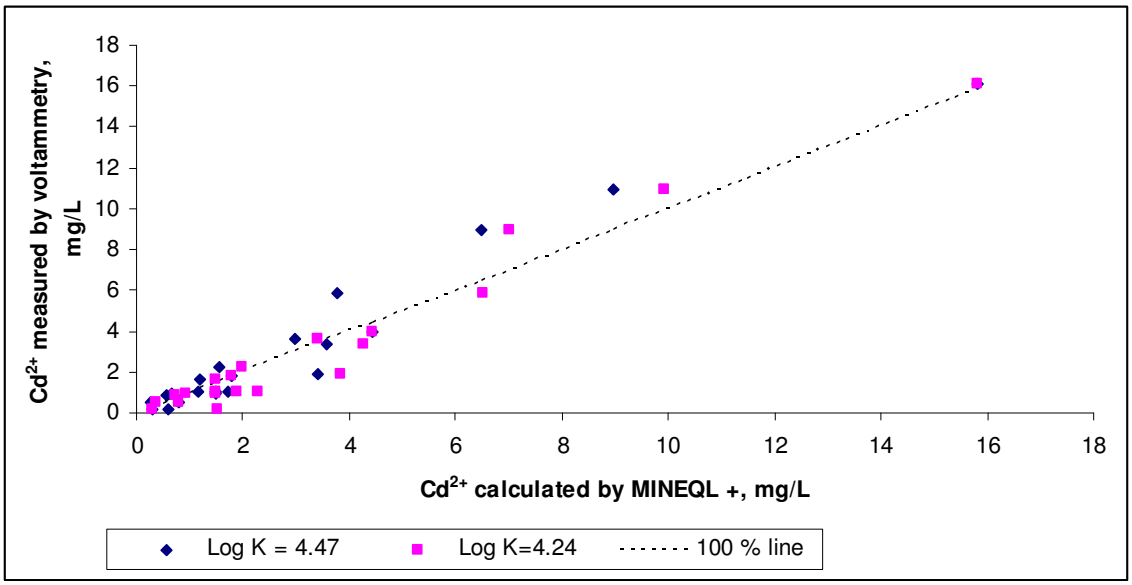

Figure 6.29. Correlation between Cd^{+2} calculated by MINEQL+ and measured by voltammetry

6.3.4. Kinetic Parameters of Cd Biosorption

In order to investigate the mechanism of biosorption, the rate constants for Cd biosorption were determined using first-order expression and pseudo-second-order expressions. For this purpose the biosorption kinetics were investigated by using the data obtained from both adsorption (Section 6.3.1) and the ammonium utilization rate experiments (Section 6.3.2).

The kinetic modelling of Cd sorption to nitrifying biomass has been carried out using the Lagergren first-order kinetic equation:

$$\ln(q_e - q_t) = \ln(q_e) - k_1 t \qquad (6.10)$$

where q_e is the mass of metal adsorbed at equilibrium (mg/g), q_t is the mass of metal adsorbed at time "t" (mg/g) and k_1 is the first-order rate constant for sorption (min^{-1}).

Biosorption data were plotted in the form of ln(qe-q_t) versus time as shown in Figure 6.30 to test the first-order rate kinetics. Lagergren equation provides a poor description of the data (R^2= 0.7897-0.9786).

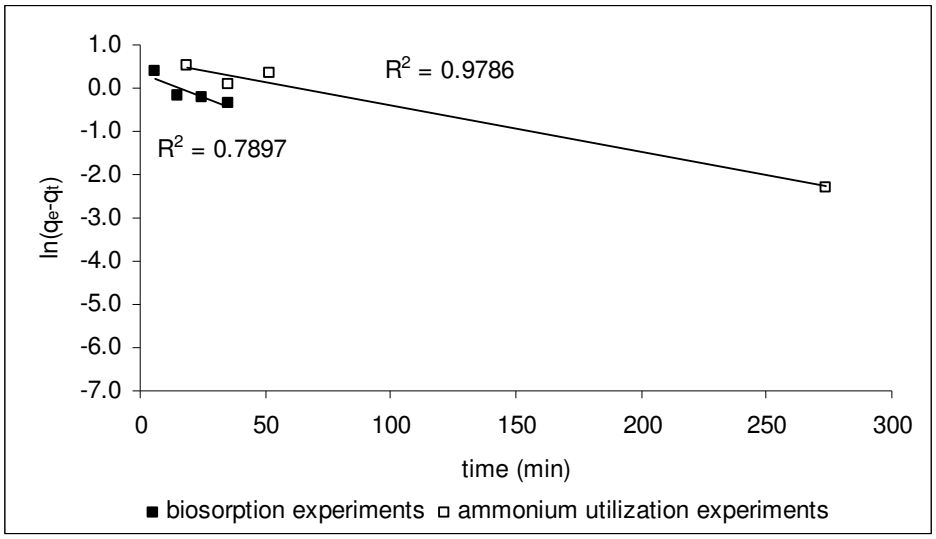

Figure 6.30. Linearization of cadmium biosorption kinetics by Lagergren first-order plots (Initial Cd = 5 mg/L)

When the data did not follow first-order kinetics, a pseudo-second-order kinetic equation was tried to describe the sorption. This equation is given as:

$$\frac{1}{(q_e - q_t)} = \frac{1}{q_e} + k_2 t \qquad (6.11)$$

where q_e is the mass of metal adsorbed at equilibrium (mg/g), q_t is the mass of metal adsorbed at time "t" (mg/g) and k_2 is the second-order rate constant for sorption (g.mg^{-1}min^{-1}). Equation 6.11 can be rearranged to obtain a linear form:

$$\frac{t}{q_t} = \frac{1}{k_2 q^2 e} + \frac{1}{q_e} t \qquad (6.12)$$

When biosorption data was plotted in the form of t/q versus time, a straight line was obtained as shown in Figure 6.31. The pseudo-second order model represented the Cd biosorption kinetics (R^2=0.99).

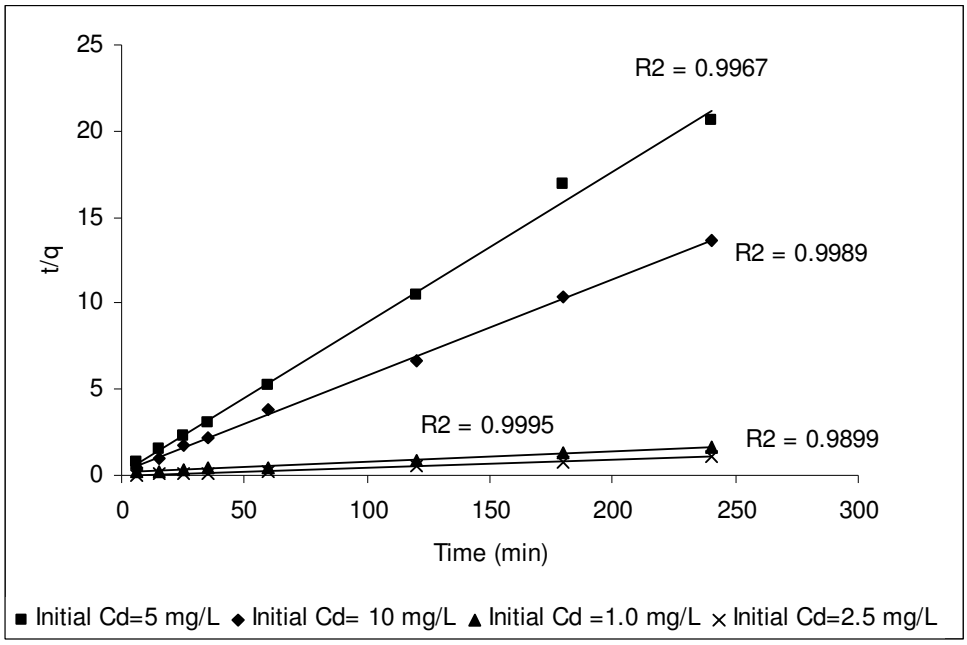

Figure 6.31. A plot of t/q vs. time according to the pseudo-second order adsorption kinetics for various initial Cd concentrations

The pseudo-second order rate constant for various initial Cd concentrations was found from the slope and intercept of the plot and summarized in Table 6.10. As seen in Table 6.10, the second-order rate constants were not significantly different from each other for various initial Cd concentrations except 1 and 15 mg/L initial Cd. Moreover, the biosorption kinetics of Cd in different test mediums such as biosorption and ammonium utilization rate experiments was similar. The latter test medium consists of some anions and cations besides Cd and SO_4^{-2}.

Adequate representation of Cd biosorption with pseudo-second-order model with a very high correlation coefficient indicates that the chemisorption may be the rate-controlling mechanism in Cd sorption onto nitrifying biomass (Ho, 2003).

Table 6.10. Pseudo-second-order rate constants of Cd biosorption in different test mediums

Initial Cd, mg/L	Source of data	k_2 ($g.mg^{-1}min^{-1}$)	R^2
1	Biosorption exp.	$2.41x10^{-4}$	0.989
2.5	Ammonium utilization exp.	$1.48x10^{-2}$	0.991
15	Ammonium utilization exp.	$1.20x10^{-2}$	0.991
10	Biosorption exp.	$1.46x10^{-2}$	0.998
10	Ammonium utilization exp.	$1.38x10^{-2}$	1.0
15	Ammonium utilization exp.	$1.93x10^{-3}$	0.998
15	Ammonium utilization exp.	$1.61x10^{-2}$	0.999

6.4. The effect of Zn on Nitrification in Batch Reactor Systems

6.4.1. The effect of Zn on specific ammonium utilization rate (q_{NH_4-N}) and specific oxygen utilization rate (SOUR)

The influence of Zn on the specific ammonium utilization (q_{NH4-N}) was evaluated with respect to the initial labile and total Zn concentration as shown in Figure 6.32 and summarized in Table 6.11. The extent of inhibition increased almost linearly when the initial labile Zn was between 0-2.97 mg/L and total Zn was between 0-6 mg/L. It reached a saturation value of approximately 94 %. After that point, further increase in Zn did not change the extent of inhibition. A saturation type relationship between q_{NH_4-N} inhibition and initial labile Zn was clearly seen (Figure 6.32b) contrary to the inhibition data observed in the case of Cd (Figure 6.9b). EC_{50} concentration with respect to total Zn and initial labile Zn was found as 2.5 and 0.566 mg/L, respectively.

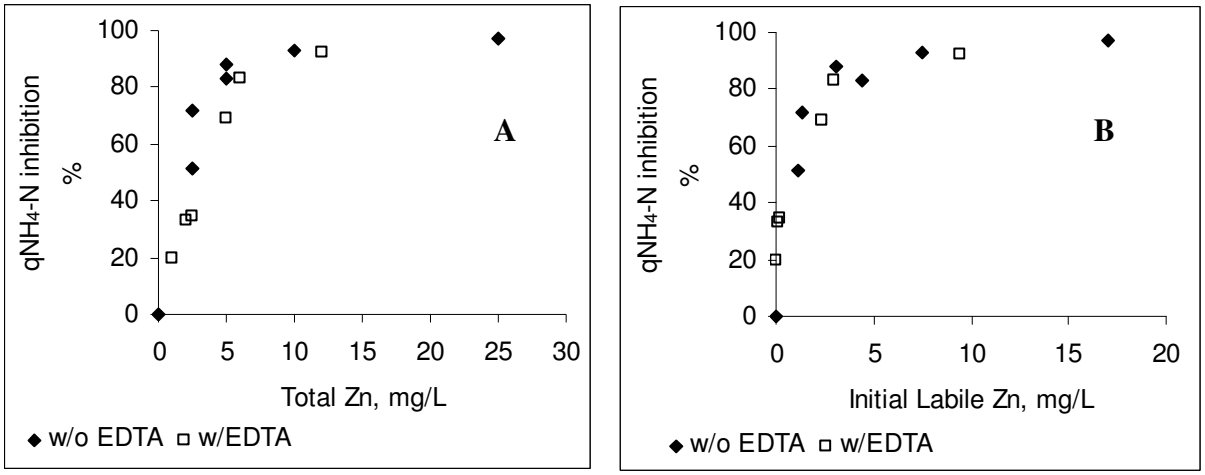

Figure 6.32. Inhibition of specific ammonium utilization rate at various a) total and b) initial labile Zn (Zn_{volt}) concentrations

Table 6.11. Summary of ammonium utilization rates and SOUR of Zn experiments

Experiment No	VSS	pH	Total Zn	Zn_{volt}		EDTA	Specific Ammonium Utilization Rate (qNH_4-N)		Specific Oxygen Uptake Rate (SOUR)		Percent reduction in qNH_4-N		Percent reduction in SOUR	
	mg/L	-	mg/L	mg/L		mol/L	mg NH_4-N /g VSS.h		mg O_2/g VSS.min		%		%	
				Initial	Final		Initial	Final	Initial	Final	Initial	Final	Initial	Final
1	240	7.7	1	0.05	0.011	$2x10^{-5}$	28.77	26.03	1.89	1.70	28	34	18	26
2	240	7.5	2	0.113	0.111	$2x10^{-5}$	20.63	18.75	1.49	1.44	48	53	35	37
3	232	7.5	2.5	1.348	0.68	-	18.4	18.4	-	-	54	54	-	-
4	410	7.5	2.5	1.708	0.544	-	19.51	19.51	1.70	1.61	51	51	53.4	53.4
5	316	7.7	2.5	0.251	0.248	$2x10^{-5}$	28	24	1.76	1.57	35	35	23	32
6	256	7.6	5	3.113	1.55	-	9.4	4.2	-	-	72	88	-	-
7	373	7.6	5	4.381	1.497	-	5	5	0.96	0.93	83	83	58.1	59.5
8	316	7.5	5	2.336	1.523	$2x10^{-5}$	19	17	0.72	0.64	52	57	64	68
9	240	7.7	6	2.967	1.619	$2x10^{-5}$	9.30	6.98	1.186	1.116	77	83	48.4	51.5
10	267	7.5	10	7.5	3.847	-	2.5	2.5	-	-	93	93	-	-
11	423	7.5	12	9.442	5.98	$2x10^{-5}$	13.64	12.40	0.417	0.179	65	69	82	92
12	257	7.5	25	16.998	11.35	-	2.1	1.1	-	-	94	97	-	-

Specific oxygen uptake rates (SOUR) were evaluated with respect to initial Zn concentrations in the range of 1-12 mg/L as shown in Figure 6.33 and summarized in Table 6.11. The percent decrease in SOUR increased as the initial total and labile Zn concentration increased linearly. The EC_{50} value was found to be around 6 mg/L in terms of total initial Cd and 2.97 mg/L in terms of initial labile Zn. Inhibition levels determined with SOUR measurements were almost the same as those determined with q_{NH_4-N} measurements. Thus, it can be concluded that nitrite oxidation step was not inhibited or inhibited to such a low extent that could not be determined by OUR measurements. The results with Zn and Cd showed that nitrite oxidizers are less sensitive to heavy metal inhibition.

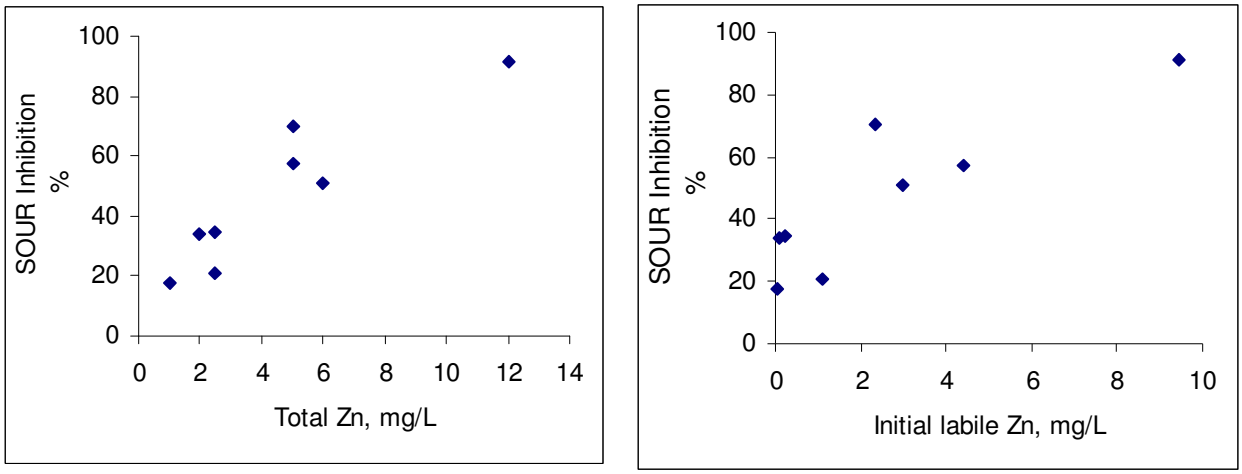

Figure 6.33. Inhibition of specific oxygen uptake rate various total at various a) total and b) initial labile Zn (Zn_{volt}) concentrations

6.4.2. Effect of Zn exposure time on nitrification inhibition

The effect Zn exposure on nitrification inhibition was investigated in long-term SOUR experiments. In this case, Zn was added to the respirometric at the beginning of the vessel. Therefore, the inhibition of SOUR started immediately with Zn addition at the beginning of experiment. The shape of the SOUR profile in the presence of Zn changed with the extent of inhibition. Some typical SOUR profiles in the presence and absence of Zn are shown in Figure 6.34. In the absence of metal, initial SOUR values were in the range of 1.88-2.11 mg O_2/g

VSS.min and reached a maximum value of 2.6-3.0 mg O_2/g VSS.min. If there was not a severe inhibition such as in the case of 1 mg/L Zn, the shape of the SOUR profile was similar to those in the absence of metals (control reactor in Figure 6.34). SOUR reached to a maximum value in a longer period of time. On the other hand, the initial and maximum SOUR values in the presence of 5 mg/L Zn and 5 mg/L Zn along with $2x10^{-5}$M EDTA which caused moderate inhibition levels, SOUR decreased immediately with Zn addition and stayed constant during the course of the experiments (Figure 6.35). Although further increase of Zn decreased the SOUR with time, this was not as drastic as in the case of Cd.

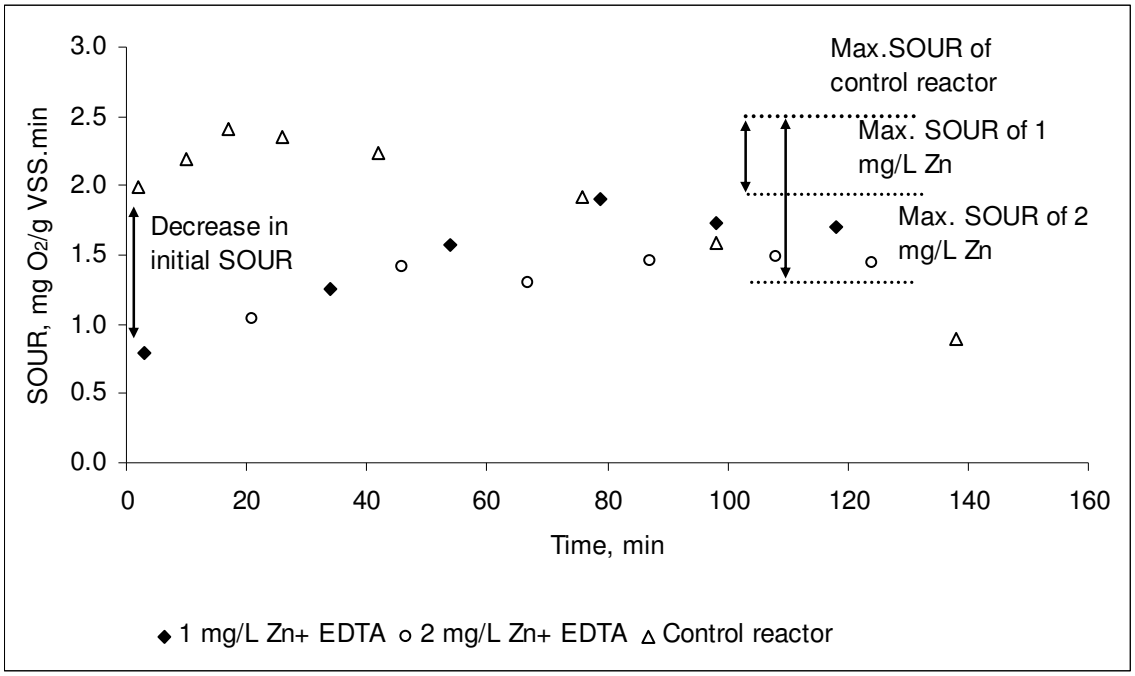

Figure 6.34. SOUR profiles in the absence and presence of 1 and 2 mg/L Zn

For the comparison of the exposure time effects on the inhibitory characteristics of Cd and Zn, the SOUR profiles of Cd and Zn were drawn on the same graph (Figure 6.36). The initial labile concentration of Cd (Cd_{volt}) and Zn (Zn_{volt}) were almost identical in these experiments. 9.44 mg/L Zn severely inhibited (%82) and caused a rapid decrease in SOUR level in 15 minutes and inhibition reached 92% after 115 minutes (Figure 6.37). On the other hand, 10.7 mg/L Cd caused only 50% inhibition in 16 minutes and reached to 95% after 200

minutes. Interestingly, the final or equilibrium degree of inhibitions was very similar. This observation showed that Zn and Cd has similar inhibitory characteristics.

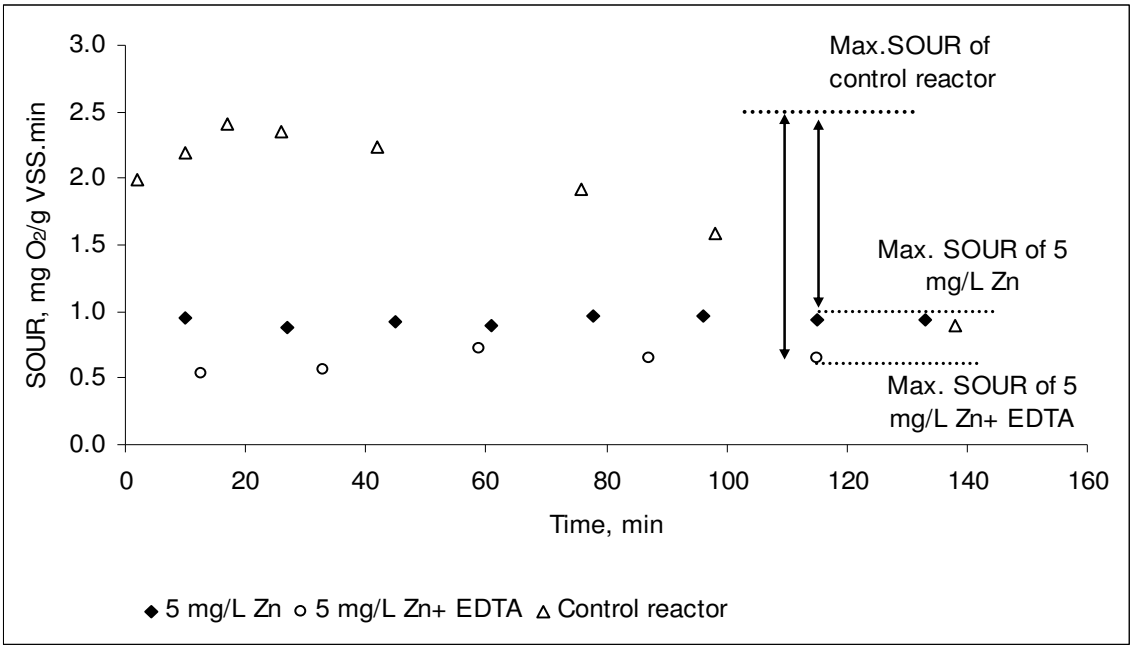

Figure 6.35. SOUR profiles in the absence and presence of 5 mg/L Zn and 5 mg/L Zn and $1x10^{-2}$ M EDTA

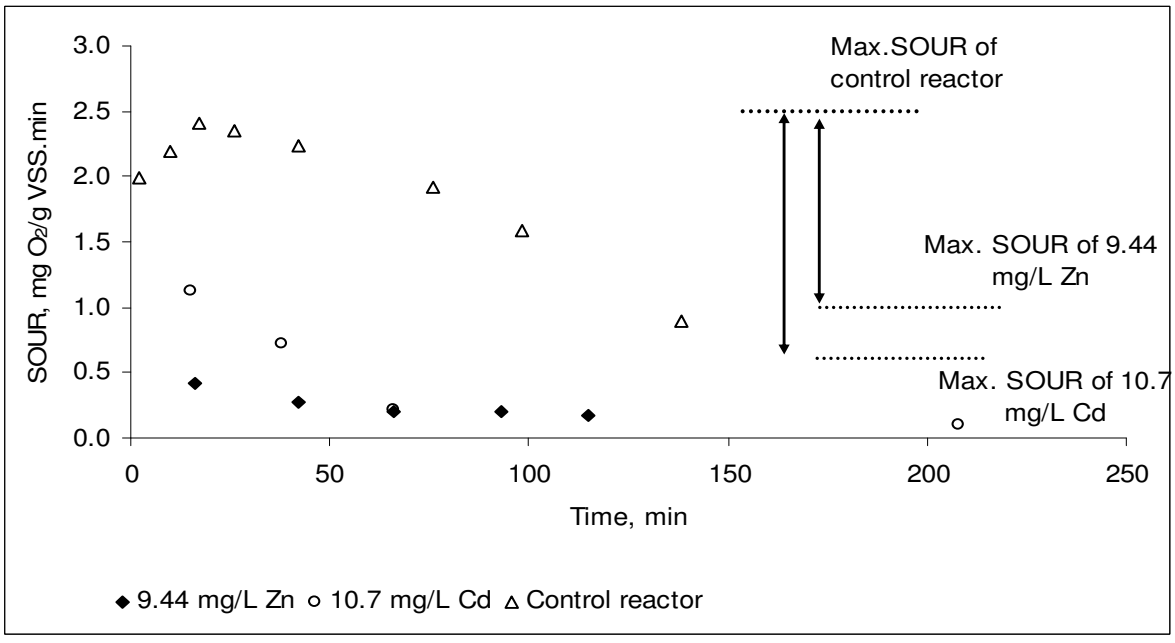

Figure 6.36. SOUR profiles in the absence and presence of 9.44 mg/L Zn and 10.7 mg/L Cd

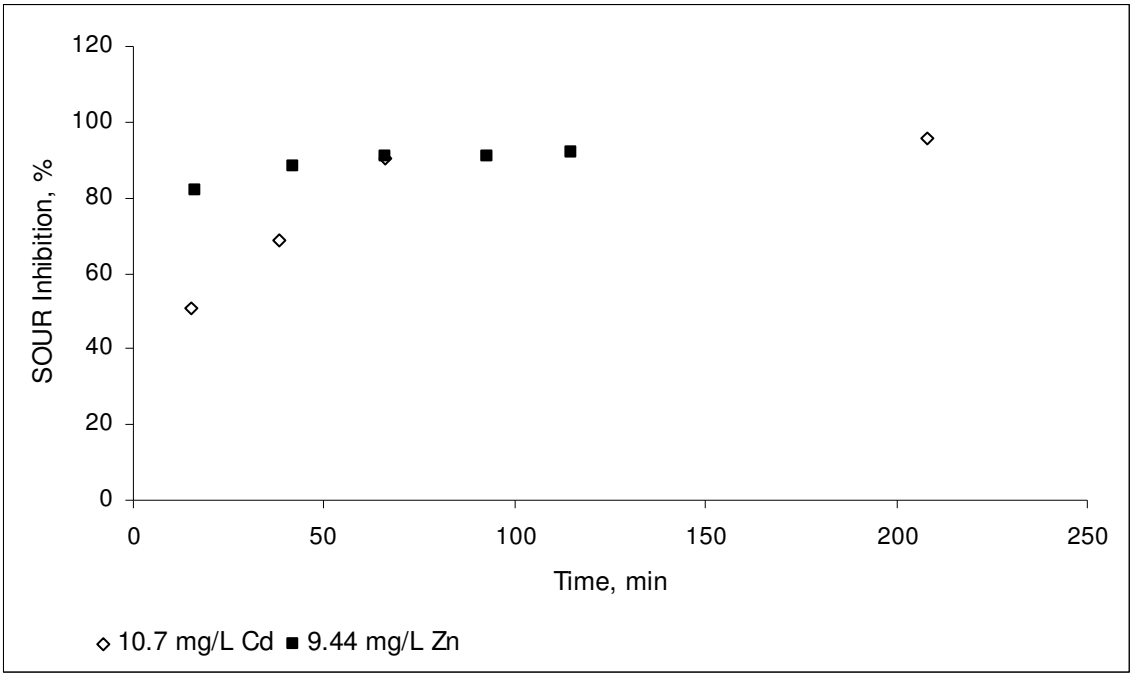

Figure 6.37. Variation in the extent of SOUR inhibition with exposure time to 9.44 mg/L Zn and 10.7 mg/L Cd

During the course of a batch operation, the inhibitory effect of Zn on nitrification stayed almost constant. It is very well known that the rate of intracellular uptake is very slow compared to extracellular uptake in most of the cases (Slaveykova et al., 2005). The extent of inhibition increases with exposure time, when inhibition is due to the binding of metal at intracellular active sites (Hu et al., 2003). In our experiments, no distinction was made between intra- and extracellular metal concentrations. This approach is termed as "the total body burden" and was used for determination of stability constant and binding site concentration. As a result, no correlation could be made between intra- and extracellular metal fractions and nitrification inhibition as it was done in a previous study (Hu et al., 2003). In our experiments, Zn inhibition did not change with exposure time (Figure 6.38), which indicated that there may be no change in intracellular Zn in the time frame of experiments. Therefore, it was concluded that nitrification inhibition was caused by the Zn binding onto bacterial cell walls rather than at intracellular active sites. Indeed, extracellular Cd fraction was found to be responsible for the nitrification inhibition as explained previously in Section 6.2.6. Ma et al. (2003) and Campbell et al. (2002) reported similar results. They concluded that the

extracellular metal, or in other words, the surface complex, {M-X-cell}, was involved in metal toxicity.

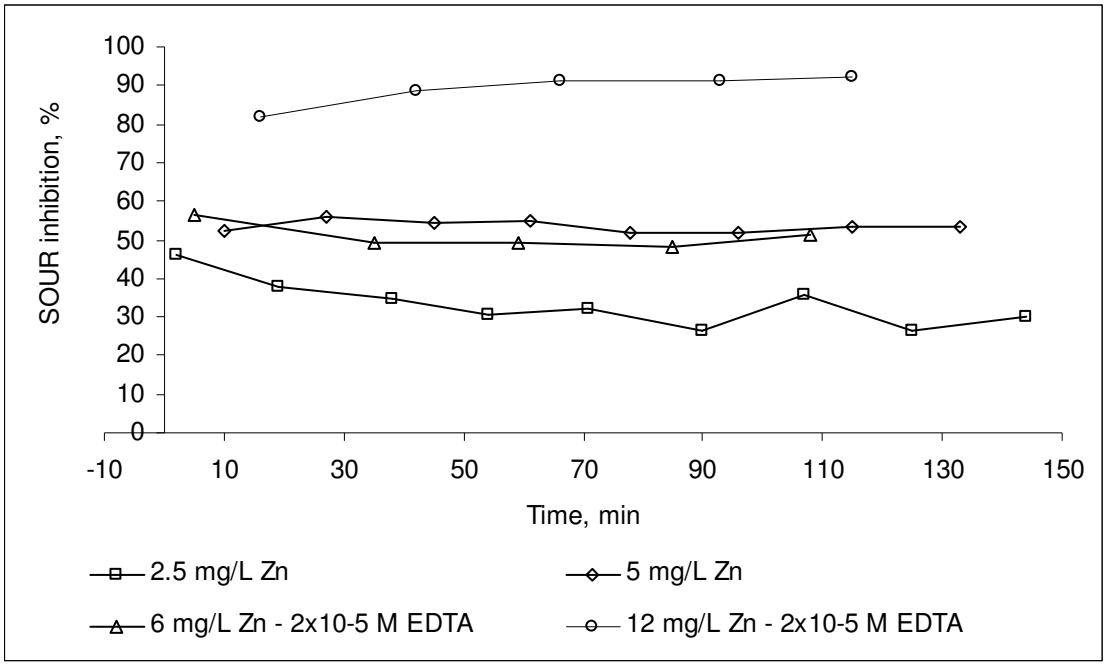

Figure 6.38. Variation in the extent of SOUR inhibition with exposure time to Zn

6.4.3 Effect Zn-EDTA Complexation on Nitrification

To assess the effect of Zn-EDTA complexation on nitrification, the total concentration of Zn was varied in a range of 3.82×10^{-5} to 1.83×10^{-4} M (2.5-12 mg/L) while keeping EDTA concentration constant at 2×10^{-5} M. Thus, inhibition was tested in a wide range of free and labile Zn. The fractions of free and labile Zn at equilibrium in the presence of EDTA ranged between 1.1 to 3.6 % and 1 to 50%, respectively. The inhibition progressed linearly and reached saturation as shown in Figure 6.39.

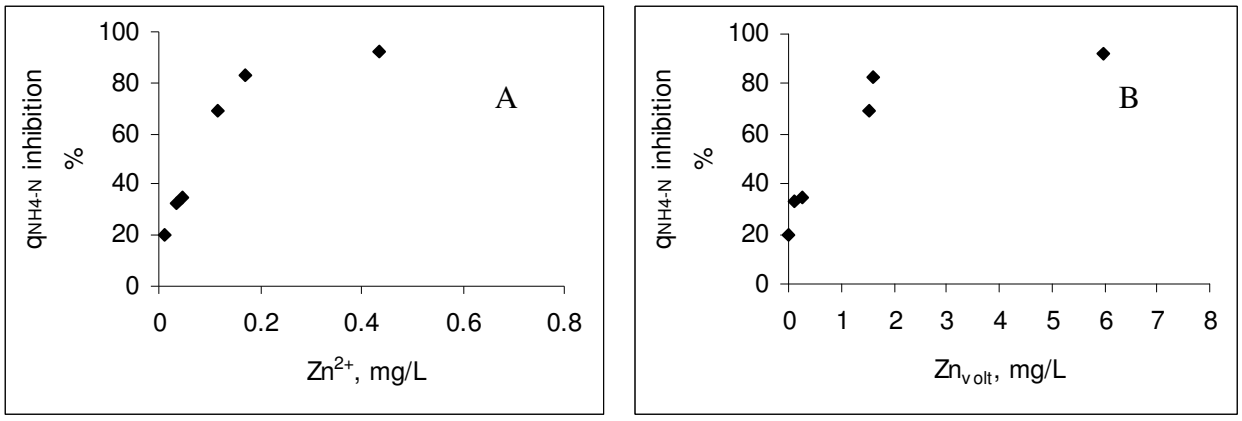

Figure 6.39. Inhibition of specific ammonium utilization rate at various a) free and b) labile Zn (Zn_{volt}) concentrations

6.4.4 The Effect of Zn Speciation on Nitrification

In order to evaluate the effects of Zn speciation on nitrification inhibition, percent reductions in specific ammonium utilization rates (*i*) (Table 6.11) were correlated to different Zn forms (Table 6.12) in the test medium (Table 4.1). Equilibrium concentrations of different Zn forms were used through in modeling. Equilibrium concentrations of Zn species in soluble phase and Zn bound to the surface of the bacteria were calculated thermodynamically by MINEQL+ (version 4.5) as explained in Section 5.3.3. Besides the free Zn and surface-bound Zn, labile Zn measured by voltammetry (as shown Zn_{volt}) during specific ammonium utilization rate experiments was used to correlate the nitrification inhibition to labile Zn.

Correlations of ammonium utilization rate inhibition (*i*) with different forms of Zn were given in Figure 6.40a-c. A saturation type relationship as in Equation 6.3 was obtained between inhibition and different forms of Zn.

Least square nonlinear regression was applied to find the model parameters in Equation 6.5 using the data given in Table 6.11 and 6.12. Then, maximum inhibition percent, i_{max} and EC_{50} (or K_M) values were obtained for each form of Zn as shown on related Figures 6.40a-c.

With these values the model curves in Figure 6.40a-c were drawn to compare experimental and modeling results.

Inhibition of nitrification could be expressed using all three forms of Zn (Figure 6.40a–c). This suggested that both the FIAM and BLM models were applicable under the conditions of this study. In each case, the nonlinear regression had a high correlation coefficient (R^2=0.85) and the residuals were randomly distributed (Figure 6.41). The 95% confidence intervals shown in Figures 6.41a-c further demonstrate the validity of the models.

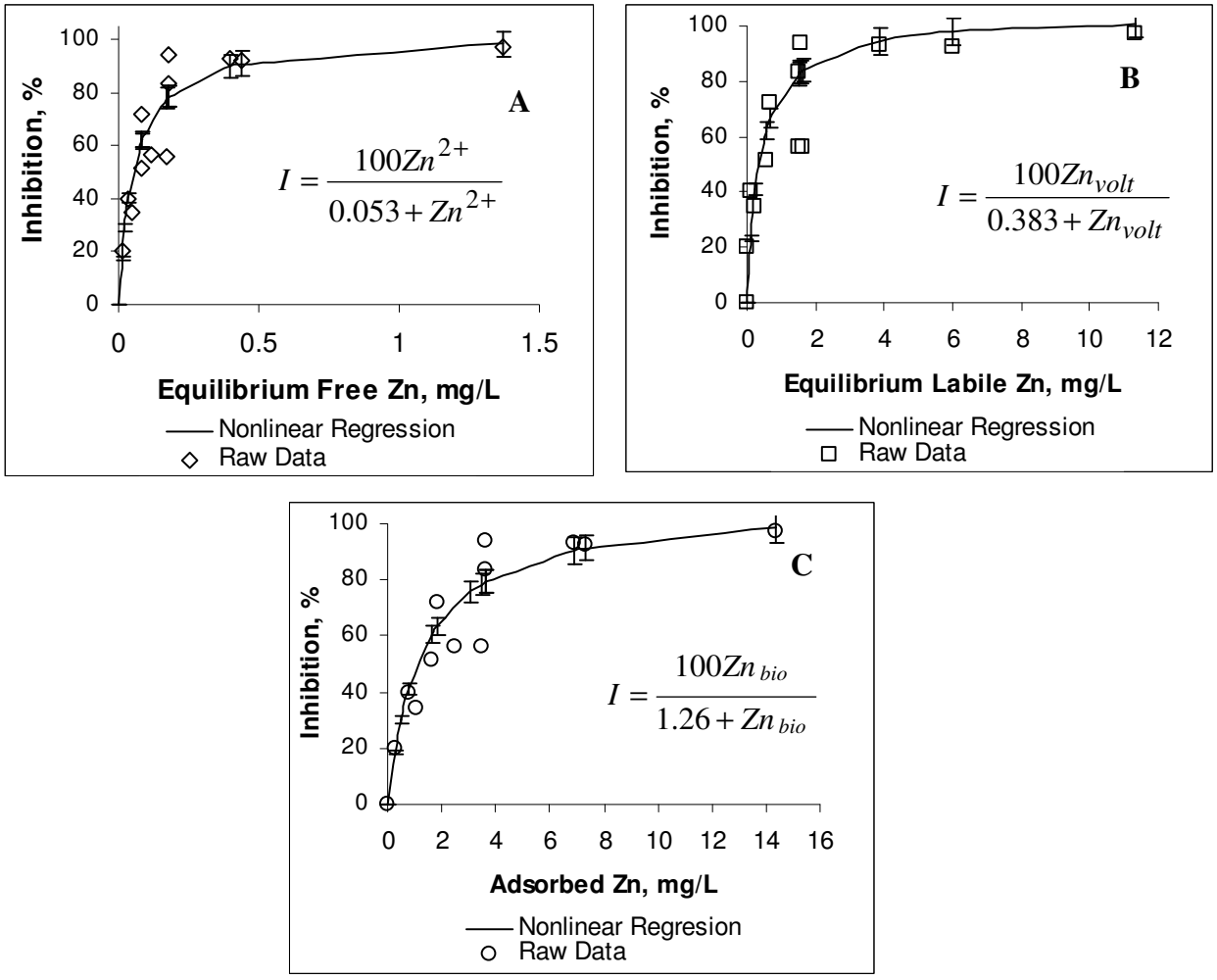

Figure 6.40. Relationship between inhibition and different forms of Zn (a) eq. free Zn calculated by MINEQL, (b) eq. labile Zn measured with voltammetry, (c) equilibrium adsorbed Zn calculated with MINEQL

Tablo 6.12 Zinc speciation in ammonium utilization rate experiments at equilibrium

Total Zn , mol/L	Calculated Labile Zn (freeZn + Zn in weak inorganic complexes), mol/L			Zn in strong complexes, mol/L	Surface bound Zn (Zn_{bio}), mol/L	Zn measured by volt., mol/L
	Zn^{2+}	Inorganic Zn complexes	Total Labile	ZnEDTA	Zn-Bacteria	Zn_{volt}
$3.8x10^{-5}$	$1.29x10^{-6}$	$8.73x10^{-6}$	$1x10^{-5}$	-	$2.82x10^{-5}$	$1.04x10^{-5}$
$7.66x10^{-5}$	$2.73x10^{-6}$	$1.84x10^{-5}$	$2.12x10^{-5}$	-	$5.53x10^{-5}$	$2.37x10^{-5}$
$1.53x10^{-4}$	$6.10x10^{-6}$	$4.13x10^{-5}$	$4.74x10^{-5}$	-	$1.05x10^{-4}$	$5.88x10^{-5}$
$3.83x10^{-5}$	$2.09x10^{-5}$	$1.41x10^{-4}$	$1.62x10^{-4}$	-	$2.20x10^{-4}$	$1.0x10^{-4}$
$7.6x10^{-5}$	$2.73x10^{-6}$	$1.84x10^{-5}$	$2.12x10^{-5}$	-	$2.51x10^{-5}$	$2.29x10^{-5}$
$3.8x10^{-5}$	$1.14x10^{-6}$	$1.20x10^{-5}$	$1.31x10^{-5}$	-	$2.75x10^{-5}$	$8.65x10^{-6}$
$7.6x10^{-5}$	$1.26x10^{-6}$	$3.21x10^{-5}$	$3.34x10^{-5}$	$1.78x10^{-5}$	$3.8x10^{-5}$	$9.767x10^{-5}$
$3.8x10^{-5}$	$3.27x10^{-7}$	$3.03x10^{-5}$	$3.06x10^{-5}$	$1.54x10^{-5}$	$1.61x10^{-5}$	$2x10^{-5}$
$1.5x10^{-5}$	$1.73x10^{-7}$	$1.17x10^{-6}$	$1.34x10^{-6}$	$9.92x10^{-6}$	$4.03x10^{-6}$	1.68e-08
$3x10^{-5}$	$5.30x10^{-7}$	$4.91x10^{-6}$	$5.44x10^{-6}$	$1.44x10^{-5}$	$1.21x10^{-5}$	$1.68x10^{-6}$
$9.2x10^{-5}$	$2.61x10^{-6}$	$1.76x10^{-5}$	$2.03x10^{-5}$	$1.84x10^{-5}$	$5.30x10^{-5}$	$2.48x10^{-5}$
$1.84x10^{-5}$	$6.67x10^{-6}$	$4.51x10^{-5}$	$5.18x10^{-5}$	$1.93x10^{-3}$	$1.12x10^{-4}$	$9.14x10^{-5}$

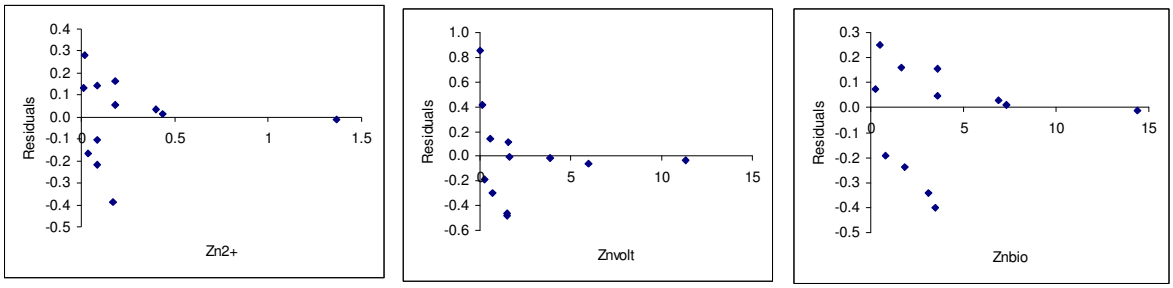

Figure 6.41. Residuals plots for the Zn inhibition models

Inhibition could be expressed with all three forms of Zn: Zn^{2+}, Zn_{volt} and Zn_{bio}. This suggested that both FIAM and BLM models were applicable under the conditions of the study. Pseudo-equilibrium was established between the free and labile Zn in bulk solution and extracellular Zn (biosorbed). Labile Zn concentration was successfully measured by voltammetry which differentiates labile and strongly complexes in bulk solution. There is no evidence for inhibition caused by intracellular Zn.

Results of the batch experiments showed that Cd and Zn caused severe inhibition to nitrifying bacteria. Zn showed its adverse affect in a short period of time. On the contrary, longer contact times were necessary for Cd. The dependence of Cd inhibition on contact time could be due to its slow uptake kinetics. On the other hand, Zn is an essential metal and bacterial cells accumulate zinc by a fast, unspecific uptake mechanism and it is normally found in higher concentrations (Spain, 2003). Short-term activity measurements could be suitable for the essential metals such as Zn, Cu and Fe in contrast to Cd and maybe other toxic metals such as Pb.

The major findings in this part were reported in a paper (Semerci and Çeçen, 2006).

6.5. Biosorption of Zn onto Nitrifying Biomass

As explained in Section 5.4, uptake of Zn onto biomass was studied under the following test mediums conditions;

1. Biosorption of Zn onto biomass in test mediums consisting of Zn and SO_4^{-2} for an initial Zn range of 1-150 mg/L
2. Biosorption of Zn onto biomass in ammonium utilization rate (q_{NH_4-N}) experiments. In these experiments test mediums inorganic complexing ions such as HCO_3^-, CO_3^{-2}, SO_4^{-2}.

6.5.1. Biosorption of Zn in the presence of SO_4^{-2}

Changes in labile Zn (Zn_{volt}) concentration for an initial Zn range of 1-10 and 25-100 mg/L during the course of the adsorption experiments are shown in Figure 6.42 and 6.43, respectively. For all initial Zn concentrations, there was an initial rapid uptake stage followed by a second slow uptake as illustrated in Figure 6.44 and 6.45 which was similar to Cd biosorption characteristics (Section 6.3.1). Adsorption occurred rapidly and nearly reached equilibrium within approximately 30 for all initial Zn concentrations of 1-10 mg/L which is consistent with previous studies. The adsorption at 25, 50 and 100 mg/L Zn was completed in 5 minutes.

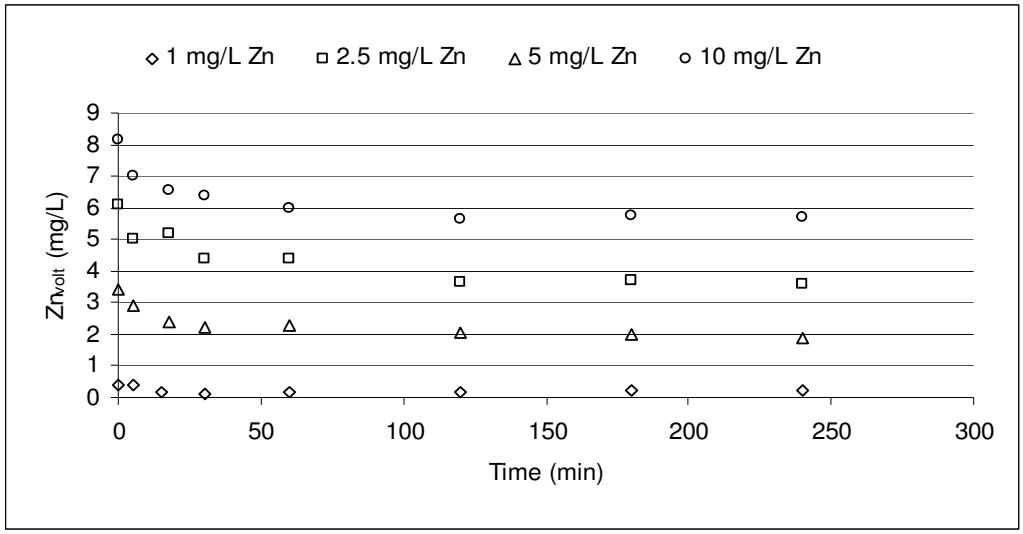

Figure 6.42. Change in bulk labile Zn with time for an initial Zn range of 1-10 mg/L

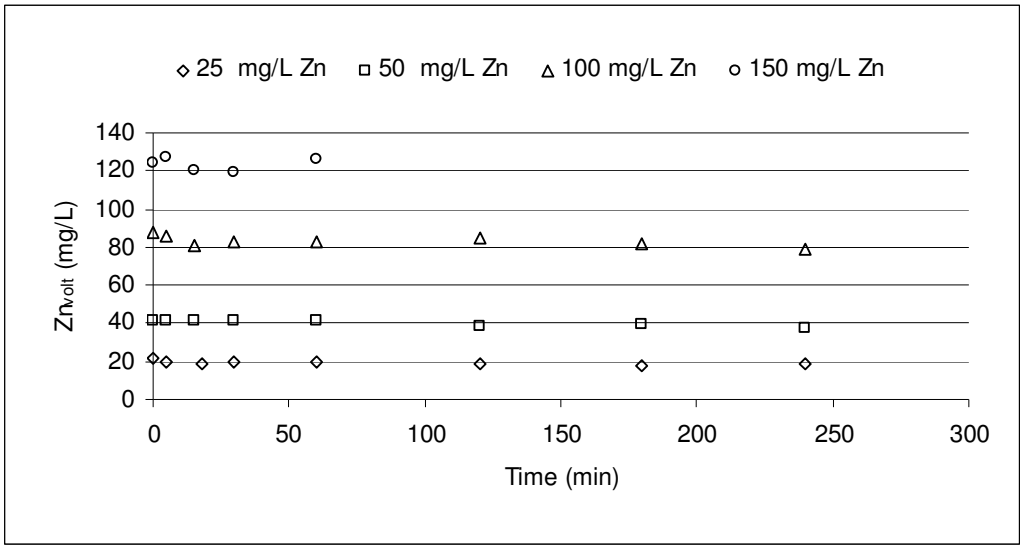

Figure 6.43. Change in bulk labile Zn with time for an initial Zn range of 25-150 mg/L

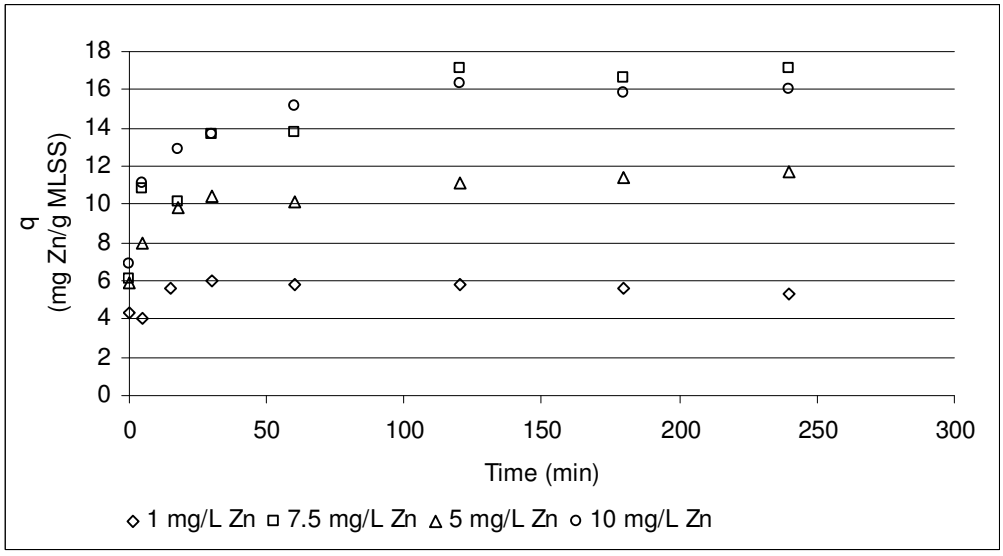

Figure 6.44. Adsorption capacity of for an initial Zn concentration of 1-10 mg/L

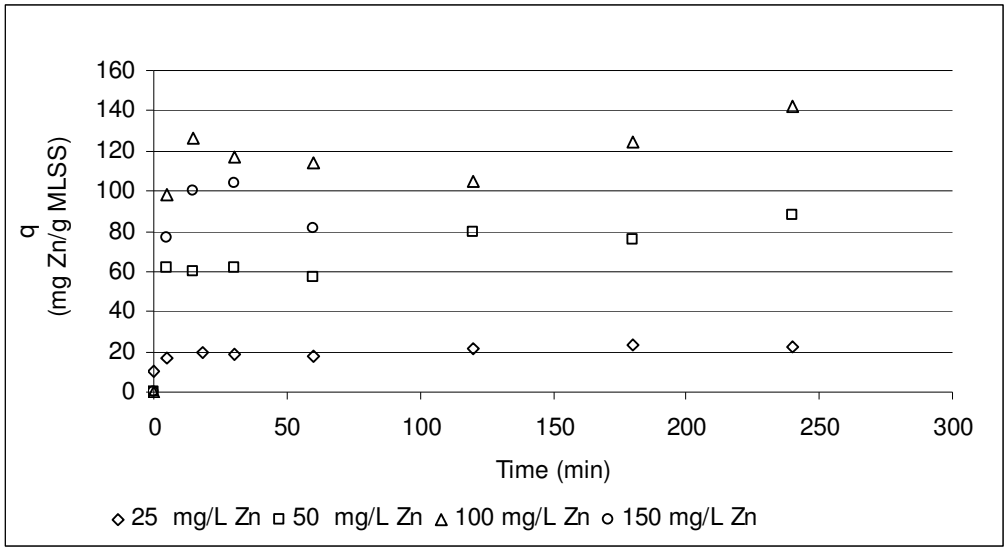

Figure 6.45. Adsorption capacity of for an initial Zn concentration of 25-150 mg/L

Equilibrium concentrations of Zn were used to construct an adsorption isotherm. The adsorption isotherm data were plotted in Figure 6.46. Both Langmuir and Freundlich adsorption models were applied to experimental data (Table 6.13 and Figure 6.46). Although Langmuir isotherm represents the equilibrium data reasonably well, the fit is not as good as the Freundlich isotherm.

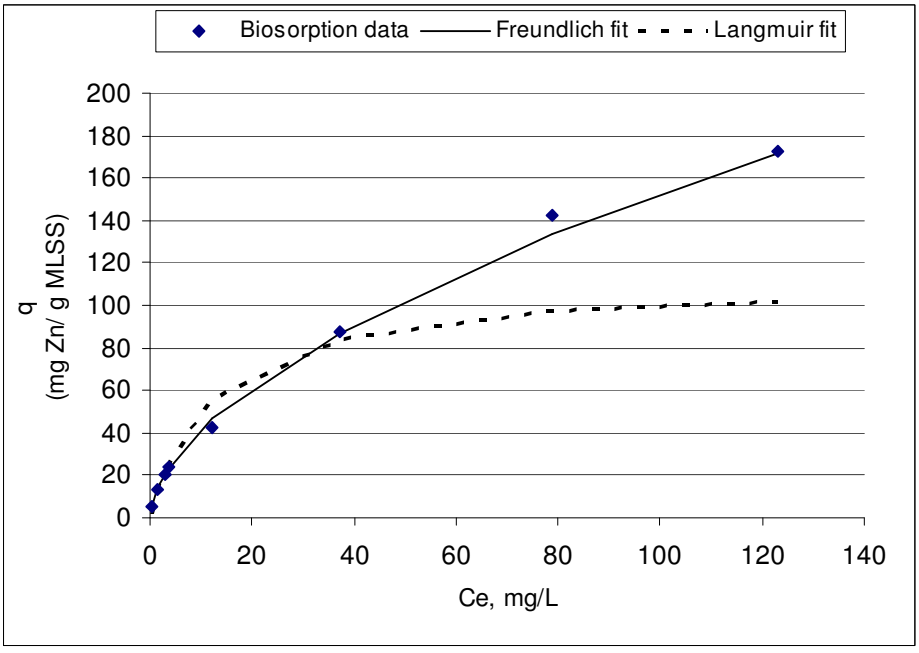

Figure 6.46. Zn Adsorption according to Freundlich and Langmuir fits

Table 6.13. Adsorption Isotherm Constants for Zn

Freundlich Isotherm Constant		
K_f	1/n	R^2
11.2±0.014	0.6±0.017	0.9967
Langmuir Isotherm Constant		
q_m	K_m	R^2
112.4±0.007	12.4±0.002	0.979

6.5.2. Biosorption of Zn onto biomass in the test mediums used in ammonium utilization rate experiments

Uptake of Zn onto activated sludge was followed in ammonium utilization rate experiments for an initial Zn range of 1-25 mg/L. Adsorption occurred rapidly and nearly reached equilibrium within 60 minutes. The adsorption isotherm data were plotted in Figure 6.47 together with those in Figure 6.46. They had almost similar characteristics. Since the initial Zn concentrations were in the range of 1-25 mg/L, the adsorption capacities fall into the linear region of the isotherm curve.

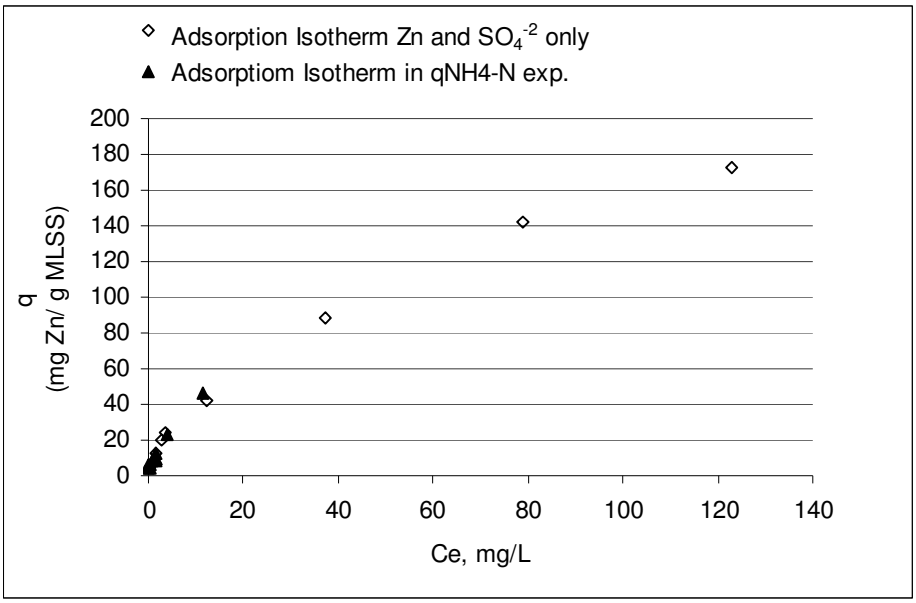

Figure 6.47. Comparison of adsorption isotherm in the presence and absence of cations and anions

6.5.3 Determination of the Conditional Stability Constant and Complexation Capacity for Zn Binding to Bacterial Sites

Two straight lines were obtained when C_e/q_e was plotted against Ce concentrations as illustrated in Figure 6.48. This showed that there were two different sites available for Zn binding which was contrary to the Cd-sludge binding characteristics (only one straight line was observed, Section 6.3.3). The conditional stability constants and binding site concentration of both sites were found from Figure 6.48 and given in Table 6.14. The partition coefficient or conditional stability constant values of the second binding site are relatively lower than the first one (log K_2 values lower than log K_1 values). This indicates that at low Zn concentrations the complexation was controlled mainly by stronger binding sites (site 1) whereas at high Zn concentrations the stronger sites became fully occupied and weaker sites started to effect complexation (site 2). However, the concentration of second binding sites available for participation in the second type of complex was greater than those available for participation in the first type. The existence of multiple sites would be more likely for the essential metal, including Zn, than for toxic metals (e.g. Cd), which was also pointed out by Hassler et al. (2004b).

Table 6.14 Partition coefficient and conditional stability constant for Zn binding to bacteria

	Partition coefficient, K_p, L/g		Conditional stability constant, LogK		Site concentration for the Zn-bacteria mol Zn/g MLSS	
	1^{st} site	2^{nd} site	1^{st} site	2^{nd} site	1^{st} site	2^{nd} site
Uptake of Zn in the presence of SO_4^{-2} only	5.63	1.16	4.21	2.88	$8.39x10^{-4}$	$4.51x10^{-3}$
Uptake of Zn in the presence of inorganic and organic ligands	3.78	-	6.57	3.52	$1.45x10^{-4}$	$1.99x10^{-3}$

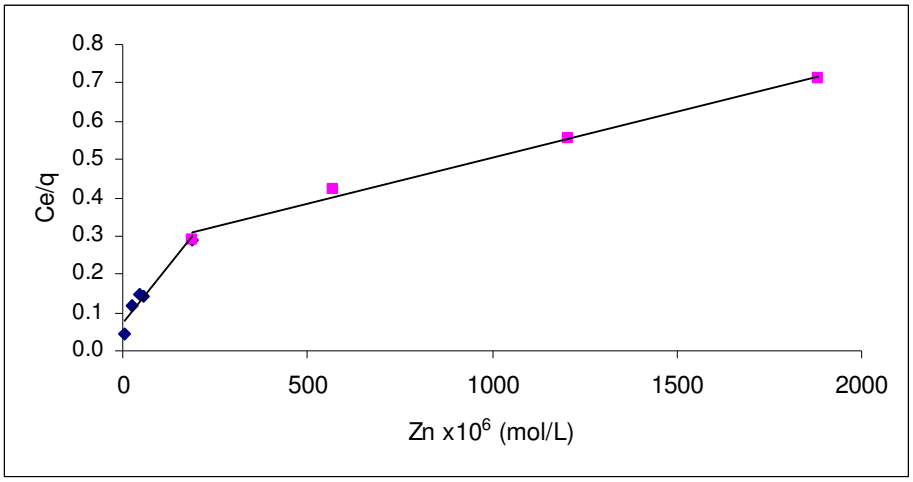

Figure 6.48. Linearization plot of Langmuir isotherm for determination of conditional stability constant for Zn binding to bacterial sites

As seen in Table 6.14., the conditional stability constants in the presence inorganic ligands and organic ligands were higher, whereas the complexation capacities were lower. Since the applied Zn concentration range was between 1-20 mg/L, the conditional stability constants and binding site concentration of the first site were used in MINEQL calculations. Comparison of the conditional stability constants of Cd for different types of organisms are presented in Table 6.15. As seen in Table 6.15, conditional stability constants are very close to values in previous studies especially for bacterial cases.

Table 6.15 Conditional stability constants for binding of Zn to different organisms

Organism		Log K	Ref.
Bacteria	nitrifying bacteria (mixed culture)	4.47	this study
Bacteria	*Rhodococcus erythropolis*	4.9, 2	Plette et al., 1996
Phytoplankton	*Scenedesmus subspicatus*	6.9	Bates et al., 1982
Fish	*Oncorhynchus mykiss (rainbow trout)*	5.1-5.6	Alsop and Wood, 2000

Comparison of the labile Zn concentration at equilibrium calculated with MINEQL and measured with voltammetry is shown in Figure 6.49. The t-test was applied and the results were not significantly different from each other ($p > 0.05$) for all Zn concentration studied.

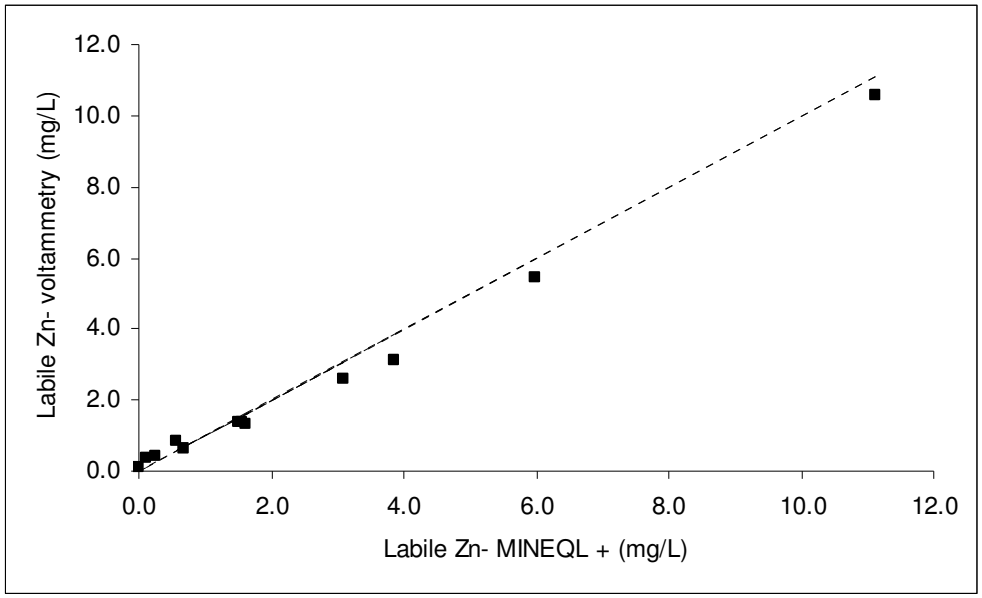

Figure 6.49. Correlation between labile Zn calculated by MINEQL+ and measured by voltammetry

6.5.4. Biosorption Kinetics of Zn

The kinetics of Zn biosorption were investigated in the Zn range of 1-150 mg/L. The pseudo-first (Eq. 6.10) and pseudo-second order (6.11) kinetic models were applied in order to investigate the mechanism of biosorption. Biosorption data were plotted in the form of ln(qe-qt) versus time in Figure 6.50 to test the first-order rate kinetics.

From the slope and intercept of the line, the first-order rate constant was found as k_1=0.078 min^{-1} (R^2=0.959). Lagergren equation provides a poor description of data (R^2= 0.959). When biosorption data was plotted in the form of t/q versus time, a straight line was obtained as shown in Figure 6.51. The pseudo-second order model represented the Zn biosorption kinetics better than pseudo-first order model (R^2=0.99). The pseudo-second order rate constant for various initial Zn concentrations were found from the slope and intercept of the plot and summarized in Table 6.16. As seen in Table 6.16, the second-order rate constant changed with initial Zn concentrations. Moreover, the biosorption kinetics of the Zn in different test mediums such as biosorption and ammonium utilization rate experiments was similar. The latter test medium consists of some anions and cations besides Zn and SO_4^{-2}.

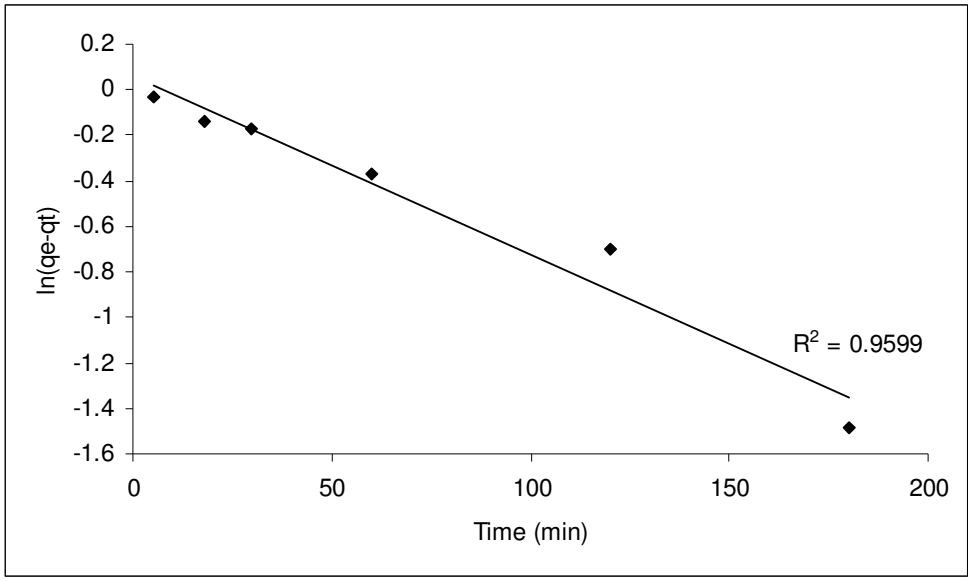

Figure 6.50. Linearization of zinc biosorption kinetics by Lagergren first-order plots (Initial Cd = 5 mg/L)

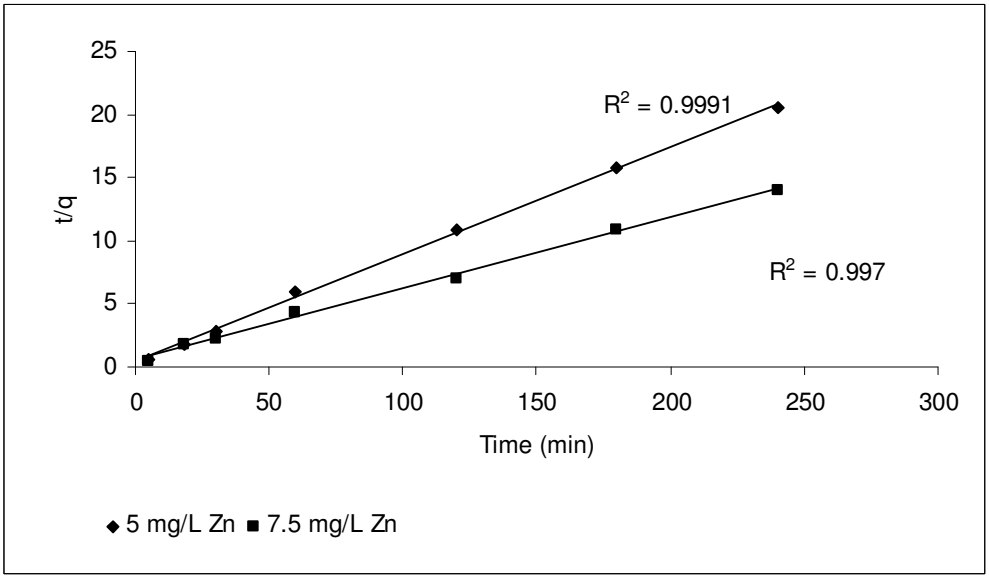

Figure 6.51. A plot of t/q vs. time according to the pseudo-second order adsorption kinetics

Table 6.16. Pseudo-second-order rate constants of Zn biosorption in different test mediums

Initial Zn, mg/L	Source of data	k_2 ($g.mg^{-1}min^{-1}$)	R^2
5	Biosorption exp.	$1.68x10^{-2}$	0.999
7.5	Biosorption exp.	$5.74x10^{-3}$	0.997
10	Biosorption exp..	$1.52x10^{-2}$	0.999
25	Ammonium utilization exp.	$6.16x10^{-3}$	0.999
10	Ammonium utilization exp.	$6.77x10^{-3}$	0.999
5	Ammonium utilization exp.	$6.03x10^{-2}$	0.999

Similar to the biosorption kinetics of Cd, Zn biosorption was adequately represented with pseudo-second-order model with a very high correlation coefficient. This indicates that the chemisorption process may be the rate-controlling mechanism of the sorption of Zn onto nitrifying biomass. The second-order constant for Zn is higher than Cd which showed the equilibrium reached in shorter period of time.

6.6. Continuous-Flow Experiments in a Nitrifying Reactor

6.6.1. Nitrification Efficiency in the absence of Cd

In the first phase of experimental period, the continuous-flow reactor was operated at various ammonium loadings as shown in Figure 5.4 to assess the nitrification efficiency and biokinetic parameters. In this period, NH_4-N, NO_2-N, NO_3-N and MLVSS concentrations were daily measured as shown in Figure 6.52. In the start up period, NH_4-N, NO_2-N, NO_3-N and MLVSS measurements were also made in samples taken from the supernatant and the sludge. The results showed that no nitrification or denitrification took place in the secondary clarifier. Steady-state values at each NH_4-N loading are summarized in Table 6.17. At all NH_4-N loadings, 98% of the influent ammonium was removed except for the transition phase in which the efficiency dropped to 91% for one day only.

The effluent NH_4-N concentration on Day 61 increased to 92 mg/L as a result of pH drop to 4 which was due to a failure in pH control system. In parallel to NH_4-N increase, nitrite oxidation decreased gradually. This resulted in nitrite accumulation with a maximum NO_2-N concentration of 110 mg/L. Dependence of nitrite accumulation on free ammonia concentration is illustrated in Figure 6.53. The recovery from free ammonia inhibition lasted 6 days (Figure 6.55). Another nitrite accumulation was observed during the transition period where the applied ammonium loading increased from 0.19 to 0.37 mg NH_4-N/mg VSS.day, the NH_4-N removal ceased for a certain period of time (Figure 6.52). Nitrite accumulation in this period was also due to the increase in free ammonia concentration (Figure 6.55).

However, nitrite accumulation in the first and second stages was different from each other. In the literature, the threshold NH_3-N concentration for nitrite oxidation inhibition was reported as 0.1 mg/L (EPA, 1993). In our system, only 50% inhibition was observed around 1 mg/L NH_3-N (Figure 6.56), although it was ten times higher than the reported value. For 0.16 mg/L NH_3-N, the decrease in nitrite oxidation was around 14%. On the other hand, in the second case, nitrite oxidation inhibition started at much lower free ammonia concentration which was around 0.07 mg/L. As seen in Figure 6.56b, inhibition

percentage was around 50% at 0.16 mg/L NH_3-N. As it would be expected, nitrite oxidation inhibition recovered after the MLVSS concentration in the reactor reached to a certain level which was around 300 mg/L. These findings suggested that the threshold NH_3-N concentration could depend on the quantity of nitrite oxidizers in a nitrifying culture. If the quantity of nitrite oxidizers is high enough to resist free ammonia inhibition, the nitrite oxidation proceeds until to a certain level of free ammonia concentration which was the first case in our system. The results would be explained in a better way by comparing the quantity of nitrite oxidizers in two different period of the reactor operation. For both cases, nitrite oxidation inhibition due to the free ammonia inhibition was reversible.

To investigate the relationship between bulk free ammonia and nitrite oxidation inhibition, percent inhibition in nitrite oxidation ($i_{NO2\text{-}N}$) was calculated as described in Eqn. 6. 9

$$i_{NO_2-N}(\%) = \frac{q_{NO_2-N}}{qNH_4-N} \tag{6.9}$$

Figure 6.56 illustrates the relationship between free ammonia concentration and nitrite oxidation inhibition. The shape of the inhibition curve for the first case looked like a dose response curve (Figure 6.56a), whereas saturation type relationship was obtained for the second one (Figure 6.56b). The inhibition data given in Figure 6.56b were modeled by assuming a saturation type relationship in which the maximum inhibition percentage was less than 100%. The model equation is given in Figure 6.56b.

Table 6.17. Steady-State Results of Continuous-Flow Experiments at Various Ammonium Loadings

Exp. No	Description of the Experiment	Flowrate	Steady state ave. pH	Temperature	Steady-state influent NH_4-N	Steady state- NH_4-N loading	Steady grab effluent NH_4-N	Steady state composite effluent NH_4-N	Steady- state MLSS	Steady- state VSS	Ammonium utilization rate	Steady grab effluent NO_2-N	Steady state composite effluent NO_2-N	Steady grab effluent NO_3-N	Steady state composite effluent NO_3-N	Steady state Nitrate production rate
		L/day	-	^{0}C	mg/L	mg /gVSS.day	mg/L	mg/L	mg/L	mg/L	mg /gVSS.day	mg/L	mg/L	mg/L	mg/L	mg /gVSS.day
1	Continuous feeding with 50 mg/L NH_4-N	10	7.5	25	50	230	0.5	1.0	110	109.8	297	0.62	1.12	49.86	47	247
2	Continuous feeding with 200 mg/L NH_4-N	10	7.60	25	208	450	1.5	2.1	251	238	530	4.1	1.9	218	201	551
3	Continuous feeding with 250 mg/L NH_4-N	10	7.55	26	248.2	510	3.0	3.5	281	263.6	551	59	-	215	-	516
4	Continuous feeding with 50 mg/L NH_4-N	10	7.65	26	56.2	190	1.2	0.8	153	145	490	0.36	-	62	-	490
5	Continuous feeding with 200 mg/L NH_4-N	10	7.50	26	223	370	0.8	0.9	334	308	577	3	20	221	230	588

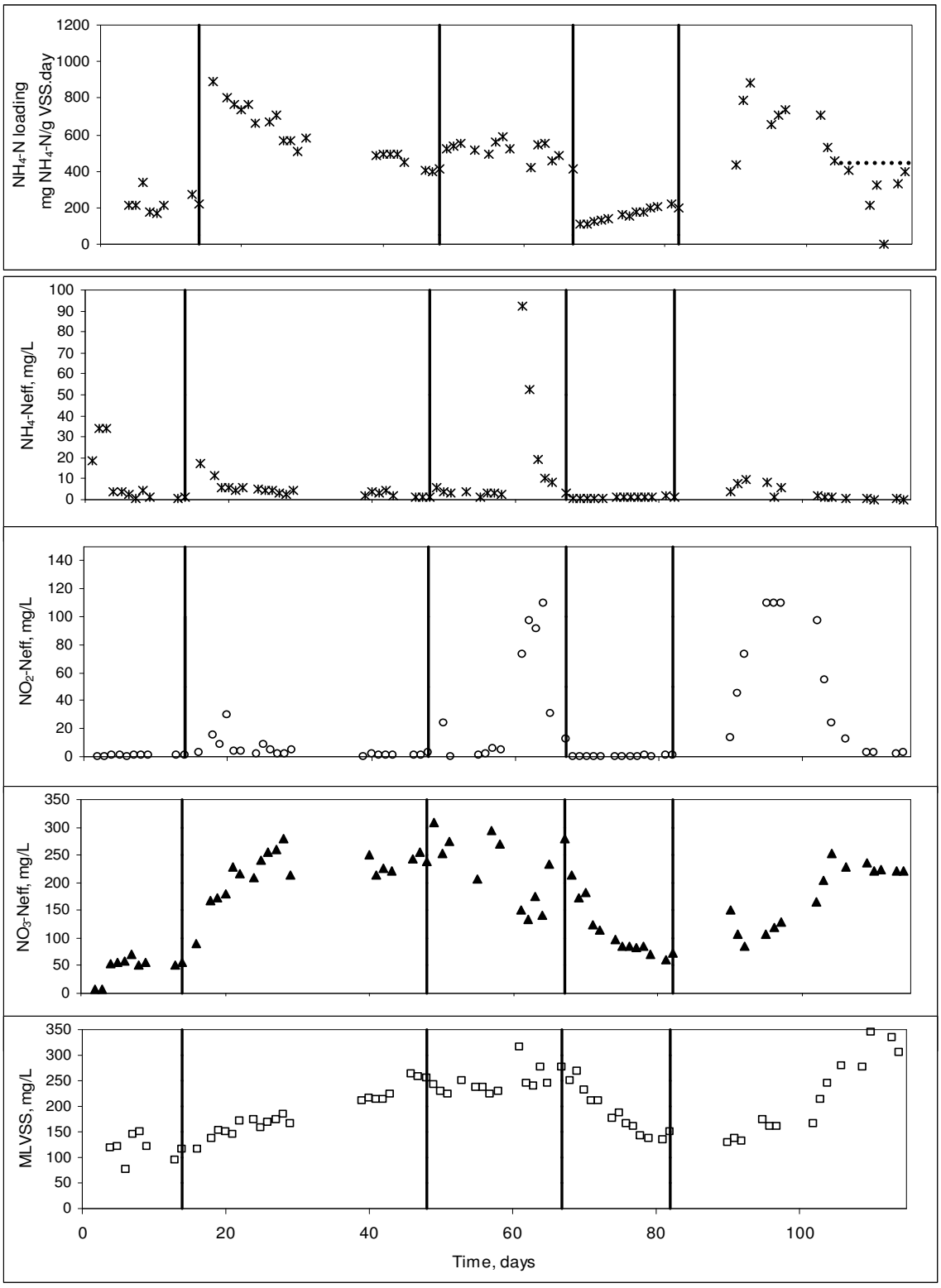

Figure 6.52. Daily ammonium loadings, effluent NH_4-N, NO_2-N, NO_3-N and bulk MLVSS measurements (Dotted lines show the steady-state concentrations).

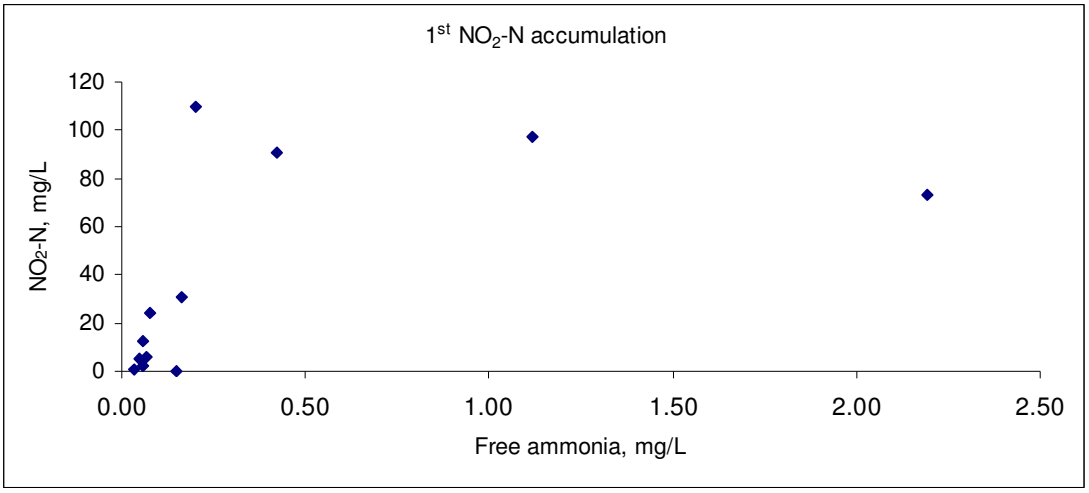

Figure 6.53. Dependence of nitrite accumulation on free ammonia (NH_4-N= 250 mg/L, NH_4-N loading = 510 mg NH_4-N/g VSS.day)

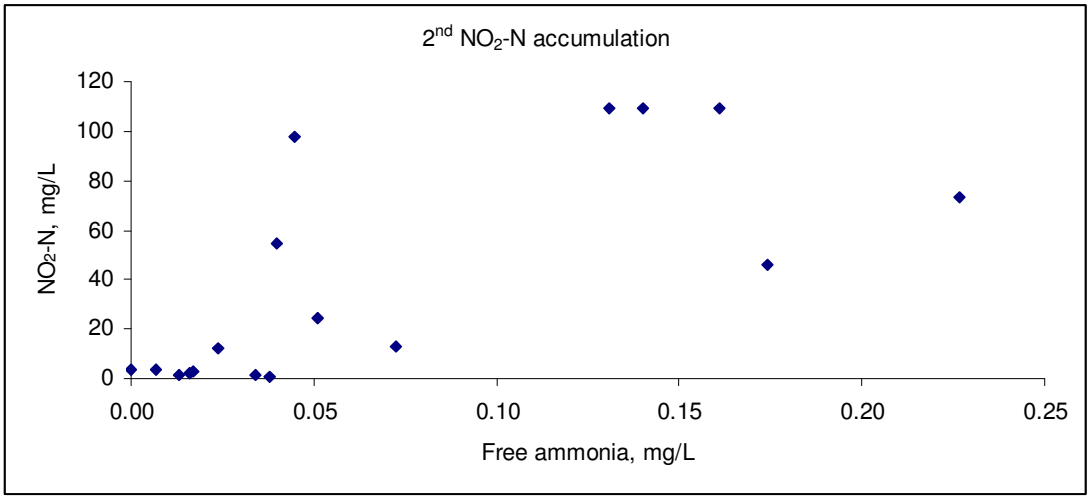

Figure 6.54. Dependence of nitrite accumulation on free ammonia (NH_4-N= 200 mg/L, NH_4-N loading = 370 mg NH_4-N/g VSS.day)

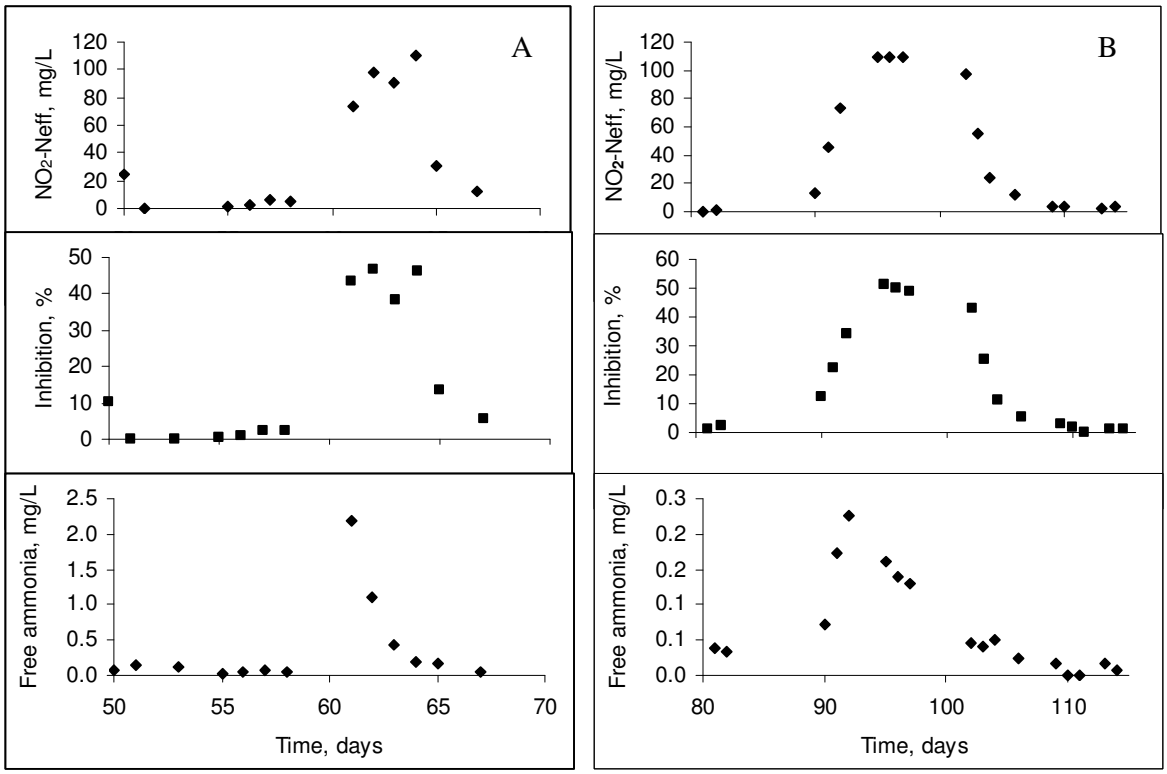

Figure 6.55. NO_2-N accumulation profiles during a) Day 50-67 b) Day 81-114

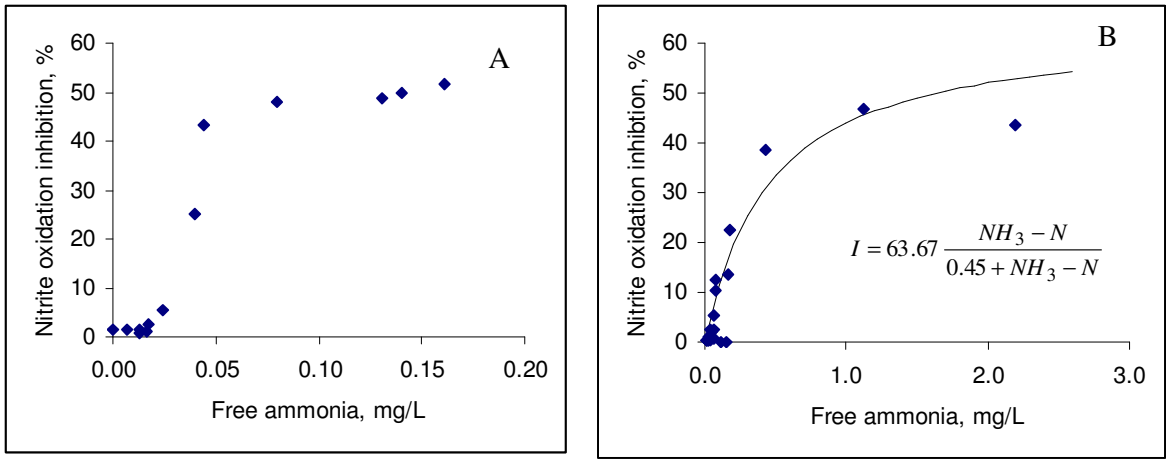

Figure 6.56. Relationship between free ammonia concentration and nitrite oxidation inhibition a) Day 81-114 b) Day 50-67

6.6.2 Estimation of Biokinetic Parameters in the Continuous-flow Reactor

Steady-state ammonium utilization and nitrate production rates in the absence of Cd were first determined at each influent NH_4-N loadings as shown in Figure 6.57 and Table 6.17. The runs at 50 and 200 mg/L influent NH_4-N were conducted twice to check the repeatability of results. Even at different time periods (Day 1 and 66 for 50 mg/L, Day 47 and 106 for 200 mg/L) for the same influent conditions, almost the same results were obtained indicating no change in nitrifier activity and fraction (Figure 6.57). The half-saturation constant for ammonium utilization, K_{S,NH_4-N}, the maximum ammonium utilization rate, $q_{\max,NH_4-N}$ and the maximum nitrate production rate, $q_{\max,NO_3-N}$ were estimated by using the steady-state rates and steady-state bulk NH_4-N concentrations (Figure 6.58). Lineaweaver-Burk, Hanes-Woolf and Eadie Hofstee linearization methods were used in the analysis of data shown in Figure 6.58.

Also, nonlinear regression was applied using the Graph PAD package program. The K_{S,NH_4-N} values obtained by different numerical techniques were comparable with literature values (Gerneay et al., 1997) and statistically acceptable (R^2=0.88-0.99). As seen from Table 6.18, evaluation of the data with respect to the bulk NH_4-N concentrations resulted in $q_{\max,NH_4-N}$, $q_{\max,NO_3-N}$ and $K_{S,N}$ values in the ranges of 608-769 mg NH_4-N/g VSS.h, 667-769 mg NO_3-N/g VSS.h and 0.48-0.92 mg NH_4-N/L, respectively as shown in Table 6.18. The comparison of experimental data with the model results is illustrated in Figure 6.58. The maximum ammonium utilization and nitrate production rates are very close to each other, indicating total oxidation of ammonium into NO_3-N. According to the results of the evaluation, the reactor was operated with an influent NH_4-N of 200 mg/L through the rest of the study.

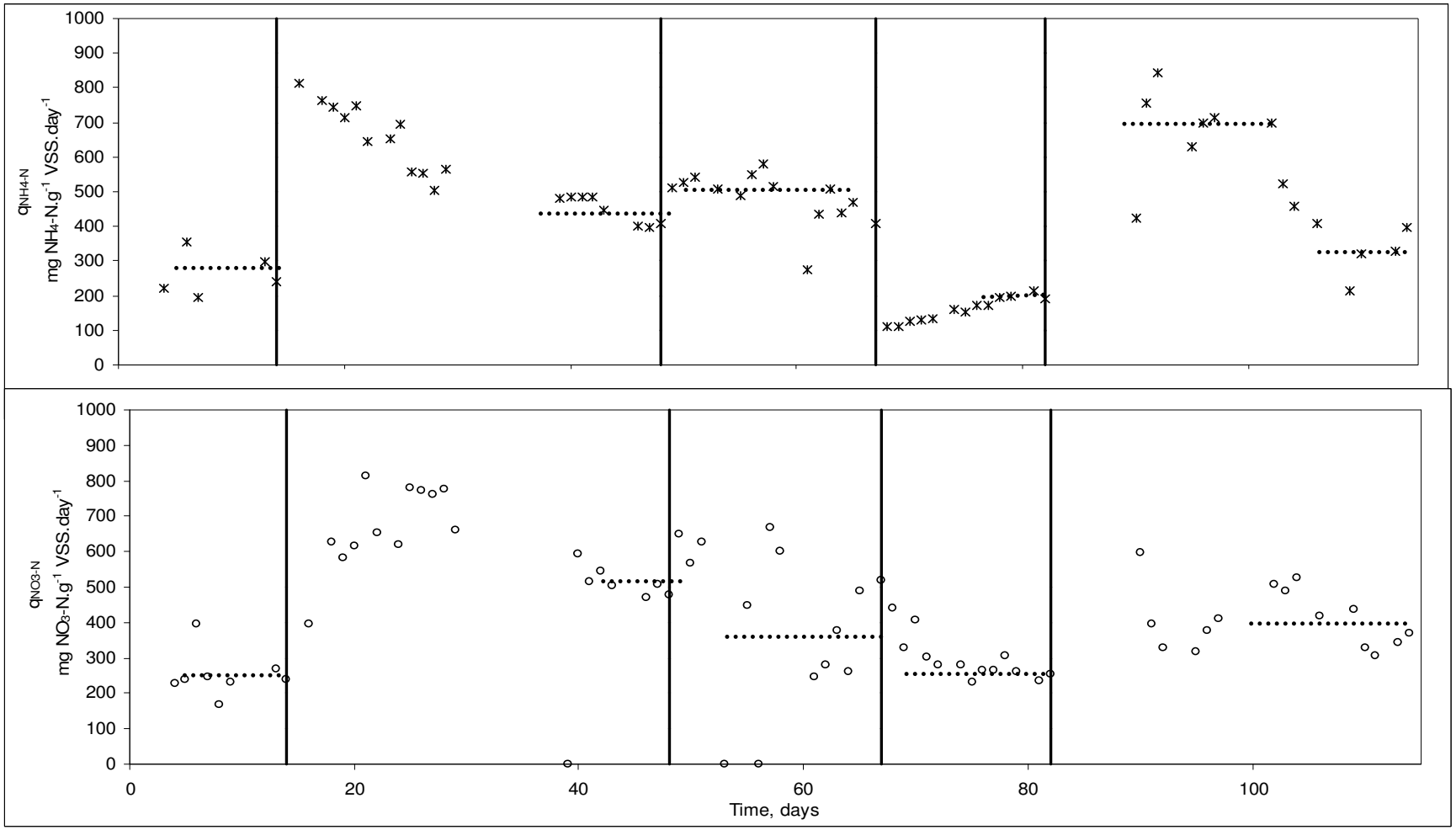

Figure 6.57. Ammonium utilization and nitrate production rates in Phase I at different influent NH_4-N loadings (Dotted lines show the steady-state rates)

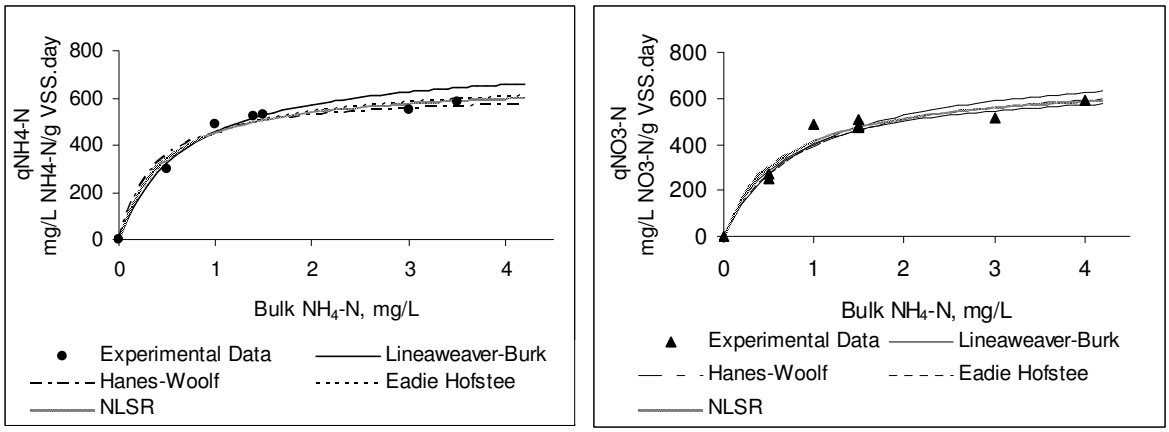

Figure 6.58. Steady-state q_{NH_4-N} and q_{NO_3-N} values at various bulk NH_4-N concentrations

Table 6.18. Maximum Specific Ammonium Utilization Rate ($q_{\max,NH_4-N}$) and Half Saturation Constant ($K_{S,N}$) in Ammonium Utilization in Continuous-Flow Experiments

Method	R^2	K_{S,NH_4-N} mg/L	$q_{\max,NH_4-N}$ mg NH_4-N/g VSS. day	R^2	K_{S,NH_4-N} mg/L	$q_{\max,NO_3-N}$ mg NO_3-N/g VSS. day
Lineaweaver-Burk	0.93	0.69	769	0.93	0.92	769
Hanes-Woolf	0.99	0.38	625	0.98	0.67	667
Eadie Hofstee	0.92	0.23	608	0.88	0.82	713
NLSR	0.89	0.48	671	0.96	0.65	685

6.6.3. Effects of Cd on Ammonium Utilization

To determine the changes in ammonium utilization and nitrate production rates in the presence of Cd, the continuous-flow system was operated at various influent Cd concentrations (Figure 5.4). In this period, NH_4-N, NO_2-N, NO_3-N and MLVSS were daily measured as shown in Figure 6.59. Steady state ammonium utilization and nitrate production rates at various influent Cd are shown in Figure 6.60 and summarized in Table 6.19.

Although addition of 1 mg/L of Cd initially decreased the specific ammonium utilization and nitrate production rates by approximately 30% (Figure 6.60), there was no measurable impact and there were essentially no changes in effluent pH, NH_4-N, NO_2-N and NO_3-N compared to the baseline (before Cd addition) effluent concentrations. Ammonium removal was approximately 90% throughout the continuous feeding period with 1 mg/L Cd. The system was continuously fed with 1 mg/L of Cd for 16 days. After the influent Cd concentration was increased to 2.5 mg/L, specific ammonium utilization rate decreased to 269 mg NH_4-N /g VSS.day corresponding to 47% inhibition. The system was continuously fed with 2.5 mg/L of Cd for 25 days. Contrary to previous batch experiments (Section 6.2.3), there was a 24% decrease in nitrite oxidation that caused nitrite accumulation with 58 mg/L NO_2-N. Upon observing 47% inhibition at 2.0 mg/L influent Cd, continuous feeding of Cd was stopped to see if any recovery took place. Nitrification inhibition recovered only partially by about 20% (Figure 6.59 and 6.60).

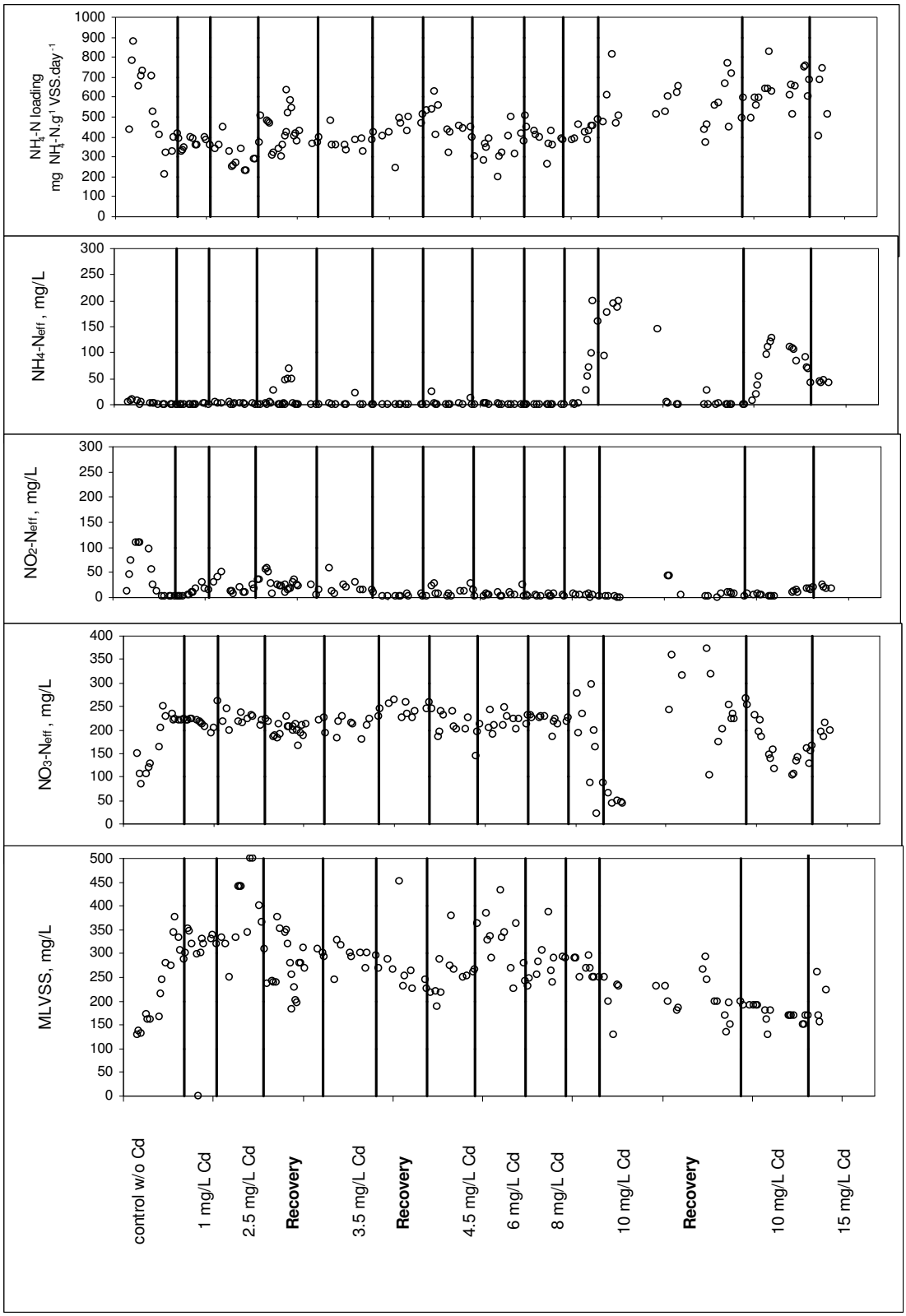

Figure 6.59. Daily ammonium loadings, effluent NH_4-N, NO_2-N, NO_3-N and bulk MLVSS measurements in Phase II with Cd.

Table 6.19. Results of continuous-flow experiments at various ammonium loadings in the presence of Cd

Exp. No	Description of the Experiment	Influent Flowrate	Steady-state ave. pH	Temperature	Steady state influent NH_4-N	Steady-state-NH_4-N loading	Steady grab effluent NH_4-N	Steady-state composite effluent NH_4-N	Steady-state MLSS	Steady- state VSS	Ammonium utilization rate	Steady grab effluent NO_2-N	Steady-state composite effluent NO_2-N	Steady grab effluent NO_3-N	Steady-state composite effluent NO_3-N	Steady-state Nitrate production rate
		L/day	-	^{0}C	mg/L	mg /gVSS.day	mg/L	mg/L	mg/L	mg/L	mg /gVSS.day	mg/L	mg/L	mg/L	mg/L	mg /gVSS.day
1	Continuous feeding with NH_4-N only	10	7.5	25	223	370	0.8	0.9	334	308	577	3.0	0.5	221	230	583
2	Continuous feeding with NH_4-N & 1 mg/L Cd	10	7.55	25	254	395	0.53	0.5	330	330	371	0.2	18	205	212	345
3	Continuous feeding with NH_4-N & 2.5 mg/L Cd	10	7.65	27	226	322	1.83	2.1	515	360	303	2.4	9	230	220	286
4	Continuous feeding with NH_4-N only (recovery period)	10	7.70	26	226	386	1.2	1.0	352	300	392	14	26	210	220	361
5	Continuous feeding with NH_4-N & 3.5 mg/L Cd	10	7.60	26	210	414	1.0	0.5	325	260	370	26	20	210	230	365

Table 6.19. (Continued)

Exp. No.	Description of the Experiment	Influent Flowrate	Steady-state ave. pH	Temperature	Steady-state influent NH_4-N	Steady-state NH_4-N loading	Steady grab effluent NH_4-N	Steady-state composite effluent NH_4-N	Steady-state MLSS	Steady state VSS	Ammonium utilization rate	Steady grab effluent NO_2-N	Steady-state composite effluent NO_2-N	Steady grab effluent NO_3-N	Steady-state composite effluent NO_3-N	Steady-state Nitrate production rate
		L/day	-	^{0}C	mg/L	mg /gVSS.day	mg/L	mg/L	mg/L	mg/L	mg /gVSS.day	mg/L	mg/L	mg/L	mg/L	mg /gVSS.day
6	Continuous feeding with NH_4-N only (recovery period)	10	7.55	26	222	455	0.7	0.9	312	250	422	1.8	3	240	270	464
7	Continuous feeding with NH_4-N & 4.5 mg/L Cd	10	7.60	26	220	451	2.0	1.8	312	250	466	12.3	11.5	220	215	447
8	Continuous feeding with NH_4-N & 6 mg/L Cd	10	7.65	26	222	379	1.1	1.0	375	300	347	1.6	5	225	230	349
9	Continuous feeding with NH_4-N & 8 mg/L Cd	10	7.7	26	220	451	0.4	0.7	315	250	397	1	3	220	210	420

Table 6.19. (Continued)

Exp. No	Description of the Experiment	Influent Flowrate	Steady-state ave. pH	Temperature	Steady-state influent NH_4-N	Steady-state NH_4-N loading	Steady grab effluent NH_4-N	Steady-state composite effluent NH_4-N	Steady-state MLSS	Steady state VSS	Ammonium utilization rate	Steady grab effluent NO_2-N	Steady-state composite effluent NO_2-N	Steady grab effluent NO_3-N	Steady-state composite effluent NO_3-N	Steady-state Nitrate production rate
		L/day	-	^{0}C	mg/L	mg /gVSS.day	mg/L	mg/L	mg/L	mg/L	mg /gVSS.day	mg/L	mg/L	mg/L	mg/L	mg /gVSS.day
10	Continuous feeding with NH_4-N & 10 mg/L Cd	10	7.8	26	224	441	53	98	325	260	45	4.4	3.4	164	199	45
11	Continuous feeding with NH_4-N only (recovery period-I)	10	7.9	26	224	766	198	200	262	150	136	4.7	1.6	45	53	136
12	Continuous feeding with NH_4-N only (recovery period II)	10	7.7	26	210	598	0.1	0.7	280	180	563	7.2	1.8	225	240	638
13	Continuous feeding with NH_4-N & 10 mg/L Cd	10	7.9	26	215	644	120	107	250	171	407	8.6	4.8	130	120	491
14	Continuous feeding with NH_4-N & 15 mg/L Cd	10	7.8	27	230	589	120	120	300	200	417	17	9.7	200	190	417

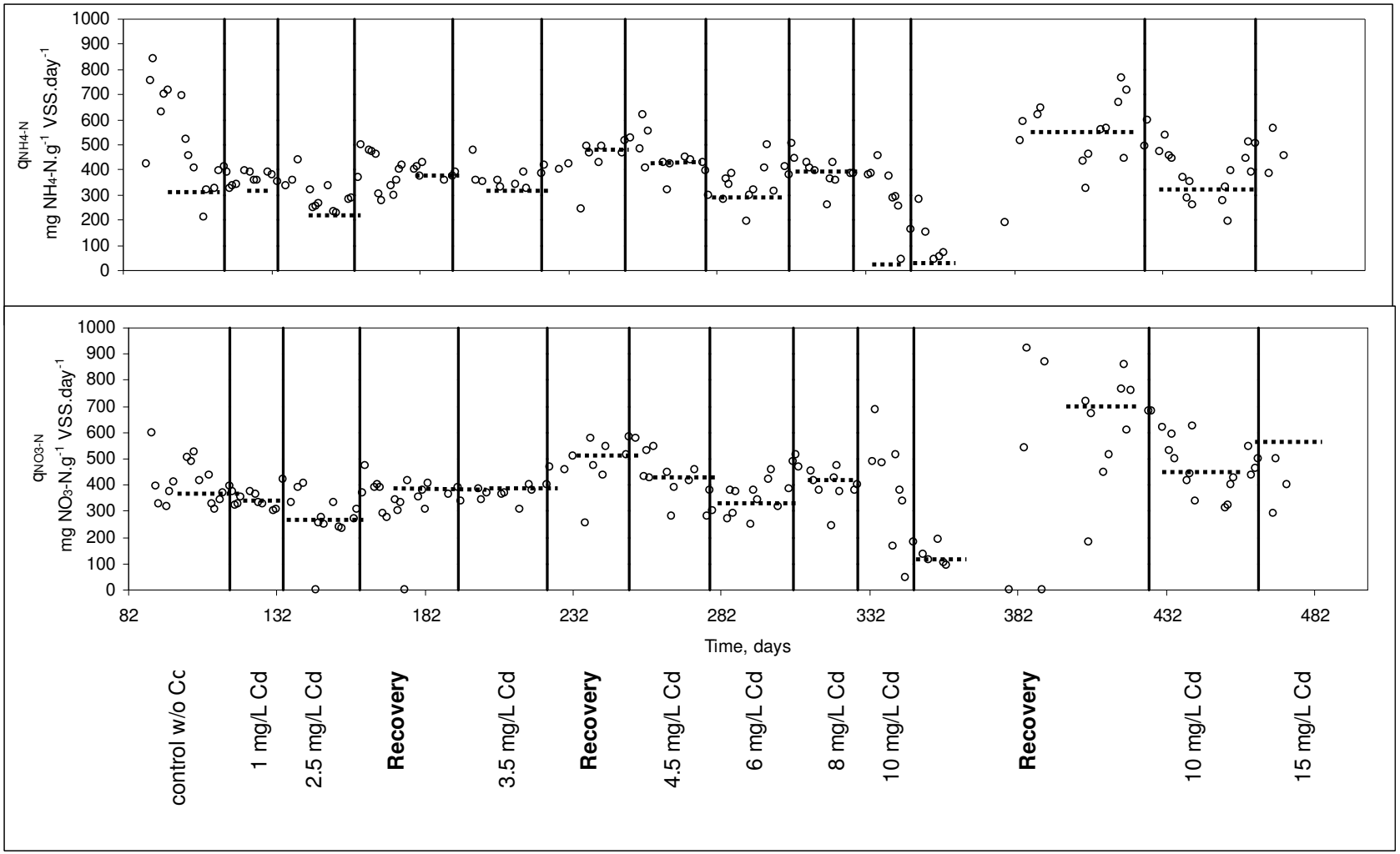

Figure 6.60 Ammonium utilization and nitrate production rates in Phase II with Cd (Dotted lines show the steady-state rates)

No further increase in inhibition was exhibited until the influent Cd concentration was increased up to 10 mg/L in new runs and inhibition ranged from 20 to 40%. At an influent Cd level of 10 mg/L, ammonium concentration increased gradually to 200 mg/L which was accompanied by a decrease in nitrate to 22 mg/L. The $q_{\max,NH_4-N}$ and $q_{\max,NO_3-N}$ were inhibited by 90% as shown in Figure 6.61. On the contrary, a serious nitrite accumulation was not observed during this period. This indicates that ammonia oxidizers are more sensitive than nitrite oxidizers as shown in previous studies (Lee et al., 1997). Continuous feeding of 10 mg/L Cd was stopped and the changes in inhibition levels were followed. After the stop of continuous Cd feeding, the recovery lasted very long, for about 37 days. Interestingly, higher nitrate production rates were observed during this recovery period (Figure 6.60). After attainment of recovery, 10 mg/L Cd was continuously fed to the system for the second time. Contrary to the previous results, there was only 20% decrease in ammonium removal efficiency and 50% decrease in $q_{,NH_4-N}$ and q_{NO_3-N}. As a final step, the influent Cd concentration increased to 15 mg/L and no change was observed in inhibition level and removal efficiency.

Although the free ammonia concentration increased to maximum 5 mg/L during the Cd addition period, the nitrite oxidation inhibition was below 30% all the time. The nitrite oxidation inhibition level ranged between 50-60% according to the empirical equation proposed in Section 6.6.1 (data not shown). The low nitrite oxidation inhibition at such high free ammonia concentration could be the result of the acclimation of nitrite oxidizers to free ammonia. This was also consistent with previous findings (Ning, 2004).

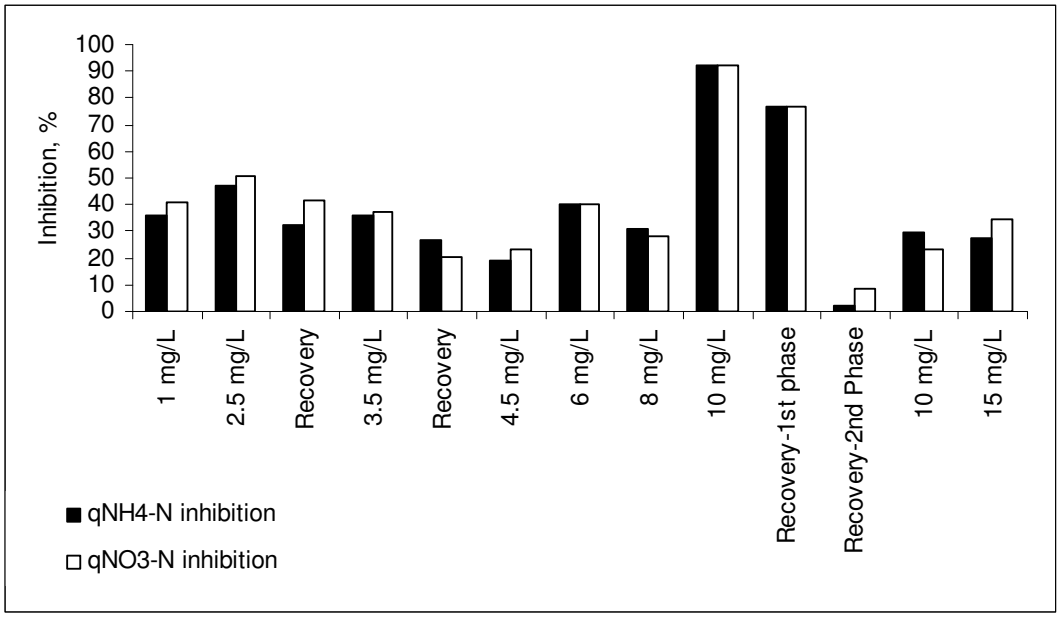

Figure 6.61. Inhibition in $q_{\max,NH_4-N}$ and $q_{\max,NO_3-N}$ with respect to influent Cd concentrations

The specific ammonium utilization rate in the continuous nitrification system in the presence of noncompetitive inhibitors can be predicted by Equation 6.2. The maximum ammonium utilization rate and half-saturation constants were determined in the first phase of the study. In previous batch experiments, the inhibitor coefficient, K_i, was determined in terms of free, labile and biosorbed Cd (Section 6.2.7). Since bulk labile Cd concentration was measured by voltammetry in continuous-flow experiments, the inhibitor coefficient in terms of labile Cd was used for the application of Equation 6.2. The observed q_{NH_4-N} at various bulk labile Cd concentration were compared with the q_{NH_4-N} calculated according to the noncompetitive inhibition models (Equation 6.2). Comparison of the rates is shown in Figure 6.48. As seen, during the initial periods of Phase II, the observed q_{NH_4-N} values were very close to the predicted rates and decreased with Cd concentration. In the range of 3.5 to 10 mg/L influent Cd, the observed q_{NH_4-N} values differed from the predicted ones considerably. According to noncompetitive model results, the rates should be 3.4 times lower than the observed ones. Moreover, although the bulk labile Cd concentration in 3.5 to 8 mg/L influent Cd feeding periods was higher than the 1 to 2 mg/L influent Cd feeding periods, the observed q_{NH_4-N} were higher than or close to

the latter one (Figure 6.62). The potential reasons for this result will be discussed in following sections.

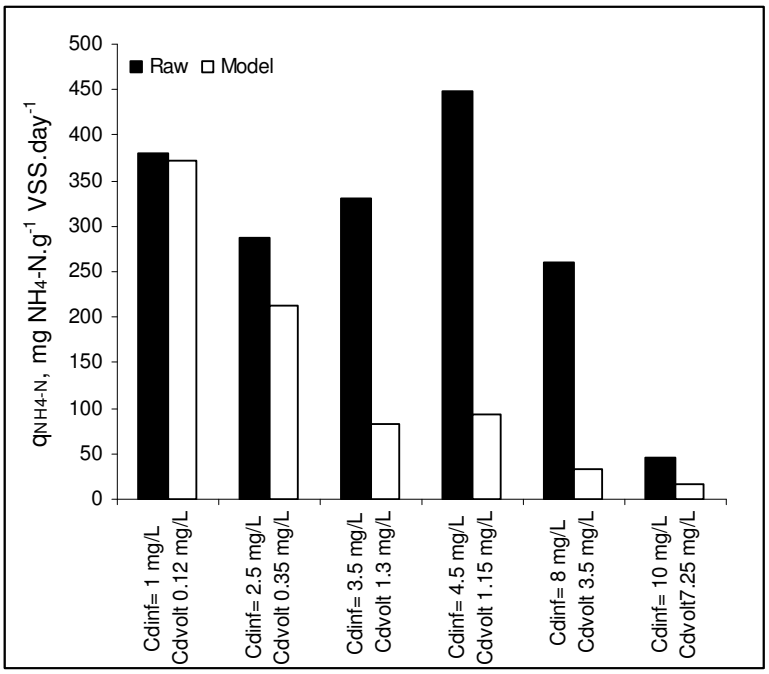

Figure 6.62. Comparison of the observed and predicted q_{NH_4-N} values at various influent and bulk labile Cd concentrations

6.6.4. Relationship Between Inhibition and Cd Biosorption

For each influent Cd concentration, the soluble Cd (Cd_{volt}) in the aeration tank increased. A constant value was reached in terms of soluble and biosorbed Cd (Figure 6.63). Steady-state concentrations of Cd in soluble (labile Cd) and in suspended phases increased as the influent Cd increased (Figure 6.64 and 6.65). For example, increase of influent Cd from 1 to 2.5 mg/L almost led to a doubling of biosorbed Cd from 5.5 to 11 mg Cd/g MLSS. The corresponding inhibition levels in terms of $q_{\max,NH_4-N}$ or $q_{\max,NO_3-N}$ were 30% and 47%, respectively, which was also consistent with the findings of our batch studies (Section 6.2.7). After 2.5 mg/L Cd feeding was stopped, in the recovery period Cd-efflux occurred. This resulted in a gradual decrease of biosorbed Cd from 11 to 5 mg Cd/g MLSS in 9 days and did not change during the rest of the recovery period. Desorption of Cd during the recovery period supported the existence of efflux pumping system that is

activated in the presence of toxic materials and increases the resistance of the microorganisms to toxicity (Nies, 1999). But, all of the Cd could not be pumped out of the cell by this mechanism. The inhibition level decreased from 47% to 27% with the decrease of biosorbed Cd from 11 to 5 mg Cd/g MLSS in the recovery period. Similarly, during 1 mg/L Cd feeding, the biosorbed Cd and corresponding inhibition were 5.5 mg Cd/g MLSS and 30%, respectively. Obviously, there is a strong relationship between biosorbed Cd and inhibition.

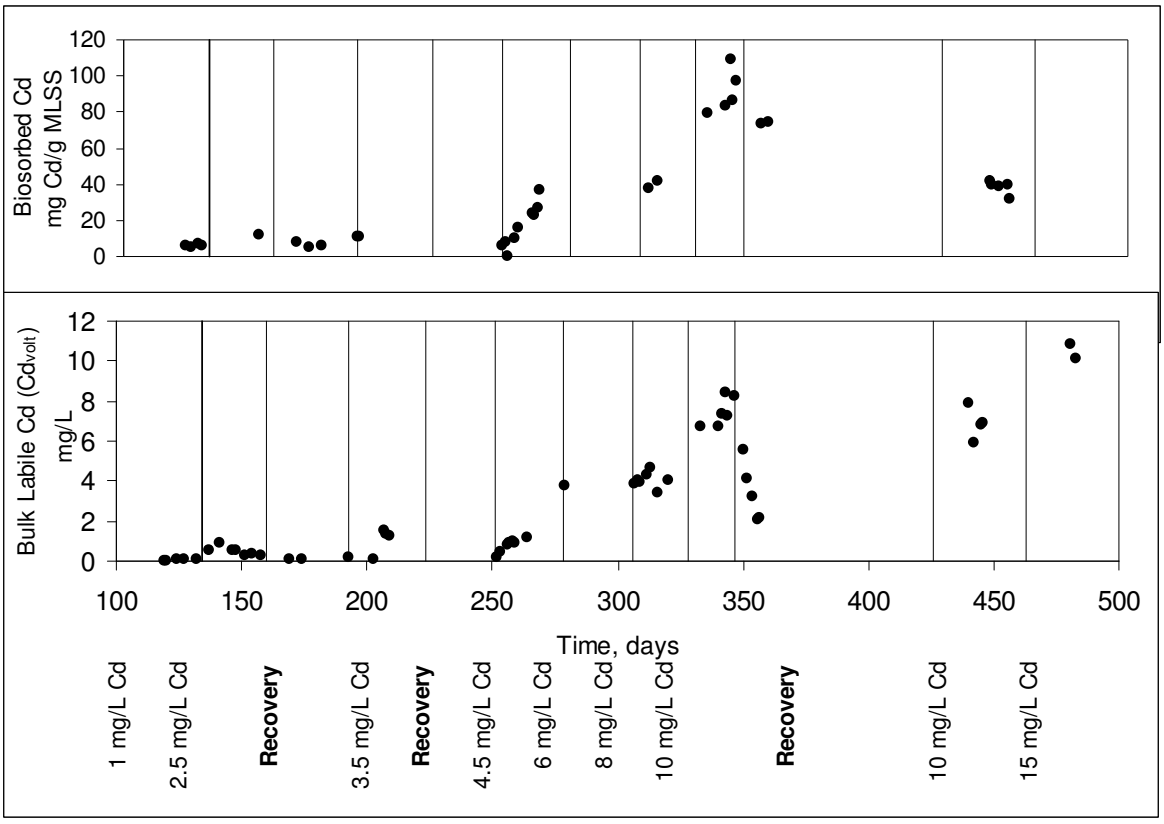

Figure 6.63. Bulk labile Cd (Cd_{volt}) and biosorbed Cd in Phase II

After the first recovery period, the influent Cd concentration was increased stepwise from 3.5 to 10 mg/L. At 4 and 8 mg/L influent Cd concentrations, biosorbed Cd ranged between 36-41 mg Cd/g MLSS and the maximum Cd adsorption capacity in previous batch adsorption experiment was reached (Section 6.3.1). Interestingly, no inhibition was observed throughout these periods as explained previously (Section 6.6.3). Further increase in influent Cd to 10 mg/L resulted in maximum uptake of Cd onto sludge and the biosorbed Cd was about 98 mgCd/g MLSS, which was far beyond the maximum

adsorption capacity in batch adsorption studies (Section 6.3.1). Hence, maximum inhibition was observed in this period. Acclimation was found to enhance the sorptive capacity of nitrifying bacteria which was consistent with another study conducted with nickel in an activated sludge system (Arican and Yetiş, 2003).

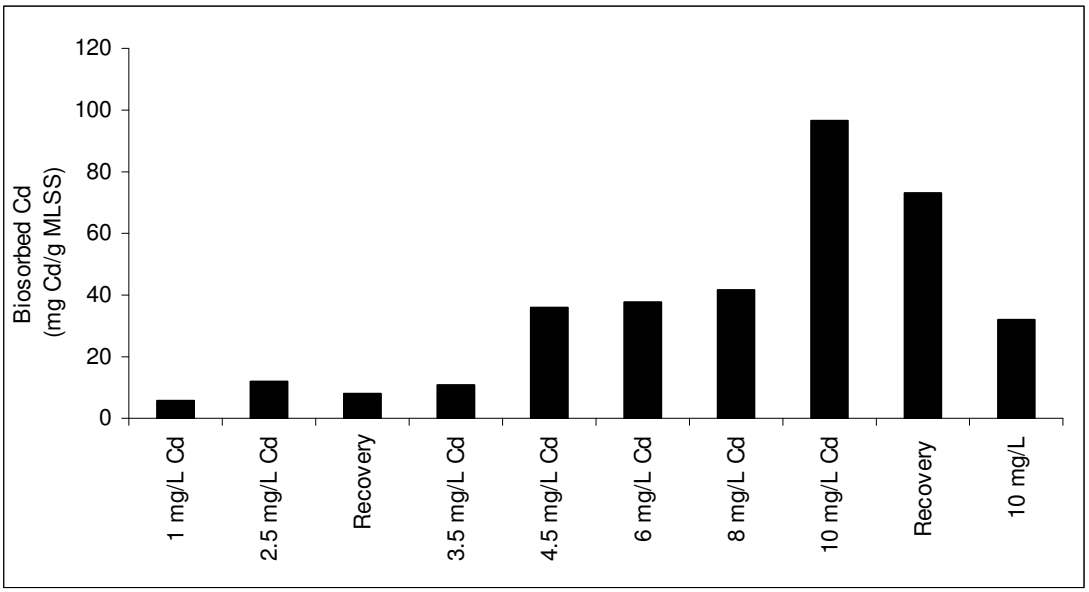

Figure 6.64. Steady-state biosorbed Cd in continuous-flow experiments

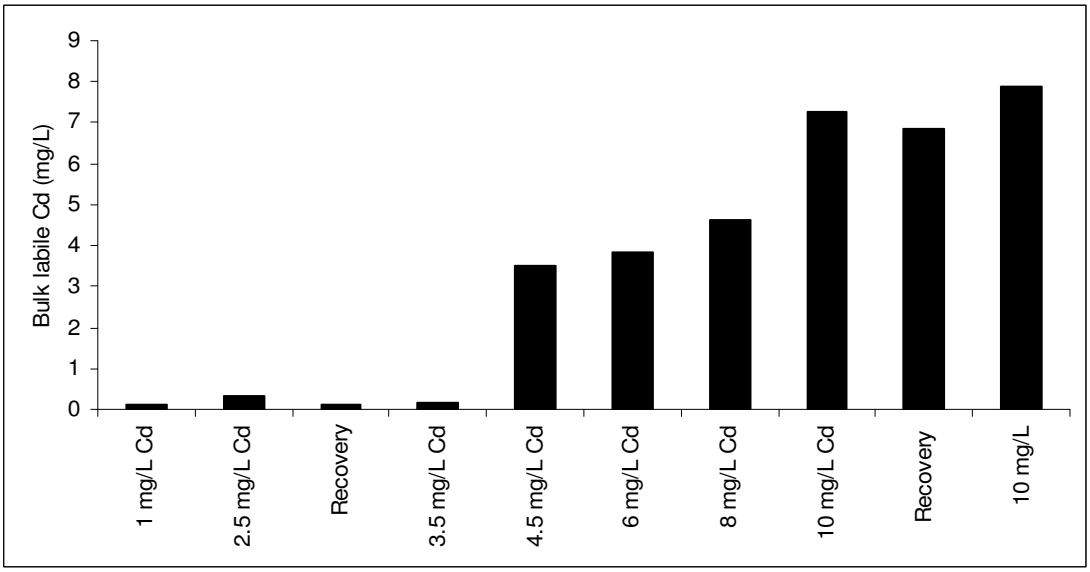

Figure 6.65. Steady-state soluble bulk labile Cd concentrations in continuous-flow experiments

Our previous studies had showed that inhibition could be expressed in terms of free, labile or biosorbed Cd concentrations in batch systems (Section 6.2.7). On the other hand, in this study, inhibition could not be represented in terms of biosorbed or bulk labile Cd (Figure 6.66). The inhibition level for labile Cd concentrations of 1.15 and 4 mg/L should be 71 and 82%, respectively, according to the model equations developed in the batch experiments. On the contrary, the observed inhibition level at these Cd concentrations was only 30 to 40% in this study. There may be two explanations for observing a relatively low inhibition at high bulk Cd concentration in continuous-flow experiments. Microorganisms can develop a heavy metal resistance system (Nies, 1999). This system is mediated by a series of systems like the permeability barrier, intra- and extra-cellular sequestration, active transport efflux pump, enzymatic detoxification and reduced sensitivity of cellular targets to metal ions. The primary mechanism of metal removal takes place by a metabolism-independent process (passive uptake) through ion-exchange phenomena, complexation with negatively charged groups, adsorption and precipitation by extracellular polymeric substances (EPS) (Principi et al., 2006). Such EPS contribute to the removal of organic and inorganic substances, and favor floc formations by promoting microorganism aggregation (Principi et al., 2006).

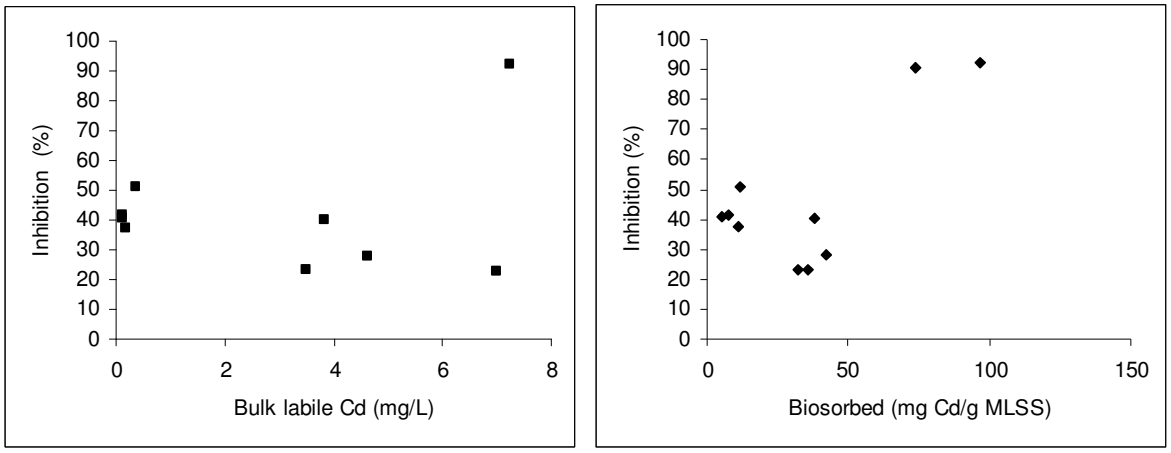

Figure 6.66. Relationship between inhibition and different forms of Cd (a) bulk labile Cd (b) biosorbed Cd

In our system, the biofloc structure differed significantly before and after continuous Cd loading. As a result of continuous Cd addition, biomass seemed to deflocculate. Deflocculation entails the breakup of biomass flocs, which results in particles that can not

be removed using conventional gravity processes and causes increased effluent suspended solids. In our study, the sludge volume index (SVI) increased to 200 from 95 L/g after Cd addition that indicated deterioration in sludge settling properties. Galil et al. (1998), Neufeld (1976) and Zarnovsky et al. (1994) found that phenol and heavy metals can induce deflocculation in a conventional activated sludge. Bott and Love (2002) also showed that shock loads of electrophilic chemicals (e.g. chloro-2,4-dinitrobenzene, N-ethylmaleimide, 2,4-dinitrotoluene and cadmium) induce deflocculation. They hypothesized that a physiological bacterial stress response mechanism existed, called the glutathione-gated potassium efflux (GGKE) system, which is a significant contributor to activated sludge deflocculation. They observed significant potassium (K^+) efflux from activated sludge flocs to the bulk liquid in response to sublethal (concentration less than the required to reduce the specific oxygen uptake rate by 50%) shock loads of cadmium and chloro-2,4-dinitrobenzene, N-ethylmaleimide, 2,4-dinitrotoluene. The existence of K^+ efflux systems supported the observed increase in effluent turbidity. Bott and Love (2002) hypothesized that the short-term increase in bulk soluble potassium increases the monovalent to divalent cation ratio in the floc, which causes deflocculation by weakening cation-bridged links within the flocs. The resistance of bacteria to heavy metal inhibition may be attributed to the glutathione-gated potassium efflux (GGKE) system. Since the bulk K^+ concentration was not measured in this study, this hypothesis could not be supported. Another explanation may be the shifts and changes in nitrifying structure as a result of Cd inhibition. It is well known that some bacterial species are more resistant to toxic chemicals and dominate in a toxic environment (Tsai et al., 2006). Shifts and changes in nitrifying structure as a result of Cd inhibition were further discussed in detail in the following section.

6.6.5. Microbial Community Analyses

FISH results showed that the ammonia oxidizers constituted the majority of all microorganisms (Figure 6.67), since the NSO190 probe hybridizes to rRNA of a broad range of *Nitroso*-type bacteria (e.g. *Nitrosomonas eutropae*, *Nitrococcus mobilis*). Figure 6.67 shows that ammonia oxidizers form dense subclusters within the floc. Although nitrite oxidation took place in whole operational period of the continuous-flow reactor, no hybridization signals could be observed for nitrite oxidizers with the use of NIT3 and NTSPA662 probes. It may be due to the insufficient quantity of nitrite oxidizers (*Nitrospira* and *Nitrobacter*).

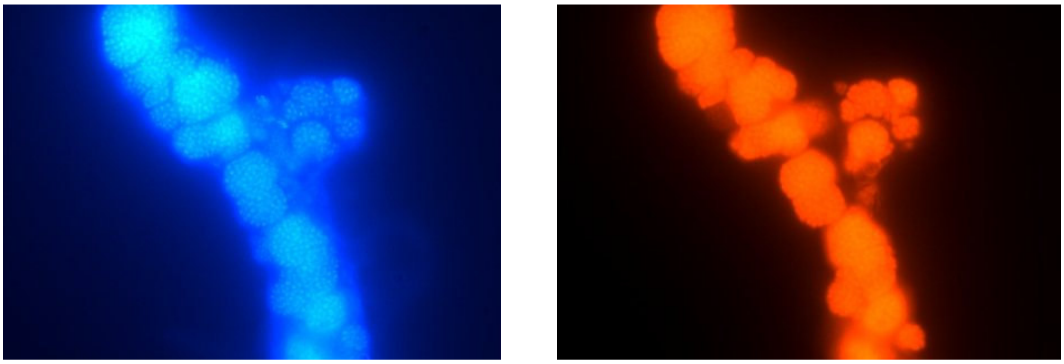

(A) (B)

Figure 6.67. Photomicrographs of FISH images, (A) All microorganims visualized with DAPI staining (blue) (B) FISH with oligonucleotide probes NSO190 (red) for *Nitrosomonas* species

The quantity changes and variations of all microbial species were investigated by the Slot-blot hybridization technique. For this purpose, the DNA was extracted from sludge samples taken at regular time intervals in continuous-flow experiments. Sampling information is given in Table 6.20. The results of these analyses are shown in Figure 6.68. Names and specificities of the probes used in Slot-Blot analysis are shown in Table 6.21. In the slot-blot hybridization method used in the determination of bacterial diversity and quantity according to time, DNA/RNA extracted from the cell, are transferred on the nylon or nitrocellulose membranes without any processing. In this study, because of the low bacteria amount, species and quantity diversity in bacteria are searched in the PCR amplified samples. Since the quantification with PCR amplification is not a reliable

method, the results was evaluated relative to the thickness of blank DNA band of each probe.

Table 6.20. Sampling Information for Slot-Blot Hybridization and DGGE analysis

Sample Name	Influent NH_4-N (mg/L)	Influent Cd (mg/L)	Sample Date- day
S1	200	-	03.15.2005-47
S2	250	-	05.11.2005-104
S3	200	1	05.20.2005-113
S4	200	2.5	06.13.2005-137
S5	200	2.5	06.26.05-153
S6	200	3.5	08.18.05-193
S7	200	recovery period	09.16.2005-232
S8	200	6	11.28.2005-306
S9	200	10	12.21.2005-280
S10	200	10	1.04.2006-342
S11	200	recovery period-1st phase	01.18.2006-357
S12	200	recovery period-2nd phase	03.29.2006-426
S13	200	15	05.10.2006-468
S14	200	15	05.22.2006-480

Table 6.21. Names and specificity of the probes used in slot-blot analysis

Probe	Specificity
EUB 338	Bacteria Domain
NSO190	*Nitrospira briensis, Nitrosovibrio tenuis, Nitrosolobus multiformis, Nitrosomonas europea, Nitrosomonas eutropha, Nitrocossus mobilis* and *Nitrosomonas C56*
NSM 156	*Nitrosomonas C56, Nitrosomonas europea, Nitrosomonas eutropha* and *Nitrocossus mobilis*
NSV 443	*Nitrosolobus multiformis, Nitrosospira briensis,* and *Nitrosovibrio tenuis*
NIT3	*Nitrobacter* spp.
NTSPA 662	*Nitrospira* spp.

In contrast to FISH results, hybridization signals were observed not only for Bacteria domain and *Nitrosomonas* species, but also *Nitrobacter* and *Nitrospira* species. No significant changes occurred in the quantity of Bacteria domain *Nitrobacter* spp. and *Nitrospira* spp. during the operation of the continuous-flow nitrifying reactor in the presence and absence of Cd. The band thickness observed for *Nitrobacter* spp. and *Nitrospira* spp. indicated that the quantity of these species were almost equal to each other and also ammonia-oxidizing β-Proteobacteria (NSO190). On the other hand, the quantity of the *Nitrosomonas C56, Nitrosomonas europea, Nitrosomonas eutropha* and *Nitrocossus mobilis* (NSM 156) seemed to be decreased near the end of the study. In this respect, it may be concluded that *Nitrospira briensis, Nitrosovibrio tenuis* and *Nitrosolobus multiformis* dominated in the system as a result of Cd inhibition. Although the NSV 443 probe which was designed to hybridize *Nitrosolobus multiformis, Nitrosospira briensis,* and *Nitrosovibrio tenuis* species was also used to search the existence of these species, no hybridization signal were observed (data not shown). It could be due to the operating conditions of the slot-blot analysis.

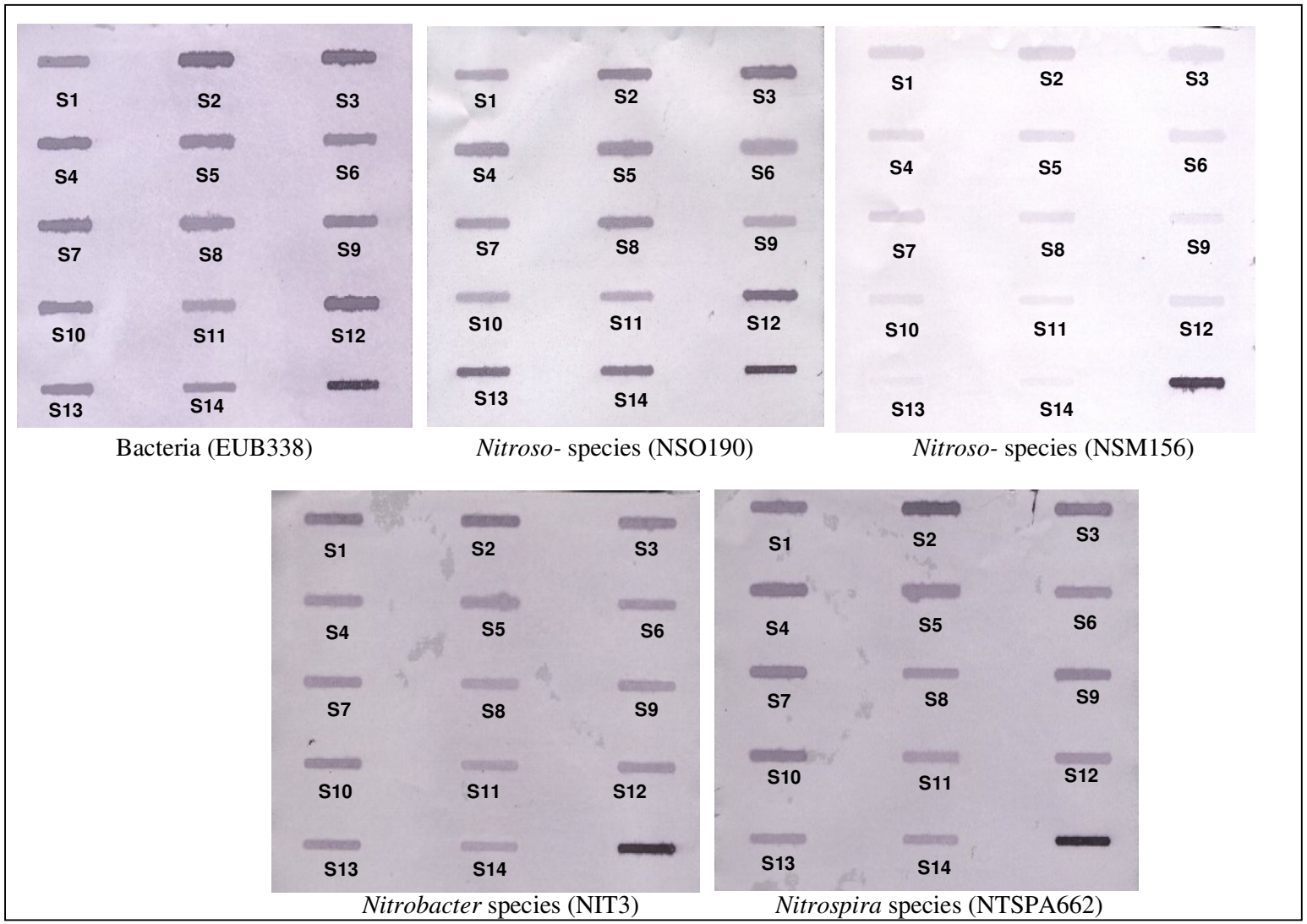

Figure 6.68. Results of slot-blot analyses

The possible changes and shifts in the diversity of nitrifying bacteria in Phase I and II were examined with DGGE analysis (Figure 6.69). The active AMO gene of the ammonia oxidizers was used for this purpose. The sampling information is given in Table 6.20.

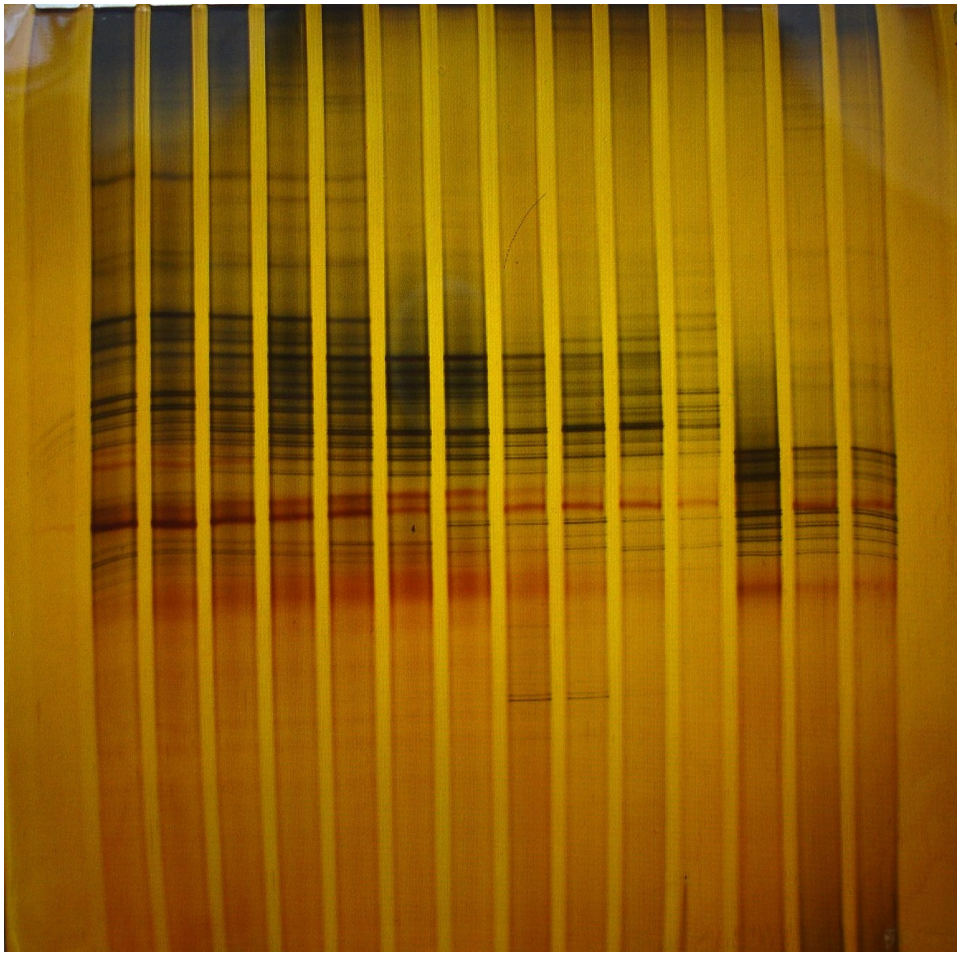

Figure 6.69. DGGE results of PCR amplified amoA genes (Sample dates are given in Table 6.20)

The operational period can be divided into three phases in terms of the changes in nitrifying species. The first phase covers samples S1 to S5 (47 to 153 days). It consists of the operation of the reactor in the absence of Cd and operation with continuous feeding of 1 and 2.5 mg/L influent Cd. The results of cloning and sequence analysis of

sample S1 revealed that initially the active species in this phase were *Nitrosomonas sp.* clone Y34, Uncultured *Nitrosomonas sp.* clone Y35 and *Nitrosomonas eutropha.* The effect of Cd on the diversity of the *Nitrosomonas* species was not observed throughout S1 to S5. The second phase started with the addition of 3.5 mg/L Cd. *Nitrosomonas sp.* clone Y34 and Uncultured *Nitrosomonas sp.* clone Y35 disappeared and *Nitrosomonas eutropha and Nitrococcus mobilis* became dominant in the system (samples S6 to S11) during this phase. There was a big difference in this period between observed and predicted $qNH_4 - N$ as explained before. Furthermore, the observed inhibition throughout this period was inconsistent with previous batch experiments. The reason could be the change in microbial species. Biokinetic parameters had been determined with a biomass in which *Nitrosomonas sp.* clone Y34, uncultured *Nitrosomonas sp.* clone Y35 and *Nitrosomonas eutropha* were dominant.

A major change occurred in the diversity of ammonia oxidizers as a result of severe inhibition caused by 10 mg/L Cd (Figure 6.61). Cd addition exerted its major effect in samples from S12 to S14. As shown in Figure 6.61, the recovery period consisted of two phases. During the first phase, inhibition continued for a certain period of time despite the stop of continuous Cd feeding. *Nitrosomonas eutropha and Nitrococcus mobilis* were still present during this phase (sample S11). In the second phase, recovery was observed as indicated by an increase in $q_{\max,NH_4-N}$ and $q_{\max,NO_3-N}$. These rates increased even to higher values than before Cd addition (Figure 6.60). The S12 sample was taken in the second phase of the recovery period. The location of the bands in the DGGE analysis changed for samples S11 and S12 (Figure 6.69) which was an indication of a change in microbial community in this period (see Table 6.20). Heavy metal resistant species became dominant in the system. A new Cd input of 10 mg/L of Cd and then another dosing at 15 mg/L Cd did not cause an inhibition as expected (Figure 6.61). Cloning and sequence analysis of the samples from S12 to S14 showed that this new metal resistant species was *Nitrosospira sp.*

Continuous-flow experiments reflected the response of microbial species subject to prolonged toxic metal exposure in real activated sludge systems. A constant input of

Cd to a nitrification system for a long period of time allowed us to follow the performance and microbial changes in nitrifying culture.

Exposure of nitrifying bacteria to 1 to 2.5 mg/L of Cd inhibited nitrification moderately. The inhibition during this period could be predicted with the model developed from batch experiments. Increase of influent Cd concentration to 3.5 mg/L and further to 8 mg/L did not inhibit the system. This was unexpected and also was not consistent with previous batch experiments. Acclimation enhanced the biosorptive capacity and the resistance of nitrifying bacteria to Cd. Acclimation occurred by the selection of heavy metal resistant species. Dependent on the level of metal feeding, sensitive nitrifying species disappeared and heavy metal resistant bacteria became dominant in the sludge. At moderate inhibition levels *Nitrosomonas sp.* clone Y34, Uncultured *Nitrosomonas sp.* clone Y35 species were present, but these species disappeared. Instead, *Nitrosomonas eutropha and Nitrococcus mobilis species* became dominant in the sludge. *Nitrosospira sp. was* found to be the most resistant species. When this species became dominant in the system only 50% inhibition was observed at 10 and 15 mg/L Cd.

Cd addition induced the deflocculation and deteriorated the settling characteristics of the sludge. The settling characteristics of the sludge did not improve during the recovery periods and throughout the study.

The results of continuous-flow experiments also showed that activity of nitrifying bacteria could change as a result of shifts in microbial community. The great difference between the inhibition levels reported in various studies (Lee et al., 1997, Gerneay et al.,1998, Hu et al., 2002) for the same metal could be due to the existence of different nitrifying species in each system. This study is a good example on the importance of incorporation of molecular tools into heavy metal inhibition studies. As far as we know, there is not such a study searching the long-term effects of Cd in an enriched nitrifying system by evaluating the operational results together with molecular techniques.

7. CONCLUSIONS AND RECOMMENDATIONS

Within the scope of this study, inhibitory effects of Cd and Zn on nitrification were investigated through batch and continuous-flow experiments using enriched nitrifying biomass. The summary of the results is as follows:

Both Cd and Zn have an inhibitory effect on ammonium and nitrite oxidizing bacteria in batch nitrification systems. The inhibitory levels were found to be dependent on the chemical Cd and Zn speciation and exposure time as summarized below:

Both the FIAM and BLM models basing on free metal ion activity and biosorbed metal concentration were successfully applied. The good correlation between labile Cd (or Zn) and nitrification inhibition indicated that also weak Cd (or Zn) complexes could contribute to inhibition besides free Cd (or Zn). This leads to the result that the labile metal concentration should also be considered in reporting inhibition levels. A novelty of the study was to determine labile Cd (or Zn) analytically by voltammetry for nitrification inhibition. Voltammetry was employed to differentiate between the total (complexed and uncomplexed metal) and the labile Cd. Hence, the use of voltammetry is recommended in the assessment of the relationship between inhibition and metal speciation.

The use of phosphate buffer in metal inhibition tests for pH adjustment is not recommended since it caused to observe lower inhibition levels for Cd and Cu by decreasing the initial labile metal concentration.

The influence of the exposure time on inhibition level determination depends on the concentration and type of metal. Use of short-term oxygen uptake rate experiments to determine (e.g. 10 min) the inhibitory levels in nitrification systems was observed to be not appropriate and led to misinterpretation of results for the metals having slow uptake kinetics like Cd and Cu. During the course of a batch operation, the inhibitory effect of Cd on nitrification increased tremendously. On the contrary, the results of

short-term and long-term experiments would be the same for the essential Zn metal under similar test conditions (e.g. chemical speciation, test culture and pH etc.).

The existence of sensitive sites (extracellular sites) on the membranes was realized by using EDTA as a washing agent. The long-term oxygen uptake rate measurements also allowed to follow the existence of two different inhibition stages, an initial rapid stage followed by a second slower one, which is very similar to the metal uptake profiles. The first rapid inhibition phase was completed in 60 minutes for all metal concentrations and corresponded to inhibition of passive metal uptake sites (extracellular sites) while the slow stage may be due to the inhibition of metabolism dependent active metal uptake sites (intracellular sites).

Both Cd and Zn exhibited noncompetitive inhibitor characteristics in ammonium utilization. The affinity of free Zn for active site enzyme was found to be significantly higher than that of free Cd. On the contrary, the affinity of labile and biosorbed Cd and Zn for the active site enzyme was found to be similar. The toxicity of metals in activated sludge systems has been studied in detail while the inhibition kinetics has been studied to a lesser extent. Specifically, there are only a few studies that investigated the inhibition type and kinetics of Cd and Zn in an enriched nitrification system. In this study, empirical noncompetitive inhibition equations were proposed in terms of free, labile or biosorbed Cd (or Zn) concentrations in batch nitrification systems. These equations can be used to predict the effects of shock loads of Cd and Zn in nitrification systems. Especially, the inhibition equation based on labile metal concentration could be very useful since it only requires the measurement of labile metal.

Biosorption of Cd was expressed with Langmuir isotherm whereas Freundlich isotherm represented biosorption of Zn onto nitrifying biomass. Biosorption of Cd and Zn followed pseudo-second order kinetics. The second-order constant for Zn is higher than Cd showing that equilibrium was reached in shorter period of time. Furthermore, capacity and kinetics of Zn and Cd biosorption did not change in the presence of anions and cations. That may indicate the high affinity of sensitive sites to these metals.

Biosorption experiments with Zn showed that there were two different sites available for Zn binding which was contrary to the case of Cd binding. This may support the existence of multiple sites for an essential metal like Zn.

Consistent results were obtained from the comparison of the labile Cd measured with voltammetry and calculated with MINEQL. This showed that voltammetry may eliminate the use chemical equilibrium models such as MINEQL 4.5 for the determination of free metal ion concentration or metal speciation. Conditional stability constant determined for Zn and Cd were found to be very close to the values given in literature, especially for bacteria. That indicated that nitrifying bacterial surfaces contained similar functional groups as the other bacteria species.

Both batch and continuous-flow studies showed that ammonium oxidizing bacteria (AOB) were more sensitive to metal inhibition than nitrite oxidizing bacteria (NOB).

Continuous-flow experiments performed at various ammonium loadings showed that free ammonia inhibited nitrite oxidizing bacteria more severely than ammonium oxidizing bacteria. The threshold free ammonia concentration that inhibits nitrite oxidation could change with the quantity of nitrite oxidizing bacteria.

Cd addition induced the deflocculation and deteriorated the settling characteristics of the sludge. The settling characteristics of the sludge did not improve during the recovery periods and throughout the study. Nitrifying bacteria may activate the glutathione-gated potassium efflux (GGKE) system, which is a physiological bacterial stress response mechanism to Cd shock load.

Contrary to the findings of batch experiments, in the continuous-flow reactor inhibition could not be expressed in terms of free, labile or biosorbed Cd concentrations. Acclimation was found to enhance the sorptive capacity of nitrifying bacteria which was consistent with literature findings.

FISH results showed that the ammonia oxidizers constituted the majority of all microorganisms and formed dense subclusters within the floc. No hybridization signals could be observed for nitrite oxidizers with the use of NIT3 and NTSPA662 in FISH analysis. In contrast to FISH results, hybridization signals were observed not only for Bacteria domain and *Nitrosomonas* species, but also *Nitrobacter* and *Nitrospira* species in Slot-blot analyses. The quantity of *Nitrobacter* spp. and *Nitrospira* spp. did not change during the operation of the continuous-flow nitrifying reactor in the presence and absence of Cd. This also showed the low sensitivity of nitrite oxidizing bacteria (NOB) to heavy metals.

DGGE analysis of amoA genes allowed tracking the shifts and changes in ammonia oxidizers during the whole experimental period. The results of cloning and sequence analysis of selected samples revealed that *Nitrosomonas sp.* clone Y34 and Uncultured *Nitrosomonas sp.* clone Y35 were the species that were most sensitive to Cd inhibition whereas *Nitroosomonas eutropha and Nitrococcus mobilis* species were moderately sensitive. *Nitrosospira* was found to be the most resistant species to Cd among ammonia oxidizers.

The results of continuous-flow experiments also showed that activity of bacteria and inhibition levels of toxic chemicals (organic or inorganic) should be reported with the name and if possible with the quantity of the species present in a culture. Hence, molecular tools and activity or inhibition measurements should be carried out simultaneously.

In view of the findings of this study, the following recommendations are made for future researches:

1) In the present study, the individual effects of Cd or Zn were investigated and modelled separately. But in real cases, metals are simultaneously present in a wastewater. Furthermore, heavy metals can be present with other toxic organic compounds or complexing agents. Therefore, the inhibitory characteristics of a metal mixture and changes in inhibition coefficients should be investigated. Also,

application of FIAM and BLM models in the presence of different metals is another area requiring additional research.

2) We have successfully predicted the labile metal concentration in the presence of complexing agents (e.g. EDTA, HCO_3^-, SO_4^{2-} and a biotic ligand, bacteria) with the help conditional stability constants. The prediction of labile metal concentration in a more complex environment (e.g. mixture of metals or other bacteria species) should also be investigated.

3) The response of nitrifying species subjected to prolonged exposure to essential metals such as Zn or Cu should be investigated. This can lead us to understand the heavy metal resistance mechanisms in the presence of essential metals.

4) In the present work, the cloning and sequence analyses were carried out only for ammonia oxidizing species. The possible shift and changes in nitrite oxidizers could not be evaluated with the help of molecular techniques. Observing different threshold free ammonia concentrations could be due to the existence of different nitrite oxidizers. Therefore additional research could be made in this area.

8. REFERENCES

http://www.cpp.org.pk/articles/heavy_metals.html

Alder, C. A., Siegrist, H., Gujer, W., Giger, W., 1990. Behaviour of NTA and EDTA in biological wastewater treatment. Water Research, 24, 733-742.

Allison J. D., Brown D. S., Novo-Gradac K. J.,1991. MINTEQA2/PRODEFA2, A Geochemical Assessment Model for Environmental Systems: Version 3.0 Users Manual. U. S. Environmental Protection Agency, Athens, GA, EPA/600/3-91/021.

Alpaslan K. B. and Çeçen F., 2005. Cometabolic degradation of TCE in enriched nitrifying batch systems, Journal of Hazardous Materials, B125, 260-265.

Alsop, D.H., and Wood, C.M., 2000. A kinetic analysis of zinc accumulation in the gills of juvenile rainbow trout: the effects of zinc acclimation and implications for biotic ligand modelling. Environmental Toxicology Chemistry, 19, 1911-1918.

Arican, B., Yetiş, Ü., 2003. Nickel sorption by acclimatized activated sludge culture. Water Research, 37, 3508-3516.

Artola, A., Balaguer, M. D., Rigola, M., 1997. Heavy metal binding to anaerobic sludge, Water Research., 31 (5), 997-1004.

Barth E. F., Salotto, B. V., McDermott, G. N., English, J. N., Ettinger, M. B., 1963. Effects of a mixture of heavy metals on sewage treatment processes. Proceeding of the 18th Industrial Waste Conference, Purdue University, 115, 616-635.

Battistoni P., Fava, G., Ruello, M. L., 1993. Heavy metal shock load in activated sludge uptake and toxic effects. Water Research, 27 (5), 821-827.

Bates, S. S., A. Tessier, P. G. C. Campbell, and J. Buffle, 1982. Zinc adsorption and transport by *Chlamydomonas variabilis* and *Scenedesmus subspicatus* (Chlorophyceae) grown in semicontinuous culture. Journal Phycology, 18, 521-529.

Beg, S. A., Atiqullah, M., 1983. Interactions of noncompetitive inhibitors on the nitrification process. Journal Water Pollution Control Federation, 35 (8), 1080-1086.

Beg, S. A., Siddiqi, R. H., Ilias, S., 1982. Inhibition of nitrification by arsenic, chromium, and flouride. Journal Water Pollution Control Federation, 54 (5), 482-488.

Benguella, B., Benaissa, H., 2002. Cadmium removal from aqueous solution by chitin: kinetic and equilibrium studies. Water Research, 36, 2463–2474.

Braam F., Klapwijk, Abraham., 1981. Effect of copper on nitrification in activated sludge. Water Research, 15, 1093-1098.

Brown, P. L., Markich, S. J., 2000. Evaluation of the free ion activity model of metal-organism interaction: extension of the conceptual model. Aquatic Toxicology, 51, 177-194.

Bruins, M., R., Kapil, S., Oehme, F. W., 2000. Microbial resistance to metals in the environment. Ecotoxicology and Environmental Safety, 45, 198-207.

Bott, A. W., 1995. Voltammetric determinations of trace concentrations of metals in the environment, Current Separations, 14:1, 24-30.

Bowles, K. C., Apte, S. C., Batley, G. E., Hales, L. T., Rogers, N., J., 2006. A rapid Chelex column method for determination of metal speciation in natural waters. Analytica Chimica Acta, 558, 237-245.

Bux, F., Atkinson, B., Hasan, H. C., 1999. Zinc biosorption by waste activated and digested sludges. Water Science and Technology, 39 (10-11), 127-130.

C. P. Leslie Grady, Jr., Henry, C. Lim., 1980. Biological Wastewater Treatment Theory and Applications, CRC Press, Inc.

Campbell, P.G.C., Errécalde, O., Fortin, C., Hiriart-Baer, V. P., Vigneault, B., 2002. Metal bioavailability to phytoplankton-applicability of the biotic ligand model. Comparative Biochemistry and Physiology Part C 133:189-206.

Campbell, P.G.C.**,** 1995. Interactions between trace metals and aquatic organisms: a critique of the free ion activity model. In Tessier, A. and D.R. Turner: Metal Speciation and Bioavailability in Aquatic Systems, John Wiley & Sons, Chichester :45-102.

Cheng, M. H., Patterson, J. W., Minear, R. A., 1975. Heavy metals uptake by activated sludge. Journal. WPCF, 47 (2), 362-376.

Chu, K. H., Hashim, M. A., Phang, S. M., Samuel V. B., 1997. Biosorption of cadmium: adsorption and desorption characteristics. Water Science and Technology, 35 (7), 115-122.

Codina, J. C., Perez-Garcia, A. and de Vicente, A., 1994. Detection of heavy metal toxicity and genotoxicity in wastewaters by microbial assay. Water Science Technology, 30 (10), 145-151.

Cornish-Bowden, A., 1995. Fundamentals of Enzyme Kinetics. Portland Press Ltd., London.

Çeçen, F. and Gürsoy, G., 2000. Characterization of landfill leachate and studies on heavy metal removal. Journal of Environmental Monitoring, 2, 436-442.

Çeçen, F. and Gürsoy, G., 2001. Biosorption of heavy metals from landfill leachate onto activated sludge. Journal of Environmental Science and Health, A36 (6), 987-998.

Daughney, C.J., Fein, J.B., 1998. The effect of ionic strength on the adsorption of H^+, Cd^{2+},Pb^{2+}, and Cu^{2+} by Bacillus subtilis and Bacillus licheniformis: A surface complexation model. Journal of Colloid and Interface Science, 198, 53-77.

Degryse, F., Smolder, E., Merckx, R., 2006. Labile Cd complexes increase Cd availability to plants. Environmental Science Technology, 40 (3), 830-836.

Dilek , F. B., Gökçay, C. F. and Yetiş, Ü., 1998. Combined effects of Ni(II) and Cr(VI) on activated sludge. Water Research, 32 (2), 303-312.

Dilek F.B., Yetiş, Ü., 1992. Effects of heavy metals on activated sludge process. Water Science and Technology, 26, 801-813.

Escher, B., Sigg, L., 2004. Chemical speciation of organics and of metals at biological intephases. van Leeuwen, H. P. van, Köster, W., (eds.) 206-269 Physicochemical kinetics and Transport at Biointerfaces, John Wiley & Sons, Ltd.

EPA (U. S. Environmental Protection Agency), 1993. Nitrogen Control Manual, Report No. EPA/625/R-93/010.

Florence T.M., 1986. Electrochemical approaches to trace element speciation in waters: A review. Analyst, 111, 489-505.

Figueria, M. M., Volesky, B., Ciminelli, V. S. T., 1997. Assessment of Interference in Biosorption of a Heavy Metal. Biotechnology and Bioengineering, 54 (4), 344-350.

Figura, P. McDuffie, B., 1979. Use of chelex resin for determination of labile trace metal fractions in aqueous ligand media and comparison of the method with anodic stripping voltammetry. Analytical Chemistry, 51 (1)120-125.

Galil, N., Scwhartz-Mittelman, A., Saroussi-Zohar, O., 1998. Biomass deflocculation and process disturbances exerted by phenol induced transient load conditions. Water Science and Technology, 38 (8/9), 105

Gardiner, J., 1975. Complexation of trace metals by ethylenediaminetetraactic acid (EDTA) in Natural Waters. Water Research, 10, 507-514.

George R. Helz , Lewis M. Horzempa, 1983. EDTA as a kinetic inhibitor of copper (II) sulfide precipitation. Water Research, 17, 167-192.

Gernaey K, Verschuere L, Luyten L, Verstraete W. (1997) Fast and sensitive acute toxicity detection with an enrichment nitrifying culture. Water Environ Research, 69, 1163–1169.

Gikas, P., Romanos, P., 2006. Effects of tri-valent (Cr(III)) and hexa-valent (Cr(VI)) chromium on the growth of the activated sludge. Journal of Hazardous Materials B133, 212-217.

Gökçay, C. F., Yetiş, Ü., 1991. Effect of chromium (VI) on activated sludge. Water Research, 25, (1), 65-73.

Harper S. C., Manoharan R., Mavinic, D. S., Randall, C. W., 1996. Chromium and nickel toxicity during biotreatment of high ammonia landfill lechate. Water Environment Research, 68(1), 19-24.

Hart BA, Bertram PE, Scaife BD., 1979. Cadmium transport by Chlorella pyrenoidosa. Environ Research,18(2), 327–335.

Hassler, C. S., Sloveykova, V. I., Wilkinson, K. J., 2004a. Some fundamental (and often overlooked) considerations underlying the free ion activity and biotic ligand models. Environmental Toxicology and Chemistry, 23 (2), 283-291.

Hassler, C. S., Sloveykova, V. I., Wilkinson, K. J., 2004b. Discriminating between intra- and extracellular metals using chemical extractions. Limnology and Oceanography: Methods 2: 234-247.

Hu Zhiqiang, Chandran K., Grasso D., Smets, B. F., 2002. Effect of nickel and cadmium speciation on nitrification inhibition. Environmental Science and Technology, 36, (14), 3074-3078.

Hu Zhiqiang, Chandran K., Grasso D., Smets, B. F., 2003. Impact of metal sorption and internalization on nitrification inhibition. Environmental Science and Technology, 37 (4), 728-734.

Hu Zhiqiang, Chandran K., Grasso D., Smets, B. F., 2004. Comparison of nitrification inhibition by metals in batch and continuous flow reactors. Water Research, 38, 3949-3959.

Jakumnee, J., Suteerapataranon, S., Vaneesorn, Y., Grudpan, K., 2001. Determination of cadmium, copper, lead and zinc by flow voltammetric analysis. Analytical Sciences, Vol.17.

Jansen, S., Blust, R., van Leeuwen, H.P. 2002. Metal speciation dynamics and bioavailability. Zn(II) and Cd(II) uptake by mussel (*Mytilus edulis*) and carp (*Cyprinus carpio*). Environmental Science and Technology, **36**, 2164-2170.

Janssen, C. R., Heijerick, D. G., Scheamphelaere, K. A. C., Allen, H. E., 2003. Environmental risk assessment of metals: tools for incorporating bioavailability. Environmental International, 28, 793-800.

Jönsson, K., Aspichueta, E., Sota, A de la., Jansen, J. la C., 2001. Evaluation of nitrification-inhibition measurements. Water Science and Technology, 43 (1), 201-208.

Jianlong, W., Ning, Y., 2004. Partial nitrification under limited dissolved oxygen conditions. Process Biochemistry, 39, 1223-1229.

Karia, F. G., Giger, W., 1996. Speciation and fate of ethylenediaminetetraacetate (EDTA) in municipal wastewater treatment. Water Research, 30, 122-134.

Kelly, D. P., Norris, P. R., Brierly, C. L., 1979. Microbiological Methods for Extraction and Recovery of Metals in Microbial Technology, Current State, Future Prospects, Bull, A. T., Ellwood, D. C., and Ratledge, C. (eds.), Cambridge University Press.

Kratochvil, D., Volesky, B., 1998. Biosorption of Cu from ferruginous wastewater by algal biomass. Water Research, 32 (9), 2670-2678.

Lee, Y-W., Ong, S-K., Sato, C., 1997. Effects of heavy metals on nitrifying bacteria. Water Science and Technology, 36 (12), 69-74.

Lewandowski, Z., 1987. Behaviour of biological reactors in the presence of toxic compounds. Water Research, 21 (2), 147-153

Loveless J. E., Painter H. A. 1968. The influence of metal ion concentrations on the growth of *Nitrosomonas* strain isolated from activated sludge. Microbiology, 52, 1-14.

Ma, M., Zhu, W., Wang, Z., Witkamp, G. J., 2003. Accumulation, assimilation and growth inhibition of copper on freshwater alga (*Scenedesmus subspicatus* 86.81 SAG) in the presence of EDTA and fulvic acid. Aquatic Toxicology, 63, 221-228.

Madoni, P., Davoli, D., Guglielmi, L., 1999. Response of SOUR and AUR to heavy metal contamination in activated sludge. Water Research, 33 (10), 2459-2464.

Manahan, Stanley E., 1994. Environmental Chemistry, 6th Edition, CRC Press Inc., U.S.A.

Mazierski, J. 1995. Effect of Chromium (Cr^{VI}) on the Growth Rate of Activated Sludge. Water Research, 29, 1479-1482.

McCarthy, P. L., 1964. Anaerobic wastewater treatment fundamentals, Part III. Toxic materials and their control, Public works, 95 (11), 91-99.

Metcalf and Eddy, Inc., 2003. Wastewater Engineering Treatment and Reuse. McGraw Hill Inc., 4th Edition, New York .

Morel, F. M. M., 1983. Principles and Applications of Aquatic Chemistry, Wiley-Interscience, Newyork.

Moussa, M.S., Sumanasekera, D.U., Ibrahim, S. H., Lubberding, H. J., Hooijmans, C. M., Gijzen, H. J., van Loosdrecht, M.C.M., 2006. Long term effects of salt on activity, population structure and floc characteristics in enriched bacterial cultures of nitrifiers. Water Research, 40 (7), 1377-1388.

Nelson, P. O., Chung, A. K. and Hudson, M. C., 1981. Factors affecting the fate of heavy metals in the activated sludge process. Journal WPCF, 53 (8),.1323-1333.

Neubecker, T. A. and Herbert E. A., 1983. The measurement of complexation capacity and conditional stability constants for ligands in natural waters. Water Research, 17, 1-14.

Neufeld, R. D., Hermann, E. R., 1975. Heavy metal removal by acclimated activated sludge. Journal WPCF, 47 (2), 310-329.

Nies, D. H., 1999. Microbial heavy-metal resistance. Applied Microbial Biotechnology, 51, 730-750.

Playle, R. C., 1998. Modelling metal interactions at fish gills. Science Total Environment, 219 (2-3), 147-163

Plette A. C. C., M. F. Benedetti, W. H. van Riemsdijk, 1996. Competitive binding of protons, calcium, cadmium, and zinc to isolated cell walls of a gram-positive soil bacterium. Environmental Science and Technology, 30, 1902-1910.

Principi, P., Villa, F., Bernasconi, M., Zanardini, E., 2006. Metal toxicity in municipal wastewater activated sludge investigated by multivariate analysis and in situ hybridization. Water Research, 40, 99-106.

Ren, S. and Frymier, P.D. 2003 Kinetics of the toxicity of heavy metals to luminescent bacteria, Advances in Environmental Research, 7 (2), 537-547.

Rossiter, W. J., Vangel, M. G., Mcknight, M. E., Signor, A., Byrd, W. E., 2001. Ultrasonic Extraction/Anodic Stripping Voltammetry for Determining Lead in Household Paint: A Laboratory Evaluation, NISTIR 6571.

Saari, R. B., Stansbury, J. S., Laquer, F. C., 1998. Effect of sodium xylenesulfonate on zinc removal from wastewater. Journal of Environmental Engineering, 124 (10), 939-944.

Saatci, A. M., Çeçen, F., Yükselen, M. A., Çallı, B., Mertoğlu, B., Girgin, E., 2006. Biyolojik Atıksu Arıtma Sistemlerindeki Nitrifikasyon Türlerinin ve Aktivitelerinin Belirlenmesi, TÜBİTAK İÇTAG-Ç106, Sonuç Raporu, Temmuz 2006.

Savvides, C., Papadopoulos A., Haralambous, K. J ., Loizidou, M. 1995. Sea sediments contaminated with heavy metals : metal speciation and removal. Water Science Technology, 32, (9-10), 65-73.

Schecher, W. D., McAvoy, D. C., 1998. MINEQL+: A Chemical Equilibrium Modeling System, Version 4.5 for Windows, Environment Research Software.

Scoullos, M. J. and Pavlidou, A. D., 2000. Metal speciation studies in a brackish/marine interface system, Global Nest: the International. Journal, 2 (3), 225-264.

Semerci, N., Çeçen, F., 2006. Importance of free Zn species in batch nitrification systems, Water Practice and Technology, 1 (3), **doi10.2166/wpt.2006.0053**

Semerci, N., Çeçen, F., 2007. Importance of cadmium speciation in nitrification inhibition Journal of Hazardous Materials (accepted for publication). doi:10.1016/j.jhazmat.2007.01.041

Settle, 1997. Handbook of Instrumental Techniques for Analytical Chemistry, Prentice Hall PTR.

Shammas, N. K., 1986. Interactions of Temperature, pH, and Biomass on the Nitrification Process. Journal of Water Pollution Control Federation, 58 (1), 52-59.

Simkiss, K., Taylor, G., 1995. Transport of metal across membranes. In a Tessier and D. R. Tunrer (eds.) Metal Speciation and Bioavailability in Aquatic Systems. John & Wiley & Sons Ltd., Chichester, England, 1-44.

Slaveykova, V. I., Wilkinson, K. J., 2005. Predicting the bioavailability of metals complexes: critical review of the biotic ligand model. Environmental Chemistry, 2, 9-24.

Spain, A., 2003. Implications of microbial heavy metal tolerance in the environment. Reviews in Undergraduate Research, 2, 1-6.

Stoveland, S., Lester, J. N., Perry, R., 1979. The influence of Nitriloacetatic Acid on Heavy Metal Transfer in The Activated Sludge Process-I. At Constant Loading. Water Research, 13, 949-965.

van Sprang, PA., Jansen, C. R., 2001. Toxicity Identification of Metals: Development of Toxicity Identification Fingertrips. Environmental Toxicology and Chemistry, 20 (11), 2604-2610.

Volesky, B., Holan, Z. R., 1995. Biosorption of Heavy Metals. Biotechnology Progress, 11 (3), 235-250.

Volesky, B., 1999. Biosorption for the next century, International Biohydrometallurgy Symposium El Escorial. http://biosorption.mcgill.ca/publication/BVspain/BVspain.htm.

Wagner, M., Rath, G., Amann, R., Koops, H.-P., Schleifer, K. H., 1995. In situ identification of ammonia-oxidizing bacteria. Applied Microbiology,18, 251-264.

Wang, J., Huang, C. P., Allen, H. E., Poesponegoro, I., Poesponegoro, H., 1999. Effects of dissolved organic matter and pH on heavy metal uptake by sludge particulates exemplified by Copper (II) and Nickel (II) : Three Variable Model. Water Environment Research, 71, 2, 139-147.

Williamson, K.J., and P.L. McCarty, 1975. Rapid measurement of Monod half-velocity coefficients for bacterial kinetics. Biotechnology. Bioengineering, 14: 915.

Woodiwiss, C. R., Walker, R. D., 1979. Concentration of nitrilotriacetate and certain metals in Canadian wastewaters and streams. Water Research, 13, 599-612.

Teske, A., Alm, E., Regan, J. M., Toze, S., Rittmann, B. E., Stahl, D. A., 1994. Evolutionary relationships among ammonia and nitrite oxidizing bacteria. Journal Bacteriology, 176, 6623.

Thomas, F. G., Henze, G., 2001. Introduction to Voltammetric Analysis, Csiro Publishing, Australia.

Ting, Y. P., Prince, I. G., Lawson, F., 1989. Uptake of cadmium and zinc by the alga *Chlorella vulgaris* II. Multi-ion situation, Biotechnology and Bioengineering, 37(5), 445-455

Tsai, Y.P., You, S.J., Pai, T.Y. Chen, K.W., 2006. Effect of Cd(II) on different bacterial species present in a single sludge activated sludge process for carbon and nutrient removal, Journal Environ. Engineering, 132 (2), 173-180

Tünay, O., Kapdaşlı, I., Taşli, R., 1994. Pretreatment of Complexed Wastewaters, Water Science and Technology, 9, 265-274.

Twiss, M. R., Errecalde, O., Fortin, C., Campell, P.G.C., Jumarine, C., Denizeau, F., Berkelaar, E., Hale, B., Rees K. V., 2000. Guidelines for studies of metal bioavailability and toxicity-why metal speciation should be considered and how!, Canadian Network of Toxicology Centres.

Twiss, M. R., Errecalde, O., Fortin, C., Campell, P.G.C., Jumarine, C., Denizeau, F., Berkelaar, E., Hale, B. Rees K. V., 2001. Coupling the use of computer chemical speciation models and culture techniques in laboratory investigations of trace metal toxicity. Chemical Speciation and Toxicity, 13 (1), 9-24.

Tyagi, R. D., Couillard, D. Tran, F. T., 1991. Analysis of final settling tank in relation to control of metal inhibition in the activated sludge process. The Canadian Journal of Chemical Engineering, 69, 534-543.

Yetiş, Ü., Gökçay, C. F., 1989. Effect of Nickel (II) on Activated Sludge. Water Research, 23 (8), 1003-1007.

Yetiş, Ü., Özcengiz, G., Dilek, F. B., Ergen, N., Erbay, A., Dölek, A., 1998. Heavy metal biosorption by white-rot fungi, Water Science and Technology, 38, (4-5), 325-330.

Yoo, H., Ahn, K-H., Lee, H-J., Lee, W-H., Kwak, Y-J., Song, K-G., 1999. Nitrogen removal from synthetic wastewater by simultaneous nitrification and denitrification via nitrite in an intermittently-aerated reactor. Water Research, 33 (1), 145-154.

Zarnozsky, L., Derco., J., Kuffa, R., Drtil, M., 1994. The influence of cadmium on activated sludge activity. Water Science and Technology, 30 (11), 235-242.

APPENDIX A

NH_4-N, NO_2-N, NO_3-N and MLVSS MEASUREMENT DURING THE START-UP PERIOD OF THE NITRIFYING BIOMASS

Table A.1 Performance of the main reactor used in batch experiments

	Total N influent of the reactor, mg/L			Total N effluent of the reactor, mg/L			MLSS, mg/L	MLVSS, mg/L	pH	Temp., ^{0}C
Date	NH_4-N	NO_2-N	NO_3-N	NH_4-N	NO_2-N	NO_3-N				
07.05.2003	610	30.43	869.57	0.25	304	1146	2885	1980	8.34	23.3
08.05.2003	590	76	574	3	258	1242	2160	1780	8.41	22
09.05.2003	590	76	574	0	6.08	908.92	1880	1520	8.50	21.7
12.05.2003	500	30	229	0.5	149	506	1960	1615	8.58	23
13.05.2003	560	15.21	164	1	471	219	1965	1660	8.36	23.4
14.05.2003	605	106.52	173	0	529		2000	1675	8.42	23.9
20.05.2003	420	6.69	94.56	0	3.04	476.96	1980	1660	6.66	24.5
21.05.2003	385	0.76	119.24	0.05	6.08	383.92	2200	1770	8.20	25
22.05.2003	385	4	128.5	0.15	0	430	1835	1515	8.32	25
23.05.2003	410	0	150	0.05	28.9	351.1	1905	1570	8.15	25
24.05.2003	375	9.13	115.87	0.05	0.3	399.7	1910	1625	8.32	25
25.05.2003	-	-	-	-						
26.05.2003	300	4.56	140.44	0.2	1	286.5	1600	1330	8.35	24
27.05.2003	380	4.86	50.14	1.95	24.34	405.66	1470	1250	8.44	24.8
28.05.2003	350	15.21	66.29	0.2	18.26	414.24	-	-	8.50	25
29.05.2003	395	6.08	74.92	0.5	-	-	-	-	-	25
30.05.2003	-	-	-	-	-	-	-	-	-	25.2
31.05.2003	-	-	-	-	-	-	-	-	-	24.8
09.06.2003	-	-	-	0.1	0.3	-	-	-	8.52	25
10.06.2003	335	-	-	0.11	0.3	-	-	-	8.12	25
11.06.2003	355	-	-	0.10	0.3	-	-	-	8.43	25
01.07.2003	355	-	-	0.14	0.3	-	760	780	7.58	26
02.07.2003	350	-	-	0.2	0	-	770	730	8.16	25
03.07.2003	350	-	-	0.15	1	-	845	780	8.43	27

Table A.1 (Continued)

	Total N influent of the reactor, mg/L			Total N effluent of the reactor, mg/L			MLSS, mg/L	MLVSS, mg/L	pH	Temp., ^{0}C
Date	NH_4-N	NO_2-N	NO_3-N	NH_4-N	NO_2-N	NO_3-N				
04.07.2003	350	-	-	0.10	0.2	315	790	760	8.12	29
07.07.2003	415	-	92	0.10	0.2	350	860	780	8.37	27
11.07.2003	400	-	-	0.31	1	380	-	-	-	25
12.07.2003	425	-	-	0.2	0.30	380	-	-	-	
15.07.2003	450	-	-	1	1	-	-	-	-	-
16.07.2003	450	-	-	1	0	-	-	-	-	
20.07.2003	450	-	-	0.16	0.30	-	-	-	-	25
22.07.2003	450	-	-	0.26	-	-	-	-	8.15	28
23.07.2003	450	-	-	0.16	-	-	-	-	8.08	27
27.08.2003	450	-	-	0.11	-	-	1080	780	8.10	27
28.08.2003	450	-	-	0.2	2.13	-	990	760	8.09	27
03.09.2003	450	-	-	-	-	-	950	760	-	-
08.09.2003	450	-	-	0.75						
14.01.2004	200	66.43	418.48	399	0	388	-	-	-	-
15.01.2004	300	245	228.2	446.8	35.75	311.96	-	-	-	-
16.01.2004	650	637.5	-	-	0.25	450	380	300	8.80	25
19.01.2004	267	265	109.56	158.44	0.5	182.60	380	350	8.54	22
20.01.2004	466	465	36.52	127.48	-	-	362	262	8.5	24
22.01.2004	666	-	-	-	0.33	22.82	-	-	8.3	25
26.01.2004	340	330	15	332	-	167.39	350	300	8.33	25
27.01.2004	340	-	-	-	-	-	388	330	8.3	25
06.02.2004	666	-	-	-	-	7.60	638	570	8.3	25
09.02.2004	350	-	-	-	-	-	756	662	8.3	25
24.03.2004	350	0.5	0.015	352.5	-	-	-	-	7.75	21.1
26.03.2004	350	0.25	7.6	295	-	-	634	576	7.5	22
27.03.2004	350	-	60.8	-	-	-	628	562	-	-

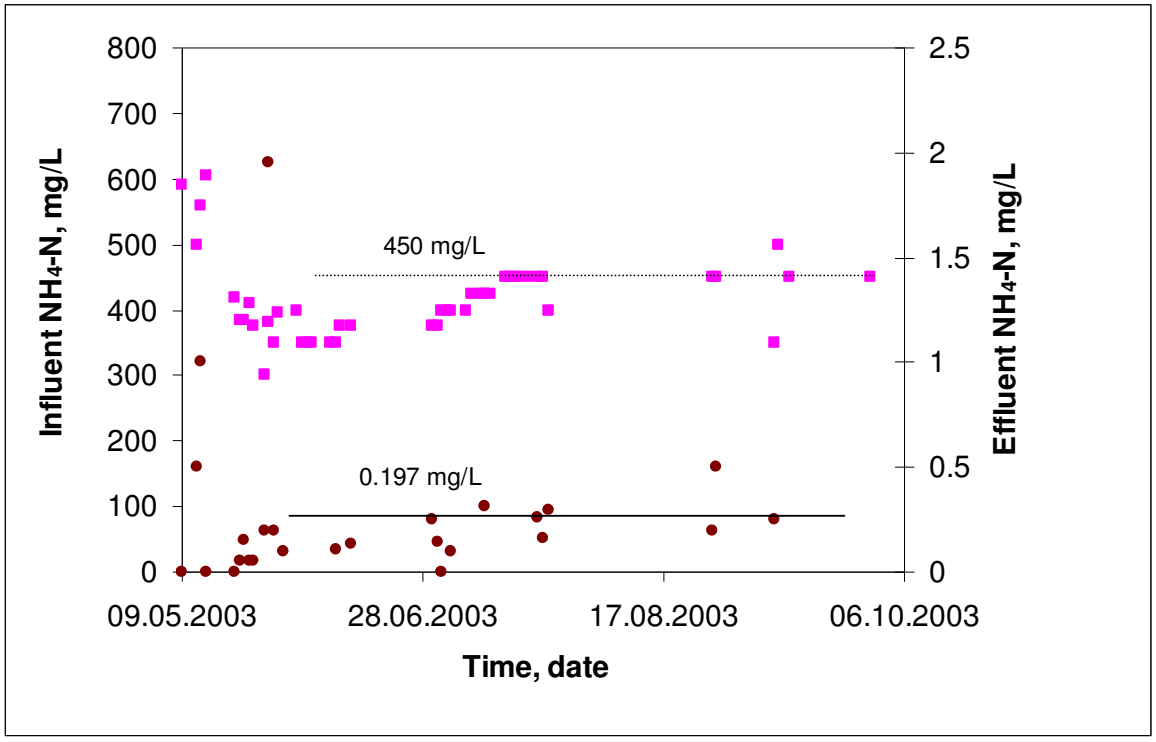

Figure A1. Influent and effluent NH_4-N concentrations in stock enriched nitrifying culture during start-up and steady state conditions

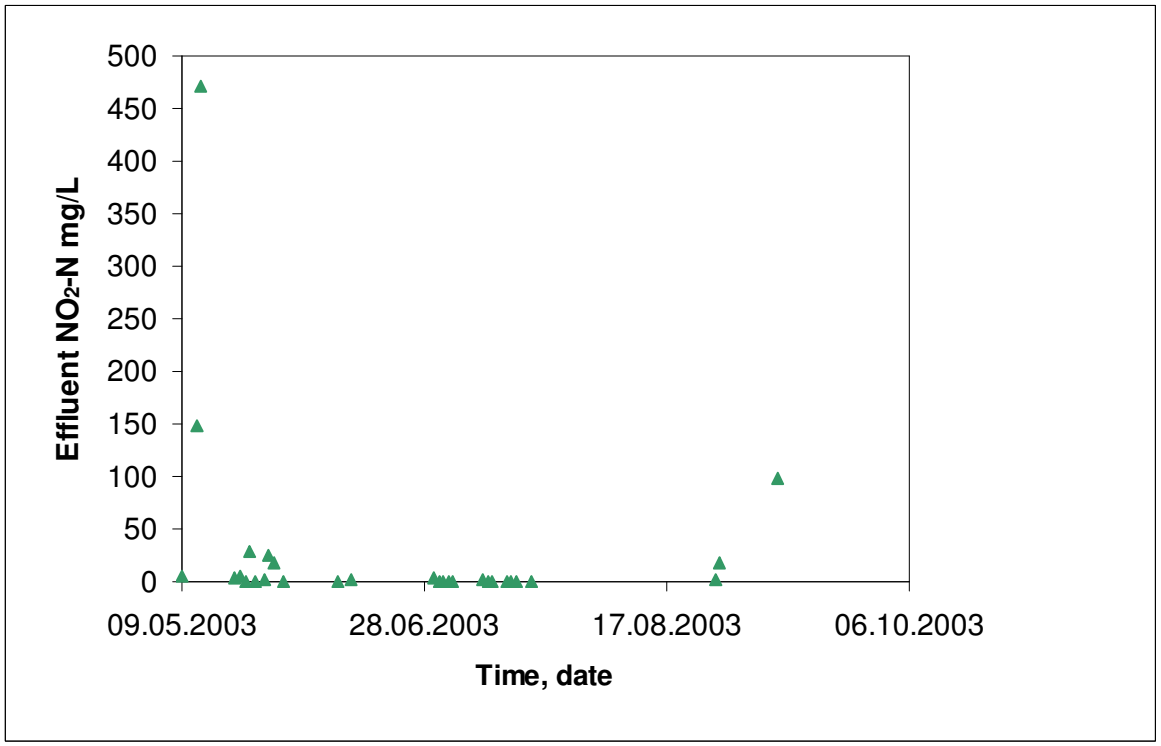

Figure A2. Effluent NO_2-N concentrations in stock enriched nitrifying culture during start-up and steady state conditions

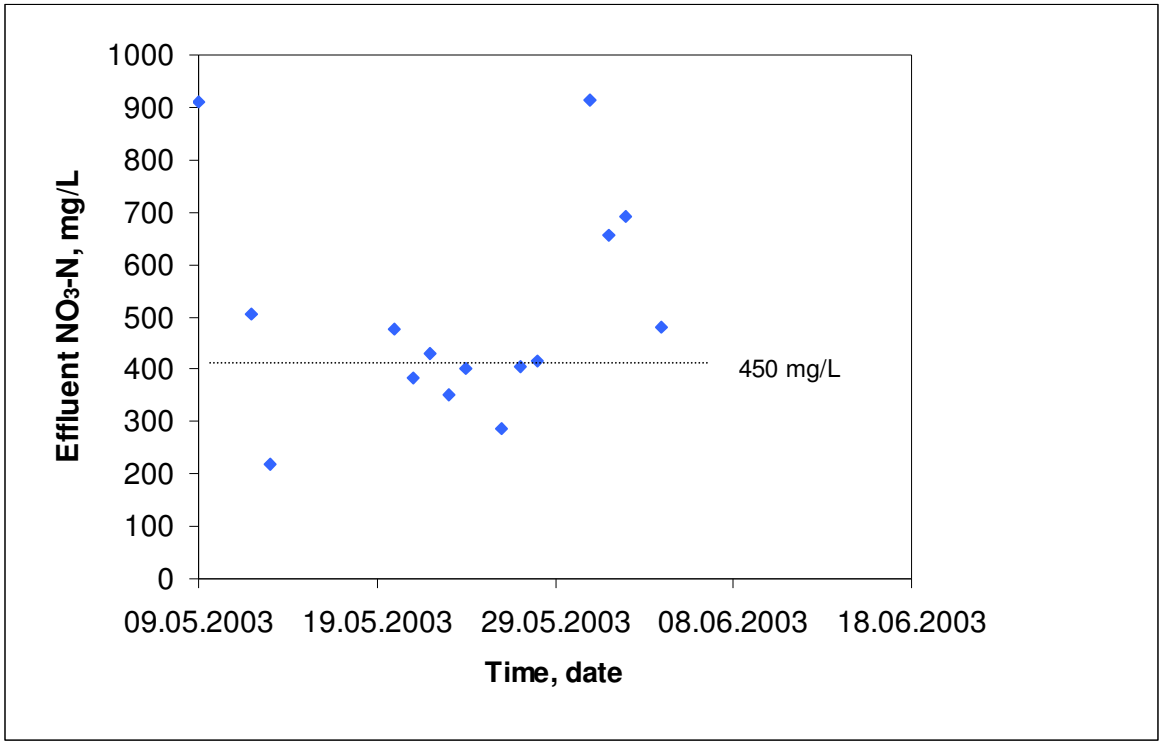

Figure A3. Effluent NO_3-N concentrations in stock enriched nitrifying culture during start-up and steady state conditions

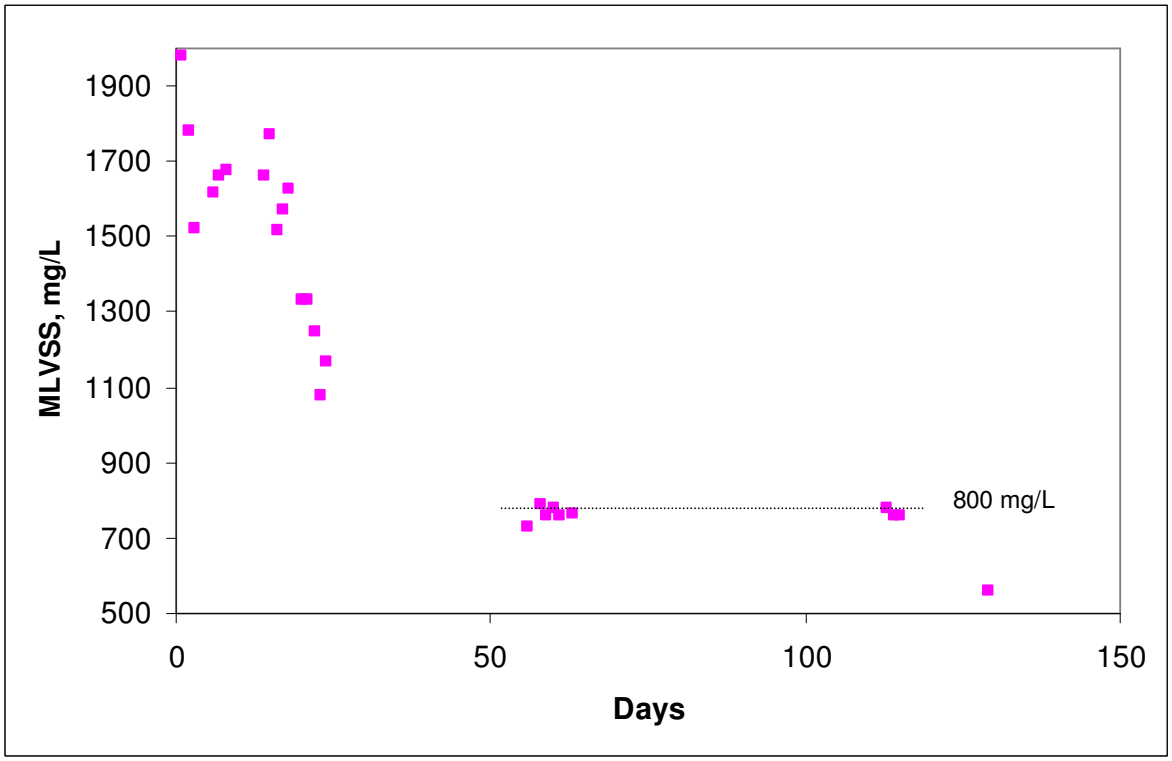

Figure A4. Biomass Concentration in stock enriched nitrifying culture during start-up and steady state conditions

APPENDIX B

NH_4-N CONCENTRATION PROFILES DURING AMMONIUM UTILIZATION RATE EXPERIMENTS FOR BIOKINETIC PARAMETER ESTIMATION

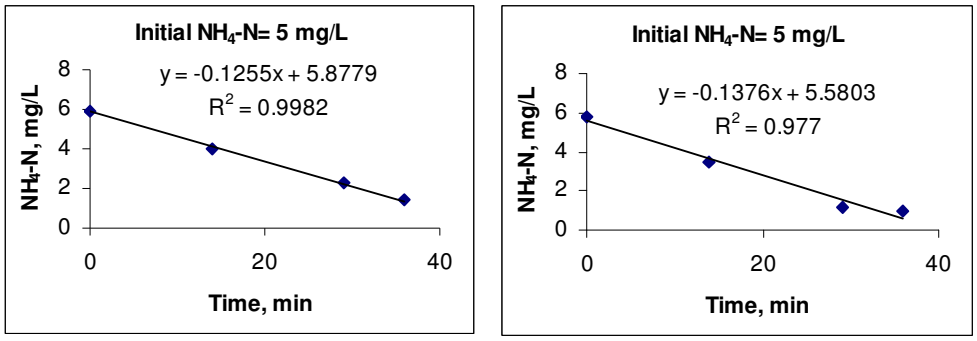

Figure B1. NH_4-N utilization profile in batch reactors, a) Reactor 1: Initial NH_4-N=5 mg/L, MLVSS = 732 mg/L, pH=7.45, T= 26^0C, DO=8-9 mg/L b) Reactor 2: Initial NH_4-N=5 mg/L, MLVSS = 1012 mg/L, pH=7.46, T= 25^0C, DO=8-9 mg/L

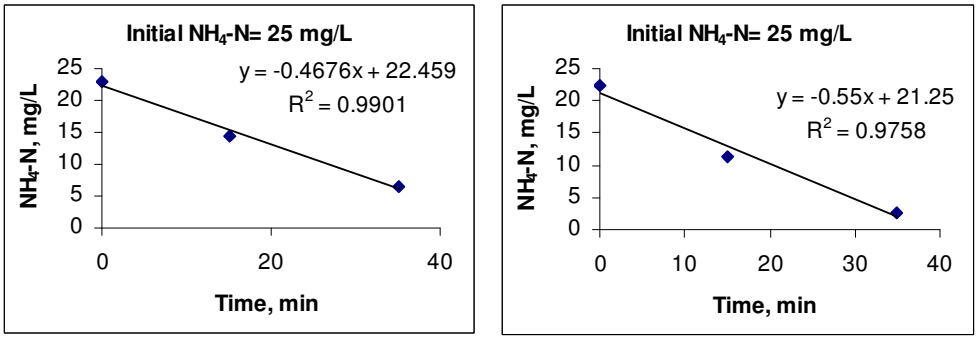

Figure B2. NH_4-N utilization profile in batch reactors, a) Reactor 1: Initial NH_4-N=25 mg/L, MLVSS = 535 mg/L, pH=7.55, T= 25^0C, DO=8-9 mg/L b) Reactor 2: Initial NH_4-N=25 mg/L, MLVSS = 640 mg/L, pH=7.57, T= 25^0C, DO=8-9 mg/L

APPENDIX B (continued)

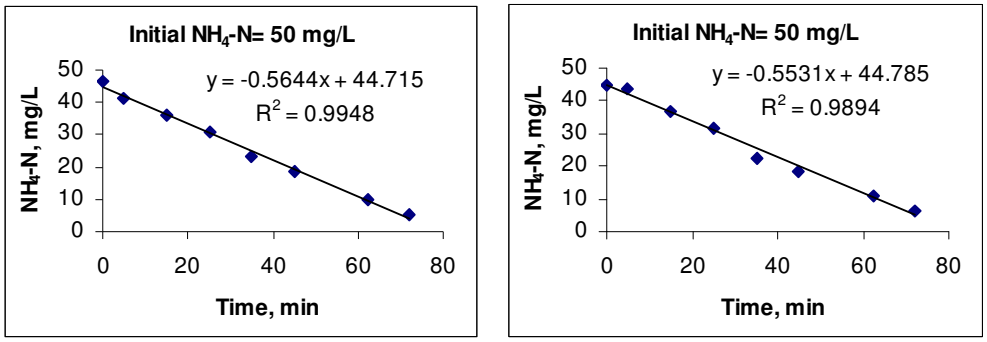

Figure B3. NH_4-N utilization profile in batch reactors, a) Reactor 1: Initial NH_4-N=50 mg/L, MLVSS = 488 mg/L, pH=7.54, T= 25^0C, DO=8-9 mg/L b) Reactor 2: Initial NH_4-N=60 mg/L, MLVSS = 407 mg/L, pH=7.55, T= 25^0C, DO=8-9 mg/L

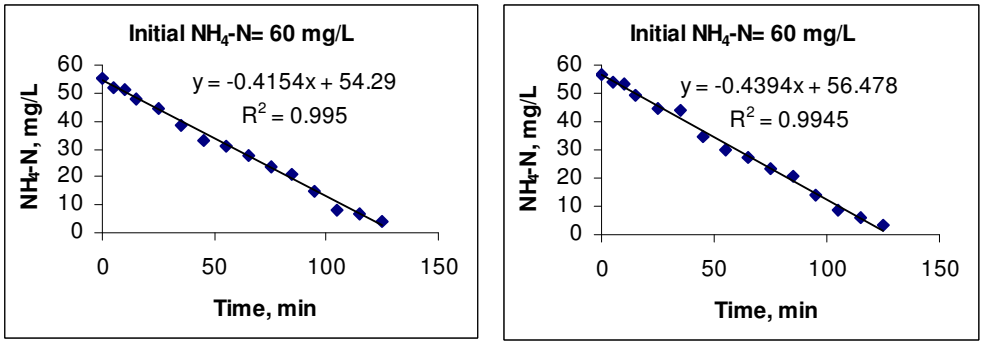

Figure B4. NH_4-N utilization profile in batch reactors, a) Reactor 1: Initial NH_4-N=60 mg/L, MLVSS = 436 mg/L, pH=7.49, T= 25^0C, DO=8-9 mg/L b) Reactor 2: Initial NH_4-N=60 mg/L, MLVSS = 366 mg/L, pH=7.51, T= 25^0C, DO=8-9 mg/L

APPENDIX B (continued)

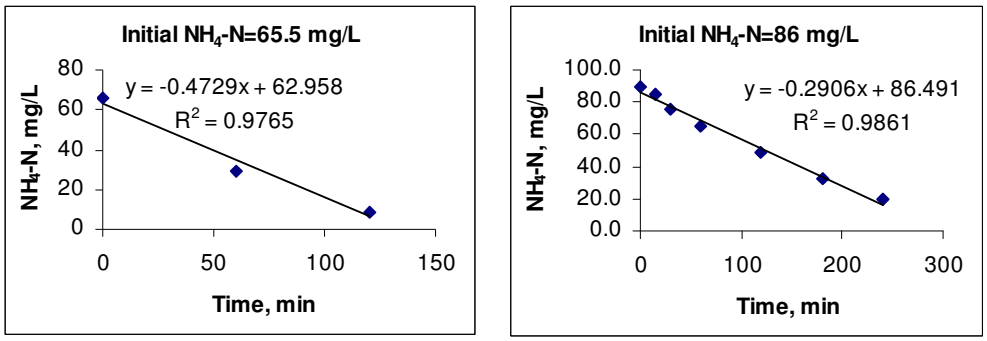

Figure B5. NH_4-N utilization profile in batch reactors, a) Reactor 1: Initial NH_4-N=65.5 mg/L, MLVSS = 402 mg/L, pH=7.45, T= 25^0C, DO=8-9 mg/L b) Reactor 2: Initial NH_4-N=86 mg/L, MLVSS = 312 mg/L, pH=7.70, T= 25^0C, DO=8-9 mg/L

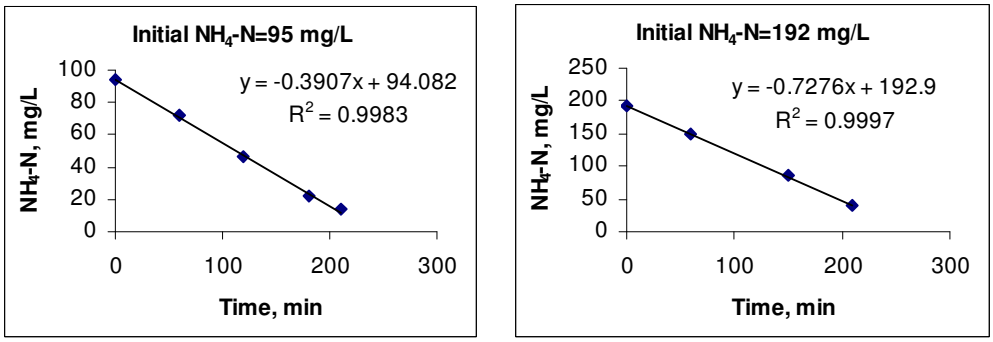

Figure B6. NH_4-N utilization profile in batch reactors, a) Reactor 1: Initial NH_4-N=95 mg/L, MLVSS = 312 mg/L, pH=7.45, T= 25^0C, DO=8-9 mg/L b) Reactor 2: Initial NH_4-N=192 mg/L, MLVSS = 522 mg/L, pH=7.70, T= 25^0C, DO=8-9 mg/L

APPENDIX B (continued)

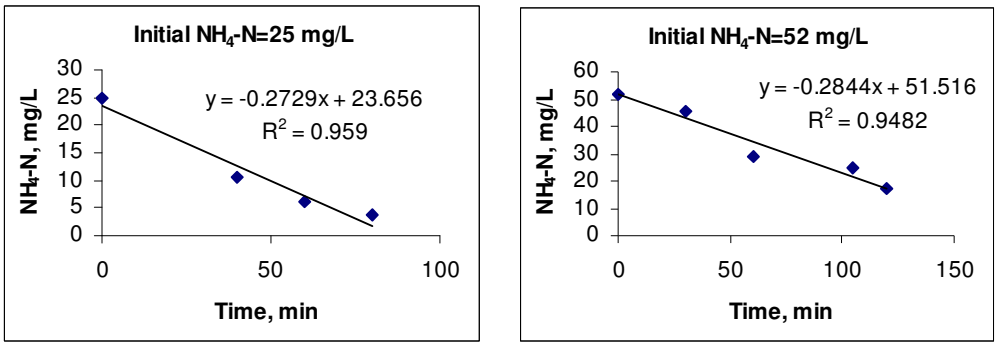

Figure B7. NH_4-N utilization profile in batch reactors, a) Reactor 1: Initial NH_4-N=25 mg/L, MLVSS = 380 mg/L, pH=7.46, T= 25^0C, DO=8-9 mg/L b) Reactor 2: Initial NH_4-N=52 mg/L, MLVSS = 294 mg/L, pH=7.46, T= 25^0C, DO=8-9 mg/L

APPENDIX C

NH_4-N CONCENTRATION PROFILES IN AMMONIUM UTILIZATION RATE EXPERIMENTS IN THE PRESENCE AND ABSENCE OF Cd

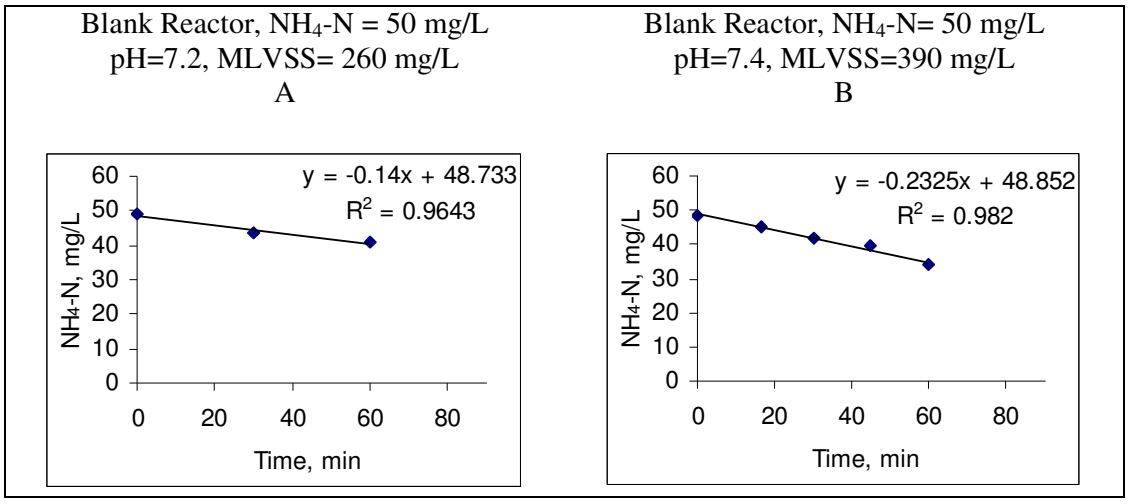

Figure C1. NH_4-N utilization in batch reactor (a) Exp. No. 1 (b) Exp. No.2

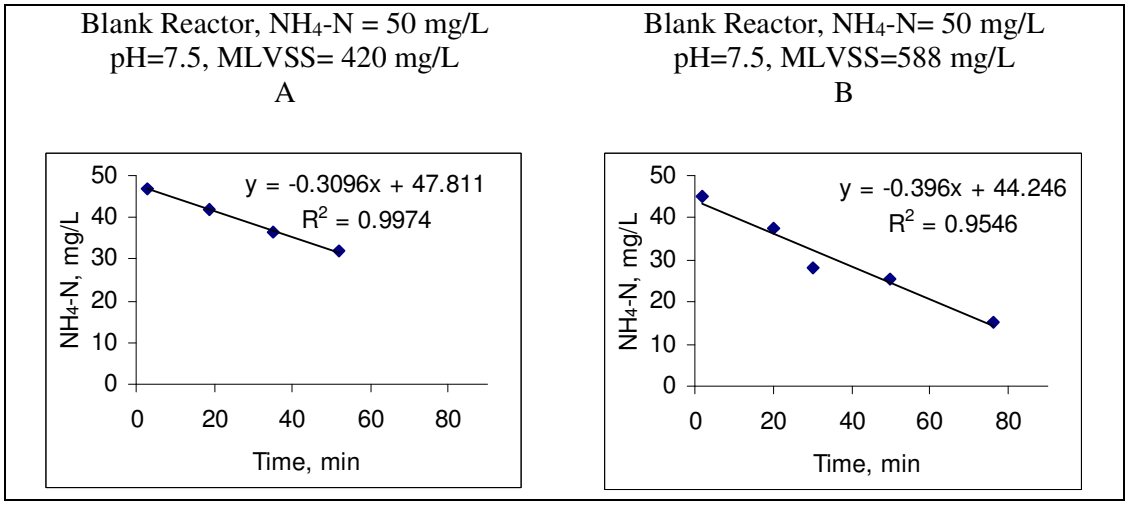

Figure C2. NH_4-N utilization in batch reactor (a) Exp. No. 3 (b) Exp. No.4

APPENDIX C (Continued)

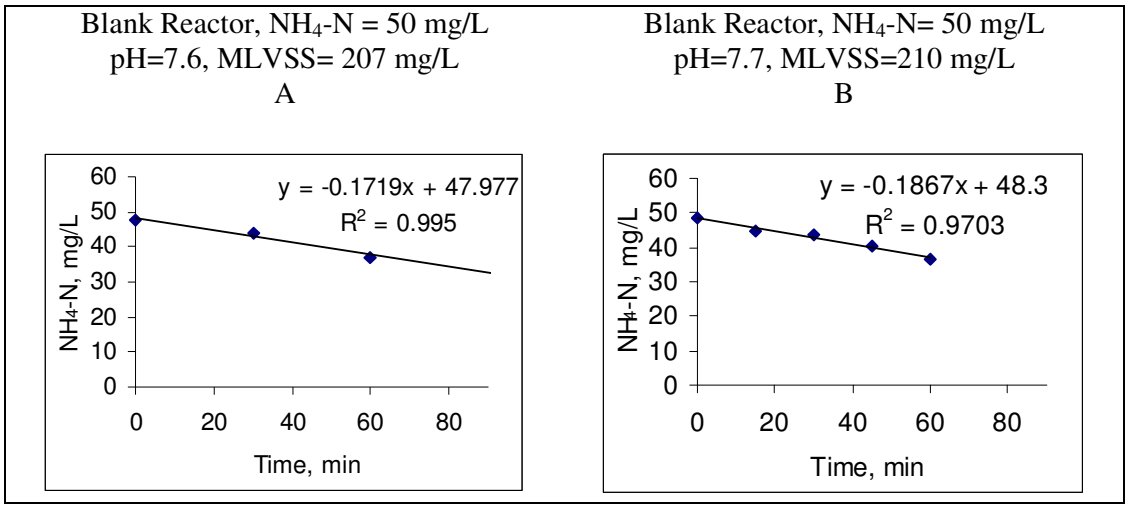

Figure C3. NH_4-N utilization in batch reactor (a) Exp. No. 5 (b) Exp. No.6

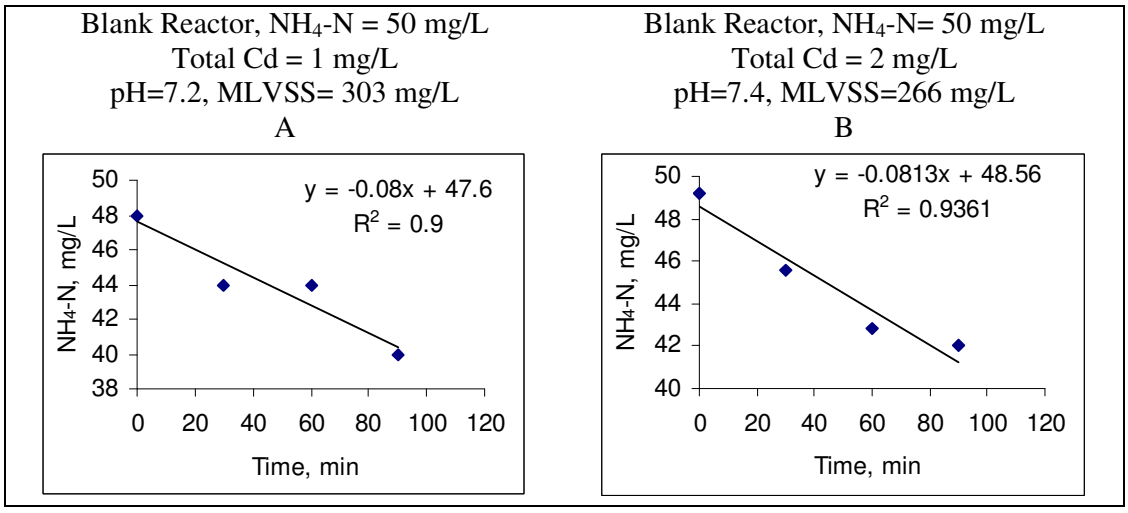

Figure C4. NH_4-N utilization in batch reactor (a) Exp. No. 7 (b) Exp. No.8

APPENDIX C (Continued)

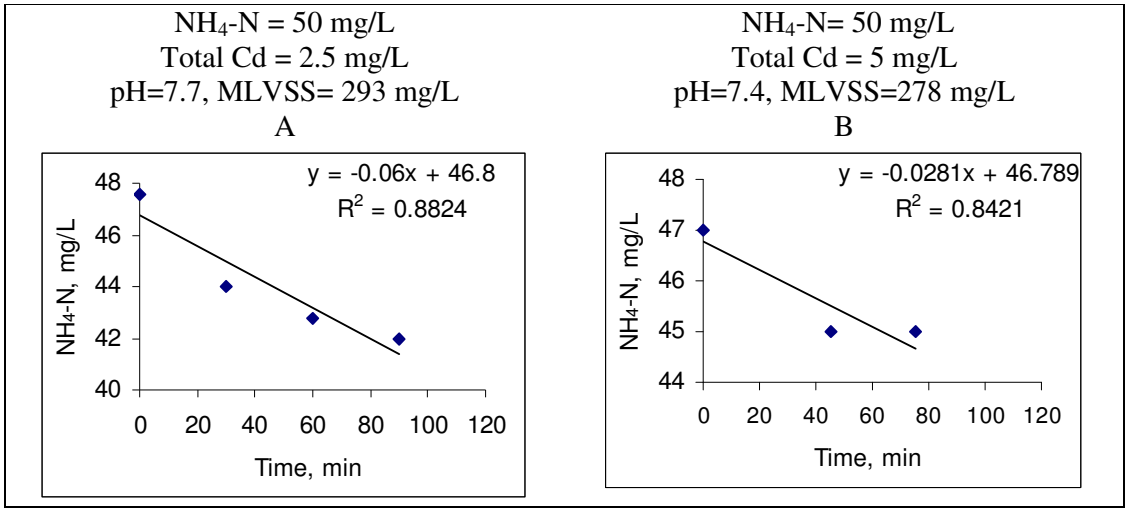

Figure C5. NH_4-N utilization in batch reactor (a) Exp. No. 9 (b) Exp. No.10

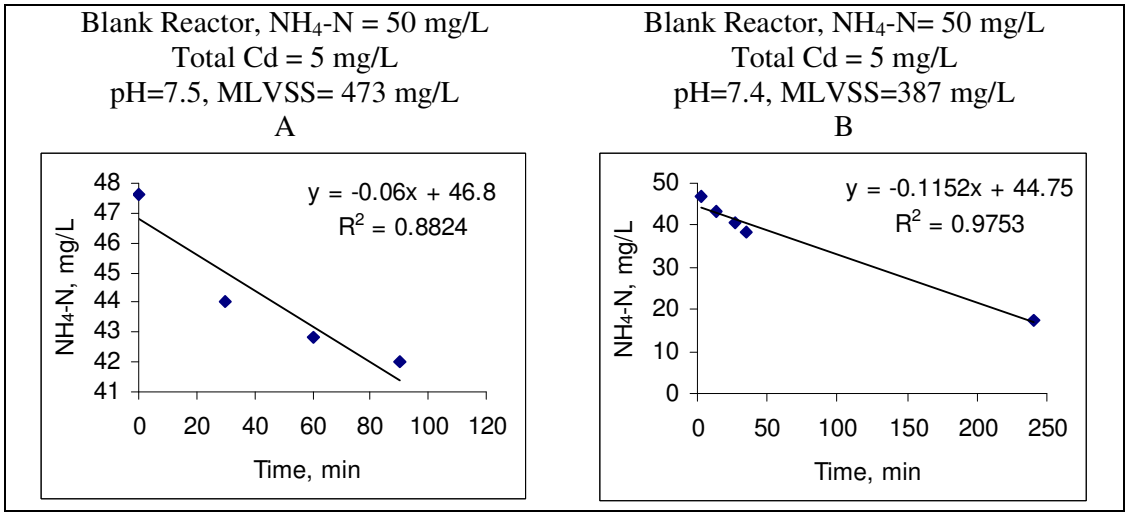

Figure C6. NH_4-N utilization in batch reactor (a) Exp. No. 11 (b) Exp. No.12

APPENDIX C (Continued)

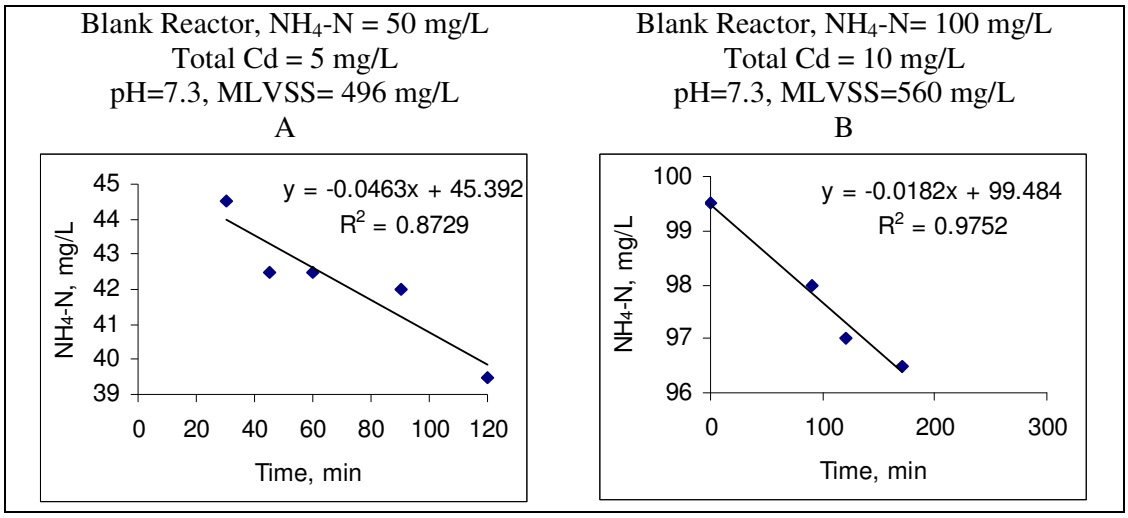

Figure C7. NH_4-N utilization in batch reactor (a) Exp. No. 13 (b) Exp. No.14

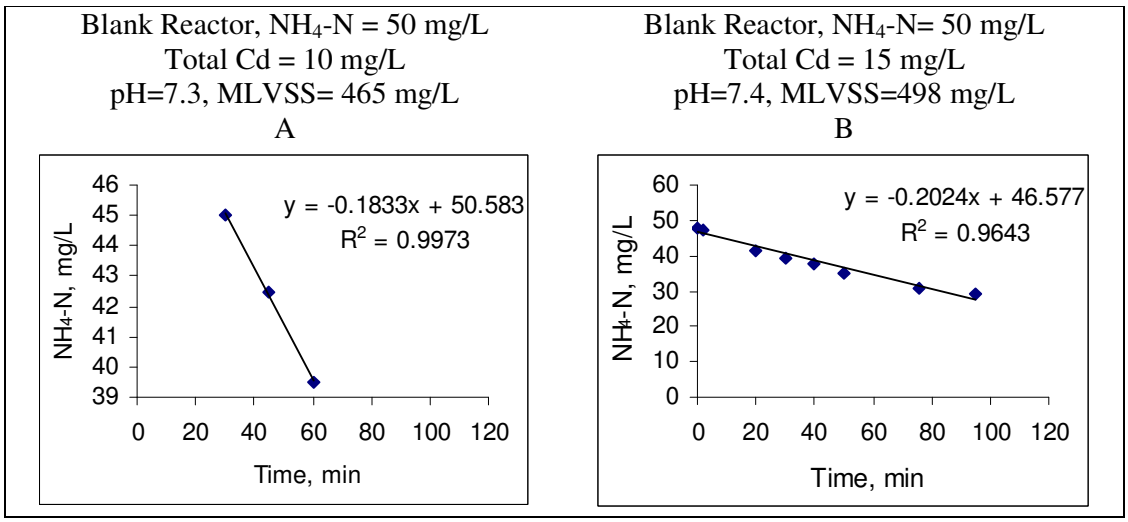

Figure C8. NH_4-N utilization in batch reactor (a) Exp. No. 15 (b) Exp. No.16

APPENDIX C (Continued)

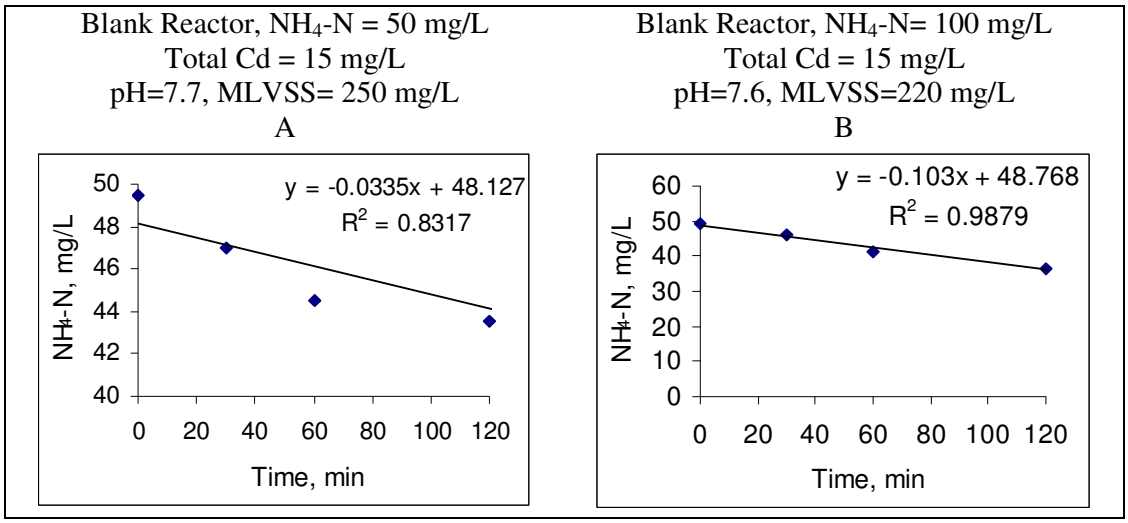

Figure C9. NH_4-N utilization in batch reactor (a) Exp. No. 17 (b) Exp. No.18

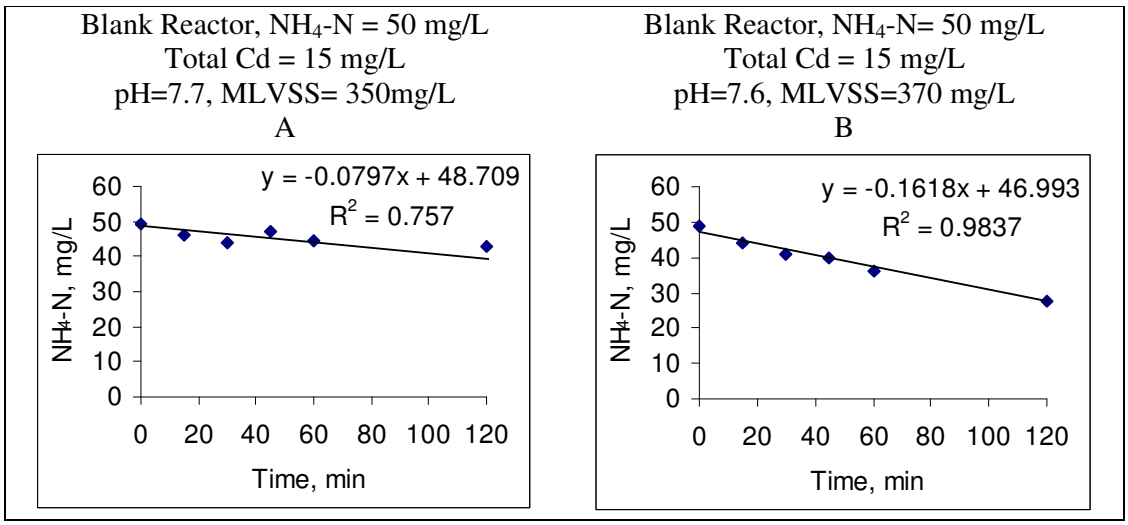

Figure C10. NH_4-N utilization in batch reactor (a) Exp. No. 19 (b) Exp. No.20

APPENDIX C (Continued)

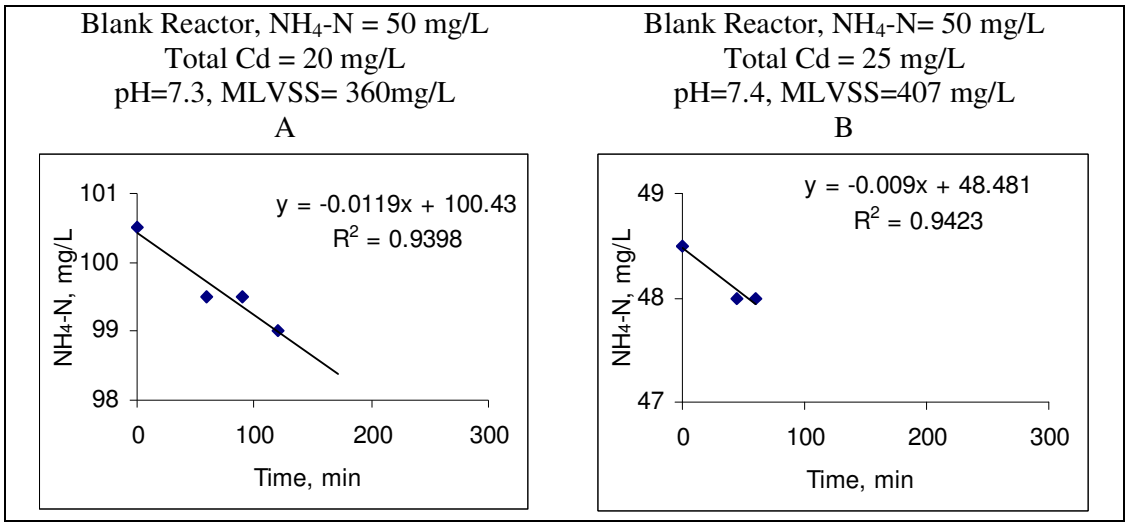

Figure C11. NH_4-N utilization in batch reactor (a) Exp. No. 21 (b) Exp. No.22

APPENDIX D

OUR MEASUREMENT EXPERIMENTS IN THE PRESENCE AND ABSENCE OF Cd

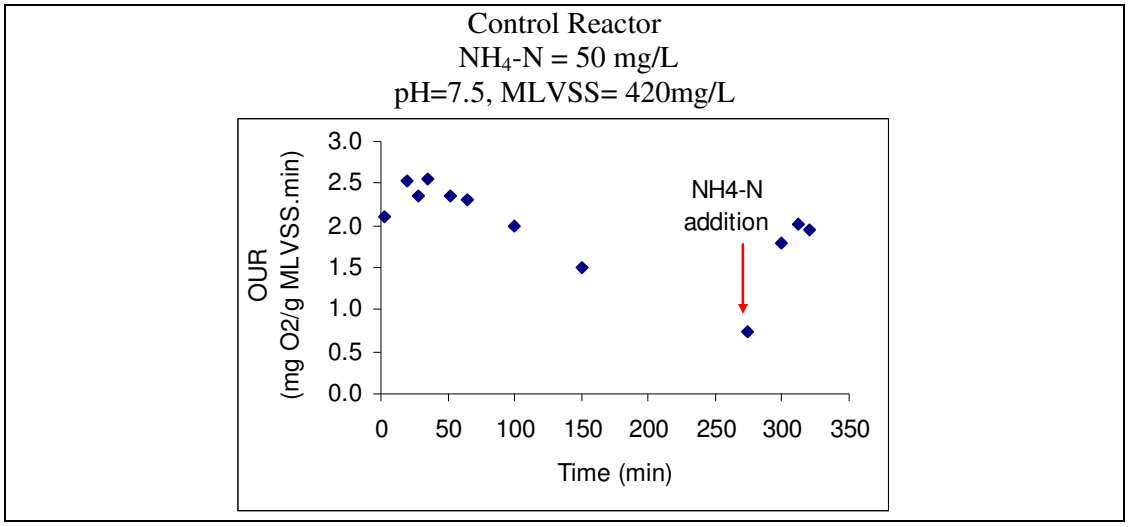

Figure D1. OUR measurements in qNH$_4$-N experiments (Exp. No. 3)

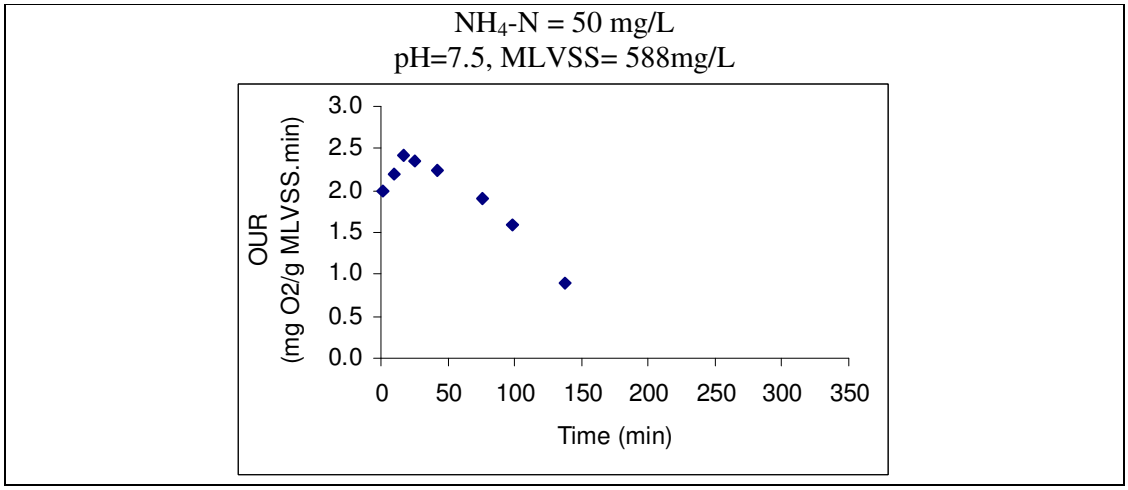

Figure D2. OUR measurements in qNH$_4$-N experiments (Exp. No. 4)

APPENDIX D (Continued)

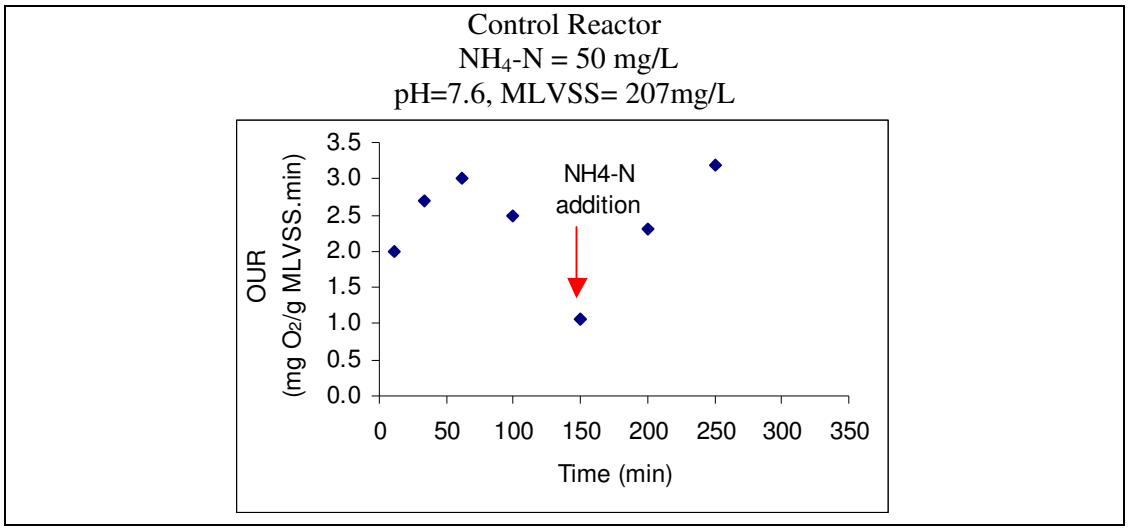

Figure D3. OUR measurements in qNH$_4$-N experiments (Exp. No. 5)

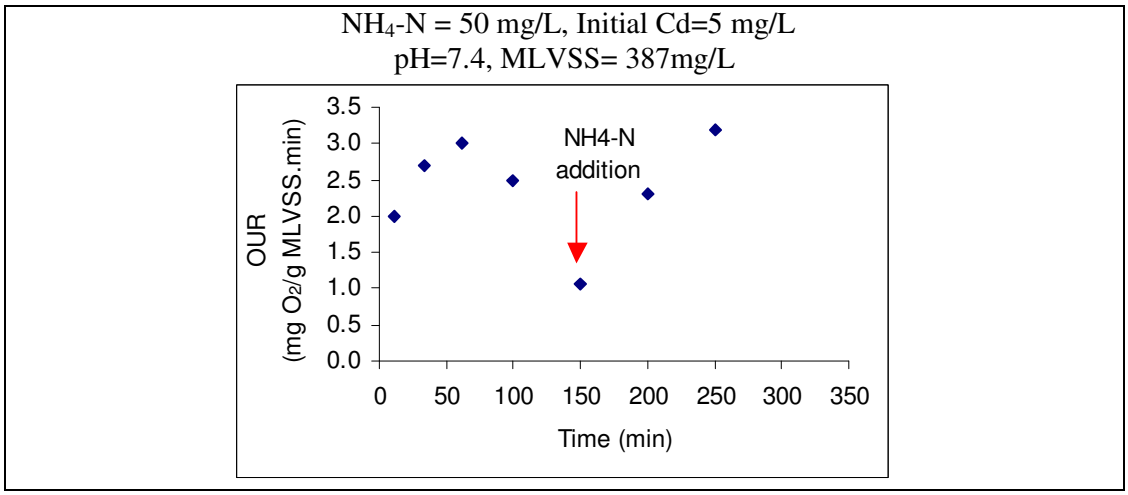

Figure D4. OUR measurements in qNH$_4$-N experiments (Exp. No. 12)

APPENDIX D (Continued)

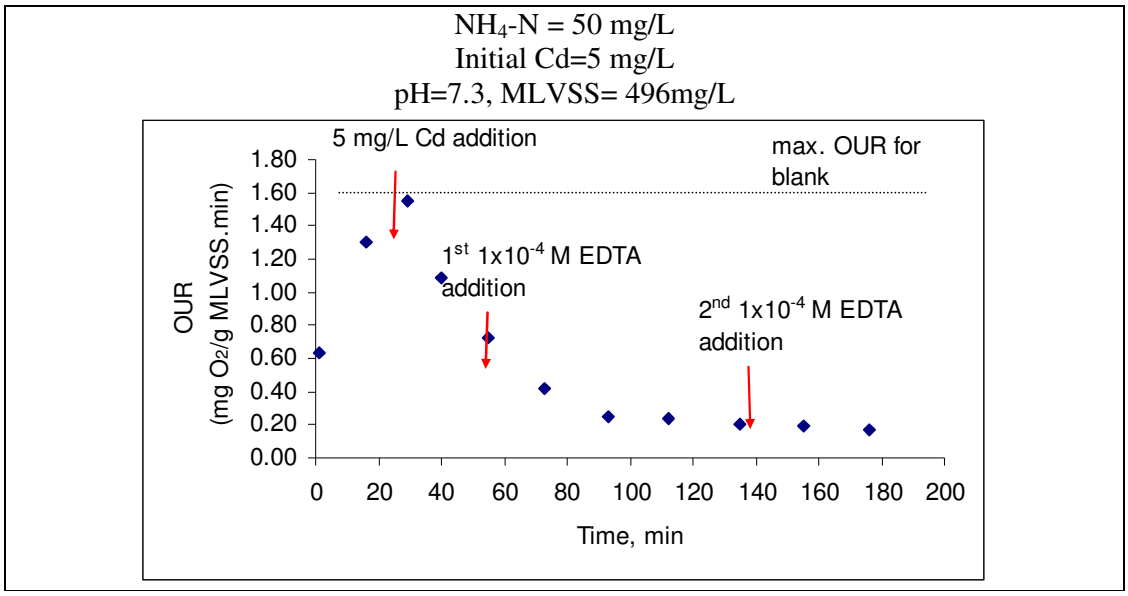

Figure D5. OUR measurements in qNH$_4$-N experiments (Exp. No. 14)

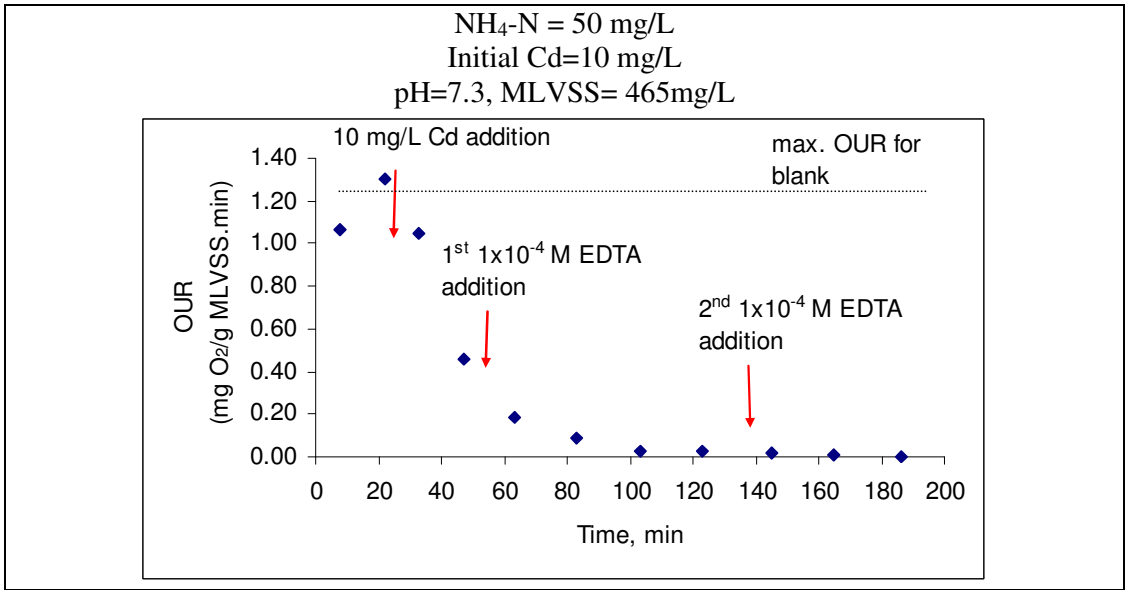

Figure D6. OUR measurements in qNH$_4$-N experiments (Exp. No. 17)

APPENDIX D (Continued)

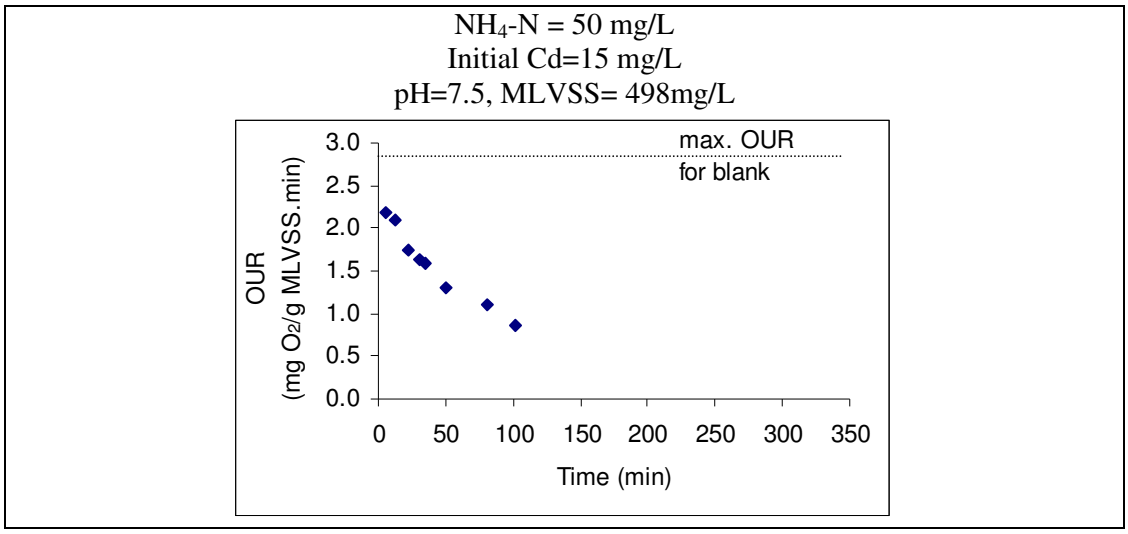

Figure D7. OUR measurements in qNH$_4$-N experiments (Exp. No. 18)

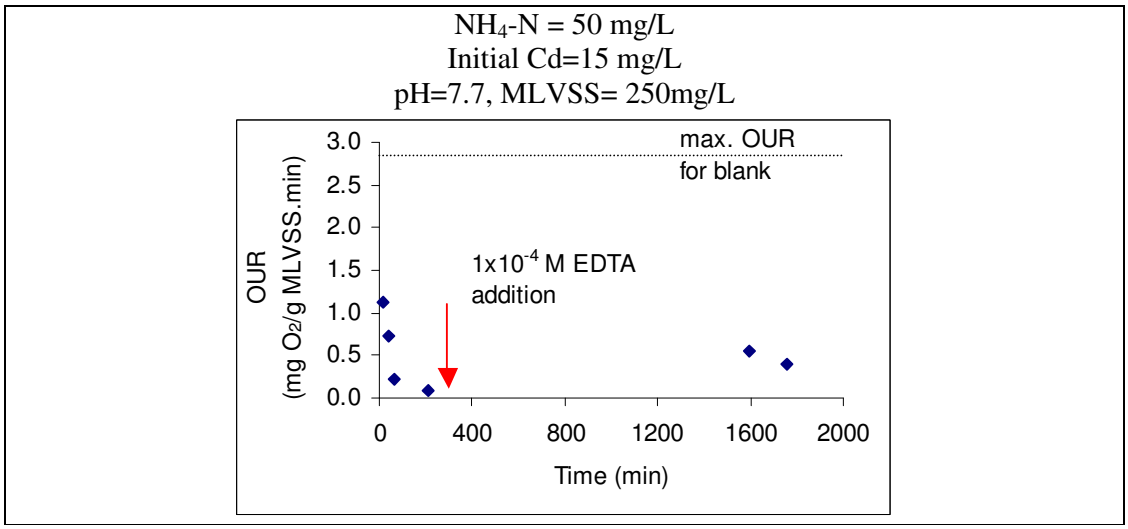

Figure D8. OUR measurements in qNH$_4$-N experiments (Exp. No. 19)

APPENDIX D (Continued)

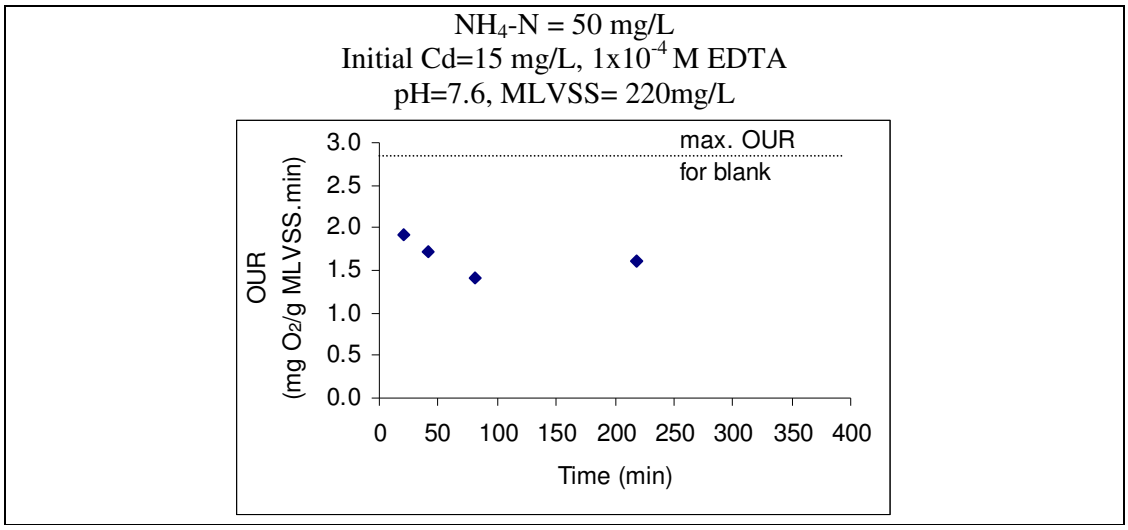

Figure D9. OUR measurements in qNH$_4$-N experiments (Exp. No. 20)

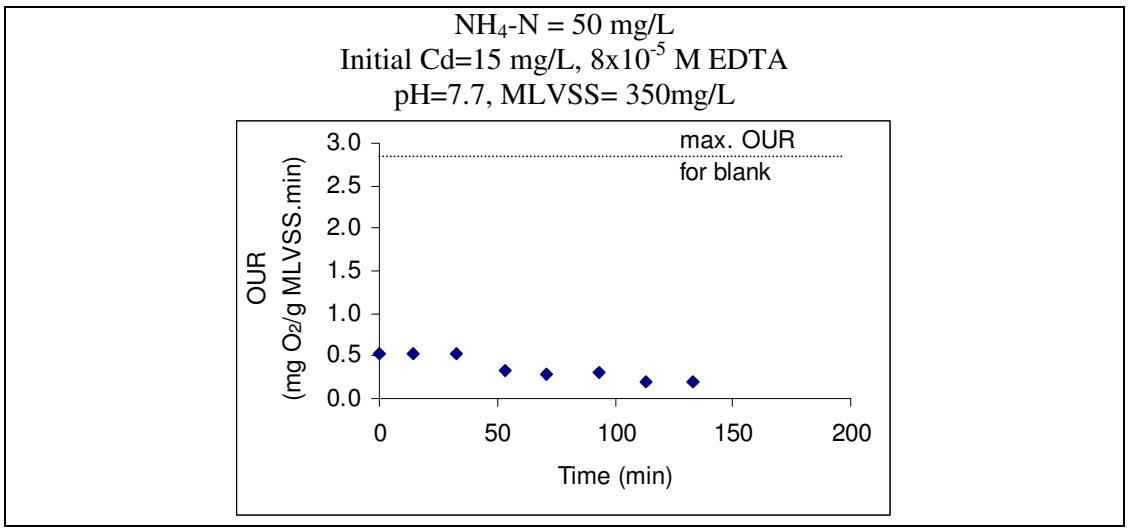

Figure D10. OUR measurements in qNH$_4$-N experiments (Exp. No. 21)

APPENDIX D (Continued)

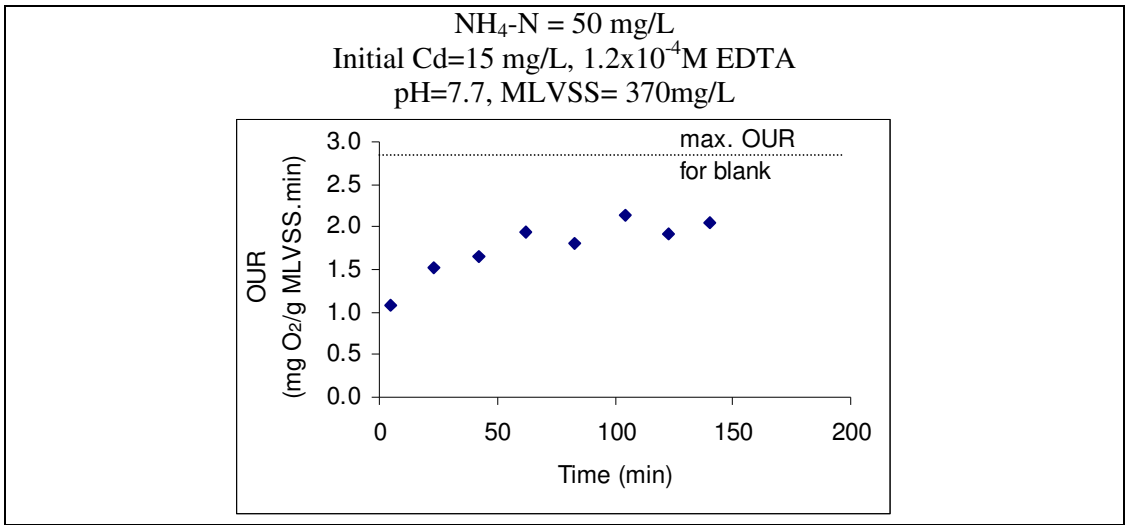

Figure D11. OUR measurements in qNH4-N experiments (Exp. No. 22)

APPENDIX E

Cd UPTAKE MEASUREMENTS IN AMMONIUM UTILIZATION RATE EXPERIMENTS

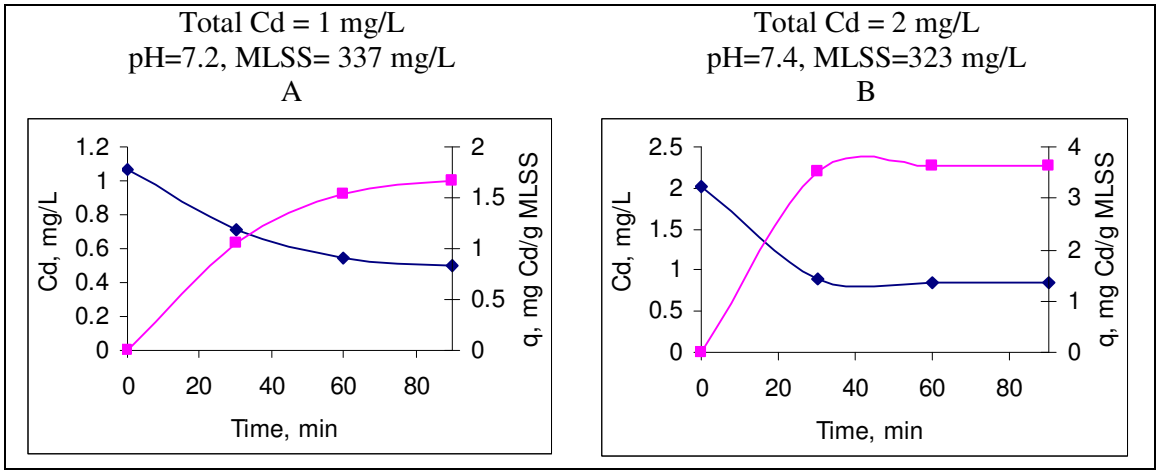

Figure E1. NH_4-N utilization in batch reactor (a) Exp. No. 7 (b) Exp. No.8

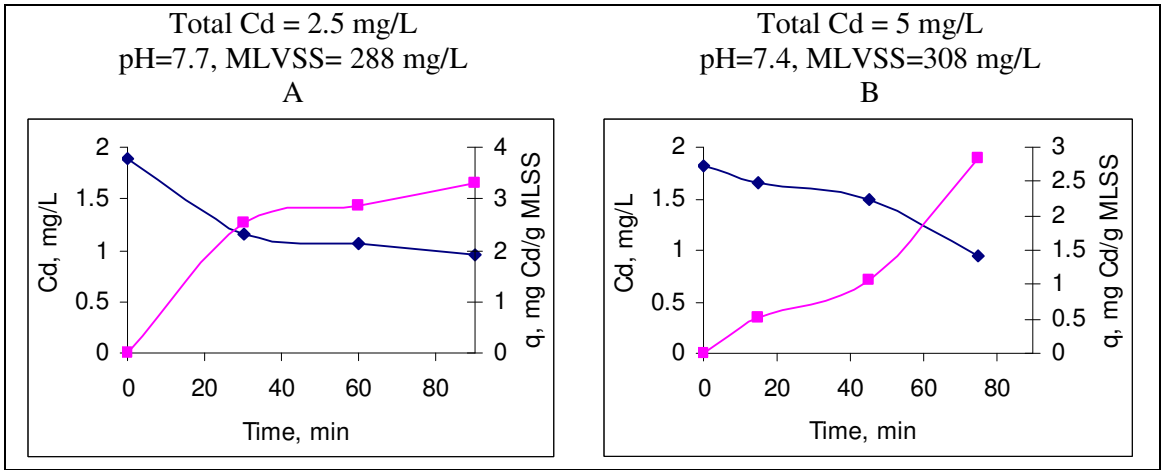

Figure E2. NH_4-N utilization in batch reactor (a) Exp. No. 9 (b) Exp. No.10

APPENDIX E (Continued)

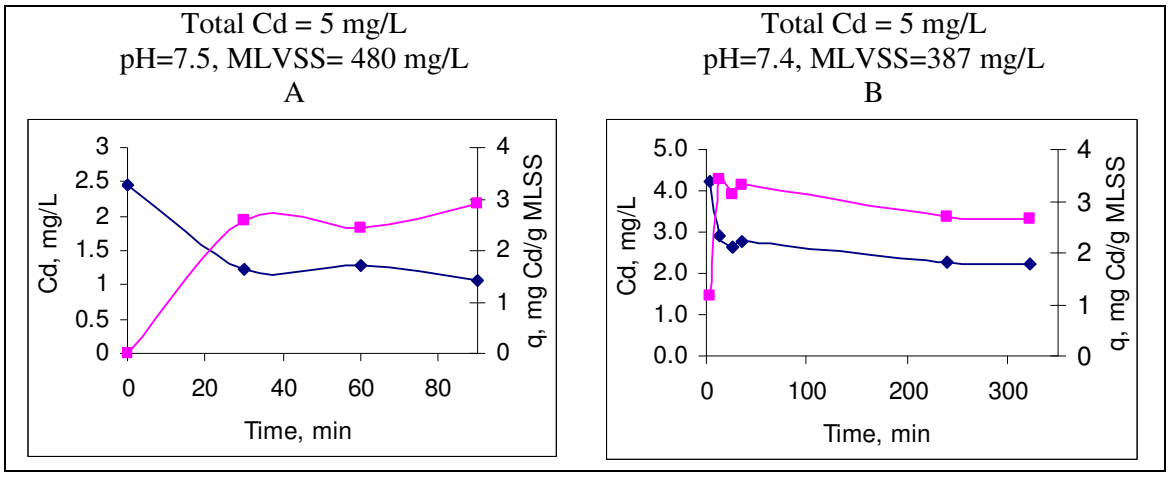

Figure E3. NH_4-N utilization in batch reactor (a) Exp. No. 11 (b) Exp. No.12